IMPACTS OF CLIMATE CHANGE ON RIVER HYDROLOGY AND ENERGY ECONOMICS IN BUDHIGANDAKI RIVER BASIN

A THESIS SUBMITTED TO THE

CENTRAL DEPARTMENT OF HYDROLOGY AND METEOROLOGY

INSTITUTE OF SCIENCE AND TECHNOLOGY

TRIBHUVAN UNIVERSITY

NEPAL

FOR THE AWARD OF

DOCTOR OF PHILOSOPHY

IN HYDROLOGY AND METEOROLOGY

BY

SURESH MARAHATTA

MAY 2022

IMPACTS OF CLIMATE CHANGE ON RIVER HYDROLOGY AND ENERGY ECONOMICS IN BUDHIGANDAKI RIVER BASIN

A THESIS SUBMITTED TO THE

CENTRAL DEPARTMENT OF HYDROLOGY AND METEOROLOGY

INSTITUTE OF SCIENCE AND TECHNOLOGY

TRIBHUVAN UNIVERSITY

NEPAL

FOR THE AWARD OF

DOCTOR OF PHILOSOPHY

IN HYDROLOGY AND METEOROLOGY

BY

SURESH MARAHATTA

MAY 2022

DECLARATION

Thesis titled “Impacts of Climate Change on River Hydrology and Energy Economics in Budhigandaki River Basin” which is being submitted to Central Department of Hydrology and Meteorology, Tribhuvan University; Nepal for the award of the degree of Doctor of Philosophy (Ph.D.) is a research work carried out by me under the supervision of Prof. Dr. Deepak Aryal and co- supervision of Academician Dr. Laxmi Prasad Devkota, Nepal Academy of Science and Technology between February 2018 to January 2022. I declare that the work is my own and has not been submitted for a degree of another university.

_____

Suresh Marahatta

IOST Registration No: 74-2074/75

Central Department of Hydrology and Meteorology

Tribhuvan University

RECOMMENDATION

This is to recommend that Mr. Suresh Marahatta has carried out research titled "Impacts of Climate Change on River Hydrology and Energy Economics in Budhigandaki River Basin" under our supervision. To our knowledge, this work has not been submitted for any other degree. He has fulfilled the entire requirement laid down by Institute of Science and Technology, Tribhuvan University for the submission of thesis and for the award of the degree.

_____

Prof. Dr. Deepak Aryal
Head
Central Department of Hydrology and Meteorology
University Campus
Kirtipur, Kathmandu, Nepal

_____

Dr. Laxmi Prasad Devkota
Academician
Nepal Academy of Science and Technology
Lalitpur, Nepal

May 8, 2022

May 8, 2022

LETTER OF APPROVAL

This is to recommend that Mr. Suresh Marahatta has carried out research titled "Impacts of Climate Change on River Hydrology and Energy Economics in Budhigandaki River Basin" under our supervision. To our knowledge, this work has not been submitted for any other degree. He has fulfilled the entire requirement laid down by Institute of Science and Technology, Tribhuvan University for the submission of thesis and for the award of the degree.

_____

Prof. Dr. Deepak Aryal
Head
Central Department of Hydrology and Meteorology
Tribhuvan University, Kathmandu, Nepal

ACKNOWLEDGEMENT

First of all, I would like to express my deepest gratitude to my supervisor Prof. Dr. Deepak Aryal and co-supervisor Dr. Laxmi Prasad Devkota for their invaluable advice, continuous support, patience, scholarly supervision and constantly guiding me during the research work. Their encouragement, suggestions and guidance were extremely fruitful in the outcome of this research. I gratefully acknowledge the University Grants Commission (UGC), Nepal for the Ph.D. fellowship. I am extremely grateful to Prof. Dr. Binil Aryal, Dr. Surendra Kumar Gautam, Dean and Assistant Dean respectively and all the administrative staffs of Institute of Science and Technology (IOST).

I am obliged to my friends Dr. Binod Pokharel, Dr. Loknath Adhikari, and Mr. Utsav Bhattarai for their suggestions, comments and review of the manuscript from proposal phase to the entire study period. I am grateful to Prof. Dr. Sunil Adhikary, Prof. Dr. Tek Bahadur Chhetri, and all the faculties and members of the Central Department Research Committee of Central Department of Hydrology and Meteorology (CDHM). I would like to thanks all administrative staff of CDHM for their support.

I am grateful to Prof. Dr. Sudha Tripathi, Prof. Dr. Ramesh Prasad Bhattarai, Mr. Kiran Shankar Yogacharya, Mr. Ajaya Mani Dixit, Prof. Dr. Sadhana Pradhananga, Prof. Dr. Prem Chandra Jha, Dr. Arun Bhakta Shrestha, Dr. Dilip Kumar Gautam, Dr. Dinesh Raj Bhuju and Dr. Rijan Bhakta Kayastha for their constructive feedback, and suggestion to my research work. I received input from Mr. Dibesh Shrestha, Mr. Sunil Pokharel, Mr. Rakesh Kayastha, and Mr. Joshan Maharjan, particularly on hydro-climatic modelling. Moreover, I am thankful to my friends Prof. Dr. Vishnu Prasad Pandey, Dr. Rohini Prasad Devkota, Dr. Ganesh Nath Tripathi, Dr. Deepak Chamlagain, Mr. Dharmendra Prakash Rajbhandari, Mr. Bikram Zoowa, Mr. Resham Baniya, Mr. Prem KC, Mr. Pawan Khatri and Mr. Kiran Pandey for their valuable inputs and suggestions during the research. I would also like to thank Mr. Nabaraj Dhakal, Mr. Shankar Sharma, Mr. Raju Pokharel and all the staffs of RECHAM Consult (Pvt.) Ltd. for their help during my Ph.D.

I would like to thank my wife Sanam Poudel, for her continuous encouragement and support. I could not have done it without your generous support. Often times, I could not be there for our sons; Agrim and Aaryak Marahatta and you had to single-handedly raise them. My mother is the source of inspiration. I am grateful to my parents-in-law

for their support and blessings. I would also like to acknowledge all the respondents of the studied basins and the gauge readers and station observers, who collected hydro-climatic data and the hydrologists/meteorologists who processed the raw data. I would like to express my special thanks of gratitude to my all teachers who taught me from pre-school to university as well as during the professional career.

Last but not the least, special thanks go to Department of Hydrology and Meteorology (DHM) for hydro-climatic data, Central Bureau of Statistics (CBS), Department of Water Resources and Irrigation (DoWRI), Nepal Electricity Authority (NEA), Department of Electricity Development (DoED), Budhigandaki Hydroelectric Development Committee (BGHDC), International Center for Integrated Mountain Development (ICIMOD), private hydroelectricity developers and all other agencies for providing published/unpublished data, necessary reports and related documents.

Thank you.

Suresh Marahatta
Balaju, Kathmandu
January 20, 2022

ABSTRACT

Water management has become a challenging task due to the increasing population, rapid urbanization and industrialization. Availability of observed hydro-meteorological data plays a crucial role in water budgeting for the country like Nepal that relies heavily on hydroelectricity for its energy needs. Quantification of available water at the local scale and examining how it is impacted by climate change (CC) is extremely important from the water management perspective at the river basin level. Budhigandaki River Basin (BRB) of Nepal, was chosen for this study in assessing climate change impact on river hydrology utilizing well calibrated and validated Soil Water Assessment Tool (SWAT), consequent impact on hydroelectric energy generation. Extending this aspect further, the micro-economic assessment of the Budhigandaki hydroelectric project was also made in this study.

This study assessed the interannual variability of hydroclimatic condition of the BRB using daily hydrological and meteorological data for the period from 1983 to 2012. To evaluate the impact of climate change on hydrological phenomenon in the study basin, future climate data under two Representative Concentration Pathways (RCP 4.5 and RCP 8.5) with four climatic conditions (cold-wet, warm-wet, warm-dry and cold-dry) for each RCP were considered. Digital elevation model (DEM) data, land use and land cover, and soil data of the basin are the spatial data required in the hydrological simulation that were utilized. The climate change impact on flow, hydroelectric energy generation and energy economics were evaluated by comparing these variables with the baseline.

Historical data shows that there is a very high variability in daily, monthly, seasonal and interannual flow in the study basin. Future annual precipitation in BRB varies significantly and is projected from -9% to 23% for RCP 4.5 and -11% to 21% for RCP 8.5 scenarios compared to the baseline value (1530 mm). The mean annual temperature increases 1.7^{o}C for RCP 4.5 and 3.9^{o}C for RCP 8.5 by the end of this century. SWAT model was calibrated and validated at Arughat gauging station considering 30 years daily flow data. Model evaluation using four statistical parameters (NSE, PBIAS, RSR and KGE) showed that the developed model performed very well to simulate river flow. Additional validation of the model done at three supplementary points; two in the upstream and one in the downstream of calibration point (Arughat) also showed that

the developed SWAT model for BRB is well calibrated. To compare the performance of flow simulation methods in the basin level, a new evaluation statistical index, the Global Performance Index (GPI), was introduced in this study. SWAT hydrological model preformed the best among the different methods considered for flow estimation as evaluated by GPI in BRB.

Annual mean flows are projected to increase in the future scenarios; 10 to 31% in RCP 4.5 and 5 to 57% in RCP 8.5 scenarios with respect to the baseline flow of 240 m^3/s. The analysis of future extreme flow shows an increasing trend in case of annual maximum one-day flow and a decreasing trend in low flow case. These results indicate a need to alter the design of hydraulic structures and selection of storage project over runoff-river project for climate resilience. Future annual energy of the Budhigandaki Hydroelectric Project is expected to increase by 9 to 13% compared to the baseline value (3385 GWh) that is equivalent to annual revenue of 20 to 28 million USD.

Results of this study show that storage hydroelectric projects with the provision of flexible operating rules are desirable. Financial policies related to hydroelectricity need to be revised with the changes in the future climatic conditions. The findings of this study are expected to be useful for hydrologists, economists and decision-makers to plan the use of available water judiciously in the future.

Keywords: Climate change, river hydrology, hydroelectricity, energy economics, GPI, SWAT, Budhigandaki

LIST OF ABBREVIATIONS AND ACRONYMS

ANN	Artificial Neural Network
AR5	Fifth Assessment Report
AR6	Sixth Assessment Report by IPCC
ARS	Agricultural Research Service
ASCE	American Society of Civil Engineers
BGHDC	Budhigandaki Hydroelectricity Development Committee
BGHP	Budhigandaki Hydroelectric Project
BP	British Petroleum
BRB	Budhigandaki River Basin
BS	Bikram Sambat
CanESM	Canadian Earth System Model
CC	Climate Change
CCAM	Conformal Cubic Atmospheric Model
CDD	Consecutive Dry Days
CN	Curve Number
COP	Conference of Parties
CSDI	Cold Spell Duration Index
DAR	Drainage Area Ratio
DEM	Digital Elevation Model
DHM	Department of Hydrology and Meteorology
ET	Evapotranspiration
ETCCDI	Expert Team on Climate Change Detection and Indices
FDC	Flow Duration Curve

FF	Far Future
FY	Fiscal Year
GCMs	Global Climate Models
GeoSFM	Geospatial Stream Flow Model
GFDL	Geophysical Fluid Dynamics Laboratory
GHG	Green House Gas
GIS	Geographic Information System
GJ	Giga Joule
GLOF	Glacial Lake Outburst Flood
GoN	Government of Nepal
GPI	Global Performance Index
GR4J	Génie Rural à four paramètres Journalier
GRFM	Geomorphic Recession Flow Model
GT	General Transposition
GW	Ground Water
HadGEM	Centre Global Environment Model
HBV	Hydrologiska Byråns Vattenbalansavdelning
HEC-HMS	Hydrologic Engineering Center—Hydrologic Modeling System
HEP	Hydroelectric Project
HRU	Hydrological Response Units
HYMOD	Hydrological Model
ICIMOD	International Centre for Integrated Mountain Development
IEA	International Energy Agency
IPCC	Intergovernmental Panel on Climate Change

KGE	Kling–Gupta Efficiency
KW	Kilo Watt
LDOF	Landslide Dam Outburst Flood
LOCI	Local Intensity Scaling
LTMA	Long Term Mean Annual
LULC	Land Use and Land Cover
MBT	Main Boundary Thrust
MCT	Main Central Thrust
MCTCA	Ministry of Culture Tourism and Aviation
MDAR	Multiple Gauging Stations Drainage Area Ratio
MF	Mid Future
MIKE SHE	Variant of Système Hydrologique Européen
MoEWRI	Ministry of Energy, Water Resources and Irrigation
MoF	Ministry of Finance
MoFE	Ministry of Forest and Environment
MoWR	Ministry of Water Resources
MPI	Max Plank Institute for Meteorology
MRE	Mean Square Error
MW	Mega Watt
NAP	National Adaptation Plan
NEA	Nepal Electricity Authority
NF	Near Future
NOAA	National Oceanic and Atmospheric Administration
NPC	National Planning Commission

NPR	Nepalese Rupees
NRB	Nepal Rastra Bank
NSE	Nash-Sutcliff Efficiency
O & M	Operation and Maintenance
OECD	Organization for Economic Co-operation and Development
P	Precipitation
PBIAS	Percent Bias
PET	Potential Evapotranspiration
PPA	Power Purchase Agreement
PRC	People's Republic of China
PRoR	Peaking Run-off-River
QM	Quantile Mapping
RAFT	Runoff Analysis and Flow Training
RCMs	Regional Climate Models
RCPs	Representative Concentration Pathways
RMSE	Root Mean Square Error
RoR	Run-off-River
RSR	Ratio of Root Mean Square Error to Standard Deviation
SAC-SMA	Sacramento Soil Moisture Accounting
SCS	Soil Conservation Service
SIMHYD	Simplified Version of the HYDROLOG
SNURCM	Seoul National University Regional Climate Model
SOTER	Soil Terrain Database Programme
SRM	Snowmelt Runoff Model

SRTM	Shuttle Radar Topography Mission
STP	Storage Type Project
SWAT	Soil and Water Assessment Tool
TOPMODEL	Topographic Hydrologic Model
TU	Tribhuvan University
TWh	Terawatt hour
UN	United Nations
UNDP	United Nations Development Program
UNEP	United Nations Environment Program
UNESCO	United Nations Educational, Scientific and Cultural Organization
UNFCCC	United Nations Framework Convention on Climate Change
UNICEF	United Nations International Children's Emergency Fund
US	United States
USD	United States Dollar
USDA	United States Department of Agriculture
VELMA	Visualizing Ecosystem Land Management Assessments
VIC	Variable Infiltration Capacity
WECS	Water and Energy Commission Secretariat
WED-DHM	Water and Energy Budget-Based Distributed Hydrological Model
WMO	World Meteorological Organization
WSDI	Warm Spell Duration Index
WY	Net Water Yield

LIST OF SYMBOLS

$	US Dollar
%	Percentage
A	Reservoir water surface area
y	Reservoir water depth
α	Multiplicative coefficient
β	Power coefficient
SW_t	Final soil water content (mm)
SWo	Initial soil water content (mm)
R_{day}	Amount of precipitation on day i
Q_{surf}	Amount of surface runoff on day i
E_a	Amount of evapotranspiration on day i
W_{seep}	Amount of water entering the vadose zone from soil profile on day i
Q_{gw}	Amount of return flow on day i
I_a	Initial abstraction (mm)
S	Relation parameter
SNO_i	Water content (mm) on day i
P_s	Solid precipitation (mm) on day i
SNO_{mlt}	Daily snowmelt amount (mm)
E_{sub}	Evaporation lost by sublimation (mm)
mm	Millimeter
Q_{0i}	Observed discharge of day i
Q_{ei}	Estimated discharge of day i
b_{mlt}	Daily melt factor (mm day^{-1} $°C^{-1}$)

SNO_{cov}	Daily melt factor (mm day^{-1} $°C^{-1}$)
T_{sno}	Daily snowpack temperature (°C)
T_{max}	Daily maximum air temperature (°C)
λ	Latent heat of vaporization (MJ/kg)
Eo	potential evapotranspiration (mm/d)
Ho	extra-terrestrial radiation ($MJ/d.m^2$)
Tavg	Average air temperature per day (^OC)
$\overline{Q_0}$	Mean of the observed discharges.
V_o	Observed volumes of water for day i.
V_e	Simulated volumes of water for day i.
σ_o	Standard deviations of observed flows
r	Correlation coefficient
σ_e	Standard deviations of simulated flows
ΔT	Percentage change of mean temperature
ΔP	Percentage change in annual precipitation
TX_{ij}	Daily T_{max} on day i in period j
TN_{ij}	Daily T_{min} on day i in period j
$X_{future,t}^{GCM}$	$X_{future,t}^{corr}$ is the corrected estimate of GCM
$X_{future,t}^{corr}$	Corrected estimate of $X_{future,t}^{GCM}$
$ecdf$	Empirical cumulative distribution function for reference time period
$X_{future,t}^{GCM}$	GCM (projected value) in future at time t,
$ecdf_{baseline}^{GCM}$	Empirical cumulative distribution function of GCM for baseline period

$F^{obs}_{baseline}$	Empirical cumulative distribution function of observation for baseline period.
$\bar{O}proj$	Bias corrected temperature for future.
M^{T}_{ref}	month-wise bias correction such that and represent means in reference time.
M^{O}_{ref}	month-wise bias correction in reference time
σ^{T}_{ref}	standard deviations of daily values for month under consideration in reference time
σ^{O}_{ref}	Standard deviations of daily values for month under consideration in reference time
H	Available net head (m)
P	Power generation (MW)
Q_{max}	Maximum allowable discharge to the turbine
P_{max}	Maximum possible power generation for the base case
η	Overall efficiency of the plant
γ	Unit weight of water (9.8 kN/m^3)
Q_T	Average discharge available for the turbine (m^3/s)
E	Total energy generated (GWh)
$\Delta E_{i,j}$	Change in the total energy generated expressed as percentage
$E_{i,j,CC}$	Total energy generated in the i^{th} month of the j^{th} year of the CC scenario
$E_{i,base}$	Total energy generated in the i^{th} month of the base case
DR_j	Total dry season revenue
WR_j	Total wet season revenue
AR_j	Total annual revenue

$R_{i,base}$	Total monthly revenue generated in the baseline period
$R_{i,j,CC}$	Total monthly revenue generated in the CC scenario
$\Delta R_{i,j}$	Change in the total revenue
ΔDR_j	Change in the dry season revenue
ΔWR_j	Change in the wet season revenue
ΔAR_j	Change in the annual revenue
π_j	Total annual profit
$C_{O\&M,j}$	Total annual operation and maintenance cost

LIST OF TABLES

LIST OF FIGURES

TABLE OF CONTENTS

CHAPTER 1

INTRODUCTION

1.1 General

Complex interactions between the atmospheric system and the underlying topography determine flow of the river. The is a part of rainfall that appears in a stream and represents the total response of a basin. Surface flow, subsurface flow, base flow and precipitation that directly falls on the stream constitutes the total discharge in the river (Chow et al., 1988; Zhang et al., 2018). Historical time series of discharge data is one of the most important requirements for planning, operation and control of all water resources projects (Dobriyal et al., 2017; Loukas and Vasiliades, 2014; Tallaksen, 1995) at both local and national scales (Razavi and Coulibaly, 2016; Shin et al., 2021). However, availability of measured flow data in many cases is either inadequate or not available at all (Loukas and Vasiliades, 2014; Young, 2006). Such situations create challenges not only for the optimal use of water resources in ungauged river basins for various development works like domestic water supply and sanitation, irrigation, hydroelectricity production etc. but also in flood control works (Devkota et al., 2017; Mwakalila, 2003). Underestimation of the flows could lead to rejection of attractive projects whereas overestimation could have huge implications on the physical infrastructure and overall economic feasibility of the projects (Devkota et al., 2020; Devkota and Maraseni, 2018).

Accurate flow estimates are, therefore, necessary at these basins where water resources projects are developed. However, measured flow data are not available in most of the cases in such project sites (Loukas and Vasiliades, 2014). It is because of the lack of sufficient flow gauging stations in most river basins. The situation is more severe in mountainous basins (Shin et al., 2021) because of the inaccessibility of most of these sites for on-site observations. It is the reason why water budget analyses in such basins are not as easy as in the other gauged basins (Alford et al., 2011; Alford and Armstrong, 2010; Hishinuma et al., 2014; Viviroli et al., 2011, 2007). To address the challenge of non-availability of observed data at local level for water resources planning and utilization in the river basin, hydrologic simulation method has been widely used in

recent years (Jain et al., 2017; Marahatta et al., 2021b; Meng et al., 2020; WMO, 1989). Simulation models provide excellent platforms for evaluating various options for water resources as well as environmental planning (Abbaspour et al., 2015; Pandey et al., 2020a). In hydrological simulation, a hydrologic model which is a simplified software representation of the hydrological processes within a basin boundary, is used to generate the flow at required locations of the river basin.

Several studies around the globe have chosen Soil and Water Assessment Tool (SWAT), to assess the water availability including either impact of climate change or land use changes or both (Tan et al., 2019). The result reveals that SWAT is a suitable tool for modelling hydrological responses in both rain-fed and snow-fed basins of Nepal. For examples: the SWAT model are used by (Bajracharya et al., 2018) in Kaligandaki basin; (Dahal et al., 2016; Lamichhane and Shakya, 2019) in Bagmati basin; (Pandey et al., 2020b) in Karnali basin; (Bhatta et al., 2019) in Tamor basin, and (Bharati et al., 2016) in Koshi basin for the assessment of the climate change impact on river hydrology.

Since the beginning of the industrial age, the ability to harness and use different forms of energy has led to global economic growth; increase in production and consumption which enabled people to perform increasingly productive tasks as well as improve the living standards of billions of people (Mohajan, 2019; Stern, 2012). However, scientific evidences indicate that huge emission of CO_2 and other greenhouse gases (GHGs) in the atmosphere is associated with the increasing use of fossil fuel (IPCC, 2015; Yoro and Daramola, 2020). The industrial revolution era can, thus, be taken as the starting point of Climate Change (CC) as the scientific community has defined it today (Stern et al., 2006a). With the widespread use of fossil fuel and human interventions after the first industrial revolution, global warming has emerged as a critical environmental issue that has brought the world attention (Le Treut et al., 2005).

Climate change, rapid population growth, urbanization, industrialization and economic development will clearly affect the availability of potential water resources in numerous regions (Touseef et al., 2020). Climate change is a global issue; however, researchers are more interested in its impact at the local level where planning of water resources projects mostly commonly takes place (Li et al., 2021; Touseef et al., 2021). The global climate models (GCMs) and regional climate models (RCMs) have been found to be

effective tools in developing a better understanding of CC by predicting future climate projections (Robock et al., 1993; Tapiador et al., 2020). Lately, it has become very convenient to use these GCM/RCM datasets in hydrological models for the impact of CC studies on river hydrology and water resources. Comparing future climate projections with the baseline period to reach meaningful conclusions have been a routine procedure in the hydrological modelling and CC domains. For examples, water availability studies using the output of climate models have been carried out at global (Barnett et al., 2005), regional (Lutz et al., 2016) and local scales (Dahal et al., 2020). Results of such studies vary considerably across the spatial and temporal scales and thus a generic conclusion on the impact of CC in water availability cannot be reached deterministically. Quantification of available water at the local scale and examining how it is impacted by CC is extremely important from the water management perspective at the river basin level. One of the main objectives of this study is to analyse the impact of CC on the hydrology. Budhigandaki River Basin (BRB) of Nepal, was chosen for this study in assessing climate change impact by utilizing SWAT hydrological model, and its consequent impact on the hydroelectric energy generation.

Hydroelectricity is mainly dependent on the temporal variation of river flow, which in turn is, largely impacted by CC. Generally, run-of-the-river (ROR) facilities are more affected than storage type plants (STPs). Several studies have analyzed how runoff will change at the global (Turner et al., 2017b, 2017a; Zhou and Hanasaki, 2018), regional (Ali et al., 2018; Zhong et al., 2019) and local (Devkota and Gyawali, 2015; Kaini et al., 2020; Marahatta et al., 2021b; Pandey et al., 2019) scales in the future due to CC. A common inference from all these studies is that the CC impacts on hydroelectricity is largely influenced by the geographical location of the hydroelectricity plant and choice of climate models despite high levels of uncertainty in the direction and magnitude of the predictions (Marahatta et al., 2021b).

Despite the worldwide consensus regarding transition to renewables, most studies on renewable energy are no longer interested in hydroelectricity because of the resource availability, climate change, environmental, social and geo-political concerns. However, hydroelectricity is extremely important for countries like Congo, Paraguay and Nepal which have abundant water resources, naturally gifted terrain extremely favorable for hydroelectricity generation and lack the capital to invest in other expensive modern renewable technologies. Nepal is a unique Himalayan country with

an economically feasible hydroelectricity potential exceeding 50,000 MW – one of the highest in the world (Alam et al., 2017; Jha, 2011). Therefore, hydroelectricity should be promoted as an efficient, economical and clean source of energy in this part of the world giving due care to minimize the environmental impacts and social issues associated with it. Moreover, we find that there are very few studies on the impacts of CC focused on hydroelectricity in the Hindu Kush Himalayas (HKH) region and the Nepalese Himalaya in particular.

The current research trend on energy economics is found to be largely focused on fossil fuels (Barreto, 2018; Belfiori, 2020; Hanif et al., 2019; Rehman et al., 2021) and other water management issues (Pakhtigian et al., 2020). However, research on the effects and economic aspect of hydroelectricity is limited (Mattmann et al., 2016). Extending this gap further is the micro-economic assessment of the cost and revenue aspects of hydroelectricity linked to CC at the project level. Another major aim of this study is to address this niche and to pave a way for integrated economic evaluations of the hydroelectricity sector.

1.2 Research questions

Based on the research gaps identified from the literature review, following research questions are established in this study:

i. How have precipitation, temperature and runoff patterns of the Budhigandaki basin changed historically?

ii. How well can the hydrological model, SWAT, simulate the river hydrology of the study basin?

iii. How does hydrological model output compare with existing methods of flow estimation in the study basin?

iv. What would the impact of climate change be on the river hydrology?

v. How would climate change affect hydroelectric energy generation and consequent energy economics?

1.3 Objectives the study

The main objective of the study is to assess the impact of climate change on river hydrology, hydroelectric energy generation and consequent energy economics in the Budhigandaki river basin. The specific objectives of the study are:

i. To quantify variation in precipitation, temperature and runoff patterns at different temporal scales.
ii. To develop well calibrated and validated hydrological model, SWAT, for the study basin.
iii. To evaluate the performance of the SWAT against existing methods of flow estimation.
iv. To assess the impact of climate change on river hydrology under different climatic conditions and scenarios for twenty first century.
v. To analyze the climate change impact on the hydroelectric energy generation and its implication on energy economics.

1.4 Limitations

This research has been carried out with the following limitations:

i. The uncertainties associated with the selection of climate models and scenarios are the data and model-related limitations of this study.
ii. Impact of land use change on river hydrology is not considered in this study.
iii. There are various forms of energy available for different uses. In this study only hydroelectric energy is considered while assessing the impact of climate change on energy economics.
iv. Energy economics of a hydroelectric project encompasses mainly two aspects: Cost (capital and recurrent expenditures) and Revenue. The study focuses on energy economics as a consequence of change in river hydrology due to climate change impact, impact of hydraulic and other structures resizing and operational modification are not investigated. These aspects may impact in cost stream of the project. Revenue aspect is only considered while performing economic analysis in the study.

v. Per unit energy price may increase or decrease in the future. However, current power purchase rate is considered while calculating the revenue of the project even for the future. Further, the exchange rate is also assumed to not change in future.

vi. A number of other direct and indirect benefits such as irrigation, domestic and industrial water supply, recreational, fish farming, water transportation, and tourism can be accrued because of the hydroelectric project. Only revenue generated from electricity sale is considered while assessing revenue of the project. This assessment has considered only the direct costs and revenue related to the storage hydroelectricity project.

1.5 Dissertation structure

The dissertation is organized into six chapters as the main body, references and appendixes. The structure is summarized as follows.

i. Chapter 1 provides the background, statement of the problem, and objectives.

ii. Chapter 2 presents a review of the published articles, research reports, and books relevant to the objectives. Future flow and climate change studies have been reviewed. The study established hydrological models based on historical hydro-climatic data, and projected change in energy and consequence revenue change are also reviewed in this chapter.

iii. Chapter 3 deals with the detailed description of the methodology framework along with the study area in terms of physical characteristic, hydro-climate, identify/planned hydroelectric sites, and the other relevant information of the river basin.

iv. Chapter 4 provides results and discussions in line with the five objectives of this study. The results of climate change and their impacts on the flow and energy production as well as change in revenue generation are discussed adequately with reference to the findings of other relevant studies.

v. Chapter 5 comprises of conclusions and recommendations.

vi. Chapter 6 comprises of a brief summary.

CHAPTER 2

LITERATURE REVIEW

2.1 Background

This chapter presents a comprehensive review of the available literature to identify research gaps relevant to this study. Starting with general overview of the impact of climate change on water resources, review of literature begins with water resources at global and national levels. It is followed by review of different flow estimation methods commonly used in Nepal. Use of hydrological models for this purpose around the globe and in Nepal are also presented. It is followed by general findings on climate change; i.e., trend analysis of precipitation and temperature; and its consequent impact on river hydrology. Such impact on river flow affects the hydroelectricity generation, prime renewable energy in the context of Nepal. The sub-sequent section of this chapter is focused on the various forms of energy, both renewable and non-renewable, used globally and in Nepal. Then a brief review of energy economics focusing on hydroelectric energy is covered before coming to the conclusions of this chapter.

2.2 General overview

Estimation of stream flow is required for planning water resource projects in a river basin. Most of the basins in the Himalayan region are ungauged due to highly rugged mountainous terrain where it is very difficult to observe hydro meteorological data. Moreover, it is not possible to take measurements at every small catchment and at every location of the stream.

Climate change has been a major global issue since last the decade and serious concerns have arisen at national and international level to assess the nature and extent of changes. Although, climate change has global implications, studies show that the impacts of climate change have a wide range of spatial scales and its affects are also concentrated at regional scale although the water management policies target at national level. South Asia is expected to be seriously affected by the impacts of climate change due to the high dependency of economy on agriculture and water resources in the region (IPCC, 2007). Glacier melt in the Himalayas is projected to increase flooding, cause rock avalanches from destabilized slopes, and affect water resources within the next two to

three decades. This will be followed by decreased river flows as the glaciers recede (IPCC, 2007). Freshwater availability in Central, South, East and South-East-Asia, particularly in large river basins, is projected to decrease due to climate change. Along with population growth and increasing demand arising from higher standards of living, climate change could adversely affect people by the 2050s.

Himalaya regions are sometime referred as third pole which has 34660 km^2 of glacier reserve. Increasing temperatures will increase the ratio of rain to snow; accelerate the rate of snow and glacier melt; and shorten the overall snowfall season. Since the end of the Little Ice Age, the temperatures have been generally increasing and the majority of the world's glaciers are retreating (IPCC, 2014). Increasing temperature shifts the permanent snowline upward. This could cause a significant reduction of glacial water storage in the mountains, which is likely to pose serious problems of water availability to many people living downstream. The Himalayan glaciers are melting faster in recent years than before (IPCC, 2007).

This study investigates the potential impact of climate change on future water availability in Nepal. The simulation shows the water availability for future dry and wet season. In case of dry season, a decline in water availability in the near future followed by a tendency to increase to the current amounts is predicted in the late part of century. However, in case of wet season there is an increasing trend of water availability in future. Considering the whole country for dry season the water availability is expected to be decreased in the early part of the century followed by an increasing trend by the end of the century relative to present water availability for both scenarios. It is noted here that the Himalaya encompasses the world's third largest glacier systems after Antarctica and Greenland, occupying about 15% of the mountain terrain (Anthwal et al., 2006), so the study of snow melt pattern in the Himalayan River due to climate change clearly linked with the economy in terms of hydroelectricity generation.

This study is focused to evaluate the influence of climate change on energy production for a storage type project (BGHP, 2015) based on water availability generated by SWAT hydrological model as discussed in (Marahatta et al., 2021d). The effects of hydroelectricity generation depend on the size of operation and the geographical location, and the type of hydroelectric facility, e.g., run-of-the-river facilities, usually operating with constant water flows and generating electric base load, have different

effects than storage plants that rely on dams to store water, for use during times of peak demand. This study further compares the revenue generation in annual as well as wet and dry periods for future climate change scenarios with the baseline values (Marahatta et al., 2022, 2021b). This study provides insightful evidence which shall be extremely useful for the planning and design of hydroelectric projects not only within Nepal but also the South Asian region drained by numerous trans-boundary rivers such as the Budhigandaki river.

2.3 Water resources

The region's water resource is already affected by the rapid population growth, urbanization, agricultural and energy demand. Recent extreme events in Nepal shows an excess of water in monsoon season (June- September) and scarcity during the rest of months of year. In addition, the intensity of the extreme events is also expected to increase in the future (Devkota and Gyawali, 2015). Two most important problems attributed by climate change in the region are frequencies of floods and droughts. Flooding negatively affects the agricultures, livelihoods and infrastructure whereas drought affects the crop production specifically the mid and far western parts of the country. This review investigates to synthesize the literatures, documenting the potential impact of climate change on future water availability in BRB and its effect on energy economics particularly in Nepal.

Water resources is required for agricultural, industrial, and domestic activities and for environmental preservation (UNEP, 2012). With the increase in population and accelerated growth of urbanization, industrialization, and commercial development, demand for water resources of sufficient quantity and quality will continue to increase (Devkota and Maraseni, 2018; Flint, 2004; World Bank, 2017). Rivers are primary sources for water supply, industries, irrigation, hydro-electricity generation, transport and sustaining ecosystems services to the people downstream (Akhtar et al., 2008; Miller et al., 2012; Molden et al., 2016; Viviroli et al., 2011). However climate change is impacting river hydrology (Devkota and Gyawali, 2015; Pandey et al., 2020a). Variation in flow in rivers is high (BGHP, 2015; DHM, 2018) and the impact of variation in meeting daily, monthly or seasonal water requirements is seldom studied.

The design of water related structures such as dams, highway bridges, embankments, among others, consists of three basic components: hydrologic design, hydraulic design

and structural design. Hydrologic design deals with the estimation of the quantities of water to be handled at the site of the structure in terms of time distribution, time of occurrence and frequency of occurrence (Reddy, 2001). Streamflow time series is, therefore, one of the most important data required for the effective water resource planning and management at both local and national scales (Razavi and Coulibaly, 2016). However, availability of measured flow data in many cases is either inadequate or not available at all (Loukas and Vasiliades, 2014; Young, 2006). Such situations create challenges not only for the optimal use of water resources in ungauged river basins for various development works like domestic water supply and sanitation, irrigation, hydro-electricity etc. but also in flood control works (Devkota et al., 2017; Mwakalila, 2003). Under estimation of the flows could lead to rejection of attractive projects whereas overestimation could have huge implications on the physical infrastructure and overall economic feasibility of the projects (Devkota et al., 2020; Devkota and Maraseni, 2018). Accurate flow estimates are, therefore, necessary at these basins where water resources projects are developed.

2.3.1 Global water resources

Hydrological cycle is the central focus of hydrology. The cycle has no beginning or end, and its many processes occur continuously (Chow et al., 1988). Although the concept of hydrological cycle is simple, the phenomenon is extremely complex. It is just one large cycle but somewhat is composed of many interconnected processes at continental, regional and local scale. The total volume of water in the global water cycle is constant but, the spatial and temporal distribution of water of such cycle is continually changing at different scales. The regional water balance is the application of water balance equation in the surface, sub-surface as well as groundwater movement. About 96.5% of all water is found in oceans, groundwater and polar ice contains 3.4%, and surface and atmospheric system contains only 0.1% of global water (1386×10^6 km^3). It is interesting to note that such 0.1% of atmospheric water (12,900 km^3) is the driving force of the surface hydrology. About two-third (68.65%) of fresh water is stored in polar as well as other snow and ice forms, 30.1% in groundwater. Atmospheric, swamp, river and biological water are 0.04%, 0.03%, 0.006% and 0.003% respectively of the total global fresh water (UNESCO, 1978).

2.3.2 National water resources

Nepal is a country rich in water resources. Rivers originating from the Nepal Himalayas are the sources of freshwater to riparian countries of India and Bangladesh. The Rivers flowing from Nepal contribute about 70% of the dry season flow and 40% of the total annual average flow 7,125 m^3/s (225 billion cubic meters) of the Ganges (Alford, 1992). The annual average runoff within the Nepalese territory is estimated at 174 billion cubic meters (76%). The large change in elevation from the high Himalayas in the North to the plains in the south over a short width of 130 to 230 km generates substantial hydraulic head for development of hydroelectricity (WECS, 2006). Nepal's hydroelectricity potential has been estimated at 83,290 MW based on average river flow. Among 83,290 MW, 114 sites (45,610 MW) are technically potential while 66 sites (42,133 MW) are economically potential (Shrestha, 1966). However, several studies in the past have shown that the total potential in terms of installed capacity and annual energy of the identified projects are 43,000 MW and 180,000 GWh respectively (WECS, 2005). Government of Nepal has issues license of 792 projects (40,848 MW) to different public, private and international companies among them 119 projects (~1900 MW) ranging from less than 1000 KW to 456 MW are in operation. There are 3,808 glaciers covering an area of 3,902 km^2 with an estimated ice reserve of 312 km^3 with an individual average area of glaciers was estimated 1 km^2. The total glacier area retreated by 24% between 1977 and 2010, and the estimated loss in ice reserves by 29% (129 km^3) with an average receded by 38 km^2 per year (Bajracharya et al., 2014). Nepal represents nearly 13 % of the total basin area of Ganges, however, discharge from the glaciers of the three major catchments of Nepal is about 5,200 million cubic meters annually, which represents nearly 4% of the estimated 145,000 million cubic meters that flow from Nepal each year into the River Ganges (Alford, 1992; Alford et al., 2011). Besides, there are 1,466 glacial lakes in Nepal covering an total area of 65 km^2 (ICIMOD, 2011). Despite the abundance of water resources potential, less than 8% of water potential is used for irrigation in Nepal (WECS, 2011).

The government's priority is to develop hydroelectricity plants that focuses on storage projects; currently, the ratio of the reservoir based and pump storage hydroelectric projects are at 30-35%, peaking-runoff the river projects at 25-30 %, and alternative sources of electricity e.g. solar, wind, micro-hydro etc. at 5-10 % for production mix of electricity projects (NPC, 2020). This shift is useful because a storage project addresses

the seasonal variation of river hydrology by storing water during high flow period (monsoon season) for power generation during low flow period when the demand for electricity is higher in Nepal. Furthermore, they can be used as multipurpose water resources projects such as for water supplies for drinking, irrigation and industrial uses; recreation; navigation and flood control. To have a year-round irrigation especially in the fertile Terai region (Indo-Gangetic plain), reservoir projects have to be considered for irrigation policy of Nepal. Reservoir projects are not only beneficial to Nepal but also to India in terms of irrigation and flood control (Pun, 2017; Upadhyay and Gaudel, 2018). Although stored water of a reservoir can be used for multiple uses, in Nepal they are primarily used for hydroelectricity generation.

Recognizing the importance of energy for socio-economic development, the Government of Nepal has plans to replace traditional fuel by electricity and increase the per capita energy consumption. To achieve this goal, Nepal has set hydroelectricity development as a priority (WECS, 2013) using its annual average available water of 225 km^3 (WECS, 2005) and its topography favorable for hydro-electricity development. Hydroelectricity development can contribute to national development through reduced imports of fossil fuels, expand the area of land under irrigation and diversify the economy in which poor households are more integrated in the economy. It can help promote industrialization, sell electricity to neighboring countries and generate foreign currency reserves and reduce Nepal's trade deficit (Alam et al., 2017; MoWR, 2009; Thapa and Basnett, 2015).

2.4 Altered global energy pattern

Rapid technological, economic and social change that has shaped the modern world is due to the industrial revolution. This was the period of great modernization and many of the technologies we use today are inventions of the industrial revolution. Energy is the prime mover of the modern world. The industrial age began with the availability and use of cheap energy in the form of coal and then petroleum products. Subsequently, global economic growth has been based on the ability to harness and use different forms of energy (Marahatta et al., 2021b). Traditional energy sources, e.g. human labor and animal transport, were replaced with more efficient energy sources, coal and then by oil in the early 1900s for powering machines and transportation (O'Connor and Cleveland, 2014; Wrigley, 2013). This has led to an increase in the production and consumption of energy enabling people to perform productive tasks as well as to

improve the living standards (Mohajan, 2019; Stern, 2012). In fact use of and access to cheaper fossil fuels have significantly contributed to the rapid economic development at the global scale (UNDP, 2020). However, extensive use of fossil fuel since the industrial revolution has resulted in the emission of large quantities of CO_2 and other greenhouse gases in the atmosphere (IPCC, 2015; Yoro and Daramola, 2020). This has spawned CC which emerged as a major global environmental challenge and demanding the world's attention (Le Treut et al., 2005; Stern et al., 2006b).

2.4.1 Global energy perspective

The global primary energy consumption was 584 Exajoules (162,222 TWh) in 2019. Renewable energy contributed nearly ~25% of the global primary energy. Bioenergy has the largest share among renewables with approximately 10% of the total primary global energy supply. Of the total primary global energy consumption, three renewable energy sources hydroelectricity, wind and solar that contribute ~ 3%, ~1% and ~0.5% respectively (BP, 2020). Hydroelectricity accounts for 17% of the world's total electricity generated (IEA, 2020). Of the total hydroelectricity produced globally in 2019, the Organization for Economic Co-operation and Development (OECD) countries was the largest producer ~35% followed by China ~29% while the Middle East generated less than 1% (IEA, 2020).

Currently efforts are on to transition from the fossil-fuel based energy systems to renewable energy. Hydroelectricity is one of the oldest, well-tested and proven clean energy technologies in the world (Awojobi and Jenkins, 2015; Mattmann et al., 2016; Ranzani et al., 2018; Tomczyk and Wiatkowski, 2020; Wagner et al., 2019). The efficiency in terms of energy returned on investment is high for hydroelectricity compared to other renewables (García-olivares et al., 2018; Hall et al., 2014). Moreover, the per unit capital cost of this technology is much lower than the other clean energy technologies (Best, 2017).

Currently efforts are on to transition from the fossil-fuel based energy systems to renewable energy through the use of water, wind, solar, tidal and geothermal sources. Firstly, the potential energy of water is directly converted to electricity without many intermediate conversion processes common in the other renewable energy generation methods (Siri et al., 2021). Secondly, the efficiency in terms of energy returned on investment is high for hydroelectricity compared to other renewables. Significant

research and development has been carried out in the last century related to different aspects of hydroelectricity such as planning, design of hydraulic structures, electro-mechanical components, distribution systems, sediment handling, emissions and overall water environment management processes (Chang et al., 2018; Devkota et al., 2016; Janssen et al., 2021; Liu et al., 2020; Mishra et al., 2018; Qin et al., 2020).

It is seen that countries with relatively smaller energy demands and having abundant hydroelectricity potential have a larger share of hydroelectricity in their national energy generation compared to countries with high electricity demands. For example, less energy consuming countries such as Albania, Congo, Mozambique, Paraguay, Uruguay and Nepal have hydroelectricity contributions in the magnitude of 90% of the total energy supply. On the other hand, the contribution of hydroelectricity is 17%, 7%, 17%, 10%, 8% and 12% of the total energy supply in China, USA, Russia, India, Japan and France, respectively (IEA, 2020; Martins et al., 2018; Tomczyk and Wiatkowski, 2020). Interestingly, some high energy consuming countries such as Norway, Brazil and Canada have significant share (95%, 65% and 59% respectively) of hydroelectricity in their total electricity supply (IEA, 2020).

2.4.2 National energy perspective

The per capita energy consumption of 482 kg oil equivalent (total 14.464 million tonnes) in Nepal in FY 2077/078 (MoF, 2021) is very low compared to global average of 1,922 kg oil equivalent (World Bank, 2020). The total annual energy consumption of Nepal was 586.7 million GJ in the fiscal year 2018/2019 (MoF/GoN, 2020). Three categories of sources, namely, traditional, commercial and other renewables constitute the energy generation mix of Nepal. Traditional sources had the highest contribution (68%) in the mix by far compared to the others for the fiscal year 2018/2019 (MoF/GoN, 2020). Traditional sources include firewood (62% contribution), agriculture residue (3%) and dry dung (3%). Fossil fuels, namely coal and petroleum contributed 7 and 19% of the total annual energy consumption. Grid electricity had a share of about 4% while other renewable energy technologies contributed to 2% of the total annual energy consumption (MOF/GoN, 2020). Total electricity generation in the Nepal national grid was 1,458 MW (1,299 MW- hydroelectricity, 30.14 MW- solar, 53.4 MW-thermal, 72 MW- alternative energy, and 3 MW from co-generation system) in FY 2020/2021 (MoF, 2021). The per capita electricity consumption of Nepal was

260 KWh in 2021 (MoF, 2021), less than 10% of the world average of 3,132 KWh and 4% and 18% of China and India respectively (World Bank, 2020).

2.4.3 Status of hydroelectricity in Nepal

Hydroelectricity development of Nepal started in 1911 with a 500 KW plant in Pharping near Kathmandu (Dixit, 2002). It was constructed in 1882, ~30 years after the first hydroelectric plant at Fox river in Appleton, Wisconsin, USA. It is interesting to note here that the first hydroelectricity plants constructed in her neighboring countries India and China were in 1889 and 1912, respectively. Historical development of hydroelectricity in Nepal can be broadly divided into three periods; ~1MW in Rana reign, ~225 MW in democratic-panchayat era, and ~1220 MW in democratic-republic era.

At present, total hydroelectricity production in Nepal is around 1,329 MW (excluding alternative energy) as of February-March 2021 (Falgun 2077), of which storage plant contributed 104 MW (DOED, 2020; MoF, 2021). After the People's Movement-II of 2006 that transformed the country's political structure into a federal republic, the Government of Nepal (GoN) has taken new policy and project level initiatives for hydroelectricity development. A task force was formed in December 2008 to formulate programs for developing 10,000 MW in 10 years for overcoming the energy crisis (MoWR, 2009). This task force has provided the list of storage and run-off-river projects with a time-line for development. Similarly, GoN has also proposed a plan of development of 25,000 MW in 20 years in 2009 (MoWR, 2010). The government has announced plans for developing 3,000 MW of hydroelectricity in three years, 5,000 in five years and 15,000 MW in ten years, raising per capita energy consumption from 245 KWh to 700 KWh by 2022 (NEA, 2019). Moreover, roadmap of energy development has been worked out by declaring energy and resource decade from 2075 BS to 2085 BS by the GoN (MoEWRI, 2019). It includes both storage projects: (16, Total Capacity: 9,000 MW) and peaking run-of the river (PRoR) projects (16, Total Capacity: 6,000 MW) (MoWR, 2010).

The total national electricity demand of Nepal in the FY 2020/21 was 8742.30 GWh (peak demand of 1475 MW) which was met cumulatively by different producers – government, the private sector and import (NEA, 2021). Current installed capacity of

the country is 1451 MW (NEA, 2021). On the brighter side, hydroelectricity plants of cumulative installed capacity of 943 MW are under construction.

2.5 Estimation of flow at basin scale

Complex interactions between the atmospheric system and the underlying topography determine the flow of the river. It is a part of rainfall that appears in a stream and represents the total response of a basin. Surface flow, subsurface flow, base flow and precipitation that directly falls on the stream constitutes the total discharge in the river (Chow et al., 1988; Zhang et al., 2018). Historical time series of discharge data is one of the most important requirements for planning, operation and control of all water resources projects (Dobriyal et al., 2017; Loukas and Vasiliades, 2014; Tallaksen, 1995). However, measured flow data are not available in most of the cases in such project sites (Loukas and Vasiliades, 2014). It is because of the lack of sufficient flow gauging stations in most river basins. The situation is more severe in mountainous basins (Shin et al., 2021) because of the inaccessibility of most of these sites for local observations. It is the reason why water budget analyses in such basins are not as easy as in other gauged basins (Alford et al., 2011; Alford and Armstrong, 2010; Hishinuma et al., 2014; Viviroli et al., 2011, 2007). However, most of the large rivers (e.g., the Ganga, the Indus, the Brahmaputra, the Mekong, the Yellow, the Mississippi- Missouri, the Yangtze, the Rio de la Plata, the Yenisei-Angara–Selenga, the Ob-Irtysh, the Amur-Argun, the Danube, the Volga, the Loire, the Rhine and the Elbe River etc,) in the world originate from the mountains and are perennial in nature as they are constantly fed by snow and glaciers. Mountain basins might have, thus, been considered as the water towers of the world (Alford, 1992; Alford et al., 2011; Alford and Armstrong, 2010; Viviroli et al., 2011, 2007).

Although the global scientific community has put substantial efforts to resolve the issue of flow estimation in ungauged basins/sites, a universal solution method is not available till date (Zamoum and Souag-Gamane, 2019). Various methods are found in use in different parts of the world to deal with this issue. One of the oldest methods of generating flow data is the use of regression equation/s developed at the regional level (Samuel et al., 2011; Sharma and Adhikari, 2004; WECS, 1990; Young, 2006). Razavi and Coulibaly (Razavi and Coulibaly, 2016) reviewed regional methods and highlighted that those methods making use of different combinations of physiographic information and meteorological attributes, among others, were found to predict

streamflow in ungagged basins better. They listed catchment area, elevation, slope of basin, rainfall and temperature as the main parameters used in those methods. Another popular method is transposition of gauged streamflow data to ungauged sites. One of them is the drainage area ratio (DAR) method (Emerson et al., 2005; Yilmaz and Onoz, 2020). It is based on the assumption that the streamflow at the ungauged site can be estimated by multiplying the ratio of the drainage area for this site and the drainage area for the gauging site by the streamflow of the gauging site (Emerson et al., 2005). As it needs only catchments areas and the observed streamflow of the gauged station, it is considered one of the easiest methods of flow prediction and therefore popularly used in the past (Yilmaz and Onoz, 2020). One of the variants of the DAR method is MDAR (Multiple gauging stations Drainage Area Ratio). In the MDAR method, the weighted sum of more than one streamflow gauging stations is used to estimate the flow at the site of interest (Ergen and Kentel, 2016). Incorporating the basin rainfall ratio of the ungauged basin to the gauged one as a multiplier to the DAR method has been considered as an improved version of the DAR method (BGHP, 2015; Emerson et al., 2005). This method is called as a general transposition (GT) method.

Hydrological simulation method is a numerical method in which a hydrologic model, a simplified software representation of the natural rainfall-runoff process within a catchment boundary, is used to generate streamflow data at the site of interest with known meteorological data. The hydrological model is first calibrated and validated at a gauged basin and then the model parameters are used appropriately at other ungauged sites within the modeling domain to simulate the flows using the calibrated model (Loukas and Vasiliades, 2014; Wagener et al., 2004). Usually, several statistical indicators as well as visual inspection of the results (hydrographs and the water balance distribution in particular) are relied upon to determine the performance capacity and robustness of the model.

Since the simulation of the entire hydrologic cycle became a reality by Stanford Watershed Model as reported by Crawford and Linsley in 1966 (Crawford and Linsley, 1966), modeling at large spatial scales and at small temporal scales (Singh, 2018) became possible with the recent development in hardware and software capabilities at an exponential rate in the last few decades (Maraseni et al., 2021). Being able to use precise satellite data such as precipitation in hydrological models has further improved the performance and thus the overall applicability of hydrological models considerably

around the globe. In recent years, application of hydrological models is becoming popular in Nepal, for assessment of water availability, planning purposes and to examine the impact of climate change in river hydrology (Bajracharya et al., 2018; Bharati et al., 2019; Devkota and Gyawali, 2015; Devkota et al., 2017; Lamichhane and Shakya, 2019; Pandey et al., 2020a; Shrestha et al., 2016b). However, they are confined mainly to academic research studies. When the world is utilizing artificial intelligence as part of a data-driven approach to assist watershed modeling for stream flow generation (Daniel et al., 2011), most of the project level studies in Nepal are still using coarse conventional methods in ungauged sites in Nepal, especially in the study of hydroelectricity projects of different scales (BGHP, 2015; DOED, 2020, 2018a; NEA and JICA, 2003). As an awakening step, SWAT (Soil and Water Assessment Tool), a public domain hydrological model and capable for hydrological modeling in Nepalese catchments (Bharati et al., 2019; Devkota and Gyawali, 2015; Lamichhane and Shakya, 2019; Pandey et al., 2020c) was used to estimate the flow at ungauged sites in this study and compared with other commonly used methods viz. WECS/DHM 1990, NEA 1997, DHM 2004, DAR and its variant GT methods.

2.6 Hydrological modeling

A hydrological model is defined as a set of empirical equations that helps for the estimation of flow as a combined function of various hydro-climatic and spatial parameters in the river basin. Hydrological models by definition are simplifications of reality and provide a clear understanding of the complex real situations of the watershed (Chow et al., 1988; Refsgaard, 1990; Sharma et al., 2008; Sorooshian and Gupta, 1995). Models are mainly used for predicting system behavior and understanding various components and processes of the hydrological cycle. The perfect hydrological model is the one which gives the close to reality with use of minimum parameters. The parameters of a hydrological model broadly classified into two parameters; physical and process parameter. Physical parameters represent the physical properties of the river basin and are usually measurable, such as the catchment area, shape, surface slope etc. Process parameters represent basin characteristics that cannot normally be measured such as the average depth of water storage capacity, coefficient of nonlinearity controlling discharge rates from component stores, etc.

Hydrological models have become essential and important tools in every hydrological study for quantification of water quality and quantity water in the river basin and are

receiving increasing attention from researcher and policy makers. Hydrological modeling is an attractive option today for solving many practical problems of environmental engineering, flood protection, water resources management, and applied hydrology in general. Modeling includes studying the system, formulating its behavior, collecting and preparing data, building the model, testing it, using it and interpreting the results. It is very important when applying models to keep in mind that there is no perfect hydrological model which we could expect to produce an output that is the same as observed data.

2.6.1 Empirical formula to hydrological model

Hydrological modeling (rainfall-runoff modeling) is a representation of the actual hydrological processes and characteristics of a basin. Runoff (stream flow) is the part of precipitation that appears in a stream and represents the total response of a basin. The total runoff consists of surface flow, subsurface flow, ground water or base flow and the precipitation falling directly on the stream. The streamflow data is the most important data in hydrology as it is required for water budget analysis, planning, operation and control of any water resource infrastructures. A detailed history of hydrological model is given by Beven (Beven, 2001; Todini, 1988). Thomas James Mulvaney (1822-1892), an Irish engineer took initiative to use rainfall-runoff model and published his work in 1851 as the rational method. The rational method can be considered as the first hydrological model (Dooge, 1957; Todini, 1988), which relates peak flow with basin area and rainfall intensity. Until now, it is the most commonly used method for the estimation of peak discharge in the ungauged basin. Green and Ampt (Green and Ampt, 1911) derived a physical based model for infiltration, Hazen (Hazen, 1914) developed frequency analysis of instantaneous flood and water storage requirement, Richard (Richards, 1931) introduced the governing flow for unsaturated flow. The concept of unit hydrograph method to transformed effective unit rainfall to direct runoff was given by Sherman (Sherman, 1932) which became a milestone in the development of hydrological model. Horton developed (Horton, 1945, 1933) infiltration theory and description of drainage basin, and the extreme value laws derived by Gumbel for hydrological studies (Gumbel, 1941). The Stanford model developed at the Stanford University in 1960s is the first digital computer watershed model (Crawford and Linsley, 1966).

During the mid of last century, a number of conceptual and physically-based hydrological models were developed and have been extensively used for simulation of flow in gauge as well as ungauged basin for the quantification of flow. Numerous watershed models have been developed globally after the computer revolution and development of geographical information system (GIS). The high-capacity computer can able to handle the large amount of data made possible to combine different component of hydrological cycle for the quantification of hydrological cycle. HEC 1, developed in 1967 at the Hydrologic Engineering Center (HEC) (Arnold et al., 1998). A number of conceptual and physically-based models have been developed and used for simulation of flow, chemical transport, soil erosion and sediment studies during the last couple of decades for example (Beasley et al., 1980; Beven, 2019, 2001; Beven and Kirkby, 2009, 1976; Feldman, 1981; Huggins, 1966; Knisel, 1980; Odoni and Lane, 2010; Williams and Hann, 1972; Dis et al., 2015; Ross et al., 1977; Tangtham, 1978).

A mathematical model involves variables and parameters; for examples, parameters are assumed constant in the model and variables are quantities which vary in space and time. The various components of the hydrological cycle are represented by appropriate equations which are solved using appropriate computer software (models). Hydrological modeling consists of various steps. Once the objective of the model application has been decided, data availability is checked and a model is conceptualized for a basin. After having selected or developed the code and collected the necessary data, a model is designed giving due consideration to the spatial discretization of the study basin, setting boundary and initial conditions. Input of hydrological and meteorological (temporal) data along with basin characteristics (spatial data) is the subsequent step. Many hydrological models are able to simulate the basin response and generate the long-term hydrology of the river system, quantify water balances and produce flow duration curves (FDCs) at the desired locations.

2.6.2 Classification of hydrological models

Numerous attempts have been made to classify hydrological models (Clarke, 1973; Refsgaard, 1990; Singh, 1995; Singh and Frevert, 2010; Todini, 1988). Broadly, hydrological model are classified as deterministic and stochastic (Chow et al., 1988). A deterministic model is the one which doesn't consider randomness of the process i.e., certain input always produces the same output. A stochastic model has outputs that are at least partially random. The deterministic models give forecasts while stochastic

models make predictions. It is obvious that the, hydrological phenomena involve some randomness. The resulting variability in the output may be relatively small while comparing to the variability of the result from the known factor. In that situation, deterministic model is more suitable. When the random variation is large, stochastic model is appropriate.

In deterministic lump model, the system is spatially averaged and regarded as a single point or region for the simulation of hydrological process without dimension. In contract, a deterministic distributed or semi-distributed model, the system considers the hydrological processes taking at various points in space and defines the model variables as a function of the space dimension. Stochastic models are classified as space independent or space co-related according to whether or not random variables at different points in space influence each other (Chow et al., 1988). The practice of hydrologic modeling in general heavily relies on mathematics and statistics.

Empirical (black box) hydrological models called data-driven models, are the non-linear statistical relationships between inputs and outputs. Principally, they are developed from experiments or observation-oriented and depends on input accuracy (Knightes, 2017; Kokkonen et al., 2001). For simple rainfall-runoff models, inputs are observational time series rainfall and runoff, with outputs of runoff at a specific location; general governing equation for empirical models is a function of inputs. Most empirical models are black box models, does not know about the internal processes that control by what method runoff results are calculated (Beven, 2011; Granata et al., 2016).

Conceptual (gray-box) hydrological models are intermediate to empirical models and physically-based models, and they generally simplified components (consider laws of physics but in quite simplified method) in the overall hydrological cycle or water balance equation that convert the rainfall into runoff, evapotranspiration, and groundwater. It interprets reservoir storages and simplified equations of the physical hydrological process, which provide a conceptual idea of the behaviors in a catchment (Devi et al., 2015; Vaze et al., 2012). Each component in the water balance equation is estimated by mathematical equations that distribute the rainfall as an input data consider physical laws but in high simplified form.

Physical hydrological models, the process-based or mechanistic (white box) models, are based on the understanding of the governing laws of physics related to the hydrological processes (Vaze et al., 2012). Physically based equations govern the model to represent multiple parts of real hydrologic responses in the catchment. The general physical laws and principles e.g., conservation of mass and energy, water balance equations, momentum, kinematics, St. Venant, Boussinesq's, Darcy, Richard's equations etc., are some of the equations adopted by physical models (Pechlivanidis et al., 2011). Similarly, Wheater (1993) classified hydrological models based on their structure, degree of distribution of processes, stochasticity, and spatial-temporal variation. The classification of hydrological model is presented in Figure 2.1.

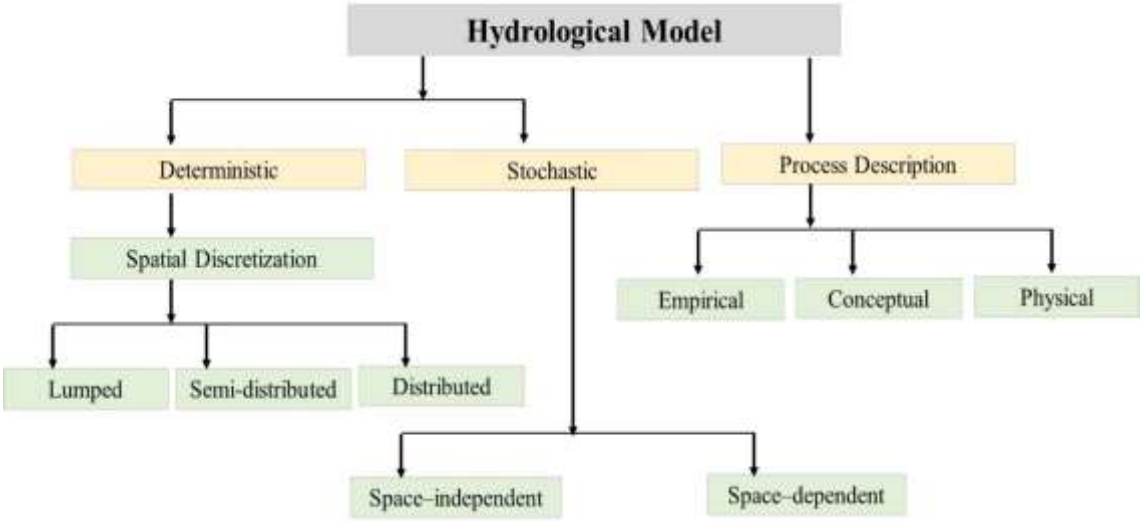

Figure 2.1: Classification of hydrological models [modified from Chow (1988)]

2.6.3 Global use of hydrological model

To address the challenge of unavailability of observed historical data at local level for water resources planning and utilization in the river basin, hydrologic simulation method has been widely used (Bierkens, 2015; Coron et al., 2012; Jiang et al., 2007; Refsgaard, 1997; Sood and Smakhtin, 2015). Simulation models provide excellent platforms for evaluating various options for water resources as well as environmental planning (Abbaspour et al., 2015). In hydrological simulation, a hydrologic model is used to generate the flow at required locations of the river basin.

Hydrological modeling has become essential in water resources research and management from small watersheds to large basins. Hydrological models help understand the past and current state of water resources in the study basin and provide

a way to explore the implications of management decisions and biophysical changes (Johnston and Smakhtin, 2014). Universities, academic institutions, research centers and consultants have developed a number of hydrological models all across the globe with specific objectives, capabilities and use. Some models are designed to look at only hydrology of a catchment whereas some have additional capabilities such as agricultural modeling, water management and energy generation, among others. Some of widely used hydrological models are; Hydrologiska Byråns Vattenbalansavdelning (HBV), GR4J (Génie Rural à four paramètres Journalier), hydrological model (HYMOD), artificial neural network (ANN) based data-driven hydrological models, simplified version of the HYDROLOG (SIMHYD), Snowmelt Runoff Model (SRM), Sacramento Soil Moisture Accounting (SAC-SMA), and TANK are lumped models while the Soil and Water Assessment Tool (SWAT), topographic hydrologic model (TOPMODEL), Variable Infiltration Capacity (VIC) and Hydrologic Engineering Center—Hydrologic Modeling System (HEC-HMS), Xinanjiang Model are semi distributed ones. Variant of Système Hydrologique Européen (MIKE SHE) and Visualizing Ecosystem Land Management Assessments (VELMA) are fully distributed models. These are either event-based (e.g., Runoff Analysis and Fow Training, RAFT) or continuous (e.g., MIKE SHE, SWAT) flow generating models.

2.7 SWAT model and its application

Recent studies on hydrological simulation by SWAT can be broadly classified into four categories; First, simulation for quantification of water (Gomes et al., 2021; Guevara-Ochoa et al., 2020; Rafee et al., 2019; Ridwansyah et al., 2019); second, sediment and land used land cover (dos Santos et al., 2017; Hosseini and Khaleghi, 2020; Ma et al., 2020; Martínez-Salvador et al., 2021; Theron et al., 2021); third sediment, water quality land use and land cover in the context of climate change (Abbaspour et al., 2015; Joorabian Shooshtari et al., 2021; Qi et al., 2020; Vilaysane et al., 2015). Fourth categories fall in hydrological extremes (Chen and Chang, 2021; Devkota and Gyawali, 2015; Khadka et al., 2014; Shrestha et al., 2016a) are some examples how SWAT is used for the different purposes. To address the challenge of non-availability of observed data at local level for water resources planning and utilization in the river basin, hydrologic simulation method has been widely used in recent years (Marahatta et al., 2021c; WMO, 1989; Jain 2017, Woolridge 2018, Meng 2020). Simulation models provide excellent platforms for evaluating various options for water resources as well

as environmental planning (Abbaspour et al., 2015). In hydrological simulation, a hydrologic model which is a simplified software representation of the hydrological process within a basin boundary, is used to generate the flow at required locations of the river basin.

With nearly 5000 publications, the SWAT is clearly one of the most extensively used ecohydrological models worldwide. The model has been widely used for projecting impacts of future hydro-climatic changes and its capabilities for application in different size of the catchment, climates and spatial variation globally (Abbaspour et al., 2015; Akoko et al., 2021; Bui et al., 2020; Chen et al., 2020; Marin et al., 2020; Priya and Manjula, 2020; Samimi et al., 2020; Tan et al., 2021a, 2020; Wang et al., 2019). Besides, it is widely used to study many issues such as flow simulation, erosion and sediment study, land use and land cover change, climate change and water quality in the six continents.

SWAT has been extensively used in large river basins, for example; The Upper Paraná river basin 900,480 km^2; Danube river basin, covering approximately 800,000 km^2; Tocantins-Araguaia Watershed 764,000 km^2, Upper Mississippi river basin 491,700 km^2; Upper Mississippi river basin area of 431,000 km^2; Mekong river drains an area of 795,000 km^2 (Chen et al., 2020; de Oliveira Serrão et al., 2020; Li and Fang, 2021; Malagó et al., 2017; Ngo et al., 2018; Rafee et al., 2019)**.**

Similarly, SWAT is used to simulate the regional scale basin, for example; southern part of Africa, Major river basin includes Orange, Limpopo, Maputo, Buzi, Save, Olifants and Groot., 2,179,400 km^2 (Chawanda et al., 2020), four watersheds in southern Saskatchewan vary between 3,900 and 17,800 km^2 (Zare et al., 2022); 14 studied basins in the Peruvian Pacific drainage (Asurza-Véliz and Lavado-Casimiro, 2020)*;* six basins at the border region between Ecuador and Peru, with areas that vary between 200 and 2642 km^2 (Oñate-Valdivieso et al., 2016); Andes, Alps, and Central Asia (Omani et al., 2017); It is also used in 36 continental scale river basins of Europe including Russia 3,669,247 km^2 (Abbaspour et al., 2015); Three, Altai Mountain, Tianshan Mountain, and Kunlun Mountain of Xinjiang (Meng et al., 2020); and 18 major Indian sub-continental basins were selected for climate change impact assessment and sensitivity analysis including Ganga-Brahmaputra-Meghna basin with area 1,100,000 km^2 (Mishra and Lilhare, 2016).

In addition to large river basin, SWAT is also widely used in micro catchments. For instance, the Lake Kyoga basin and covering an area of 31.1 km^2, Uganda (Gabiri et al., 2020); Damma glacier watershed 10 km^2, Switzerland (Andrianaki et al., 2019); The Odderbæk catchment is located in northern Denmark. The catchment has an area of 11 km^2, Black Brook Watershed about 14.5 km^2, (Qi et al., 2016); Hiso River watershed, which is located in the upper Hiso, with an area of 426 ha, Fukushima, Japan (Peng et al., 2021); A micro-watershed covering an area of 0.38 km^2, Cunha Municipality, Sao Paulo State, Brazil (Lucas-Borja et al., 2020). Rio San Giorgio basin 3082 ha, West Mediterranean Sea (Marras et al., 2021). The Heeia watershed (11.5 km^2) is located in the north-east, windward part of Oahu Island, Hawaii (Leta et al., 2016); The Pago Watershed 23.41 km^2 is located in the east of central Guam (East Pacific) (Yeo et al., 2021).

Moreover, Omani et al. (2017) used SWAT model to simulate five glacierized mountain river basins of the world that includes the Narayani (Nepal), Vakhsh (Central Asia), Rhone (Switzerland), Mendoza (Central Andes, Argentina), and Chile (Central Dry Andes, Chile). Furthermore, Damma glacier watershed in Canada (Andrianaki et al., 2019), and 46 small to medium-size catchments in Xinjiang, an arid region China watershed of the three mountains, Altai Mountain, Tianshan Mountain, and Kunlun Mountain (Meng et al., 2020). Shrestha et al. (2018) has evaluated the hydrological responses of SWAT models for 11 basins in two contrasting climatic regions (Himalayan and Tropical) of Asia. The Heihe river basin in Northwest China (Ruan et al., 2017) are some examples of snow dominated high altitude catchment where the SWAT was used to simulate the flow.

Studies in African Basins e.g., Oum Er Rbia and Souss Basin (Morocco), Mangoky basin (Madagascar), Blue Nile basin (East Africa) and Tsitsa basin of South Africa (Milewski et al., 2020; Tanteliniaina et al., 2021; Tehsome et al., 2021; Theron et al., 2021). Asian basin e.g., Upper Mekong basin (south-west China), Budhigandaki (Tibet-Nepal); Baitarni basin (India), Hailar basin (Inner Mongolia, China), Lhasa basin (Tibet) China (Ma et al., 2020; Marahatta et al., 2021a; Padhiary et al., 2020; Yan et al., 2020; Yasir et al., 2021). Australia and Oceania basin (Kundu et al., 2017; Leta et al., 2016; Marhaento et al., 2017; Tan et al., 2021b) in Murray- Darling basin (Australia), Heeia basin (Hawaii), Sami basin (Java), Kelantan basin (Malaysia). Europe (Marcinkowski and Mirosław-Świątek, 2020; Nguyen et al., 2018) Upper

Narew basin (Poland) and Lower Saxony and North Rhine-Westphalia basin (Germany). Middle east, Italy and Mediterranean basin (Hajihosseini et al., 2020; Marras et al., 2021; Peker and Sorman, 2021) Helmand basin, a transboundary in (Iran - Afghanistan), Rio San Giorgio and Rio Mannu di Fluminimaggiore basins Sardinia Island (Italy) and Murat and Karasu basins (Turkey). Black and Northeast Cape Fear basins (NC-USA), and Upper Assiniboine (Canada) of North America (Mapes and Pricope, 2020; Muhammad et al., 2020). South American basins (de Oliveira Fagundes et al., 2020; Havrylenko et al., 2016) Itapemirim River basin (Brazil) and Arrecifes basin (Argentina). Their result in all six continents reveals that SWAT is a suitable tool for modelling hydrological responses in all hydroclimatic and geographical region globally.

Recent studies on hydrological simulation by SWAT can be broadly classified into four categories; First, simulation for quantification of water (Gomes et al., 2021; Guevara-Ochoa et al., 2020; Rafee et al., 2019; Ridwansyah et al., 2019); second, sediment and land use land cover (dos Santos et al., 2017; Hosseini and Khaleghi, 2020; Ma et al., 2020; Martínez-Salvador et al., 2021; Theron et al., 2021); third sediment, water quality land use land cover in climate change context (Abbaspour et al., 2015; Joorabian Shooshtari et al., 2021; Qi et al., 2020; Vilaysane et al., 2015). Fourth category covers hydrological extremes (Chen and Chang, 2021; Devkota and Gyawali, 2015; Khadka et al., 2014; Shrestha et al., 2016a) are some examples how SWAT is used for the different purposes.

2.8 Commonly used hydrological models in the Nepalese river basins

Different hydrological models have been used in Nepalese basins by various researchers and practitioners, consultants and academia. Use and objective of the models vary which also depends on the cost of data and model, data availability and the nature of analysis. Mostly open-source hydrological models are used in Nepal. Sometimes the models are proposed by the donors or project partners who are somehow involved in the model development too. Since data availability is a major issue for Nepal, data intensive models are less preferred over those requiring less data. The hydrological models most popularly used in Nepal are HEC-HMS (Babel et al., 2013; Gautam 2015; Shrestha et al., 2014), BTOPMC (Bastola et al., 2008; Manandhar et al., 2013), snow and glacier models (Bhattarai et al., 2020; Bocchiola et al., 2020b, 2020a; Gupta et al., 2019; Kayastha et al., 2020; Khadka et al., 2014, 2020; Mimeau et al.,

2019; Pokhrel et al., 2014; Shea et al., 2015; Soncini et al., 2016; Thapa et al., 2021), J2000 and GR4J (Eeckman et al., 2019; Nepal, 2016; Nepal et al., 2017), other models ANN (Sharma et al., 2015), WED-DHM (Shrestha et al., 2012), GRFM (Magaju et al., 2020), GeoSFM (Bajracharya et al., 2017) and HBV (Bhattarai et al., 2018; Kong et al., 2021). Recently SWAT (Bajracharya et al., 2018; Bharati et al., 2019; Bhatta et al., 2020, 2019; Budhathoki et al., 2021; Chinnasamy and Sood, 2020; Dahal et al., 2020, 2016; Devkota and Gyawali, 2015; Dhami et al., 2018; Kaini et al., 2020; Kaushal et al., 2020; Lamichhane and Shakya, 2019; Maharjan et al., 2021; Marahatta et al., 2021a; Mishra et al., 2021; Mishra et al., 2018; Palazzoli et al., 2014; Pandey et al., 2020a, 2019; Shrestha et al., 2021, 2017; Shrestha et al., 2020; S. Shrestha et al., 2020) has also started gaining popularity among researchers. These studies suggest, the SWAT model can be used for assessing the water balance by the establishment of model and impacts of climate change, land use land cover changes, and soil erosion both in snow fed basins along with rainfed middle Mountain and Siwalik basins.

2.8.1 Calibration and validation

Hydrological models are developed with several model parameters, which are adjusted by the modeler during the calibration process based on his/her experience by the software or a combination of two. When the calibrated model predicts the data reasonably as suggested by literatures, it may be considered as satisfactorily simulated (Moriasi et al., 2015). Precipitation, surface runoff and sub-surface runoff, evapotranspiration, and infiltration are major components in the hydrological process in the hydrological cycle among them, precipitation and evapotranspiration are the two major components. Due to the limited meteorological stations in river basins in Nepal, scarcity of observed relative humidity, wind speed and solar radiation, the estimation of potential-evapotranspiration is rather complicated.

2.8.2 Evaluation of SWAT model

For the statistical evaluation of the hydrological model, different objective functions; e.g., Nash-Sutcliff efficiency (NSE), percent bias (PBIAS), Kling–Gupta efficiency (KGE), correlation coefficient (R^2), mean square error (MRE) and the ratio of root mean square error to standard deviation (RSR), are generally used. Besides, P-factor and R-factor are also used to evaluate model performances. There are no any specific rules regarding the statistical evaluation of the hydrological models. SWAT model is no

exception on these issues. While evaluating the SWAT model, most studies have used three objective functions (Getachew et al., 2021; Grusson et al., 2021; Martínez-Retureta et al., 2021; Peng et al., 2021; Rafiei et al., 2020; Tanteliniaina et al., 2021; Villamizar et al., 2019; Yasir et al., 2021). Some of the published works rely on only two objective functions to evaluate the performance e.g., (Akoko et al., 2020; Andrianaki et al., 2019; Aznarez et al., 2021; Hajihosseini et al., 2020; Momiyama et al., 2020; Thiha et al., 2021). However very few researcher used only one objective function for examples (Ma et al., 2020; Malagó et al., 2017; Marcinkowski and Mirosław-Świątek, 2020; Meng et al., 2020). Additionally, plenty of researcher used four or more objective functions (Aboelnour et al., 2020; Fagundes et al., 2021; Gabiri et al., 2020; Havrylenko et al., 2016; Kiprotich et al., 2021; Marhaento et al., 2017; Negewo and Sarma, 2021; Orlińska-Wozniak et al., 2020; Pulighe et al., 2021; Rafee et al., 2019; Shelton, 2021) to evaluate the model performance. It is interesting to note that Touseef (Touseef et al., 2020) used five objective functions (NSE, R^2, PBIAS, KGE and RSR) to evaluate the SWAT model in Upper Xijiang river basin, a tributaries of Pearl river basin, south China.

There is no consensus for choosing the periods (time steps) for calibration and validation in the literature in SWAT. Simulation by Abbaspour et al. (2015) in rivers of Europe, Liu in watersheds of Nevada mountains (USA) (Liu et al., 2021); Genale Dawa basin in Ethiopia (Negewo and Sarma, 2021); Budhigandaki basin in Sino-Nepal (Marahatta et al., 2021a) etc. follow the two-thirds (calibration) and one-thirds (validation) period. Most of the simulation was carried out in monthly time steps with period over > 20 years (Asurza-Véliz and Lavado-Casimiro, 2020; dos Santos et al., 2017; Getachew et al., 2021; Grusson et al., 2021; Martínez-Retureta et al., 2021; Martínez-Salvador et al., 2021; Orlińska-Wozniak et al., 2020; Padhiary et al., 2020; Pandey et al., 2021; 2021; Rafee et al., 2019; Tan et al., 2021a; Thiha et al., 2021). The studies having daily time steps with significant period (> 20 years) includes (Li and DeLiberty, 2020; Milewski et al., 2020; Moazami Goudarzi et al., 2020; Naderi, 2020; Petpongpan et al., 2021; Shah et al., 2020; Shukla et al., 2021). However, some simulations rely on one year each for calibration/validation periods, e.g.; Lake Kyoga basin in Uganda (Gabiri et al., 2020) and Cimandiri catchment of Java Indonesia (Ridwansyah et al., 2020). Rafiei et al. (2020) carried out calibration/validation period consists of six years (five normal years and one extreme dry/wet year each) in daily

time steps. While, Troin et al. (2012) considered 20 years as calibration period (ten each dry and wet) and nine years taken as validation period in monthly time scale.

2.9 Climate Change

Climate change has become a burning issue in international as well as national development forums. Evidences of increase/decrease in the river discharge due to climate change have been seen globally and at different regional and local scales due to increase in temperature and change is precipitation pattern (Khanal et al., 2021; MoFE, 2019). Himalayan region may have significant changes in precipitation, temperature as well as glacier retreat, functional changes in wetlands, increased flow variability as well as change in flow timings and amounts affecting rural livelihoods, agriculture and overall economy due to CC. Water resource is the most vulnerable sector which will have large impacts due to CC; when the river is snowfed, the impacts are even more pronounced.

2.9.1 Historical and future climatic trends

Climate change has become a major challenge and threat to the planet particularly, after World War II. Although, alteration in the Earth's climate has been going on forever, we have started acknowledging its impacts on humans and the current environment only in the second half of the twentieth century (Le Treut et al., 2005). The first world conference on environment held in Stockholm in June 1972 (United Nations, 1973) formally opened doors for a dialogue between industrialized and developing countries on the link between economic growth, pollution of the air, water, and oceans and the well-being of people around the world. Moreover, formation of the United Nations Environment Programme (UNEP) is one of the major achievements of the Stockholm conference. The UN World Meteorological Organization (WMO) and UNEP established the Intergovernmental Panel on Climate Change (IPCC) with the objective of conducting and disseminating findings of scientific research on CC in 1988 (Houghton, 1996). The Second Earth Summit organized by the UN in Rio de Janeiro, Brazil, in June 1992 formed a mechanism for cooperation between states, sectors and people on issues related to environmental protection and sustainable economic development (United Nations, 1992). Further, in 1997, the Kyoto Protocol set the first GHG emission reduction targets for industrialized nations. In this regard, a total of 192 nations of the world committed to reducing their emissions by an average of 5.2% by

2012 which is popularly referred to as Kyoto Protocol (United Nations, 1998). United Nations Climate Change Conference held in December 2009 documented that CC is one of the greatest challenges of the present day and prescribed that actions be taken to keep temperature increases to below 2°C (UNFCCC, 2010).

The 2015 Paris Conference of Parties (COP) 21, a global consensus, established that the average global warming needs to be kept below 1.5 to 2°C to avoid the irreversible threat to environmental, economic, social and political challenges by CC for years and decades to come (UNFCCC, 2016). IPCC reports all currently available global climate models (GCMs) agree on an increase in global mean temperature over the twenty-first century. The latest assessment report by IPCC (AR6) has recommended to limit global warming to 1.5°C above pre-industrial levels and related global greenhouse gas emission pathways in order to significantly reduce the risks and impacts of CC. COP 26 in November 2021 at Glasgow take a major step to address the climate crisis including a material increase in ambitions to reduce greenhouse emissions across the world. However, COP26 fell to deliver the national commitments that would together limit warming globally to 1.5°C. Furthermore, COP 26 finalised the rules on reporting emissions and international carbon trading, and the launch of a range of new initiatives and sector deals.

2.9.2 Historical and future climatic trends in Nepal

A gradual increase in maximum temperature is evident from both global and regional records. Shrestha et al. (Shrestha et al., 1999) showed that the average annual temperature is estimated to have increased by 0.04 to 0.06°C from 1977 to 1994. The warming is more pronounced in the higher altitude regions of Nepal such as middle-mountain and Himalayas, while the warming is lower or even lacking in Terai and Siwalik regions. Further, warming in the winter is more pronounced compared to other seasons. Analysis of (Shrestha et al., 1999) was extended with more recent data and was found that the warming trend is still continuing and the rate of warming has not decreased. The widespread warming in the country thus is in agreement with projections made by climate models. An increasing trend in temperature was found in Nepal (Marahatta et al., 2009). The maximum temperature increased at a greater rate (0.05ºC/year) than the minimum temperature (0.03ºC/year). A decreasing trend was found in the maximum temperature in the Terai region during the winter season. Positive trends are observed in annual (0.056ºC/year) and seasonal maximum

temperatures. The annual minimum temperature trend is also positive (0.002^{o}C/year), minimum temperature shows insignificantly positive trend only in monsoon season. However, no significant trend is observed in precipitation in any season (DHM, 2017). The average annual temperature and precipitation in Nepal might increase by 1.7 to 3.6^{0} C and 11 to 23% respectively, until the end of this century. The highest (lowest) rates of mean temperature increase by 1.8 to 2.4^{0} C (1.5 to 2.0^{0} C) are expected for the post-monsoon (winter) season. The post-monsoon season is expected to have the highest increase of 6 to 19% in precipitation by in the medium-term and about 20% in the long-term. However, it is likely to decrease in the medium-term period in pre-monsoon season nearly by 5% (MoFE, 2019).

2.10 Impacts of climate change in river hydrology

Studies have analyzed the impacts that CC could possibly have on river flows at the global (Hamududu and Killingtveit, 2016; Turner et al., 2017a, 2017b; Vliet et al., 2016), regional (Ali et al., 2018; Liu et al., 2016; Meng et al., 2021) and local (Bhatta et al., 2020; Marahatta et al., 2021d; Shrestha et al., 2021) scales. Most of these studies use global climate models (GCMs)/ regional climate models (RCMs) in hydrological models for making the assessments. It is found that snow dominated areas such as the Arctic (Russia, Scandinavian-Baltic countries, Canada, and parts of the US) and the Hindu Kush Himalayas; Caribbean countries; South-Central and North China and Central-West Africa show significant increase in runoff historically as well as in the future projections (Arriagada et al., 2019; Caceres et al., 2021; de Jong et al., 2021; Hasan and Wyseure, 2018). On the contrary, Asia Pacific, Australia including Oceania, Africa, South America, Europe (Balkan, Mediterranean, Alpine) and the Middle East have shown evidence of rapid decrease in runoff in the past, a trend which is expected to continue in the future (Bahadori et al., 2013; Caceres et al., 2021; de Oliveira et al., 2017; Fan et al., 2020; Mutezo and Mulopo, 2021; Mutsindikwa et al., 2020; Poletti and Staffell, 2021; Tobin et al., 2018; Uamusse et al., 2017).

2.11 Climatic models

General circulation models (GCMs) and regional climate models (RCMs) are the numerical models that represent physical processes in the atmosphere, ocean, cryosphere and land surface. These are the most advanced tools currently available for simulating the response of the global climate system to increasing greenhouse gas

concentrations. G/RCMs depict the climate using a three-dimensional grid over the globe, typically having a horizontal resolution of between 250 and 600 km, 10 to 20 vertical layers in the atmosphere and sometimes as many as 30 layers in the oceans. There are many G/RCMs available from different climate modeling institutions, selection of suitable G/RCMs depends on its availability as well as applicability for the study.

2.11.1 Types of climate model

The G/RCMs have been found to be effective tools in developing a better understanding of CC by predicting climate projections (Robock et al., 1993; Tapiador et al., 2020). Scientists of Geophysical Fluid Dynamics Laboratory (GFDL), National Oceanic and Atmospheric Administration (NOAA) developed the first coupled ocean-atmosphere GCM in the 1960s capable of simulating temperature and precipitation of the past 50 years (Edwards, 2011; Oceanic et al., 2006). Following GFDL, many other researches across the world have developed different climate models. For example, Hadley Centre Global Environment Model (HadGEM) (Collins et al., 2011), Canadian Earth System Model (CanESM) (Chylek et al., 2011) and Max Plank Institute for Meteorology (MPI) (Mauritsen et al., 2019) are some notable GCMs while Seoul National University Regional Climate Model (SNURCM) (Lee and Cha, 2020), Max Plank Institute for Meteorology - REMO2009 (Müller et al., 2018), Conformal Cubic Atmospheric Model (CCAM) (Thatcher et al., 2015) are popular RCMs. G/RCMs cannot represent many processes leading to precipitation occurring at a resolution smaller than the grid size, thus, downscaling based on the desired region is necessary to improve the quality of G/RCMs output to represent the local climatic condition.

2.11.2 Scenarios in climate change studies

A set of four Representative Concentration Pathways (RCPs) has been recognized in the fifth Assessment Report (AR5) by IPCC. Each of these pathways represent a bigger set of scenarios described in scientific literatures, hence named ‘representative’, and is a plausible and inherently consistent description of the future. Greenhouse gases concentrations are used in RCPs rather than ‘emission’ serving as input to climate models. Four RCPs lead to different radiative forcing levels of 8.5, 6.0, 4.5 and 2.0 W/m^2 by the end of this century (2100) and are hence named accordingly. Among these RCPs, RCP 2.6 scenario represent mitigation scenario leading to very low forcing level

with drastic changes in technologies. Besides, RCP 8.5 scenario represent very high emission scenarios. Whereas RCP 4.5 and RCP 6.0 scenarios are stabilization scenarios in which total radiative forcing is stabilized shortly after 2100 (Vuuren et al., 2011). Numerous studies in Nepal including (MoFE, 2019) used RCP 4.5 scenario, a stabilization scenario, and RCP 8.5 scenario, high emission scenario.

2.11.3 Bias correction methods

Climatic data generated from GCM models are used to force hydrological models in water resources study. These data provide valuable input to understand the possible future behavior of water resources system which is often used in decision making for water resources management at local or basin levels. However, direct application of GCM data is not carried out. It is because of the following reasons: (a) GCM models have inherent systematic biases which can be due to models' representation of physical processes and their parameterization, initializations or some modelers input, and (b) They are often incompatible in scale (because of coarser scale) that are necessary for hydrological impact studies because they lack regional or local climate information since they are focused on global scale climate (Themeßl et al., 2012). In order to apply GCM models at local scale, it needs to be made compatible at local or regional scale essentially by addressing bias they possess. When GCM model simulation of past climate is compared with observed climate, there is inconsistency. GCM model show bias in simulating past observed climate.

Different methods for bias correction for climate variables like precipitation and temperature are discussed in different literatures that ranges from simple correction in the annual or monthly mean values to complex distribution fitting that corrects entire distribution. Further, Hawkins et al. (2013) used delta approach / change factor approach in crop modelling in Europe that that are simple and popular methods that basically corrects the mean (and variance) of the distribution. Likewise, Schmidli et al. (2006) used local intensity scaling (LOCI) approach for downscaled the precipitation by using ratio of wet-day intensities between observations and the GCM with the adjusted wet-day threshold for GCM precipitation. Lenderink et al. (2007) applied linear scaling approach to estimating future discharges of Rhine River by ratio of long-term averages of observations to long-term average of control run for each 36 intervals (10-day average precipitation). Further, tool for bias correction is power transformation method for precipitation applied in various studies (Leander and Buishand, 2007;

Terink et al., 2021) corrects mean and variance of the precipitation distribution. In addition, the approach that not only corrects the mean and variance but also the whole distribution, called as Distribution mapping or quantile mapping (Maraun, 2016; Maraun and Widmann, 2018; Piani et al., 2010a; Teutschbein and Seibert, 2013) is also widely used. Furthermore, in the case of temperature, the method describe by Hawkins et al. (2013) has been widely used for bias correction.

2.12 Energy

Energy is important for economic activities and development. Sustainable economic growth is the main strategy for almost all countries around the world to achieve mainly through energy consumption (Fan et al., 2020). It increases consumption of energy, particularly commercial renewal energy like electricity, and promotes economic growth of a country (Ghosh, 2002). Due to the high demand of energy for the growing population and development in technologies, fossil fuels, a principal energy source, are rapidly depleting (Bilgili et al., 2018). Such huge exploitation of fossil fuel to fulfil the growing energy requirement is resulting in massive emissions of CO_2 and other greenhouse gases (GHGs) in the atmosphere and continually increasing since the beginning of the industrial revolution.

Traditional energy sources along with the human labor and draught transport were replaced, initially by coal and then by oil in the early 1900s for powering machines and transportation (O'Connor and Cleveland, 2014; Wrigley, 2013). Access to such cheaper fossil fuels has been a major milestone for modern development pathways (UNDP, 2020). Since the beginning of the industrial age, the ability to harness and use of different forms of energy has led to rapid global economic growth; increase in production and consumption which enabled people to perform increasingly productive tasks as well as improve the living standards of billions of people (Mohajan, 2019; Stern, 2012). However, scientific evidences indicate that huge emission of CO_2 and other GHGs in the atmosphere is associated with the increasing use of fossil fuel (IPCC, 2015; Yoro and Daramola, 2020). The industrial revolution era can, thus, be taken as the starting point of CC as the scientific community has defined it today (Stern et al., 2006a). With the widespread use of fossil fuel and human interventions after the first industrial revolution, global warming has emerged as an environmental issue that has brought the world attention (Le Treut et al., 2005).

2.12.1 Global share of total energy

The combustion of fossil fuel to generate energy in the globe ranges from 97 TWh in 1800 to 136,761 TWh in 2019 is the primary driver of global warming. The International Energy Agency's (IEA) World Energy Outlook estimates an increase of about 50% in the global energy-related CO_2 emissions by 2030. The Intergovernmental Panel on Climate Change (IPCC) has stated that emissions from fossil fuels are the dominant cause of global warming. Globally, the two biggest sectors that contribute to climate change are electricity generation (~25%) and food & land use (~24%). The share of electricity production of hydroelectricity is 17% (Fan et al., 2020; BP, 2020; Chen et al., 2017; Meng et al., 2017) in the global scale however, it varied significantly between countries. Magnitudes of GHG and CO_2 emission is directly proportional to the non-renewable energy consumption while inversely related to renewable energy consumption (Salari et al., 2021). IPCC has found that emissions from non-renewable energy sources are the dominant cause of global warming and climate change.

The developing countries are facing contradictions between limiting global warming below 1.5^{o}C (UNFCCC, 2016) and achieving economic growth. It is noted here that, without consumption of large amounts of energy, economic growth of the developing country would not be possible (Vanegas Cantarero, 2020). As a result, the entire world is facing severe environmental consequences, the severity being the most in under-developed countries which are the least capable of withstanding the impacts of climate change. There is a global unanimous agreement on the concept of transition from the current non-renewable energy production mix to renewable energy dominated mix.

2.13 Energy transition

There is a global consensus on the urgent need of transition from the current non-renewable energy production mix to renewable energy dominated mix. As a result, switching towards green energy, such as hydroelectricity, wind, solar, geothermal and wave has recently received global attention (Bogdanov et al., 2021; Davis et al., 2020; Dietzenbacher et al., 2020; Liao et al., 2021). Among the identified renewable sources of clean energy, hydroelectricity is over a century old, tested and well-proven technology with significant developments in its planning, design of hydraulic structures, electro-mechanical components as well as distribution systems. Likewise, studies have also focused on methane emissions, sediment and overall water

environment of reservoirs and dams of hydroelectricity project (Janssen et al., 2021; Li et al., 2018; Liu et al., 2020, 2019).

Hydroelectricity is one of the major contributors of electricity, with about 17% share in the total world's electricity generation (IEA, 2020, 2019; Y. Meng et al., 2020). The contribution of hydro-energy is found to be substantial in countries with a relatively smaller energy demand and high-water availability. However, it varies significantly across countries. The IEA reported that the share of hydroelectricity in the gross national supply of electricity is 100% in Albania, 99% in Congo, 97% in Mozambique, Paraguay and Uruguay, 92% in Iceland, 90% in Nepal and 66% in Venezuela (IEA, 2020). On the contrary, high energy consuming countries have a relatively smaller contribution of hydroelectricity in the current electricity supply. For example, hydroelectricity contributes, 1232 TWh (17.2%) in China, 317 TWh (7.1%) in USA, 193 TWh (17.3%) in Russia, 151 TWh (9.6%) in India, 88 TWh (8.4%) in Japan and 71 TWh (12.1 %) in France. Some exceptions of high energy consuming countries with a high share of hydro-electricity contribution in the total electricity supply are Brazil 389 TWh (64.7%), Canada 386 TWh (59%), and Norway 140 TWh (95%), etc. (IEA, 2020; Martins et al., 2018; Tomczyk and Wiatkowski, 2020). Best (Best, 2017) makes an interesting comparison showing that the capital cost of a hydroelectricity project is about 4.0 million USD per MW which is only slightly more expensive than a coal plant, two-thirds of a nuclear or geothermal plant and one-fourth of the cost of a solar power plant. However, Awojobi and Jenkins (2015) and Baurzhan et al. (2021) both compare the unit cost (MW) of hydroelectricity projects of the 2010 prices value; Asia (1.4 and 1.9) while the world average (2.4 and 1.8) million USD respectively.

The rapid reduction in the cost of renewable energy like solar and wind energy has led to these resources being the future of energy systems across the world. In addition, these clean energy sources offer pathway to reduce the impacts of CC, particularly to meet the Paris Agreement target of keeping the global temperature rise within 1.5 to 2^{o}C of the pre-industrial period by the end of this century. The countries in the region, including Nepal, India, China and the rest, have plans of adding substantial solar, wind and other renewal energy sources to meet its energy and power demand. Nepal is however unique as it still has a huge potential for development of its hydroelectricity. Hence, it is imperative that Nepal's hydroelectricity development is able to compete and support the energy and power systems of the future both nationally and regionally.

2.13.1 Global share of renewable energy

Among the identified renewable sources of energy, hydroelectricity is one of the major contributors of energy production, especially in countries with a relatively smaller energy demand. The International Energy Agency (IEA) reports that the share of hydroelectricity in the gross supply of electricity represented Albania (100%), Congo, Paraguay, Uruguay (99%), Brazil and Iceland (82%), Venezuela (66%) (IEA, 2020). Exception - high energy consuming countries (e.g. Norway (100%), Canada (58%) according to data for 2019 (Tomczyk and Wiatkowski, 2020) to fulfil their energy demand to achieve their economic growth. Climate change is one of the major factors that influence river hydrology which ultimately affect the energy generation from hydroelectricity projects.

2.13.2 Hydroelectric energy

Production of hydroelectricity is a function of flow and head. The capacity of a power plant depends on the river discharge in RoR types of projects. In a storage hydroelectricity plant, the power generation is based on the reservoir volume, inflow characteristics and purpose of its use, such as if a plant is operated for generating electricity to meet the daily demand or to meet peak hours' demand (Liu et al., 2016). Whatever the cases, river hydrology plays an important role in hydroelectricity generation. Time series of flow data is one of the most important requirements for planning, operation and control of all hydroelectric projects (Dobriyal et al., 2017; Loukas and Vasiliades, 2014). However, measured flow data are not available in most of the rivers listed as potential project sites (Loukas and Vasiliades, 2014). It is because of the lack of sufficient flow gauging stations in most river basins. The situation is more severe in mountainous basins because of the inaccessibility of most of these sites for local observations. It is the reason why water budget analyses in such basins are not as easy as in gauged basins. For such situation, hydrological simulation is an essential tool to understand the hydrological process of the basin under the various climate input and land management (Meng et al., 2020).

2.13.3 Impact of climate change on hydroelectricity

A preliminary review of available literature indicates that a significant number of studies have been conducted for the quantitative assessments of impact on hydroelectricity due to CC through different systems at various geographical scales

such as global scale. Several studies have been carried out to assess the change in energy due to impact of CC for both RoR and reservoir projects in the global scale based on 1593 large hydropower dams in more than one hundred countries. Their results reveals both loss/gain in energy simulated globally and at different regional and local scales directly affect the energy due to increase/decrease in the river discharge from climate change (Turner, Hejazi, et al., 2017; Turner, Ng, et al., 2017), Rio Jubones Basin of Ecuador by (Mehedi and Wyseure, 2018). The different hydroelectricity projects including Mattmark hydropower system is located in Visp river basin in Switzerland (Anghileri, 2018), River basins of Sumatra island in Indonesia (Meng et al., 2017), Toce basin of Italy (Ravazzani et al., 2016), Zambezi river basin in South Central Africa (Hamududu & Killingtveit, 2016), Guadalquivir river basin of Spain (Solaun and Cerdá, 2017), Shire Lake river basin, Malawi (Mtilatila et al., 2020), selected seven reservoir projects in India (Ali and Mishra, 2020), hydropower stations located in Lusatian Neisse river basins in south-west Poland at the Polish–German–Czech border (Adynkiewicz-piragas, 2020); Kaoping river basin in Taiwan (Chiang et al., 2013), Denawaka Ganga river basin, Sri Lanka (Khaniya et al., 2020); plans and developed hydroelectric projects in China (Liu et al., 2016) including Upper Yangtze river basin of China (Qin et al., 2020), Hanjiang river basin in China (Chang et al., 2018). Tobin et al. (2018) calculated the flow change due to change in different scales of temperature change. The climate change and consequences of power generation from the hydroelectric project has, merely, been studied in Nepalese catchment (Mishra et al., 2020; Shrestha et al., 2021, 2016a) have evaluated the energy generation in both storage and runoff the river as well as existing and planned projects e.g., Kulekhani, storage now in operation and Tamakoshi Peaking RoR has just commissioned.

2.14 Energy economics of hydroelectric project

Electricity is one of the key drivers for overall development of a country. Number of past studies have shown that economic development of a country is strongly correlated with the access of electricity and its consumption (Aslan, 2014; Devkota, 2020; Kamaludin, 2013; Lorde et al., 2010; Stern et al., 2019). It is because electricity brings higher agricultural productivity through powering irrigation, food and seed preservations, and contributes to effective running of industrial and service sectors. Similarly, it enhances productivity of education efforts and health services, and helps to improve clean water supply and sanitation. It also helps to create opportunities in the

application of new technologies and ease access to information (Satpathy, 2015). Furthermore, hydroelectricity development can contribute to national development through reduced imports of fossil fuels, expand the area of land under irrigation and diversify the economy in which poor households are more integrated in the economy. In the context of Nepal, increase in greater electricity generation is expected to promote industrialization, generate foreign currency reserves through export of electricity to reduce the trade deficit (Alam et al., 2017; MoWR, 2009; Thapa and Basnett, 2015). However, the cost of the electricity production is important from consumer's point of view (Devkota et al., 2022). It is essential to explain that the proposed project is economically feasible and likely to generate more benefits than the costs by calculating the benefit cost ratio. Benefit cost ratio is defined as the ratio of the annual benefits to the annual costs. Annual cost comprises of the cost of the projects, selecting interest rates, estimated lives of hydraulic structures, tax and other investment charges, relationship between expected frequencies of extreme events of stream flow, and the economic design of the hydraulic structures

2.14.1 Economic impact of electricity and cost of hydroelectricity

The world currently gets about 80% of its energy supplies from fossil fuels. However, the cost advantage of fossil fuels over renewable energy sources is decreases with the time, as the renewable energy costs decline further in the future, while price of fossil fuel rises. Thus, even without policies to promote a transition toward renewables, economic factors are currently moving us in that direction. Best (Best, 2017) makes an interesting comparison showing that the capital cost of a hydroelectricity project is about 4.0 million USD per Megawatt (MW) which is only slightly more expensive than a coal plant, two-thirds of a nuclear or geothermal plant and one-fourth of the cost of a solar power plant. Hydroelectricity remains very competitive, less than the cheapest new fossil fuel-fired cost project (IRENA, 2020).

Cost comparisons between different energy sources are made by calculating the levelized cost of energy. Levelized costs represent the present value of building and operating a plant over an assumed lifetime, expressed in real terms to remove the effect of inflation. They are USD 0.073/kWh and USD 0.047/kWh for newly commissioned geothermal and hydropower power projects respectively. It is USD 0.068/kWh for solar plants averaged globally (IRENA, 2020). Baris and Kucukali (2012) compared the cost of a renewable energy sources in Turkey and state that hydroelectricity has the lowest

investment cost of $1226/kW, among the renewable energy alternatives. Hydroelectricity is, thus, considered as the most preferred renewable energy source followed by solar and wind energies to increase their contribution to electricity generation in Turkey (Gök, and Kentel, 2015).

2.14.2 Impact of climate change in the economics of hydroelectric project

Profit of a project refers to the financial benefit realized when revenue generated from a business activity exceeds the expense of the project. Costs of a hydroelectric project occur during two distinct time frames – one, during the construction phase of the project and two, during the operation phase. Revenue is the amount of money received by selling hydroelectric energy generated by the project. It depends on the power purchasing agreement (PPA) rate made with the buying agency. Whenever, a hydroelectric project is planned, a certain amount of money is to be invested called capital investment. Capital investment is usually converted into monthly or annual investment with interest rate plus depreciation or as interest plus amortization. The appropriate factor to convert an investment into an equivalent annual cost is called capital recovery factor. Besides, the capital investment, there will be recuring annual investment on maintenance and operation (O&M) costs. Typical values of annual O&M costs range from 1% to 4%. The IEA assumes 2.2% for large hydroelectricity, and 2.2% to 3% for smaller projects, with a global average of around 2.5%. An average value for O&M costs of 2% to 2.5% is considered for large-scale projects (IRENA, 2012). This will usually include the refurbishment of mechanical and electrical equipment like turbine overhaul, generator rewinding and reinvestments in communication and control systems. The construction cost of the physical infrastructure can be assumed to remain constant and the annual O&M cost is not affected significantly while evaluating the impact of CC on electricity production (Marahatta et al., 2022; Mishra et al., 2020). It implies that the cost components of the project remain constant for the base case as well as for the future case. The change in profit from hydroelectric project due to the impact of the CC is, therefore, simply the difference between the revenue generated from the hydroelectricity sales for the base case and for the future case.

2.15 Research gap

The impact of CC on runoff and water availability for hydroelectricity projects have been studied in different countries such as Brazil, Canada, China, that have abundant

hydropower potential. There are other studies on renewable energy mostly targeted towards advancement of newer technologies and analyses of the conversion from current fossil-fuel based to a renewables-dominated. However, the current research trend on energy economics is largely focused on fossil fuels and other water management issues. Research on the effects and economic values of established technologies such as hydroelectricity is rather limited. Extending this gap further is the micro-economic assessment of the cost and revenue aspects of hydroelectricity linked to CC at the local level. This study attempts to address this research gap and paves way for integrated economic evaluations of the hydroelectricity sector. The urgent world-wide need of switching to green energy has led to hydroelectricity, wind, solar, geothermal and wave receiving global attention. Based on the literature review made in this study, the following research gaps are identified.

i. Sufficient researches are not carried out to assess the impact of climate change on river hydrology and its impact on hydroelectricity production.
ii. Impact of climate change on economics aspect of hydroelectricity project at the local level is almost non-existent.
iii. Continuum of flow, hydroelectric energy and economics is integrated considering the impact of climate change in this study

2.16 Overall summary of literature review

This review provides an analysis of the influence of climate change on energy production based on water availability by using currently available literature, scientific reports and government documents. It also provides current state of hydrological simulation methods and their applications to a broad spectrum of CC scenarios. Studies on the hydro-energy of mountainous basins in Himalayan region and its effects in the face of changing climate an economic perspective are also evaluated. This study specifically quantifies and compares the global hydroelectricity impact due to CC by using available literatures in the six continents including arctic, Mediterranean, Balkan region as a separate region. Further, comparison with the baseline information for climate resilient planning and design of hydroelectricity projects in global scenario to narrow down to complex mountainous river basins of Sino-Nepal is presented. The ever-increasing demand of water resources utilization for improvement of living standard of billions of populations in the world, particularly for energy, water supply and agriculture, is increasing pressure on water resources have been explored. Even

though water is a basic necessity for improving food production and socioeconomic well-being, it has also caused damages to the environment and its related services. Balancing water uses for humans and nature is seen as the major challenge of this century. This issue is far more complex for the semi-arid regions of Tibet Autonomous Region of Peoples Republic of China and the high precipitation area of Federal Democratic Republic of Nepal and where water is generally scarce and demands from water supply, agriculture, industry, urbanization for the rapidly growing population. The high climatic variability and expected ongoing CC further add to the pressing issues. This review provides insightful evidence which shall be extremely useful for the planning and design of hydroelectric projects not only within Nepal but also the South Asian region drained by numerous trans-boundary rivers such as the Budhigandaki river due to CC.

CHAPTER 3

MATERIALS AND METHODS

3.1 Background

This chapter describes materials and methods used for the study of flow estimation, climate change projection and energy economics in the forms of revenue change analysis for the future time window under different Representative Concentration Pathways (RCPs). Secondary data have been used for this study. Further, four different future climate scenarios of each RCPs were generated. Current and future hydrology were simulated at the dam site of Budhigandaki Storage HEP using well calibrated and validated in SWAT model. The change in revenue was assessed under CC scenarios, and is compared with base case scenario. Following sub-sections describe the methods in detail.

3.2 Study area

3.2.1 General description

The Budhigandaki River Basin (BRB) is a transboundary river basin bordered in the north by the vast Tibetan Plateau, in the south and east by the Trishuli river basin and in the west by the Marsyangdi river basin. The BRB is one of the major basins of the Narayani river basin of Nepal, which is a major tributary of the river Ganges. About one-fourth of the basin area lies in the Tibetan plateau of People's Republic of China (PRC) and the remaining part lies in the Federal Democratic Republic of Nepal (Figure 3.1).

Physiographically, the basin falls in the Middle Mountains and the Himalayas. Mount Manaslu, the eighth highest peak in the world, is situated in this basin (MCTCA, 2014). In the upper part of the basin, the valley slopes are steep, rocky and V shaped. In the lower part, the landscape is mature with smooth uniform slopes, which have been dissected by actively eroding rivers rejuvenated by the recent uplift of the Himalayas. The basin area at the confluence of Trishuli river is 4988 km^2, with an average elevation of 3723 masl (range: 315 m–8163 m). It is about 113 km long and between 15 and 30 km wide. BRB lies in Gorkha and Dhading districts in between the Bagmati and Gandaki provinces of Nepal and Kerong county of Tibetan Autonomous Region of

China between latitudes 27° 50' and 28°00' N and longitudes 84°30' and 85°10' E. The major tributaries of Budhigandaki river are Tom (Dogar), Syar and Ankhu Khola. The other tributaries of the Budhigandaki are Larke, Athahra Saya, Phurba Dhyapsa, Hinan, Gungan, Sanchu, Seran, Udilun, Sayale, Sanamchu, Chulung, Bhalu, Yaru, Pangair, Dowan, Namrung, Machi, Richet, Aarkhet, Kaste, and Jyadul Khola.

The hydrology of the basin has been established with respect to the gauging station No. 445 at Arughat, located approximately 30 km upstream of its confluence with the Trisuli River (BGHP, 2015; Marahatta et al., 2021c, 2021d, 2021b; Singh and Saravanan, 2020). Long-term annual rainfall of the BRB is 1495 mm with an extremely high spatial variability within the basin. Rainfall intensities vary throughout the basin with maximum intensity occurring on the south facing slopes of the mountains. The station Arughat receives an annual precipitation of greater than 2500 mm while the Tibetan part of the basin receives less than 700 mm. The mean annual flow of the Budhigandaki river upstream of Trishuli confluence is estimated to be 240 m^3/s (Marahatta et al., 2021b). The temperature varies from −2.0 °C in winter to 33.0 °C in summer in the study basin. The flow is minimum in the months of February and March and begins to rise with the onset of the monsoon. It peaks in July or August, after which it starts to decrease. The maximum monthly average discharge of 982 m^3/s occurs in August, while the minimum monthly average flow of 52 m^3/s in February.

The Budhigandaki River has been dammed twice near Lapubesi in 1967, and August 1, 1968. The landslide dam in 1968 blocked the river for 29 hours, created a 60 m deep lake and reduced the river depths from 4 m to 0.9 m at Arughat station. When the landslide dam breached, the water depth jumped to 14.61 m. The peak flow immediately after the breach of landslide dam outburst flood (LDOF) on August 2, 1968, was estimated ~5,210 m^3/s, more than twice the mean annual instantaneous flood of 2,380 m^3/s (Marahatta, 2015; Shankar, 1969). The flood swept 24 houses at Arughat Bazaar, and many suspension bridges downstream of the dam.

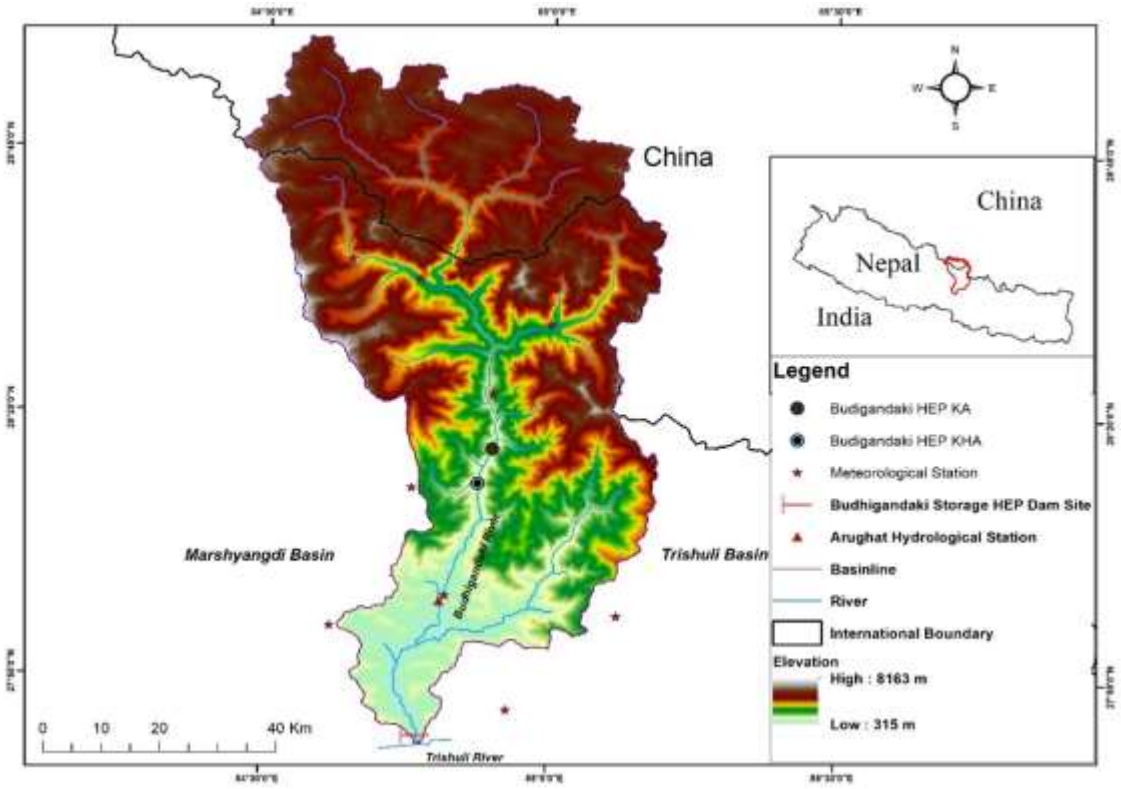

Figure 3.1: Budhigandaki River Basin

3.2.2 Demography

The BRB covers the two districts in Nepal and one county in PRC with a total population of these three administrative regions is 594,732 consisting of 48 % male and 52% female. The total number of households in the districts/county area is about 144,500 and the average household size is 4.2 persons. The percentage of male is 48% in Nepal while in Tibet it is 53%. The demographical data of the study region is shown in Table 3.1.

Table: 3.1: Demographical data of the study area

SN	District/County	Province/Prefecture	Total	Male	Female	Reference Year
1	Dhading	Bagmati	322,758	49%	51%	2021
2	Gorkha	Gandaki	254,438	48%	52%	2021
3	Kyirong	Shigatse	17,536	53%	47%	2020

3.2.3 Geology

The BRB mainly comprises lesser and higher Himalayan rock sequences. Geologically, the catchment area is intersected by two major thrusts called Main Boundary Thrust (MBT) and Main Central Thrust (MCT). Fuchs (1982) prepared a regional geological map of the entire Himalaya. Based on these two studies: extreme north of catchment comprises Tibetan Tethys sequence which is followed by Triassic–Jurassic formations comprising mainly carbonate rocks to the south. Further south, Himal Group rocks mainly garnet biotite gneisses, kyanite biotite gneisses, garnetiferous mica schist, augen gneisses etc. have been reported. Carbonaceous slates, green shales, dolomite and dolomitic limestone interbedded with slates were mapped to the south of these higher Himalayan crystalline rocks. Weak rock types and the area lying on the MCT zones may place this area relatively more susceptible to mass. The major rock types of all aforementioned formations include phyllites, shales, slates, limestones and dolomites with characteristic colors, grain size, sedimentary structures etc. unique to each formation. Areas in the vicinity of these mega geological structures may be more prone to landslide hazard and subsequently to LDOFs because of the crushed and fractured zones as a result of the past tectonic movement and high seismic activities in the region.

3.3 Data and Sources

3.3.1 Meteorological data

Meteorological data from eight stations in and around the study basin (1981–2015) were used as input to the model (Figure 3.1). Two stations have both observed precipitation and temperature data while the remaining six stations have only precipitation data. Gridded data of precipitation and temperature for the Tibet part of the basin was also used in the study. The number of years with complete daily rainfall data missing was determined during the study for a station and then percentage (%) of data missing were computed. The date of establishment of rainfall stations, the period availability of the rainfall along with their locations and percentage (%) of data availability years is presented in Table 3.2. The stations Chhekapar (833), Machha Khola (840), Barpak (850), Namrung (839) and Chumchet (869) are the most important precipitation stations in the basin. However, due to unavailability of long series of data, these stations have not been used in the analysis. Quality checking of the data was done through various methods: homogeneity test, outliers checking, inter

parameter consistency checking, spatial checking and double mass curve analysis. The average areal precipitation over the catchment was calculated by the Thiessen polygon method (Thiessen, 1911) using geographic information system (GIS). Considering the above availability of rainfall data and the necessity to give the equal weights for all the meteorological stations, the period of 35 years between 1981 and 2015 has been selected as the common base period. This is done in accordance with the WMO practice (WMO, 1989) which states a normal standard period that has 30 years of continuous mean monthly climatological data, which is required for any climatic analysis.

Table: 3.2: Meteorological stations in the study area

Name	Types of Station	Lat.	Long	Elev.	Data Available %	Available Data	Established Date
Jagat	Precipitation	28.37	84.90	1334	93.7	1957-2016	Jul-57
Larke Samdo	Precipitation	28.67	84.62	3650	90.8	1979-2016	Jun-78
Gorkha	Agro-met	28.00	84.62	1097	96.2	1957-2016	Jun-56
Gharedhunga	Precipitation	28.20	84.62	1120	95.7	1976 -2016	Jul-76
Chhekampar	Precipitation	28.48	85.00	3300	37.5	1978-2016	Jun-78
Machha Khola	Precipitation	28.23	84.87	550	89.9	2007-2020	Jun-99
Barpak	Precipitation	28.20	84.74	1889	98.8	2007-2020	Jun-99
Namrung	Precipitation	28.55	84.77	NA	71.2	2007-2019	Jun-99
Chumchet	Precipitation	28.43	84.90	NA	76.7	2012-2019	Jun-99
Timure	Climatology	28.28	85.38	1900	91.7	1956-2016	Jun-56
Arughat Bazar	Precipitation	28.05	84.82	518	70.3	1957-2016	Jun-57
Nuwakot	Climatology	27.92	85.17	1003	87.3	1956-2016	May-56
Dhading	Climatology	27.87	84.93	1420	82.2	1956-2016	May-56
Dhunche	Climatology	28.10	85.30	1982	86.7	1972-2016	Nov-71
Pansayakhola	Precipitation	28.02	85.12	1240	93.3	1973-2016	Jan-73
Tamachit	Precipitation	28.17	85.32	1847	96.6	1972-2017	Nov-71
Laprak	Precipitation	28.22	84.80	2115	91.5	2014-2020	

Name	Types of Station	Lat.	Long	Elev.	Data Available %	Available Data	Established Date
Majhimtar	Precipitation	27.80	84.95	460	81.0	2012-2020	Oct-99
Gajuri	Precipitation	27.80	84.88	NA	96.6	2008-2020	Apr-99
Sakher	Precipitation	28.23	84.38	NA	91.4	2007-2020	Apr-99
Taal	Precipitation	28.47	84.38	1600	81.9	2007-2020	Jul-99
Tibet1	Climatology	28.833	84.58	4866	100	1956-2015	
Tibet2	Climatology	28.765	84.70	4582	100	1956-2015	

3.3.2 Hydrological data

For this study, long term daily streamflow data of Budhigandaki River at Arughat is considered from 1964 to 2015 (DHM, 2018). Daily flow data (1983–2012) of Budhigandaki river at Arughat gauging station has been used for calibration and validation of the model. Similarly, short term flow data available at the damsite of the proposed Budhigandaki Storage Hydroelectric Project (2013–2014) lying downstream of the Arughat station and headwork sites of two proposed run of the river hydroelectric projects, viz., Budhigandaki *Ka* HEP and Budhigandaki *Kha* HEP (2009) lying upstream of Arughat (Figure 3.1) were also used for additional validation of the model. The available flow data of Ankhu Khola at Ankhu Bazar did not pass the quality test. Therefore, the data of Anhu Khola was not used in this study.

Table: 3.3: Hydrological stations in the study basin

Station Name	Location	Lat.	Long	Basin Area (km^2)	Data Available %	Available Data	established Date
Budhigandaki	Arughat	28.04	84.82	4270	93.3	1964-2015	Nov-63
Budhigandaki	Tatopani	28.52	84.86	3784	100	2009	Jan -09
Budhigandaki	Machha Khola	28.50	84.86	4017	100	2009	Jan -09
Budhigandaki	Sirenitar	27.83	84.77	4986	100	2013-2014	Dec -12
Ankhu	Ankhu Bazar	27.97	84.81	768	45.5	1987-2012	1967

3.3.3 Observed rainfall-runoff characteristics

Long term monthly average precipitation and observed flow (1983–2012) based on Department of Hydrology and Meteorology (DHM) at Arughat gauging station is depicted in Figure 3.2. The figure shows that the flow closely follows the precipitation pattern of the basin. Long term annual basin precipitation has been calculated as 1300 mm (maximum 278 mm in July and minimum 11 mm in November). Similarly, the long-term average and standard deviation of the annual flows are 163 m^3/s and 156 m^3/s, respectively.

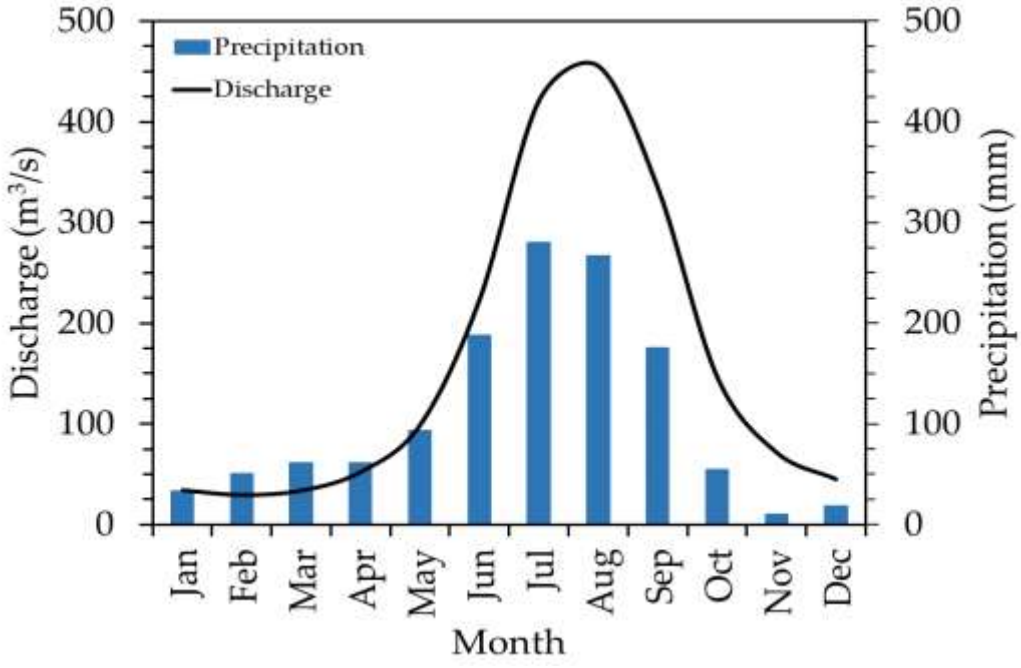

Figure 3.2: Long term rainfall-runoff pattern of the Budhigandaki river basin at Arughat

3.3.4 Spatial data

Shuttle Radar Topography Mission (SRTM; 1 arc second horizontal resolution) DEM was used to delineate the river network and sub-basins. Landuse and land cover (LULC) data were obtained from DoWRI Irrigation Master Plan Preparation through Integrated River Basin Planning (Dataset). Soil data of the Tibetan part of the basin was taken from Soil Terrain Database Programme (SOTER) which is at 1:1 million scale whereas soil data for Nepal was also obtained from DoWRI. LULC and soil maps of the basin are shown in Figure 3.3 (a-b) respectively. LULC data was categorized into nine classes while soil data was segregated into 17 classes. BRB is covered by snow and glaciers

(SNGL-29%), followed by forest (FORS-23%), barren (BARN-21%), shrub and grassland (SHGR-18%) and agriculture (AGVT, AGST, AGLT-8%). River (RIVR) and residential built-up area (RESI) covers the least portion (~1%) of the total area. It can be seen from Figure 3.3b that hard rock mass in mountainous terrain (RockRock) covers a significant part (~33%) of the basin while inceptisols with loamy sand texture (IncSand) covers about 21% of the basin area. Gelic leptosols with rocky texture (LpiRock-13%) and gelic leptosols with loamy skeletal texture (LpiSkel-10%) are also found in different parts of BRB. Entisols with sandy texture (EntSand-7%), spodosols with sandy texture (SpoSand-5%), inceptisols with loamy texture (IncLoam-3%), alfisols with loamy texture (AlfLoam-3%) and eutric leptosols with rocky texture (LpeRock-3%) are also found in small patches. Inceptisols with loamy skeletal texture (IncSkel-1%), eutric leptosols with sandy texture (LpeSand-1%), entisols with loamy skeletal texture (EntSkel-0.5%), haplic luvisols with loamy texture (LvhLoam-0.4%), mollisols with sandy texture (MolSand-0.2%), leptosols with loamy texture (LpLoam < 0.1%), leptosols with loamy skeletal texture (LpmSkel < 0.1%) and entisols with loamy texture (Entloam < 0.1%) are found in traces.

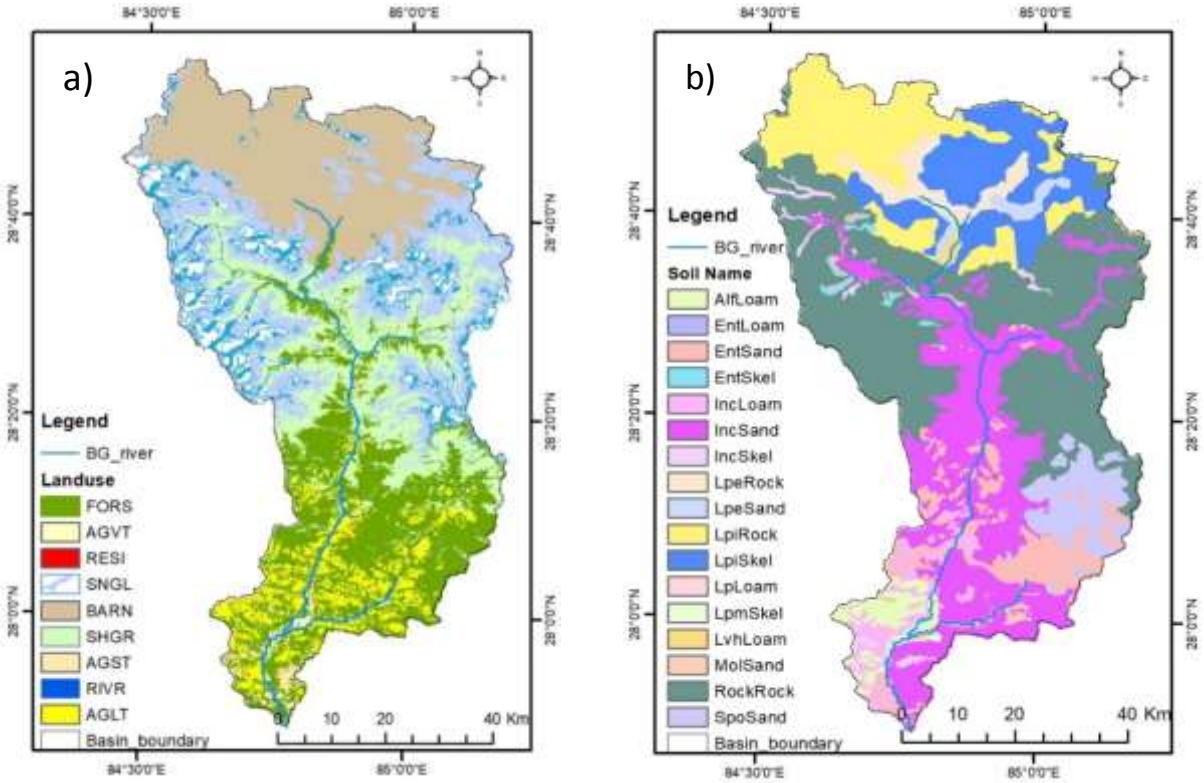

Figure 3.3: Spatial data a) Land Use and Land Cover, b) Soil map of the study basin

3.3.5 Climate change data

The United Nations Framework Convention on Climate Change (UNFCCC) in its Article1, defines climate change as: "a change of climate which is attributed directly or indirectly to human activity that alters the composition of the global atmosphere and which is in addition to natural climate variability observed over comparable time periods". The UNFCCC thus makes a distinction between CC attributable to human activities altering the atmospheric composition, and climate variability attributable to natural causes. Climate change refers to a change in the state of the climate that can be identified (e.g., by using statistical tests) or by changes in the mean and/or the variability of its properties, and that persists for an extended period, typically decades or longer. Climate change may be due to natural internal processes or external forcing such as modulations of the solar cycles, volcanic eruptions, and persistent anthropogenic changes in the composition of the atmosphere or in land use. Future data of different GCMs to assess the impact of CC on the Budhigandaki River Basin was projected for 79 years (2021-2099). Climate data were considered for two RCPs 4.5 (stabilization scenario) and 8.5 (high emission scenario) of the IPCC AR5 (Vuuren et al., 2011). Brief description of the selected GCMs and their selection criteria, bias correction methods, impact of CC on climatic parameters and hydrology, and frequency analysis of extreme flows.

Climate change presents increasing challenges for energy production and transmission. A progressive temperature increase, an increasing number and severity of extreme weather events and changing precipitation patterns will affect energy production and delivery. The supply of fossil fuels, and thermal and hydropower generation and transmission, will also be affected due to CC.

Climate change is occurring due to human interference and it poses risks for both humans and natural system. The assessment of impacts, adaptation and vulnerability must be carried out and must evaluate how patterns of risks and potential benefits are shifting due to CC. In recent decades, changes in climate have caused impacts on the natural and human system on all continents and across oceans. Evidence of climate change impacts is strongest and most comprehensive for the natural system. In many regions, changing precipitation or melting snow and ice are altering hydrological systems, affecting water resources in terms of quality and quantity. Glaciers continue

to shrink almost worldwide due to climate change affecting runoff and water resources downstream.

3.3.6 Terrain data

The reservoir water surface area (A) is estimated as a power function of its depth (y) as given in Equation 3.1 Devkota et al. (2022).

$$A = \alpha y^{\beta} \quad (3.1)$$

The best fitted value of the multiplicative coefficient (α) is 1360 and the power coefficient (β) is 2.0 which have been used for further calculations.

3.3.7 Energy and PPA rate

Energy table of BGHP (BGHP, 2015) is collected from the Budhigandaki Hydroelectricity Development Committee and power purchasing agreement (PPA) rate is adopted by the minutes of Nepal Electricity Authority (NEA) board meeting held on April 27, 2017 (NEA, 2017). The seasonal and annual revenues equivalent to the generated monthly energy for the climate change scenarios were then calculated using the power purchasing agreement PPA rates (Table 3.4) fixed by the Nepal Electricity Authority (NEA, 2017) and compared with the base case.

Table: 3.4: PPA rate for storage type projects in Nepal

Season	Rate NRs/kWh	Min. Dry season energy required
Dry (Mangsir 16-Jestha 15)	12.40	35%
Wet (Jestha 16- Mangsir 15)	7.10 If wet season energy is more than 50%, this rate shall be decreased by the excess %	
If dry season energy is less than 35% of annual energy, a storage project shall be considered as a PROR project for applying the power purchase rate.		

3.4 Methodology

3.4.1 Overall methodology

This study adopts a model-based approach to assess impacts of projected future climate on revenue generation in the BRB. Figure 3.4 depicts an overall flowchart of adopted methodology and following sub-sections describes them in detail. Future climate was projected from GCMs. Historical baseline flow, future runoff and energy generation in both baseline and future were assessed using a hydrological model developed in SWAT. Based on the research questions, the detailed flow chart of the specific objectives are shown in the subsequent section.

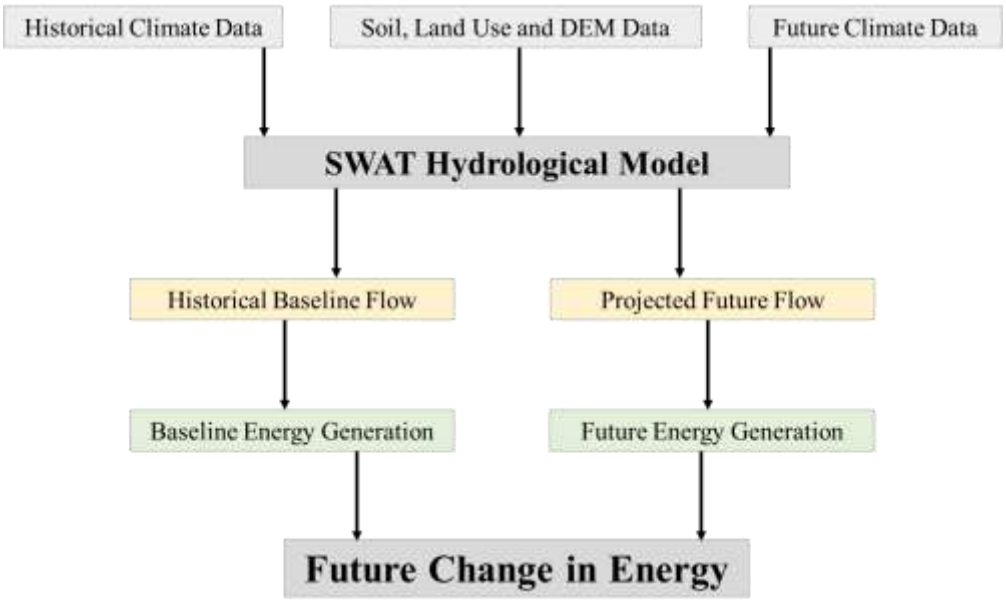

Figure 3.4: Overall methodology of the research

3.4.2 Selection of flow estimation method

Estimation of the available flows at sites of water resources project development in ungauged basins is carried out by various methods. Out of these methods, design values are fixed by the site conditions and evaluation of the designer. The approaches commonly used in Nepal are given below.

i. Hydrological Simulation Method
ii. WECS/DHM 1990 Method
iii. NEA 1997 Method

iv. DHM 2004 Method

v. Drainage Area Ratio (DAR) Method

vi. General Transposition (GT) Method

Six evaluation indicators have been compared for the different discharge estimation methods for the BRB (Marahatta et al., 2021c). All the indicators are given equal weights. The lowest performing method was assigned a value of 1 while the highest performing a value of 6 in increments of one. In case of equal values for different methods, the average value is considered. The average performance value of each approach was calculated by Global Performance Index (GPI) which is mathematically presented in Equation 3.2.

$$GPI_j = \frac{R_j^2 + MAE_j + RMSE_j + PBIAS_j + NSE_j + KGE_j}{6} \quad (3.2)$$

Where, $_j$ = index corresponding to the method under consideration

Higher value of GPI indicates better performance for monthly flow estimation and vice versa. It is noted here that GPI value of Soil and Water Assessment Tool (SWAT), hydrological simulation method was found better for the monthly flow estimation as compared to other methods. So, SWAT has been taken as the best method of flow estimation in BRB catchment.

3.4.3 SWAT hydrological model

SWAT (Arnold et al., 1998) is a continuous, semi-distributed, and process-based hydrological model with open source code developed by the U.S. Department of Agriculture Agricultural Research Service (USDA-ARS). It is widely and successfully used to simulate hydrological cycles, crop growth, sediment yields, and agricultural chemical transport on a daily time step to evaluate the effects of alternative management decisions on water resources and non-point source pollution in large river basins with varying soils, slopes and land use management conditions. SWAT was designed on the water balance concept and has been extensively used on different scales and application around the world (Akoko et al., 2020; Asurza-Véliz and Lavado-Casimiro, 2020; Brouziyne et al., 2020; Getachew et al., 2021; Guevara-Ochoa et al., 2020; Huang et al., 2020; Kundu et al., 2017; Liu et al., 2021; Malagó et al., 2017; Marahatta et al., 2021b; Marhaento et al., 2017; Marras et al., 2021; Nerantzaki et al., 2020; Omani et al., 2017; Peker and Sorman, 2021; Qi et al., 2020; S. Shrestha et al., 2020; Vanderkelen

et al., 2018; Venetsanou et al., 2020). In 1990s, the first version of SWAT 94.2 was developed and released, and for the first time, Arnold in 1994 published a peer-reviewed description of a GIS interface for SWAT. The current SWAT model contains the key elements contributed by the USDA-ARS model (Arnold et al., 1998). The purposive use of the SWAT model is to predict the impact of climate on water resources, as well as sediment and chemical yield in a large scale of the ungauged basin (Glavan et al., 2011; Hosseini and Khaleghi, 2020; Ma et al., 2020; Mapes and Pricope, 2020; Pandey et al., 2021; Rafiei et al., 2020; Ricci et al., 2018; Rodrigues et al., 2019; Theron et al., 2021). The SWAT model is used to predict the influence of land use and land cover change on water in a vast watershed over a long time with different conditions (Aawar and Khare, 2020; Joorabian Shooshtari et al., 2021; Rahimpour et al., 2021; Rani and Sreekesh, 2021; Shelton, 2021; Sinha et al., 2020; Worku et al., 2017).

SWAT simulates catchment processes such as evapotranspiration, runoff, crop growth, nutrient and sediment transport on the basis of meteorological, soil, land cover data and operational land management practices (Neitsch et al., 2011). The model discretizes a catchment into sub-catchments and further into one or more hydrological response units (HRU), which represent unique combinations of land cover/land used, soil type and slope. The discretization method employed by SWAT enables the model to simulate catchment processes in detail and to understand the response of unique HRUs to hydrological processes. An HRU is the smallest spatial response unit where many physical processes such as hydrological cycle, soil erosion, nutrient and pesticide transport are simulated. Primary input data include digital elevation model (DEM), land use, soil, and weather (i.e. precipitation, temperature, wind speed, solar radiation, and relative humidity) is simulated at the HRU scale. Water, sediment, and chemical movement in SWAT involve two phases: first, the watershed land areas control water transported to the channels together with sediment, nutrients and pesticides in each sub-watershed. Then, the movement of water and other mass through the stream network to the watershed outlet. It is used to predict the impact of land management practices on water, sediment, channel and reservoir routing and agricultural chemical yields in large complex watersheds with varying soils, land-use and management conditions over long periods of time. A more detailed description of the SWAT model can be available from online documentation (https://swat.tamu.edu/docs/). The SWAT model simulates the

various hydrological processes occurring in the river basin based on water balance within the basin as given by Equation 3.3.

$$SW_t = SW_0 + \sum_{i=1}^{t}(R_{day} - Q_{surf} - E_a - W_{seep} - Q_{gw}) \quad (3.3)$$

Where

SW_t is the final soil water content (mm),

SW_0 is the initial soil water content (mm),

t is the time in days,

R_{day} is the amount of precipitation on day i (mm),

Q_{surf} is the amount of surface runoff on day i (mm),

E_a is the amount of evapotranspiration on day i (mm),

W_{seep} is the amount of water entering the vadose zone from soil profile on day i (mm),

Q_{gw} is the amount of return flow on day i (mm).

All the processes in SWAT are simulated at HRU level and aggregated for each sub-basin, which are then routed through the river system using the variable storage or Muskingum method. SWAT facilitates an assortment of parameters defined at HRU, sub-basin or basin level. SWAT uses the climate data from the station nearest to the centroid of each sub-basin. For a given precipitation, snowfall occurs when the temperature is below threshold level. Rain first falls on the plants where canopy storage and evaporation take place. Surface runoff, depending upon local land use, soil type, and antecedent moisture condition, is estimated by SCS curve method and peak runoff estimations are based on modified Rational formula. Watershed concentration time is estimated using Manning's formula, considering both overland and channel flow. Four water storage compartments in SWAT are snow, soil profile (0-2m), shallow aquifer (2-20m), and deep aquifer.

In SWAT, the surface runoff from rainfall can be estimated using a modified soil conservation service (SCS) curve number (CN) method (USDA, 1972) or the Green and Ampt infiltration method (Green and Ampt, 1912). In this study The SCS CN

method was employed. It is computationally efficient and the most popular method, which predicts runoff with a given rainfall event mainly based on land use, soil properties and antecedent moisture conditions. The surface runoff component of the water balance is determined from the SCS CN method computes runoff using Equation 3.4 as;

$$Q_{surf} = \frac{(R_{day} - I_a)}{(R_{day} - I_a + S)} \quad (3.4)$$

Where, Ia = 0.2S and $S = 25.4(\frac{1000}{CN} - 10)$ and hence the amount of surface runoff is equated as:

$$Q_{surf} = \frac{(R_{day} - 0.2S)}{R_{day} + 0.8S} \quad (3.5)$$

Where: Ia is the initial abstraction (mm), S is relation parameter, drainable volume of soil water per unit area of saturated thickness (mm/day) and CN is curve number.

SWAT uses the climate data from the station nearest to the centroid of each sub-basin. A given precipitation is classified as solid (snow) and liquid (rainfall) based on a user-defined threshold value of mean air temperature. Snow melts when the maximum temperature on a given day exceeds the user defined threshold level. In snow covered areas, a fraction of the estimated daily potential evapotranspiration is by sublimation. The following mass balance at the HRU scale allows SWAT to keep track of the snowpack as Equation 3.6.

$$SNO_{i+1} = SNO_i + P_s - E_{sub} - SNO_{mlt} \quad (3.6)$$

Where;

SNO_i and SNO_{i+1} are respectively the water content (mm) on a day i and i+1;

P_s is the solid precipitation (mm) on day i;

E_{sub} is the evaporation lost by sublimation and

SNO_{mlt} is daily snowmelt amount (mm).

A temperature index (degree day factor) is used to obtain snowmelt amount (Neitsch et al., 2011) as given by Equation 3.7.

$$SNO_{mlt} = b_{mlt}.SNO_{cov}\left[\frac{T_{sno} + T_{max}}{2} - T_{mlt}\right] \quad (3.7)$$

Where

b_{mlt} is the daily melt factor (mm day^{-1} $°C^{-1}$),

SNO_{cov} is the fraction of HRU area covered by snow,

T_{sno} is the daily snowpack temperature (°C),

T_{max} is the daily maximum air temperature (°C) and

T_{mlt} is the base temperature above which snowmelt is allowed (°C).

SWAT uses different modules to calculate evaporation from soils and plants. The available models for estimating potential evapotranspiration (PET) are Penman-Monteith, Priestley-Taylor, and Hargreaves. Details of the SWAT model can be found in (Arnold et al., 1998; Neitsch et al., 2011; Van Liew et al., 2005). Potential soil water evaporation is estimated as a function of potential ET and leaf area index (LAI). Soil evaporation is estimated using an exponential relation of soil-depth and water-content. Transpiration is calculated using a linear function of PET, LAI, root-depth and soil-water content.

When the temperature exceeds a threshold value, snow melt occurs. Infiltration, evapotranspiration, subsurface flow and percolation occurs in multiple soil layers. Groundwater flow is simulated by routing the shallow aquifer storage to the stream. Percolation from the shallow aquifer is considered as lost from the system. The schematic representation of the different hydrological processes in SWAT is described by Figure 3.5.

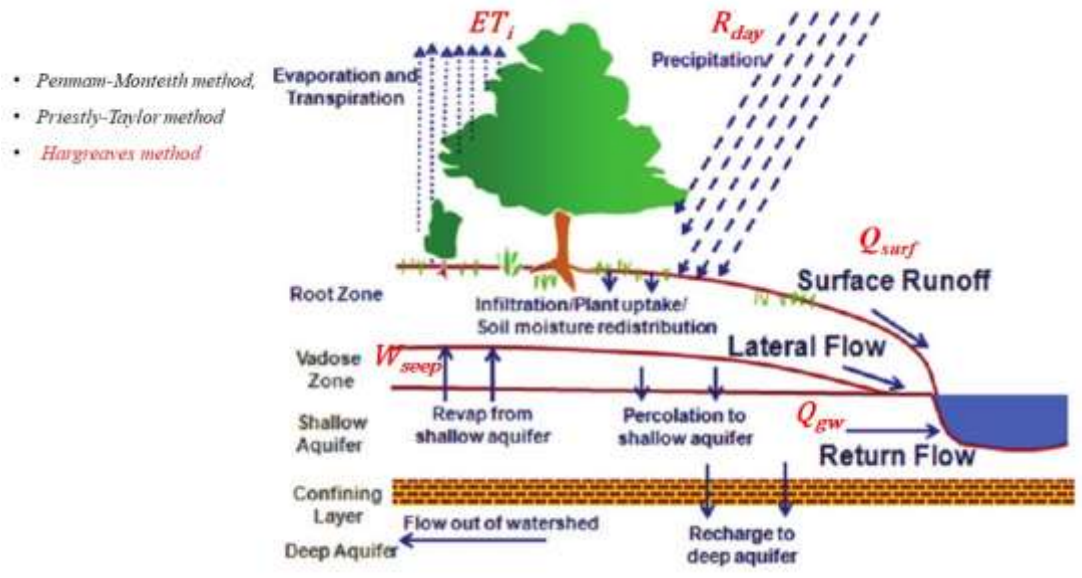

Figure 3.5: Schematic representation of the hydrologic cycle in SWAT (Neitsch et al., 2011)

To compute the potential evapotranspiration (PET), Hargreaves method was applied because it requires limited climatic data (Hargreaves and Samani, 1982)

$$\lambda E_o = 0.0023.H_o.(T_{max} - T_{min})^{0.5}.(T_{avg} + 17.8) \quad (3.8)$$

Where, λ is the latent heat of vaporization (MJ/kg), Eo is the potential evapotranspiration (mm/d), Ho is the extra-terrestrial radiation (MJ/d.m^2). T_{max}, T_{min} and T_{avg} are the maximum, minimum and average air temperature per day (^{o}C) respectively.

3.5 SWAT model evaluation criteria

3.5.1 Calibration and validation

Model calibration and validation are important and crucial steps for any model simulation. Calibration is an iterative process for assigning the values of the input parameters by comparing the simulated and observed output data series. Validation is the process in which the calibrated model is simulated for an entirely different time duration to assess its performance under different hydro-climatic conditions.

In this study, for calibration and validation of the model, manual calibration method is followed. In manual calibration, the SWAT interface provides three methods for varying the parameters. The first option allows to replace the value directly. The second method allows adding values to the initial values. And the third method allows multiplying the initial value with the drawn parameter value. Calibration and Validation was performed for daily flows. One station was chosen for the calibration while three additional gauging sites were chosen for validation purposes.

The BRB was divided into 16 sub-basins and five slope classes (0–30, 30–50, 50–70, 70–90 and >90 percent). A threshold value of 10% each for land use and land cover, soil (Figure 3.3a-b) and slopes were used to divide the subbasin into unique 344 HRUs. Further, to account for orographic effects, we generated 500 m range elevation band in each sub basin. The methodological framework for model setup and simulation is given in Figure 3.6.

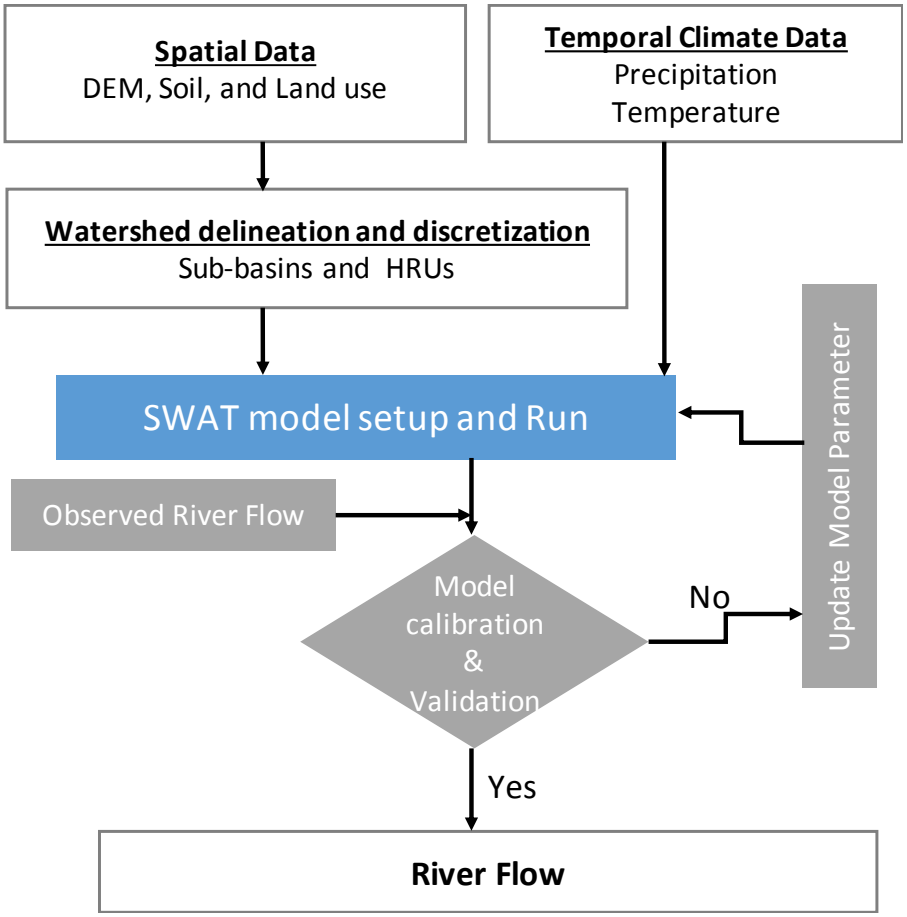

Figure 3.6: SWAT hydrological model setup diagram.

There are a large number of missing flow data of years 2013 and 2014 at Arughat station. Therefore, 30 years of observed flow data of Arughat station from 1981-2012 were used in the study. The SWAT model was calibrated and validated manually at Arughat station for the simulation period of 30 years. A warm up period of 2 years (1981-1982) to stabilize the model initially, calibration period (1983-2002) and validation period (2003-2012) was used during the calibration and validation. The model was calibrated using 20 years (two-thirds) of the study period (1983–2002) and validated using the remaining one-third i.e., 10 years (2003–2012). Based on the modeling experience in Nepalese basins and judgement of the researcher, manual method was used for calibrating the model. The 15 most sensitive parameters were selected for calibration based on the sensitivity analysis. Parameters identified from the sensitivity analysis were varied in sequence of their relative sensitivity within their recommended ranges till the desired threshold of objective function was achieved. The hydrological station used for calibration and validation is shown in Table 3.5.

Table 3.5: Hydrological stations used for SWAT simulation

SN	Station Name	Year of Record	Calibration Period	Validation Period	Subbasin ID	Remarks
1	Arughat	1964-2015	1983-2002	2003-2012	12	DHM
2	Tatopani	2009-2010		2009	10	BG Ka
3	Machha Khola	2009-2010		2009	9	BG Kha
4	Kalleri	2013-2014		2013-2014	15	BGHP

3.5.2 Performance evaluation criteria

Moriasi et al. (2007) has discussed various graphical and statistical model evaluation techniques. Among them, three well-established statistical indicators: Nash–Sutcliffe efficiency (NSE), percent bias (PBIAS), and ratio of the root mean square error to the standard deviation of measured data (RSR) were used for model evaluation (Moriasi et al., 2015, 2012, 2007). In addition to these three, Kling Gupta efficiency (KGE) prescribed by (Gupta et al., 2009; Knoben et al., 2019; Pool et al., 2018) has also been used for the purpose of evaluation of the model.

Nash–Sutcliffe efficiency (NSE) is a normalized statistic that determines the relative magnitude of the residual variance ("noise") compared to the measured data variance ("information"). NSE indicates how well the plot of observed versus simulated data fits the 1:1 line (Nash and Sutcliffe, 1970) NSE is computed using Equation 3.9.

$$\mathrm{NSE} = 1 - \left[\frac{\sum_{i=1}^{12}(\mathrm{Q_{0i}} - \mathrm{Q_{ei}})^2}{\sum_{i=1}^{12}(\mathrm{Q_{0i}} - \overline{\mathrm{Q_o}})^2}\right] \qquad (3.9)$$

where, Q_{0i} and Q_{ei} are respectively observed and estimated discharge of day i, $\overline{Q_0}$ is the mean of the observed discharges. The optimum value is 1.0, with higher value indicating better model performance.

Percent bias (PBIAS) measures the average tendency of the simulated data to be larger or smaller than their observed counterparts. The optimal value of PBIAS is 0.0, with low-magnitude values indicating accurate model simulation. Positive values indicate model underestimation bias, and negative values indicate model overestimation bias

(Moriasi et al., 2007). PBIAS is, generally, expressed in percentage and is calculated using Equation 3.10.

$$\text{PBIAS} = \frac{\sum_{i=1}^{n} V_o - \sum_{i=1}^{n} V_e}{\sum_{i=1}^{n} V_o} \% \quad (3.10)$$

Where V_o and V_e are respectively the observed and simulated volumes of water for day i.

The root mean square error (RMSE) and the **s**tandard deviation of observed flow (σ_o) can be expressed as a ratio (RSR). It is commonly accepted that the lower the RMSE the better the model performance. RSR varies from the optimal value of 0, which indicates zero residual variation and therefore perfect model simulation, to a large positive value that indicates poorer model performance (Moriasi et al., 2007). RSR is calculated using Equation 3.11.

$$\text{RSR} = \frac{\text{RMSE}}{\sigma_o} = \frac{\sqrt{\sum(Q_{oi} - Q_{ei})^2}}{\sqrt{\sum(Q_{oi} - \bar{Q}_o)^2}} \quad (3.11)$$

The Kling–Gupta efficiency (KGE) that incorporates correlation, variability bias and mean bias (Gupta et al., 2009) is increasingly used for model calibration and evaluation. It is expressed using Equation 3.12.

$$\text{KGE} = 1 - \sqrt{(r-1)^2 + \left(\frac{\sigma_e}{\sigma_o} - 1\right)^2 + \left(\frac{\overline{Q_e}}{\overline{Q_o}} - 1\right)^2} \quad (3.12)$$

where, r is the correlation coefficient between the observed and simulated flows, σ_o and σ_e are standard deviations of observed and simulated flows respectively.

Table 3.6: General performance ratings statistics

Performance Rating	NSE	RSR	PBIAS	KGE
Very Good	0.75 < NSE ≤ 1.0	0 ≤ RSR ≤ 0.50	PBIAS ≤ ±10	0.50 < KGE ≤ 1.0
Good	0.65 < NSE ≤ 0.75	0.50 < RSR ≤ 0.60	±10 ≤ PBIAS ≤ ± 15	0 < KGE≤ 0.50
Satisfactory	0.50 < NSE ≤ 0.65	0.60 < RSR ≤ 0.70	±15 ≤ PBIAS ≤ ± 25	Positive
Unsatisfactory	NSE ≤ 0.50	RSR > 0.70	PBIAS ≥ ± 25	KGE < 0

(Gupta et al., 2009; Knoben et al., 2019; Moriasi et al., 2007)

3.6 Climate model selection

Climate models are the mathematical representation of the climate. The values of the predicted variables, such as precipitation, temperature, wind, humidity and atmospheric pressure are calculated by dividing the earth, ocean and atmosphere into grid points over the time. This study used the advanced envelope-based climate selection method to assess the projected future climates as described in Lutz et al. (2016). It is based on two general criteria for the selection of GCMs: (a) GCMs should be common to a pool of models with changes in temperature and precipitation, and (b) they must be available on a continuous daily scale. Based on these two conditions, 105 models for RCP 4.5 and 78 models for RCP 8.5 scenario were included in the initial pool of models. Climatic data (mean temperature -tas and precipitation - pr) were obtained from GCMs through KNMI climate explorer interface[1] for RCP4.5 and RCP 8.5 scenarios for the study area. The applied method uses three steps connecting future projection with past performance (1981-2005) as shown in Figure 3.7.

Step 1: In the first step, projected changes in future climate from the baseline period are computed for each GCM listed in the pool of models considering warm-dry, warm-wet, cold-wet and cold-dry corners to form an envelope. The 10^{th} and 90^{th} percentile values for change in mean temperature (ΔT) and percentage change in annual precipitation (ΔP) for each scenario were determined. These values represent the four corners of the spectrum of the projections for temperature and precipitation change. The tenth percentile value of ΔT and tenth percentile value for ΔP are in the 'cold-dry' corner of the spectrum. Likewise, the tenth percentile value of ΔT and 90^{th} percentile value for ΔP are in the 'cold-wet' corner, while 90^{th} percentile value of ΔT and 90^{th} percentile value of ΔP are in the 'warm-wet' corner. Similarly, 90^{th} percentile value of ΔT and tenth percentile value of ΔP fall in the 'warm-dry' corner of the spectrum. The proximity of the model runs to the 10^{th} and 90^{th} percentile values is derived using the distance metrics recommended by (Lutz et al., 2016). The 10^{th} and 90^{th} percentile values of the projected changes led to the choice of four combinations (dry-cold, dry-warm, wet-cold, and wet-warm) for each Representative Concentration Pathways (RCPs). The model nearest to the percentile values was considered for downscaling. A total of 20 models (5 models in each four corners) were selected in this step.

[1] https://climexp.knmi.nl/start.cgi

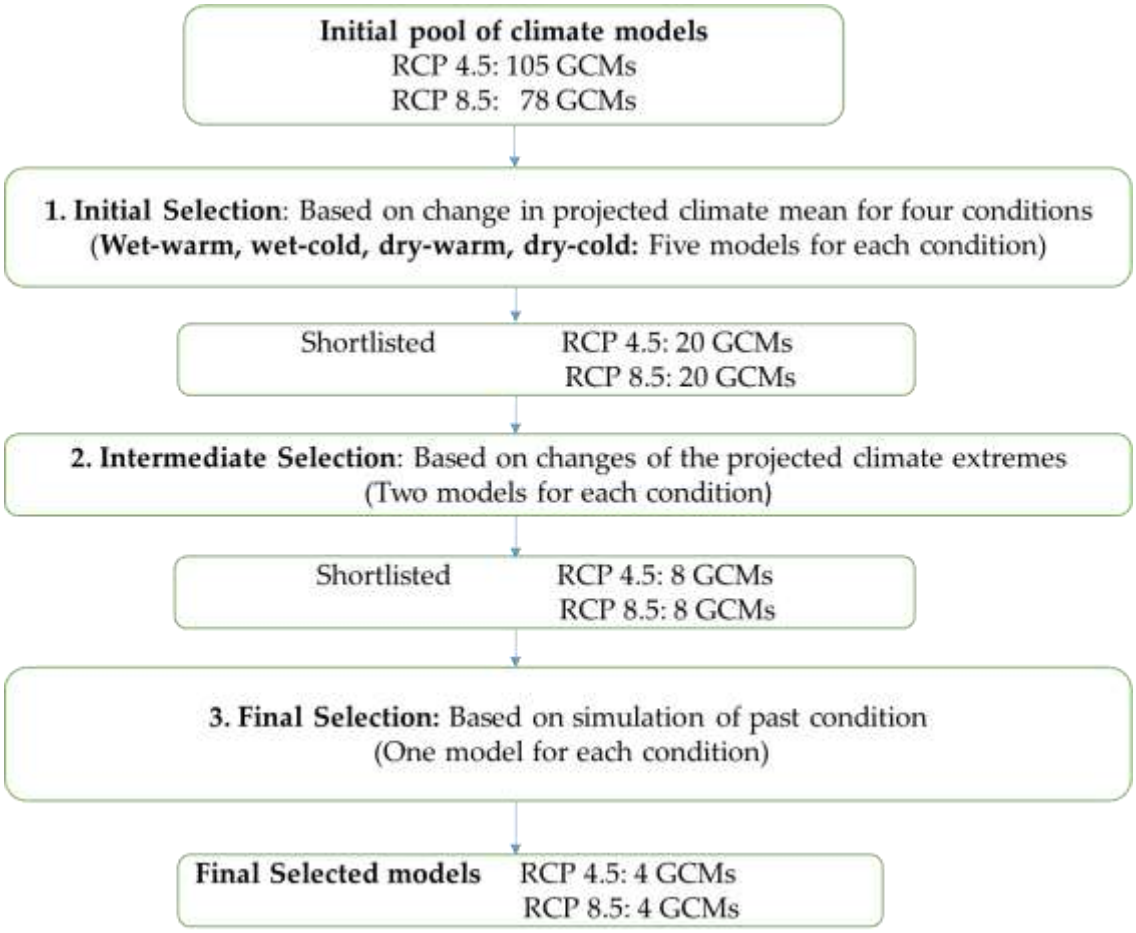

Figure 3.7: Climate model selection [Modified from (Lutz et al., 2016)]

Step 2: Two GCMs in each corner were selected in the intermediate step based on the projection of changes in climate extremes using four of Expert Team on Climate Change Detection and Indices (ETCCDI) as mentioned by (Lutz et al., 2016).They are R_{95P} [Precipitation due to extremely wet days (>95th percentile)], CDD [Consecutive dry days: maximum length of dry spell (P < 1 mm)], WSDI [Warm spell duration index: count of days in a span of at least 6 days where TX > 90th percentile (TX_{ij} is the daily T_{max} on day i in period j)] and CSDI [Cold spell duration index: count of days in a span of at least 6 days where TN < 10th percentile (TN_{ij} is the daily T_{min} on day i in period j)].

Step 3: In the final step, the ability of the selected GCMs to hindcast the past observation is evaluated between the selected two models in Step 2 of each of the four corners. In this step, Taylor method (Taylor, 2001) was used to evaluate the GCMs on the basis of three statistics: correlation coefficient, root mean squared error (RMS) and the standard deviation. The most reasonable GCM for each corner was selected from

the average of the highest Taylor score of the precipitation and temperature. In this way four models, one in each corner with the maximum score were considered for each RCP.

3.7 Bias correction method

When GCM model simulation of past climate is compared with observed climate, there is discrepancy. GCM model show bias in simulating past observed climate. This bias needs to be corrected or considered when the model is applied for any hydrological studies at regional or local level. Different methods for bias correction for climate variables like precipitation and temperature are discussed in different literatures that ranges from simple correction in the annual or monthly mean values to complex distribution fitting that corrects entire distribution.

Hawkins used delta approach/change factor approach, Lenderink used linear scaling approach for estimating future discharges of Rhine river (Hawkins et al., 2013; Lenderink et al., 2007). In this approach, the authors scaled the precipitation in control run by ratio of long-term averages of observations to long-term average of control run for each of 36; 10-day average precipitation. In case of local intensity scaling (LOCI) applied by (Schmidli et al., 2006), the precipitation is downscaled by using ratio of wet-day intensities between observations and the GCM with the adjusted wet-day threshold for GCM precipitation. Another tool for bias correction is power transformation method for precipitation discussed in various studies as, (Leander and Buishand, 2007; Terink et al., 2021) corrects mean and variance of the precipitation distribution. Besides, the approach that not only corrects the mean and variance but also the whole distribution, called as Distribution mapping or quantile mapping (Maraun, 2016; Piani et al., 2010b; Teutschbein and Seibert, 2013) is also widely used. In this study, distribution mapping was used for the bias correction.

3.7.1 Bias correction approach for precipitation

This study used the distribution mapping approach in which the mean, variance and the whole distribution is considered. Quantile mapping (QM) method was used to bias-correct the projected climate data at the climatic stations (Gudmundsson et al., 2012; Teutschbein and Seibert, 2013). QM corrects quantiles of GCM data to match those of observed data by creating suitable transfer functions explained in Equation 3.13.

$$X_{future,t}^{corr} = inverse\ ecdf\ {}_{baseline}^{obs}\left(ecdf_{baseline}^{GCM}\left(X_{future,t}^{GCM}\right)\right) \quad (3.13)$$

Where

$X_{future,t}^{corr}$ is the corrected estimate of $X_{future,t}^{GCM}$.

ecdf is empirical cumulative distribution function for reference time period,

$X_{future,t}^{GCM}$ is the raw GCM (projected value) in future at time t,

$ecdf_{baseline}^{GCM}$ is empirical cumulative distribution function of GCM for baseline period, and $inverse\ ecdf\ {}_{baseline}^{obs}$ is the inverse empirical cumulative distribution function of observation for baseline period.

We used the frequency adaptation method as described in (Themeßl et al., 2012) for the correction of extra dry days. This method was applied only in case of the frequency of dry days being higher in the baseline period in GCM data compared to the observed data.

3.7.2 Bias correction approach for temperature

In case of temperature, bias correction methodology correcting the mean and variance of temperature variable method described by Hawkins et al. (2013) is adopted in this study. This approach assumes that relationship between GCM temperature and observed temperature in reference period also remain same between future GCM projection and future observation. If $\bar{T}$ref and $\bar{O}$ref be area averaged GCM and observed temperature for reference period with means $M_{ref}^{T}$and and M_{ref}^{O} respectively and standard deviation σ_{ref}^{T} and σ_{ref}^{O} respectively and also, if $\bar{T}$proj is the GCM projected temperature in future, then corrected estimate of future observation $\bar{O}proj$ corresponding to $\bar{T}$proj is given by Equation 3.14.

$$\bar{O}proj = M_{ref}^{O} + \frac{\sigma_{ref}^{O}}{\sigma_{ref}^{T}} \times (\bar{T}proj - \bar{T}ref) \quad (3.14)$$

Where

$\bar{O}proj$ is bias corrected temperature for future. In the study, we applied month-wise bias correction such that M_{ref}^{T} and M_{ref}^{O}represent means; and σ_{ref}^{T} and σ_{ref}^{O} represent standard deviations of daily values for month under consideration in reference time.

The bias-corrected GCM data for each meteorological station was averaged to create a multi-model ensemble for each scenario. The projected future impacts of CC were

analysed based on the individual climatic scenarios and their ensembles using SWAT hydrological model.

3.8 Climatology under climate change

Percentage change in annual average precipitation and temperature under CC were compared with the baseline data for both emission scenarios (RCPs 4.5 and 8.5).

3.8.1 Climate change impact analysis of future flows

SWAT model developed and discussed in (Marahatta et al., 2021a) was applied to simulate the future flows by enforcing the projected GCMs CC data. Projected flows were divided into three 30-year time windows: Immediate Future (2021-2050), Mid Future (2046-2075) and Far Future (2070-2099). Projected flows were compared with corresponding monthly, seasonal, annual and fractional differences of extreme flows (Q_{90} and Q_{10}) of simulated baseline flows (1983-2012). Such comparison was made for all four scenario results, three future time windows and for both RCPs.

3.8.2 Frequency analysis

Annual one-day-maximum and -minimum flow series were extracted for each time window of all four scenarios for both RCPs along with baseline simulated flow. Gumbel distribution (Gumbel, 1941) was fitted to these time series in order to find the magnitude of high and low flows for selected return periods. Other flood related studies have applied hydro-economic (Devkota and Maraseni, 2018) and techno-social (Devkota and Bhattarai, 2018) perspective assessment methods.

3.8.3 Reservoir operating rule

For the change in revenue generation due to CC with respect to the baseline, this study used Budhigandaki Storage Hydroelectric Project as a case. For the planning purpose of the reservoir studies, generally applications of optimization techniques have been applied. Discussions in the American Society of Civil Engineers (ASCE) warn that gaps may exist between theory and practice, particularly in the area of real time reservoir operation (Ahmad et al., 2014; Miquel and Roche, 1986; William, 1985). The operating rules were derived such that dry season energy is maximized. Further, the inflow during the wet months first fills up the reservoir to a design level and extra water is used for energy generation (Devkota et al., 2022). Water collected in the reservoir during wet season is used up as per the operating rule in the dry months (December-May). At the

end of the dry season, the water level in the reservoir is maintained at the minimum operating level so that it can be filled by the next monsoon. The following were estimated using the derived operating rule at monthly time resolution:

i) Mean discharge (Q_T) available for the turbine,
ii) Net head (H),
iii) Power generated (P) using the average discharge and net head,
iv) Discharge (Q_{max}) available for use by the turbine after all the required conditions are fulfilled,
v) Maximum probable power and energy generation (P_{max} and E_{max}) for the baseline

3.9 Energy economics

Reservoir operating rules were derived as discussed in Section 3.8.3 based on the assumptions in (Devkota et al., 2022) such that dry season energy is maximized. These rules were applied for historical flow time-series of the baseline period. Additionally, applying the same operating rules, energy generation under RCPs 4.5 and 8.5 until the end of this century were also calculated. The physical properties of the reservoir are assumed to remain unaltered. Projected monthly, seasonal and annual energy generation was compared with the baseline values. The revenues from the generated energy for the baseline and considered climate scenarios were estimated using the power purchasing agreement (PPA) rates of the Nepal Electricity Authority (NEA 2017). The following governing equations have been used for calculating power, energy and revenue as discussed above:

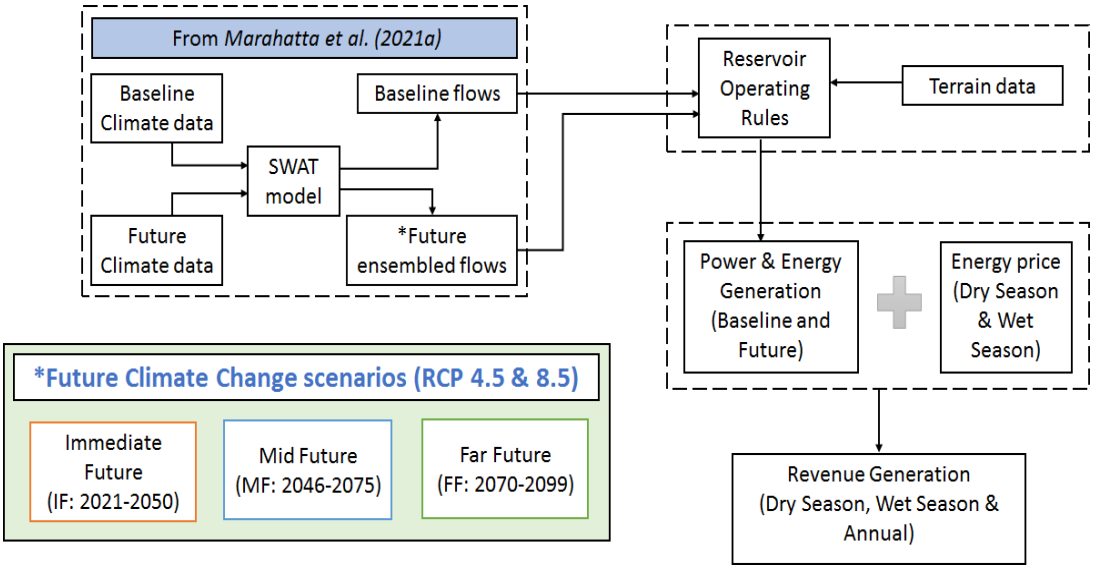

Figure 3.8: Methodological framework for energy economics study

Power generation of a hydroelectricity plant is calculated using Equation 3.15 (Devkota et al., 2022).

$$P_{i,j} = \eta . \gamma . Q_{Ti,j} . H_{i,j} / 1000 \quad (3.15)$$

Where

P = Generated power (MW)

η = Overall efficiency of the plant (0.93) (considered a constant)

γ = Unit weight of water (9.8 kN/m^3) (considered a constant)

Q_T = Flow passing through the turbine (m^3/s) and

H = Available net head (m)

i = index for the month

j = index for the year

Energy generation is estimated as the product of the power and the number of days of operation in a given month in compatible units Equation 3.16.

$$E_{i,j} = P_{i,j} . n_{i,j} . (\frac{24}{1000}) \quad (3.16)$$

Where

E = Energy generation (GWh)

n = Number of days

Change in energy generation is estimated by Equation 3.17.

$$\Delta E_{i,j} = \frac{E_{i,j,CC} - E_{i,base}}{E_{i,base}} . 100 \quad (3.17)$$

Where

$\Delta E_{i,j}$ = Change in the total energy generated expressed as percentage

$E_{i,j,CC}$= Total energy generated in the i^{th} month of the j^{th} year of the CC scenario

$E_{i,base}$= Total energy generated in the i^{th} month of the base case

The PPA rates vary with season. It is assumed that these rates do not change during the period of analysis. Adopted exchange rate is: 1 USD = 119 NRs (NRB, 2021). The revenues are calculated using the following equations:

$$R_{i,j} = E_{i,j} . PPA_i \quad (3.18)$$

$$DR_j = \sum_{i=Dec}^{May} R_{i,j} \quad (3.19)$$

$$WR_j = \sum_{i=Jun}^{Nov} R_{i,j} \quad (3.20)$$

$$AR_j = \sum_{i=Jan}^{Dec} R_{i,j} \quad (3.21)$$

Where

$R_{i,j}$= Revenue generated (USD)

DR_j = Total dry season revenue

WR_j = Total wet season revenue

AR_j = Total annual revenue

Change in revenue is estimated using the Equations 3.22 to 3.25.

$$\Delta R_{i,j} = \frac{R_{i,j,CC} - R_{i,base}}{R_{i,base}} . 100 \quad (3.22)$$

$$\Delta DR_j = \frac{DR_{j,CC} - DR_{j,base}}{DR_{j,base}} . 100 \quad (3.23)$$

$$\Delta WR_j = \frac{WR_{j,CC} - WR_{j,base}}{WR_{j,base}} . 100 \quad (3.24)$$

$$\Delta AR_j = \frac{AR_{j,CC} - AR_{j,base}}{AR_{j,base}} . 100 \quad (3.25)$$

Where

$R_{i,base}$= Baseline period monthly revenue generation

$R_{i,j,CC}$= CC scenario monthly revenue generation

$\Delta R_{i,j}$ = Difference in the total revenue

ΔDR_j = Difference in dry-season revenue

ΔWR_j = Difference in wet-season revenue

ΔAR_j = Difference in annual revenue

The annual profit/loss is calculated as the change between the revenue generation corresponding to the energy generation and the operation and maintenance (O&M) cost annually. Mathematically,

$$\pi_j = AR_j - C_{O\&M,j} \quad (3.26)$$

Where

π_j = Annual profit/loss for the j^{th} year

$C_{O\&M,j}$= Annual operation and maintenance cost

The change in annual profit is estimated by Equation 3.27.

$$\Delta\pi_j = \left(AR_{j,CC} - C_{O\&M,j,CC}\right) - \left(AR_{j,base} - C_{O\&M,j,base}\right) \quad (3.27)$$

For convenience, it is assumed that the annual O&M cost is unchanged during the baseline and CC scenarios (i.e., $C_{O\&M,j,base} = C_{O\&M,j,CC}$).

Adhering to the above assumptions, change in future revenue generation compared to the baseline case is computed using Equation 3.28.

$$\Delta\pi_j = AR_{j,CC} - AR_{j,base} \quad (3.28)$$

CHAPTER 4

RESULTS AND DISCUSSION

4.1 Background

This chapter presents a detail evaluation of energy economics of the Budhigandaki river; as a continuum of climate change-river flow-hydroelectricity generation-energy economics. The results are presented in six separate sections. Starting from the analysis of the precipitation, temperature and flow in the first section, impact of the flow variations in resources loss and power production in the second section. This study utilizes SWAT to assess the impact of CC in river hydrology of the study basin, section three is devoted to evaluate its simulated results. In the next section, i.e., in section four, why hydrological simulation technique, using SWAT model, is the best flow estimation tool in ungauged basin is revealed. The fifth section describes hydro-climate of BRB due to different projected CC scenarios and the consequent impact in river hydrology. The final section highlights the result of the changes in hydroelectric energy production because of such change in flow and subsequent revenue change compared to the baseline values of Budhigandaki Hydroelectric Project (BGHP).

4.2 Historical perspective of hydrology and climatology of the study basin

The climatic data is the most important parameter in any hydrological study. The climatic characteristics and their different parameters are all important factors in the various analyses performed in the present study. In this study altogether 9 climatic stations have been used. In addition, gridded data of two stations lies in Tibet of Peoples Republic of China have also been used.

4.2.1 Precipitation

The BRB receives nearly 1530 mm of annual precipitation with 74% of rainfall in monsoon (June-September) season (Figure 4.1). However, the high-altitude stations received 50-60% of the annual precipitation in monsoon season. The BRB receives highest rainfall in July (23%) and November is the dry month receives less than 1% of total annual precipitation, during the winter (December-February) season, the precipitation is about 4%. Windward side of the mountain barrier receives major portion of rainfall while the leeward side remains dry. The stations located at Jagat, Arughat,

Gorkha and Dhading shows the decreasing trends in precipitation and maximum 24 hours rainfall is in increasing trend however it is not statistically significant. Moreover, the increase in precipitation in pre monsoon months will have positive impact on the water availability of the rivers.

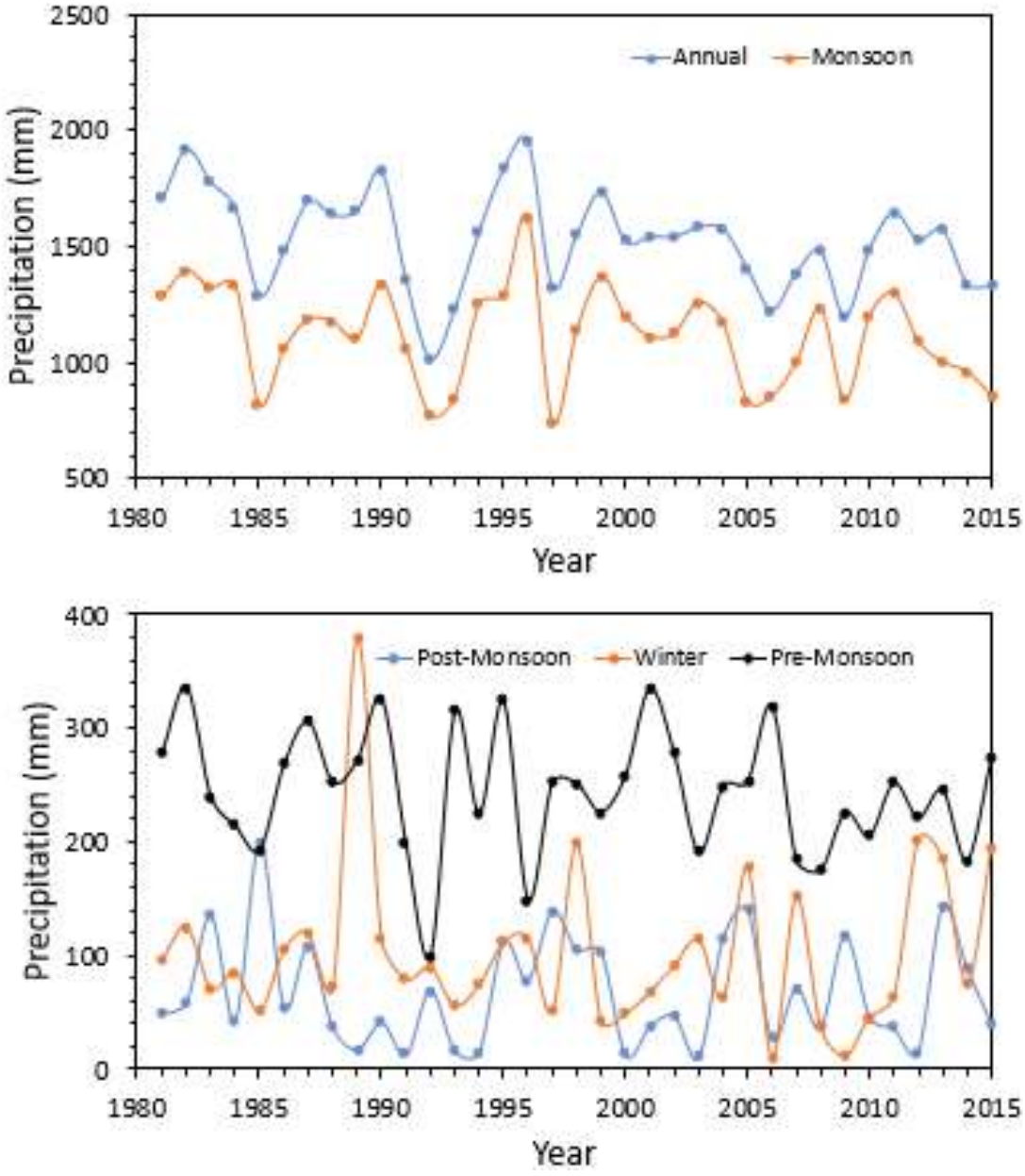

Figure 4.1: Annual and seasonal rainfall pattern of BRB

4.2.2 Temperature

May is the hottest month with mean temperature up to 24°C and maximum temperature up to 38°C in the dam site area of BGHP. Temperature is below 0°C in the high-altitude area. January is the coldest month with mean temperature ranging from 12°C to 15°C

and minimum temperature 6°C to 9°C in the dam site. Figure 4.2 depicts the variation in annual average value of the maximum temperature and the minimum temperature over the years. An increasing trend in both maximum and minimum temperature was found in BRB; the maximum temperature is projected to increase at a greater rate (0.08ºC/year, *p>0.05*) than the minimum temperature (0.04ºC/year, *p>0.05*).

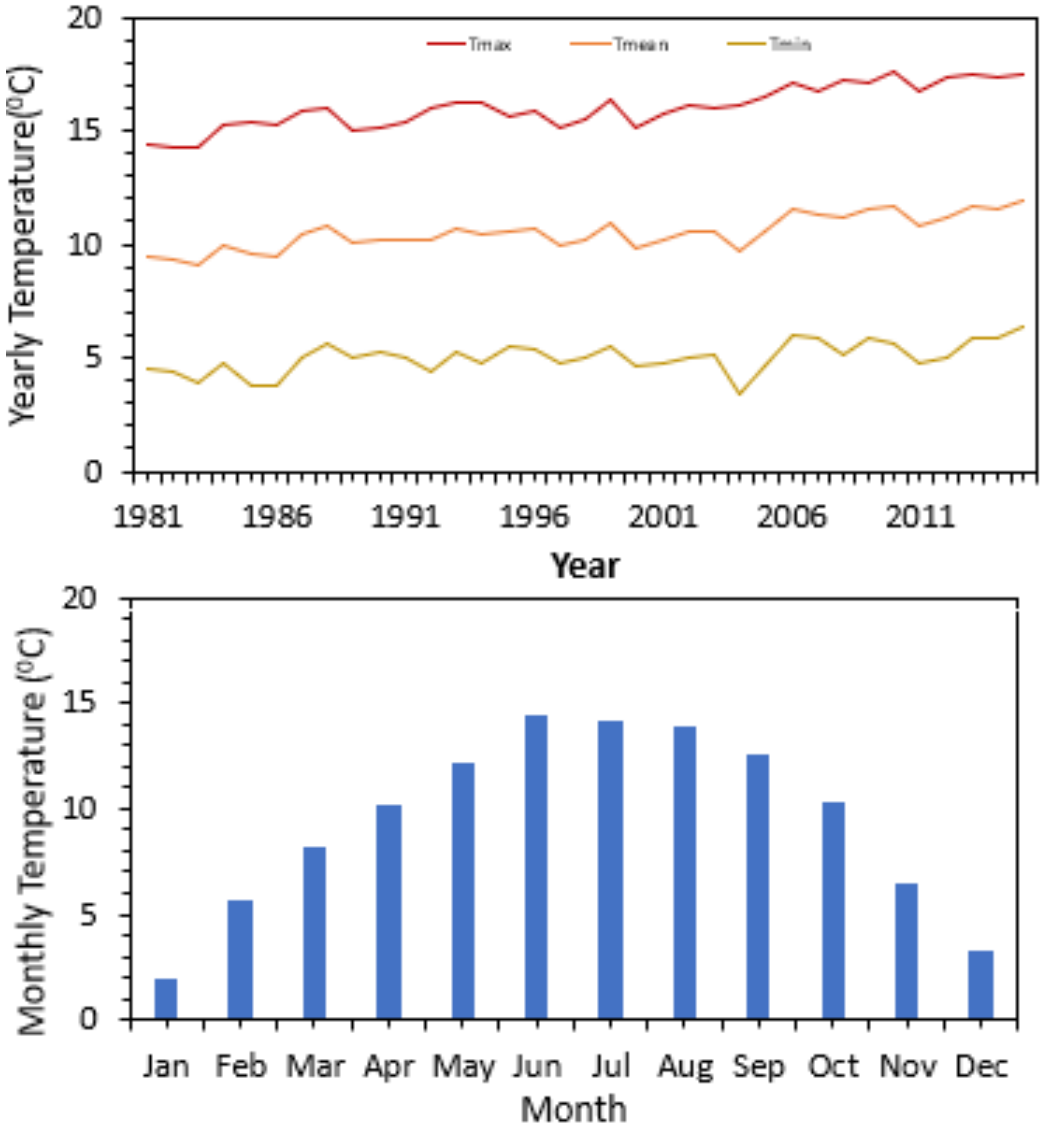

Figure 4.2: Annual maximum, minimum mean and monthly mean temperature of BRB

4.2.3 Flow analysis

i) General characteristics of flow

The stream flow data analyzed for Budhigandaki river at Arughat from 1964 to 2015 is shown in Figure 4.3. From the analysis it is found that the long-term annual average

and the standard deviation of the flow of this river at Arughat are respectively 160 and 18 m^3/s. It can be seen from Figure 4.3 that the flow in Budhigandaki river start to increase from March to August and then decreases gradually, with the minimum flow occurring in February (30 m^3/s) and maximum in August (437 m^3/s). It shows that the monthly variation in flow is as high as 15. The range of flow of each month is also presented in the figure. Maximum variation in flow (maximum flow: minimum flow) was found in the month of March (3.8) and minimum in August (1.8). The flow variation is lower for annual average, with minimum value of 120 m^3/s occurred in 2009 while the maximum value is 210 m^3/s in 2010. It is because of the smoothing phenomena. Contrary to it, the daily variation in flow is quite high, minimum 18 and maximum 1457 m^3/s.

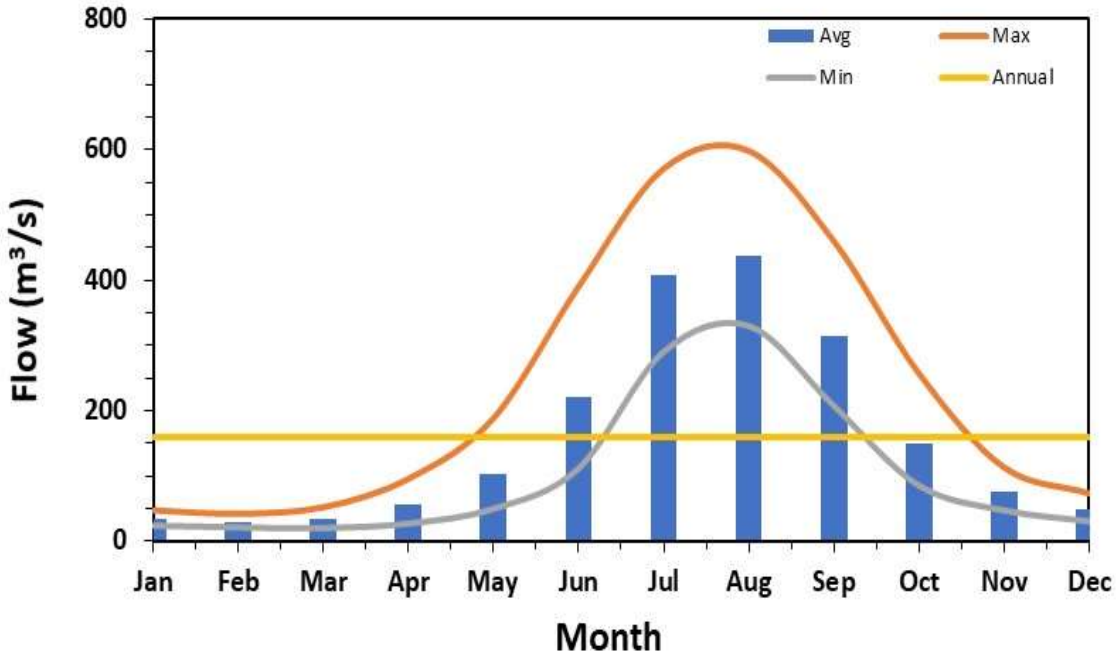

Figure 4.3: Flow statistics of Budhigandaki river at Arughat

The river flow in Nepal is high during the monsoon (June-September) because of the active south-west monsoon. The flow starts decreasing in the post monsoon (October and November) season but still remains quite high. The winter season (December-February) witnesses decreased river flows. In the pre-monsoon season (March-May), snowmelt starts due to the rise in temperature which leads to gradual increase in the river flow. The share of monsoon and post monsoon is cumulatively 84% of the total annual flow while the dry season flow contributes only 16%. The instantaneous

minimum flow which was observed in March 16, 1967 is 17 m^3/s and the maximum flow occurred in July 3, 1999 is 2060 m^3/s. It shows that the mean instantaneous flow fluctuations occurring in between 1964 to 2015 is more than 30 times.

ii) Flow duration curve

Design flow is required while designing any hydraulic structures which may be to dispose the water from the system or use of water for an intended purpose. For example, design flow in RoR hydroelectric plant is generally taken as Q_{40} of the annual flow, i.e. it is the threshold flow that equals or exceeds 40% of the days in a year (DOED, 2018b). Such design flow is estimated using flow duration curve (FDC) prepared by using historical daily flow data. It is given in Figure 4.4 for Arughat station. The FDC for Arughat (Figure 4.4) shows that the Q_{10}, Q_{40}, Q_{50}, Q_{60} and Q_{90} are respectively, 413, 125, 84, 59, and 30 m^3/s.

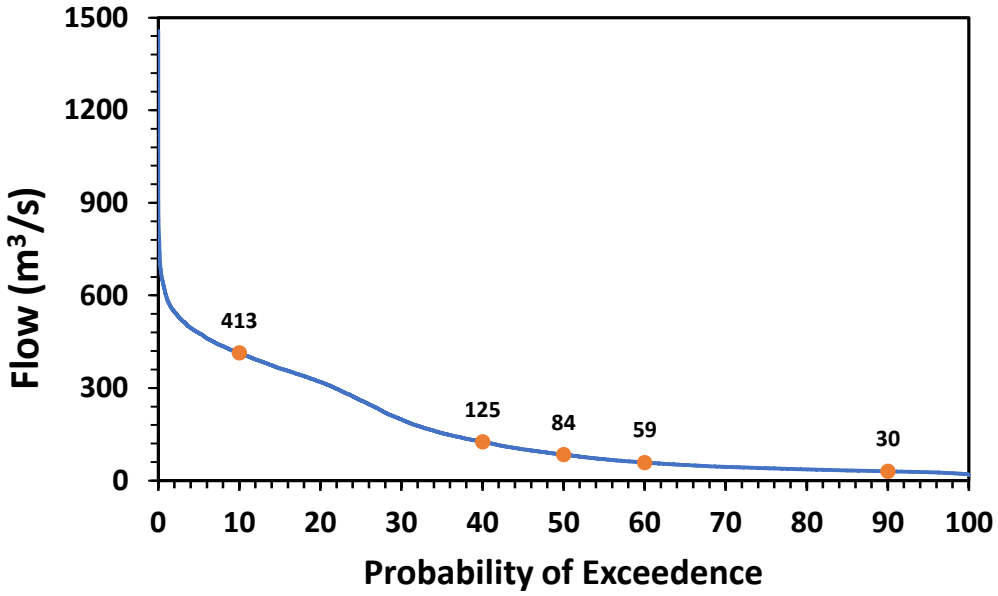

Figure 4.4: Flow duration curve of Budhigandaki river at Arughat

4.3 Impact of flow variation and power production

4.3.1 Impact of flow variation

Impact of flow variation in loss in water resources and power production was evaluated in this study considering RoR project utilizing the flow available at Arughat using the data of 1964-2015. Although the power production is a function of quantity of flow and

net head, only considering quantity of flow is enough for RoR project, as net head almost constant in both wet and dry seasons. Here, dry season refers to six months of the year (December to May) as considered as in (BGHP, 2015). The monsoon and post-monsoon months are in the contrary taken as wet months when the flow in the river is ample for power production as presented in the preceding section.

Table 4.1: Implication of flow variation for run of the river power plant

Case/Flow	**Condition**	**Loss/Gain Amount in Flow (*dQ*)**	**Power Loss or Gain with respect to Design Value**	**Remarks** **Spill: Resource Loss**
Case 1: Q1-1	$Q > Q_{LTMA}$ & $Q > Q_{design}$	0	No	Water Spill $(Q - Q_{design})$
Case 1: Q1-2	$Q < Q_{LTMA}$ & $Q > Q_{design}$	0	No	Water Spill $(Q - Q_{design})$
Case 1: Q1-3	$Q < Q_{LTMA}$ & $Q < Q_{design}$	$Q - Q_{design}$	Loss (-)	No Spill
Case 2: Q2-1	$Q > Q_{LTMA}$ & $Q > Q_{design}$	$Q_{design} - Q_{LTMA}$	Gain (+)	Water Spill $(Q - Q_{design})$
Case 2: Q2-2	$Q > Q_{LTMA}$ & $Q < Q_{design}$	$Q - Q_{LTMA}$	Gain (+)	No Spill
Case 2: 2-3	$Q < Q_{LTMA}$ & $Q < Q_{design}$	$Q - Q_{LTMA}$	Loss (-)	No Spill

The flow in a river at a particular day can be divided into 6 types with respect to long term mean monthly (Q_{LTMA}) and design flows (Q_{design}) as given in Table 4.1. These flows are clustered into two cases. Case 1 can be taken as a flow in wet season in which Q_{LTMA} is, generally, higher than the design discharge. Case 2 resembles dry season flow in which season Q_{LTMA} is generally lower than Q_{design}. The flow at a particular day can be higher or lower than both Q_{design} and Q_{LTMA} or in between them. Such deviation of

flow ($\pm dQ$)) from Q_{LTMA} can be advantageous, disadvantageous or neutral for the project as shown in Table 4.1.

As shown in Figure 4.3 the monthly discharge varies year to year significantly from the long-term average value of a considered month, say April (from 27 in 2014 to 97 m^3/s in 1982). Variation daily discharge is even higher as discussed in the previous section. Spill occurs if the daily discharge exceeds the design discharge. However, when the discharge is less than the design value, less electricity is generated. Three design discharges (Q_{90}, Q_{60} and Q_{40}) have been adopted for the analysis.

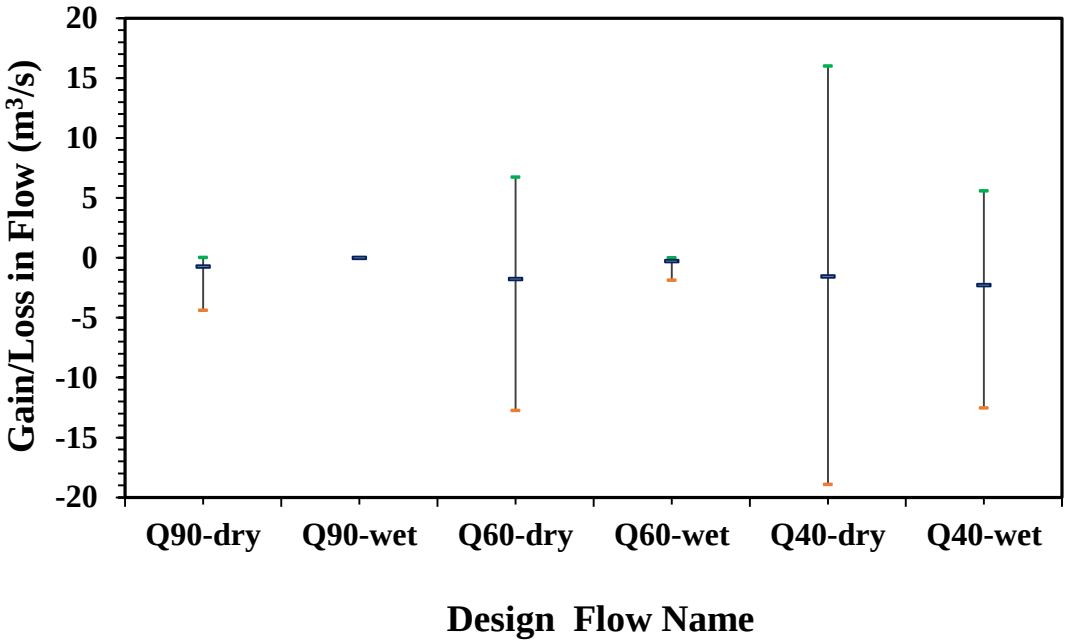

Figure 4.5: Loss/gain in flow for different probabilities of flow variation by season

Figure 4.5 depicts the range of loss/gain in flow for the different cases discussed above. It is noted here that $Q_{90\text{-dry}}$ refers to design discharge of Q_{90} season considered is dry and so on. It gives altogether 6 cases as shown in the figure. The long-term average values of loss in flow are -0.72, -1.76 and -1.54 m^3/s for the dry season and 0.0, -0.27 and -2.26 m^3/s for wet season respectively for design discharges of Q_{90}, Q_{60} and Q_{40}. These results show that in an average there is a loss of resources in RoR project because of flow variation in the river. However, the gain in resources in some years and loss in others years are there too. For example, maximum gain and loss occur for design discharge of Q_{40} i.e., 16 m^3/s gain in a year and 19 m^3/s loss in another year can be seen in Figure 4.5. The lower value of average loss for Q_{90} flow is because of smaller design

flow, which is daily flows are less likely to be less than this design flow. Even in this case some of the dry season flows are lower than this value whereas there is no loss in water resources in wet season because of all daily discharge values exceeding the design discharge. In other cases, the daily discharges may or may not be equal to long term mean values or the design discharge values. The negative impact of flow variation indicates less water available for electricity generation in all the scenarios except for Q_{90} of the wet season. Therefore, in order to assess the full extent of uncertainty in electricity generation, energy calculation needs to be based on daily flows.

Out of 51 years, the number of years in which the flow is less than the anticipated values (Q_{LTMA} for dry season and Q_{design} for wet season) are shown in Figure 4.6. From the figure we can see that the number of years in which the flow is less than 50% in all cases except the Q_{90}-wet season. The numbers of years in which wet season loses in the flow are 32 and 36 for Q_{60} and Q_{40} respectively. While, for the dry case, these values are respectively 35 and 28.

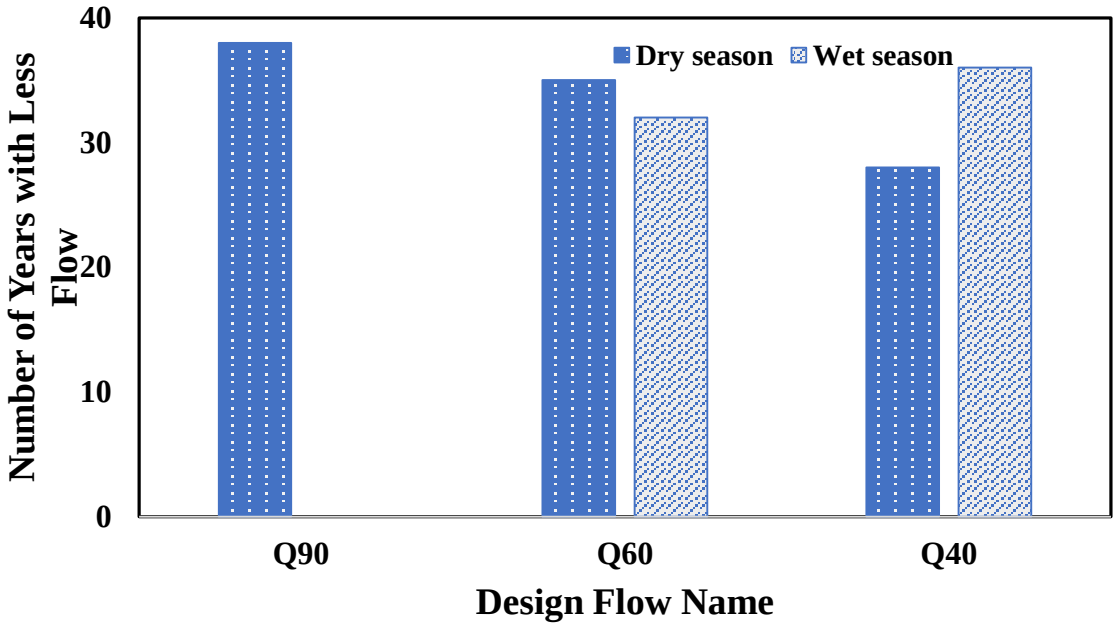

Figure 4.6: Number of loss years in different scenarios

4.3.2 Impact of flow variation on power production

The power generation depends on the daily flow for the dry season which is usually less than the design discharge. However, in the case of wet season, the power generation is governed by the design discharge which is generally less than the daily discharge. The flow is less than the long-term monthly discharge by 1.5 m^3/s (~3%) for the dry

season while it is 2.3 m^3/s (~ 2%) with respect to design discharge for the wet season. However, the annual variation in power production is quite high. It can be seen from Figure 4.7 that the probability of losing and gaining power generation in a year are as high as 40% and 30% respectively in the dry season. Likewise, the chances of power loss and gain are 10% and 5% respectively in the wet season. Additionally, the probability of producing less power than the design values are seen in 11 consecutive years (> 20%) in the dry season and 27 consecutive years (>50%) in the wet season.

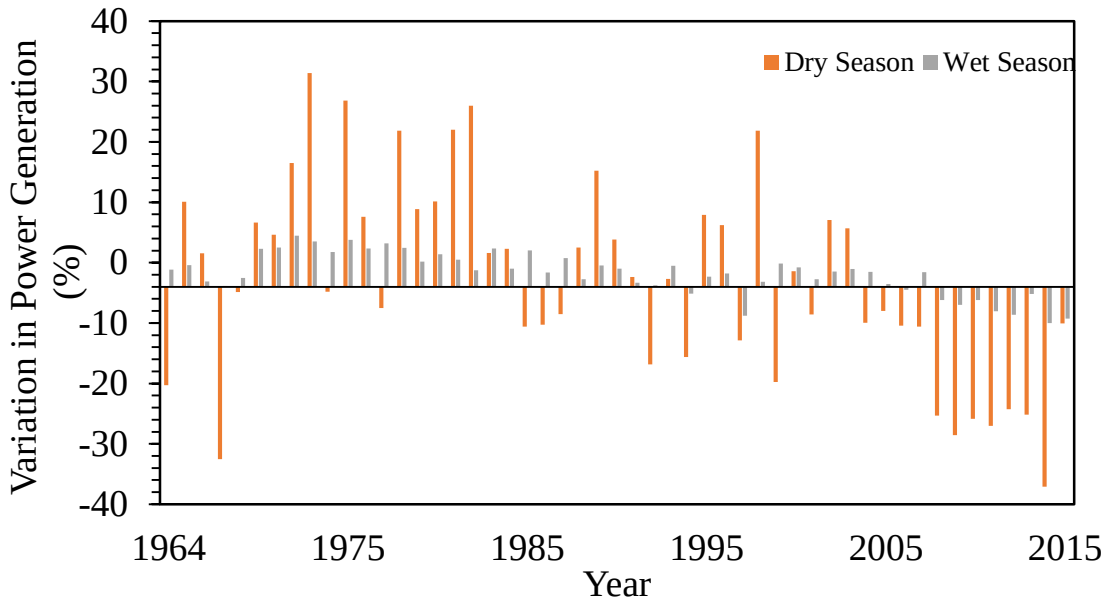

Figure 4.7: Seasonal variation in power generation of RoR projects in the BRB

The findings of the historical flow analysis of half century of the observed hydrological data at Arughat hydrological station (#445) as presented in this section is attached as **Appendix 1**.

4.4 Evaluation of SWAT model for flow simulation

4.4.1 Calibration and validation of the model

The developed SWAT model for the Budhigandaki basin, as discussed in chapter four, should be well calibrated and validated before using it for flow simulation under different climatic scenarios. In this study, the model is calibrated and validated for Arughat gauging station using 30 years of daily flow data (1983-2012). Further, calibrated model is further validated using short term data available two at upstream and one at downstream of calibrated station, i.e., (i) intake site of Budhigandaki KA

(BG KA), (ii) intake site of Budhigandaki KHA (BG KHA) lying upstream and (iii) 1200 MW Budhigandaki Hydroelectric Project (BGHP) dam site lying downstream of Arughat station.

a) Calibration and validation at Arughat gauging site

The SWAT model is calibrated using 20 years (two-thirds) of the study period (1983–2002) and validated using the remaining one-third 10 years (2003–2012) similar to the ones used by (Abbaspour et al., 2015; Aboelnour et al., 2020; Athira and Sudheer, 2021; Gupta et al., 2021; Havrylenko et al., 2016; Liu et al., 2021; Luo et al., 2020; Negewo and Sarma, 2021). The 15 most sensitive parameters were selected for calibration after the sensitivity analysis. The final adopted values of the parameters (in alphabetic order) are shown in Table 4.2. It can be seen that two different sets of parameters directly influence the surface runoff (CN2 and OV_N) and lateral flow (LAT_TIME and SURLAG) whereas five parameters (ALPHA_BF, GWDELAY, GWQMIN, SOL_AWC and SOL_Z) impact the baseflow from the basin. There are six snow related parameters (snowfall temperature (SFTMP), snowmelt temperature (SMTMP), snow cover (SNOCOVMX), degree-day factors (SMFMX, SMFMN) and temperature lapse rate (TLAPS)) which are used to calculate the snow component of the total flow. Thus, it is seen that the basin demonstrates a high degree of complexity among the different interacting components of the hydrological cycle.

Table 4.2: Selected SWAT parameters and their calibrated values.

Parameter	**Unit**	**Final Value**	**Allowable Range ***	**Impacted Component of Flow**
ALPHA_BF	day	0.01	0–1	Baseflow
CN2		50–93	35–98	Surface runoff
GW_DELAY	day	55	0–500	Baseflow
GWQMIN	mm	200	0–5000	Baseflow
LAT_TIME	day $s/m^{1/3}$	18	0–180	Lateral flow
OV_N		0.5	0.01–0.41	Surface runoff
SFTMP	°C	4.5	−5–5	Snow

Parameter	Unit	Final Value	Allowable Range *	Impacted Component of Flow
SMFMN	mm/°C/day	2.5	1.7–6.5	Snow
SMFMX	mm/°C/day	4.5	1.7–6.5	Snow
SMTMP	°C	2.5	−5–5	Snow
SNOCOVMX	mm	400	0–1.0	Snow
SOL_AWC	mm/mm	0–0.3	0–1.0	Baseflow
SOL_Z	mm	0–50	0–3500	Baseflow
SURLAG	day	1.0	1–10	Lateral flow
TLAPS	°C/km	−6.5	−10–10	Snow

(Marahatta et al., 2021d)

Simulated and observed hydrographs for the calibration and the validation periods at Arughat on daily and monthly time steps are shown in Figure 4.8 and Figure 4.9. The performance indicators (NSE, PBIAS, RSR and KGE) obtained in calibration and validation using daily data, along with mean and standard deviation of observed and simulated flows, for different periods are presented in Table 4.3. The mean and standard deviation of the observed (simulated) flows are 168 (170) m^3/s and 167 (168) m^3/s, respectively for the calibration period and 154 (181) m^3/s and 163 (180) m^3/s, respectively for the validation period (Table 4.3). It can be seen from Figure 4.8 and Figure 4.9 that SWAT simulates the discharge very well and the hydrographs are well correlated the rainfall at both daily and monthly timescales. It is also evident from the scatter plots of simulated vs. observed daily flows of these periods (Figure 4.10). The difference in cumulative volume between the simulated and observed flow is very small for the calibration period (Figure 4.11a), however, the model has over-estimated the flow in the validation period (Figure 4.11b).

The NSE, PBIAS, RSR and KGE values for the calibration period are, respectively, 0.78, −1.46%, 0.47 and 0.89. Similarly, for the validation period, the values of NSE, PBIAS, RSR and KGE are 0.81, −17.1%, 0.44 and 0.79, respectively (Table 4.3). Based on the criteria prescribed by (Gupta et al., 2009; Knoben et al., 2019; Moriasi et al., 2015, 2007; Nash and Sutcliffe, 1970; Pool et al., 2018), all these indices fall in the 'very good' category except PBIAS in the validation period ('satisfactory' range). The

model performance parameters for monthly flows are even better for monthly timesteps 0.88 (NSE), −6.5% (PBIAS), 0.35 (RSR) and 0.91 (KGE).

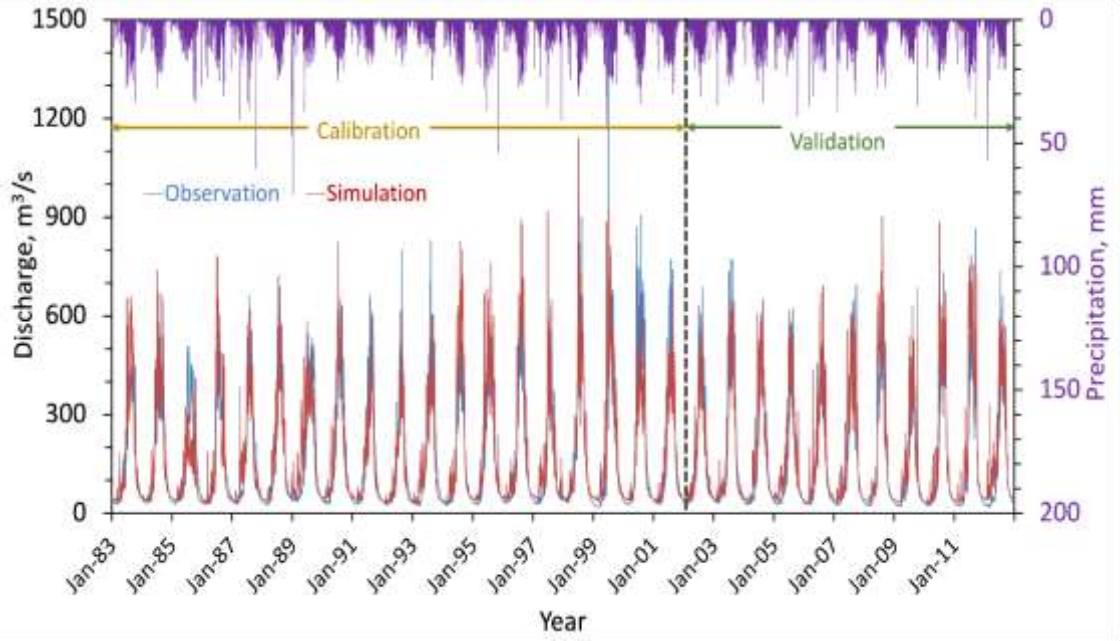

Figure 4.8: Calibration and validation hydrographs at daily timestep at Arughat station.

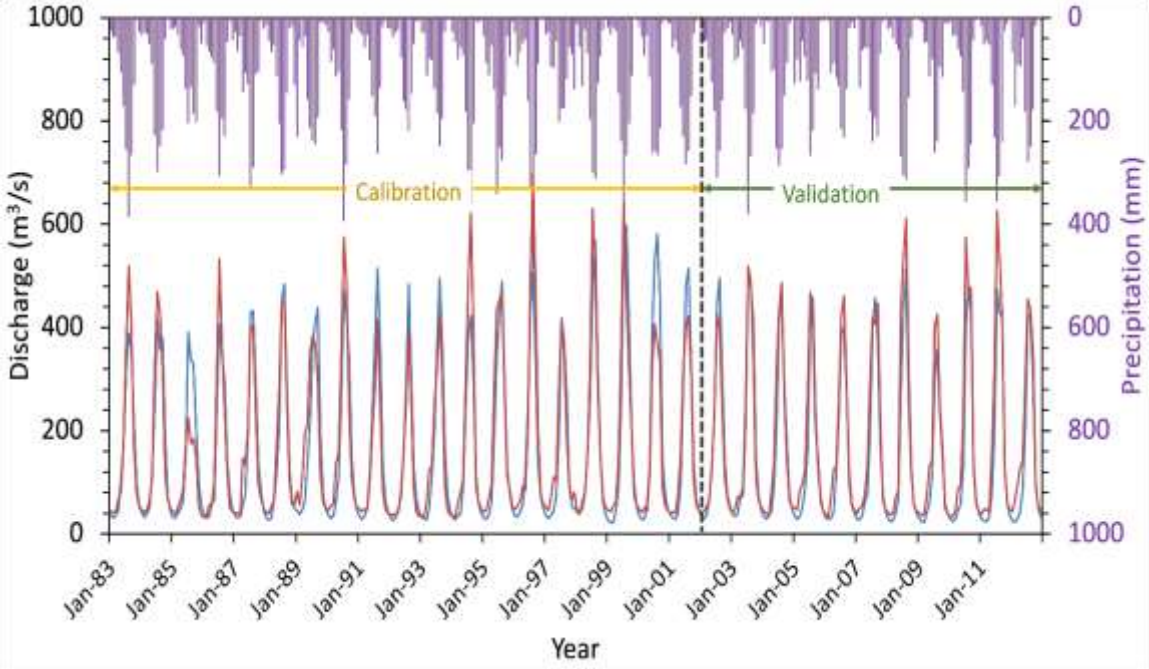

Figure 4.9: Calibration and validation hydrographs at monthly timestep at Arughat station

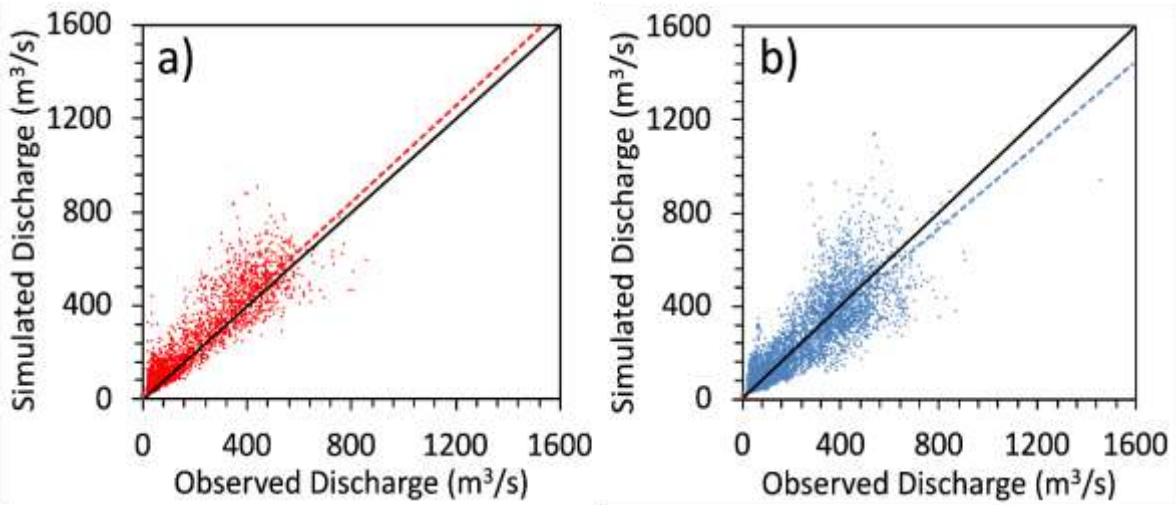

Figure 4.10: Correlation between observed and simulated daily flows in (a) calibration and; (b) validation

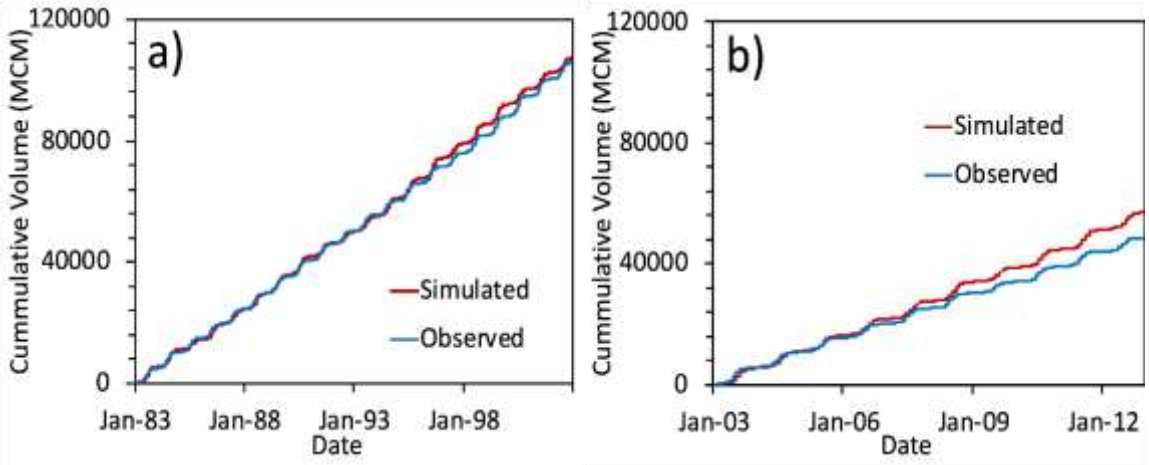

Figure 4.11: Cumulative volume balance in the (a) calibration period; and the (b) validation period

Table 4.3: Model calibration and validation statistics at Arughat station

Statistic (Years)	**Mean Flow (m^3/s)**		**Standard Deviation (m^3/s)**		**Performance Indicators**			
	Observed	**Simulated**	**Observed**	**Simulated**	**NSE**	**PBIAS**	**RSR**	**KGE**
Calibration (1983–2002)	168	170	167	168	0.78	−1.46%	0.47	0.89
Validation (2003–2012)	154	181	163	180	0.81	−17.1%	0.44	0.79
Entire Simulation (1983–2012)	163	174	166	172	0.79	−6.38%	0.46	0.88

The performance indices of this study are found better or comparable to similar studies carried out in other Nepalese basins. For example, for Chameliya, Karnali, Bheri, Kaligandaki, Indrawati, Tamakoshi, Arun and Tamor basins of Nepal, NSE (and PBIAS) values are respectively 0.75 (+5.1%), 0.84 (−14.2%), 0.70 (−4.4%), 0.78 (−4.0%), 0.72 (-), 0.76 (−1.7%), 0.81 (−6.8%) and 0.85 (+4.3%) for calibration period while these values are 0.65 (-9.3%), 0.84 (−15.4%), 0.71 (−8.9%), 0.8 (+9.6%), 0.87 (-), 0.84 (+5.2%), 0.58 (+24.6%) and 0.89 (+5.5%) respectively for validation period (Bajracharya et al., 2018; Bharati et al., 2019; Bhatta et al., 2019; Y. Mishra et al., 2018; Palazzoli et al., 2014; Pandey et al., 2020a, 2019; Shrestha et al., 2016b). Similarly, NSE (and PBIAS) values of Gilgelabay basin of Ethiopia, Gurupura basin of India and Tizinafu basin of Western China were found to be respectively 0.69 (+4.8%), 0.83 (+17.5%) and 0.71 (+5.79%) for calibration period while these values for validation period were 0.68 (+4.9%), 0.85 (−3.9%) and 0.64 (−18.0%), respectively (Duan et al., 2018; Sharannya et al., 2018; Tegegne et al., 2017). From the graphical comparison shown in Figures 4.10 to 4.13 and the performance rating given in Moriasi et al., 2007, Gupta et al., 2009 and Knoben et al., 2019 show that the SWAT model developed in this study is well calibrated and validated at Arughat.

b) Additional validation of SWAT at supplementary stations

Previous studies, e.g., Bharati et al. (2019) and Pandey et al. (2020a) have used multi-site approach to calibrate the SWAT model. However, in the current study, the model is calibrated at a single point and validated at three supplementary points too which are upstream and downstream of calibration station, Arughat. It is worth mentioning that the researcher and team carried out rigorous discharge measurements and prepared rating curves at these three locations during 2009–2010 (BG KA and BG KHA) and 2013–2014 (BGHP damsite) which has been used for the additional validation. The results of the validation have been shown in Figure 4.12 and Figure 4.13. The NSE, RSR, PBIAS and KGE values for BG KA are 0.66, 0.58, 21% and 0.59 and 0.58, 0.65, 13% and 0.54 for BG KHA, respectively. Similarly, their respective values for the BGHP damsite are 0.91, 0.31, 7.88% and 0.81. As per the rating criteria by (Gupta et al., 2009; Knoben et al., 2019; Moriasi et al., 2015, 2007; Nash and Sutcliffe, 1970; Pool et al., 2018), the model performance is “very good” at the BGHP dam site, “good” at BG KA and “satisfactory” at BG KHA. This independent validation at supplementary sites reveals that the calibrated model at Arughat can simulate the flow well for the

Budhigandaki Basin up to the Trishuli confluence, although the performance is better in the downstream reach which is the site of interest for this study.

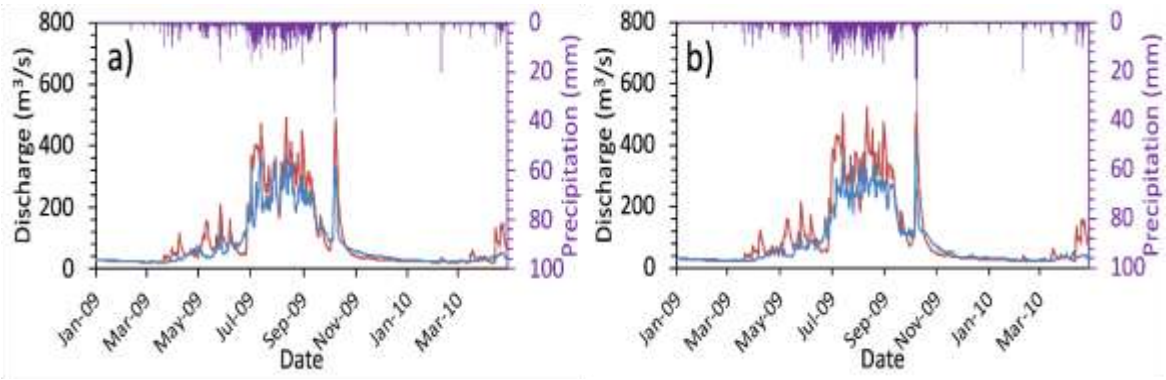

Figure 4.12: Additional validation of flows at supplementary stations in upstream site (a) Budhigandaki KA and (b) Budhigandaki KHA

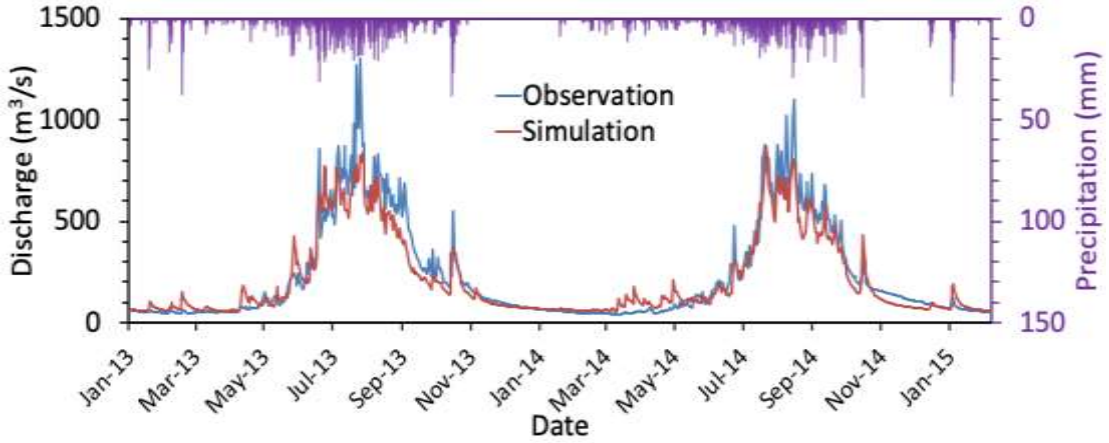

Figure 4.13: Additional validation of flows at supplementary station at BGHP dam site

c) Flow duration curve

The flow duration curve (FDC) was prepared from the observed as well as simulated daily flow data at Arughat (Figure 4.14). From the figure, it can be seen that the FDC of both observed and simulated flow are also very close to each other. All these results show that SWAT model developed for BRB is capable enough to simulate the flow in this basin for different climatic conditions.

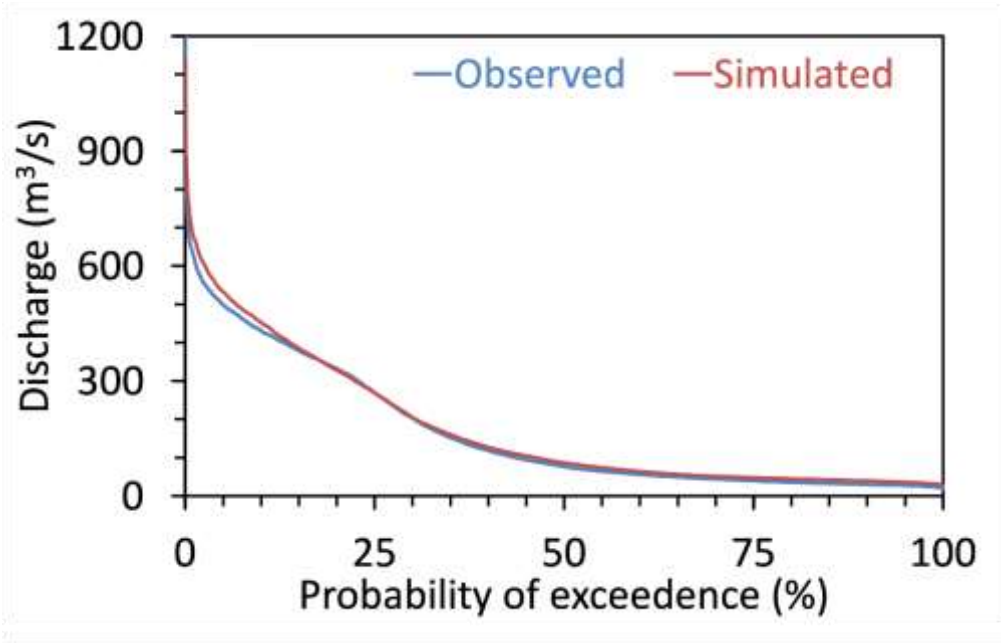

Figure 4.14: Flow duration curve generated from observed and simulated discharge

d) Water balance of the Budhigandaki River basin

Monthly simulated water balance component of the study basin is shown Figure 4.15. It depicts the distribution of water balance components, namely, precipitation (P), actual evapotranspiration (AET) and the net water yield (WY) of the study basin. The WY refers to the total flow coming as surface runoff, lateral flow, and groundwater flow minus transmission losses and pond abstractions (Arnold et al., 1998). Change in storage is defined as ΔStorage = − [(Precipitation (P) − Net Water Yield (WY) − Evapotranspiration (ET)]. It implies that if P > (WY + ET), the excess water infiltrates and is stored, as soil moisture and GW storages, of the basin. On the other hand, if (WY + ET) > P, the water deficit is met by soil and GW storages of the basin. For example, in January, some water is released from the basin to meet the WY and ET while it is stored in the soil and GW storage in July. It is noted here that Δstorage accounts for model errors too. It can be seen from the results that precipitation across the SWAT sub-basins varies from less than 700 mm (leeward side of northern Trans-Himalayan region) to above 2500 mm (foothills of the Himalayas). The average annual precipitation over the entire basin is 1528 mm. Here precipitation has been taken as the sum of annual rainfall and snowmelt (318 mm). The percentage of precipitation falling in pre-monsoon, monsoon, post monsoon and winter are respectively 16%, 74%, 4% and 6% of the total annual value. The average annual AET over the basin is 402 mm while WY is 1010 mm. The WY is about 56% during monsoon (June–September) while

it is only 28% and 9% in pre-monsoon (March–May) and post-monsoon (October and November) seasons, respectively. It is only 7% of the total annual volume for the winter season (December–February). Delta storage for the entire simulation period has been calculated to be around 8%.

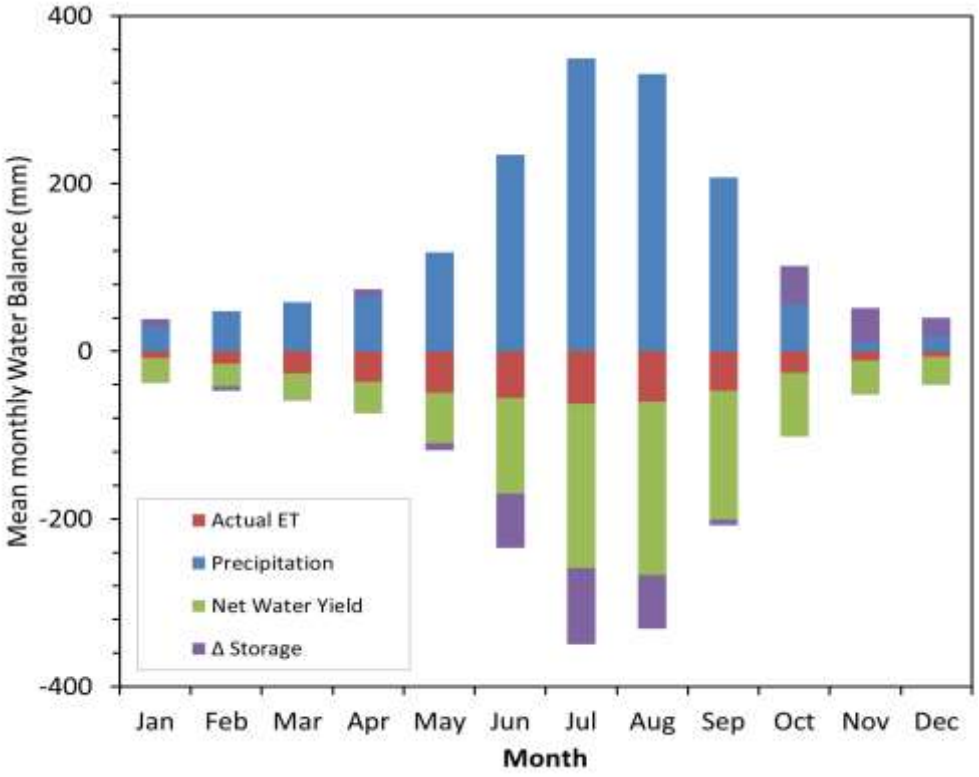

Figure 4.15: Monthly simulated water balance components in BRB

4.5 Hydrological modeling: better alternative to flow estimation

4.5.1 General approach

Various methods popular in Nepal viz. WECS/DHM 1990, NEA 1997, DHM 2004, drainage area ratio (DAR) and general transportation (GT), mentioned in Chapter 4 (Details can be found in Marahatta et al., 2021b), are used for monthly flow estimation for various purposes. Monthly flows are, generally, utilized both in RoR and storage type hydroelectric projects to estimate the power production from them. In this study mean monthly flows were estimated from each of these methods and performance indicators are calculated for each of them that includes the results of SWAT model. From the estimated flows from considered six methods and the observed discharge at the gauging stations, performance statistics are calculated. It is to be noted here that performance evaluation of simulation results, WECS 1990, NEA 1997 and DHM 2004

methods are made with respect to long term averages of observed flow (1983-2012: Obs-A). However, DAR and GT estimates are compared with the average of two years data (2013-2014: Obs-B). This limitation is because measured data at BGHP dam site is not available for the other years. It is assumed that such difference will have minimum impact on performance parameters. Utilizing different performance indicators value Global Performance Index (GPI) were calculated for each method at these two sites. This statistical analysis helps to quantify the merits of the different methods, and assists in selecting the most reliable method for the use in the BRB.

4.5.2 Performance evaluation at Arughat station

Monthly flows from the different methods and observations are shown in Figure 4.16. Numerical values of goodness-of-fit parameters of the considered methods of flow estimation for Arughat are given in Table 4.4. Considering the monthly values, the coefficient of determination (R^2) for all the methods are close and > 0.95. All the other calculated performance parameters except MAE show that the simulated flows obtained through SWAT hydrological modeling are found closer to the observed values. Even for MAE, the calculated value is very close to the NEA 1997 method. Based on GPI value as shown in Table 4.4, it can, safely, be concluded that the hydrological simulation method is the most suitable among the considered methods for simulating the monthly discharge at Arughat. Further, the method adopted by Nepal Electricity Authority (NEA 1997) and general transformation (GT) method respectively ranked second and third.

Table 4.4: Performance of considered methods at Arughat and BGHP dam site

Data Length	**Arughat: 30 years (1983-2012)**				**BGHP dam site: 2 years (2013-2014)**		
Parameters	**SWAT**	**WECS 1990**	**NEA 1997**	**DHM 2004**	**DAR**	**GT**	**Parameters**
R^2	0.98	0.97	0.97	0.96	0.99	0.99	**R^2**
MAE	21.6	60.6	20.9	61.0	52.4	30.2	**MAE**
RMSE	36.6	209.6	65.1	211.4	181.5	104.5	**RMSE**
PBIAS	-6.4	37.3	11.6	37.6	-39.5	-22.7	**PBIAS**
NSE	0.97	0.67	0.95	0.67	0.74	0.92	**NSE**
KGE	0.87	0.45	0.81	0.45	0.49	0.72	**KGE**
GPI	5.5	2.1	4.8	1.3	3.1	4.3	**GPI**
Performance Rank	**I**	**V**	**II**	**VI**	**IV**	**III**	**Performance Rank**

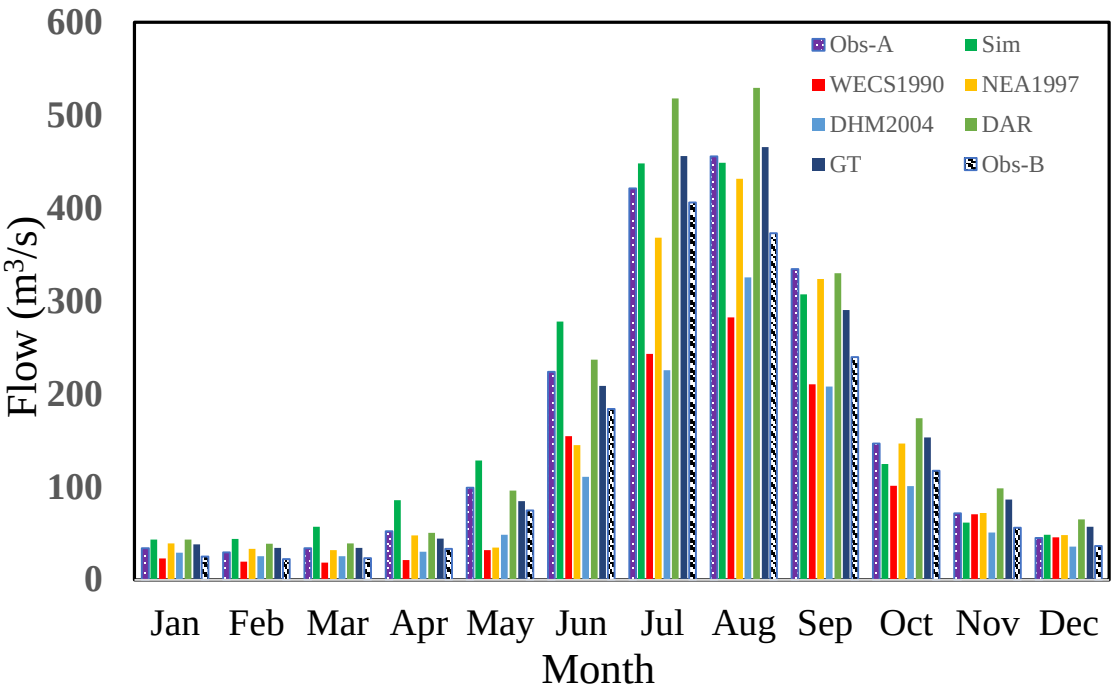

Figure 4.16: Comparison of Monthly Flows at Arughat

Seasonal variation was also evaluated at Arughat gauging station using the methods explained above. Table 4.5 ranks the performance of the flow estimation methods based on seasonal GPI value. The GT and NEA 1997 methods performed the best for dry and post-monsoon seasons. Likewise, hydrological simulation ranked second in both seasons. However, it outperforms the other methods during the monsoon. Depending on the value of the weighted-average GPI, it can be seen that GT method ranks the first while hydrological simulation and NEA 1997 rank second and third respectively. The other methods did not perform satisfactorily at the seasonal scale.

Table 4.5: Evaluation of the considered methods for seasonal discharge estimation at Arughat

GPI and Rank	**Hydro Sim**	**WECS1990**	**NEA1997**	**DHM2004**	**DAR**	**GT**
GPI-Dry Season	3.83	1.50	3.50	3.83	2.92	5.42
GPI-Monsoon	4.92	2.33	4.58	1.25	3.42	4.50
GPI Post Monsoon	4.67	3.08	5.58	2.42	1.92	3.33
GPI-Weighted Average	4.33	2.04	4.21	2.74	2.92	4.76
Rank	II	VI	III	V	IV	I

3.5.3 Performance evaluation at Budhigandaki dam site

The mean monthly discharge was estimated using different methods and compared with the observed values (Figure 4.17). Performance rating of the considered methods are given in Table 4.6. It can be seen that SWAT ranks first among the considered approaches while GT ranks second and DAR ranked the last.

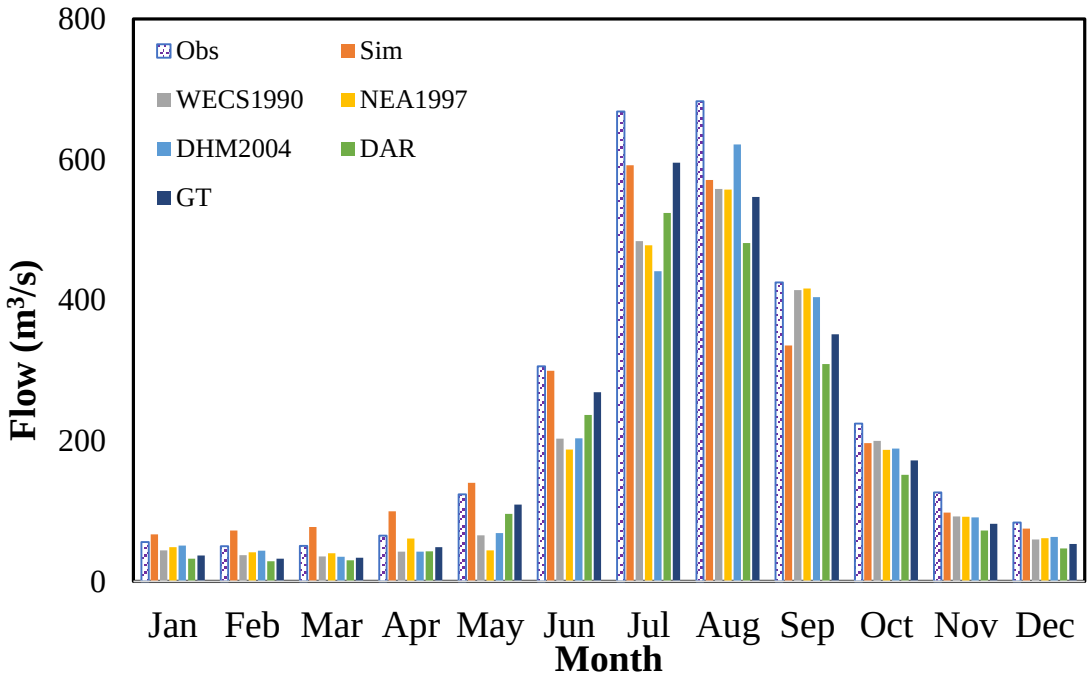

Figure 4.17: Monthly hydrographs generated by different approaches at Budhigandaki dam site

Table 4.6: Performance rating of different discharge estimation approaches at Budhigandaki Dam Site

Data length	**2 years (2013-2014)**					
Parameters	**Hydro Sim**	**WECS 1990**	**NEA 1997**	**DHM 2004**	**DAR**	**GT**
R^2	0.99	0.97	0.96	0.95	0.99	0.99
MAE	38	52	54	51	68	44
RMSE	69	181	186	176	234	153
PBIAS	8.39	21.88	22.62	21.26	28.30	18.51
NSE	0.95	0.89	0.88	0.88	0.85	0.94
KGE	0.78	0.69	0.67	0.69	0.63	0.76
GPI	5.83	3.25	2.08	3.17	1.67	5.00
Performance Rank	I	III	V	IV	VI	II

Additionally, the seasonal global performance index (GPI) of the considered methods of discharge estimation is given in Table 4.7. The performance of the GT method in the dry season is relatively better than the other methods. However, for the other two seasons, hydrological simulation performed relatively well. Similar, to the annual case, seasonal performance of SWAT simulation shown by the weighted GPI is the highest among all the other considered methods (Table 4.7). Considering the overall GPI value, SWAT ranked first, GT second while NEA 1997 ranked the last.

Table 4.7: Evaluation of seasonal discharge estimation at Budhigandaki dam site

GPI and Rank	**Hydro Sim**	**WECS1990**	**NEA1997**	**DHM2004**	**DAR**	**GT**
GPI-Dry Season	4.67	2.42	2.00	3.42	2.92	5.58
GPI-Monsoon	5.50	3.25	2.08	2.75	2.17	5.25
GPI Post Monsoon	5.50	4.83	3.17	3.83	1.42	2.25
GPI-Weighted Average	5.08	3.10	2.22	3.26	2.42	4.92
Rank	I	IV	VI	III	V	II

Results show that SWAT model performs the best among the considered six methods for the BRB. The WECS 1990, NEA 1997 and DHM 2004 are empirical methods established by regression analysis. The regression coefficients are averaged at a regional scale and therefore, the performance of these methods may vary according to the catchment. Similarly, the DAR method only considers the size of the catchment. The GT method additionally takes into account the precipitation. Hence, its performance is better compared to the regional and DAR methods. However, it does not consider the basin characteristics. Simulations using SWAT model can be customized to account for a wide range of meteorological, hydrological, geological and catchment characteristics.

4.6 Impact of climate change in river hydrology

4.6.1 Selections of climate models

First the climate model selection was made by comparing the projected mean temperature and annual precipitation changes (%) of 2021-2050 with baseline period of 1981-2005 for both RCPs, shown as dots in Figure 4.18**.** In RCP 4.5, the projected

changes in annual precipitation are in the range of -9% to +23% while most of models show increase in precipitation. Similarly, change in projected temperature ranges from +0.6°C to +3.0°C with multi-model mean showing an increase by approximately +1.7 °C. Similarly, in RCP 8.5, the projected precipitation changes range from -11% to +21%. In case of temperature, the changes are from +0.7°C to +3.1°C with the mean of +1.9°C. It is noted here that in both RCPs, greater number of models show an increase in precipitation. In this first step, 20 models (5 models for each dry, warm-wet, cold-wet and cold-dry corners, and for each RCP) were selected from 105 models for RCP 4.5 and from 78 models for RCP 8.5 scenarios as shown in Figure 4.18.

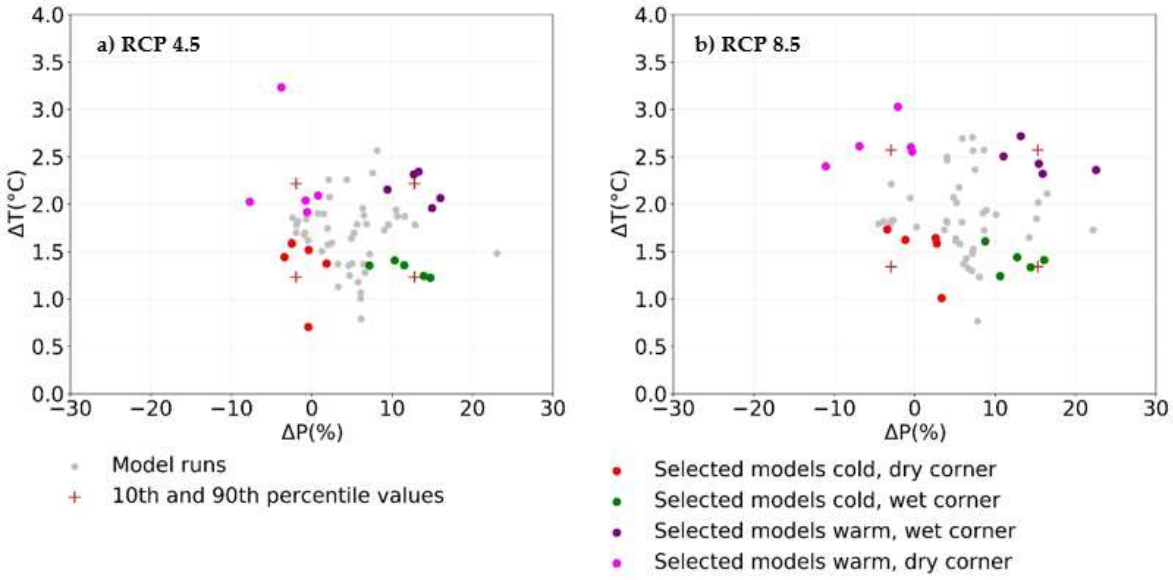

Figure 4.18: Projected changes in annual precipitation and annual mean temperature for RCP 4.5 and RCP 8.5.

Table 4.8: Summary of precipitation and temperature change indices score of selected GCMs

Condition	Model	Δr95p(%)	Δcdd(%)	Δwsdi(%)	Δcsdi(%)	ΔT(°c)	ΔP(%)	Tindex rank	Pindex rank	Combined Score
RCP 4.5										
Cold,dry	inmcm4_rcp45_r1i1p1	6.6	8.8	136.5	-21.3	0.7	-0.4	5	2	3.5
p10_10	FGOALS-g2_rcp45_r1i1p1	-8.1	-0.6	385.7	-89.9	1.4	-3.4	1	1	1
	bcc-csm1-1-m_rcp45_r1i1p1	6.4	21.1	226.5	-78.4	1.4	1.9	2	4	3
	HadGEM2-CC_rcp45_r1i1p1	0.8	44.7	564.6	-74.5	1.6	-2.5	3	5	4
	MPI-ESM-MR_rcp45_r2i1p1	-0.9	12.4	207.5	-69.2	1.5	-0.4	4	3	3.5
Cold,wet	MRI-CGCM3_rcp45_r1i1p1	55.0	-11.9	120.4	-90.0	1.2	13.9	1	5	3
p10_90	CSIRO-Mk3-6-0_rcp45_r3i1p1	34.6	-0.6	389.5	-55.9	1.2	14.8	3	3	3
	CSIRO-Mk3-6-0_rcp45_r8i1p1	16.7	3.8	223.0	-54.9	1.4	11.5	4	1	2.5
	CESM1-BGC_rcp45_r1i1p1	30.5	-8.8	218.1	-73.8	1.4	10.3	2	2	2
	GFDL-ESM2G_rcp45_r1i1p1	38.9	5.3	377.5	-28.1	1.4	7.2	5	4	4.5
Warm,wet	CanESM2_rcp45_r3i1p1	50.9	2.2	211.6	-87.0	2.3	12.7	3	4	3.5
p90_90	CanESM2_rcp45_r2i1p1	44.5	5.8	302.8	-78.8	2.3	13.3	5	3	4
	CanESM2_rcp45_r1i1p1	51.1	7.2	180.0	-79.7	2.1	16.0	2	5	3.5
	CanESM2_rcp45_r5i1p1	30.7	-8.4	149.8	-88.8	2.2	9.4	1	2	1.5
	IPSL-CM5A-LR_rcp45_r3i1p1	19.7	-0.6	279.8	-78.1	2.0	15.0	4	1	2.5
Warm,dry	CSIRO-Mk3-6-0_rcp45_r9i1p1	-4.7	28.5	683.2	-84.7	2.0	-0.8	5	5	5
p90_10	GFDL-CM3_rcp45_r1i1p1	0.3	4.5	646.5	-85.4	3.2	-3.8	4	2	3
	MPI-ESM-LR_rcp45_r2i1p1	-7.6	9.5	291.7	-81.9	2.0	-7.7	2	3	2.5
	MPI-ESM-LR_rcp45_r3i1p1	10.3	18.0	331.5	-76.2	2.1	0.8	3	4	3.5
	MIROC-ESM_rcp45_r1i1p1	8.0	-4.0	233.1	-98.2	1.9	-0.6	1	1	1
RCP 8.5										
Cold,dry	inmcm4_rcp85_r1i1p1	15.6	3.4	168.1	-37.5	1.0	3.4	5	1	3
p10_10	GFDL-ESM2G_rcp85_r1i1p1	25.8	7.2	362.5	-61.9	1.6	2.7	3	2	2.5
	HadGEM2-ES_rcp85_r4i1p1	10.0	30.0	383.8	-65.0	1.6	-1.2	2	4	3
	FGOALS-g2_rcp85_r1i1p1	6.3	9.2	281.8	-92.7	1.6	2.6	1	3	2
	HadGEM2-ES_rcp85_r1i1p1	7.4	42.3	352.8	-56.6	1.7	-3.4	4	5	4.5
Cold,wet	CSIRO-Mk3-6-0_rcp85_r8i1p1	21.6	-9.8	218.2	-57.5	1.3	14.4	3	2	2.5
p10_90	CSIRO-Mk3-6-0_rcp85_r3i1p1	30.2	-11.3	349.9	-55.4	1.4	16.1	5	3	4
	GFDL-ESM2M_rcp85_r1i1p1	44.1	-0.3	235.0	-56.7	1.4	12.8	4	4	4
	IPSL-CM5B-LR_rcp85_r1i1p1	12.8	-11.7	152.2	-69.4	1.2	10.6	2	1	1.5
	bcc-csm1-1_rcp85_r1i1p1	50.9	3.7	347.2	-82.3	1.6	8.8	1	5	3
Warm,wet	CanESM2_rcp85_r2i1p1	48.3	4.1	325.0	-90.1	2.4	15.4	4	2	3
p90_90	CanESM2_rcp85_r3i1p1	49.3	8.3	285.7	-74.2	2.7	13.2	3	4	3.5
	IPSL-CM5A-MR_rcp85_r1i1p1	43.7	1.1	347.0	-90.8	2.5	11.0	5	1	3
	CanESM2_rcp85_r5i1p1	48.8	-15.2	169.8	-91.2	2.3	15.9	1	3	2
	CanESM2_rcp85_r1i1p1	68.6	-2.8	208.9	-74.7	2.4	22.5	2	5	3.5
Warm,dry	MPI-ESM-LR_rcp85_r3i1p1	16.6	12.6	414.3	-92.6	2.6	-0.5	3	3	3
p90_10	CMCC-CMS_rcp85_r1i1p1	5.1	9.7	318.0	-89.7	2.6	-6.9	1	1	1
	GFDL-CM3_rcp85_r1i1p1	12.2	14.9	603.8	-76.7	3.0	-2.1	4	5	4.5
	MIROC-ESM-CHEM_rcp85_r1i1p1	10.0	12.8	729.1	-94.8	2.6	-0.3	5	4	4.5
	MPI-ESM-LR_rcp85_r2i1p1	-11.2	10.4	369.4	-85.2	2.4	-11.1	2	2	2

Using Taylor method (Taylor, 2001) four GCMs, one GCM for each RCP and for each corner are selected in the final step as shown in Table 4.9.

Table 4.9: Final selection GCMs using Taylor skill

Condition	GCMs	Taylor Skill		
		Precipitation	Temperature	Combined
RCP 4.5				
Cold—dry (p10_10)	inmcm4_rcp45_r1i1p1	0.707	0.835	0.771
	HadGEM2-CC_rcp45_r1i1p1	**0.792**	**0.928**	**0.86**
	MPI-ESM-MR_rcp45_r2i1p1	0.658	0.901	0.779

Condition	GCMs	Taylor Skill		
		Precipitation	Temperature	Combined
Cold—wet (p10_90)	MRI-CGCM3_rcp45_r1i1p1	0.568	0.891	0.729
	CSIRO-Mk3-6-0_rcp45_r3i1p1	0.49	0.891	0.69
	GFDL-ESM2G_rcp45_r1i1p1	**0.663**	**0.904**	**0.784**
Warm—wet (p90_90)	**CanESM2_rcp45_r3i1p1**	**0.578**	**0.829**	**0.703**
	CanESM2_rcp45_r2i1p1	0.529	0.832	0.68
	CanESM2_rcp45_r1i1p1	0.571	0.818	0.694
Warm—dry (p90_10)	CSIRO-Mk3-6-0_rcp45_r9i1p1	0.473	0.881	0.677
	MPI-ESM-LR_rcp45_r3i1p1	**0.637**	**0.886**	**0.761**
RCP 8.5				
Cold—dry (p10_10)	inmcm4_rcp85_r1i1p1	0.707	0.835	0.771
	HadGEM2-ES_rcp85_r4i1p1	0.789	0.952	0.871
	HadGEM2-ES_rcp85_r1i1p1	**0.802**	**0.947**	**0.874**
Cold—wet (p10_90)	CSIRO-Mk3-6-0_rcp85_r3i1p1	0.49	0.891	0.69
	GFDL-ESM2M_rcp85_r1i1p1	**0.66**	**0.891**	**0.775**
Warm—wet (p90_90)	**CanESM2_rcp85_r3i1p1**	**0.578**	**0.829**	**0.703**
	CanESM2_rcp85_r1i1p1	0.571	0.818	0.694
Warm—dry (p90_10)	GFDL-CM3_rcp85_r1i1p1	0.47	0.838	0.654
	MIROC-ESM-CHEM_rcp85_r1i1p1	**0.493**	**0.877**	**0.685**

Notes: Bold GCMs are selected from step 3.

HadGEM2 was selected for cold and dry condition, GFDL for cold and wet condition, CanESM2 for warm and wet condition for both RCPs. However, in case of warm and dry condition MPI-ESM for RCP 4.5 and MIROC-ESM for RCP 8.5 were selected. Summary of the selected GCMs for each RCP are presented in Table 4.10

Table 4.10: Summary of selected GCMs

RCP 4.5	GCMs	RCP 8.5	GCMs
Cold-dry (p_{10_10})	HadGEM2-CC_rcp45_r1i1p1	Cold-dry (p_{10_10})	HadGEM2-ES_rcp85_r1i1p1
Cold-wet (p_{10_90})	GFDL-ESM2G_rcp45_r1i1p1	Cold-wet (p_{10_90})	GFDL-ESM2M_rcp85_r1i1p1
Warm-wet (p_{90_90})	CanESM2_rcp45_r3i1p1	Warm-wet (p_{90_90})	CanESM2_rcp85_r3i1p1
Warm-dry (p_{90_10})	MPI-ESM-LR_rcp45_r3i1p1	Warm-dry (p_{90_10})	MIROC-ESM-CHEM_rcp85_r1i1p1

Note: p_{x_y}: x^{th} and y^{th} percentiles of temperature and precipitation.

4.6.2 Bias correction

Precipitation and temperate were bias corrected by two different approaches: Precipitation was bias corrected from the full distribution of observed and GCM by distribution mapping (quantile) method, assuming there will be match statistical moments including the mean and standard deviation between two distributions. While in case of temperature, temperature variable, method was used.

This approach assumes that relationship between GCM temperature and observed temperature in reference period also remain same between future GCM projection and future observation. Figure 4.19 shows the observed, uncorrected and bias corrected mean precipitation and temperatures for CanESM2 model for the RCP 4.5 scenario. The figure illustrates that the bias corrected values match closely with the observed data, which indicates that the climate data are well bias corrected.

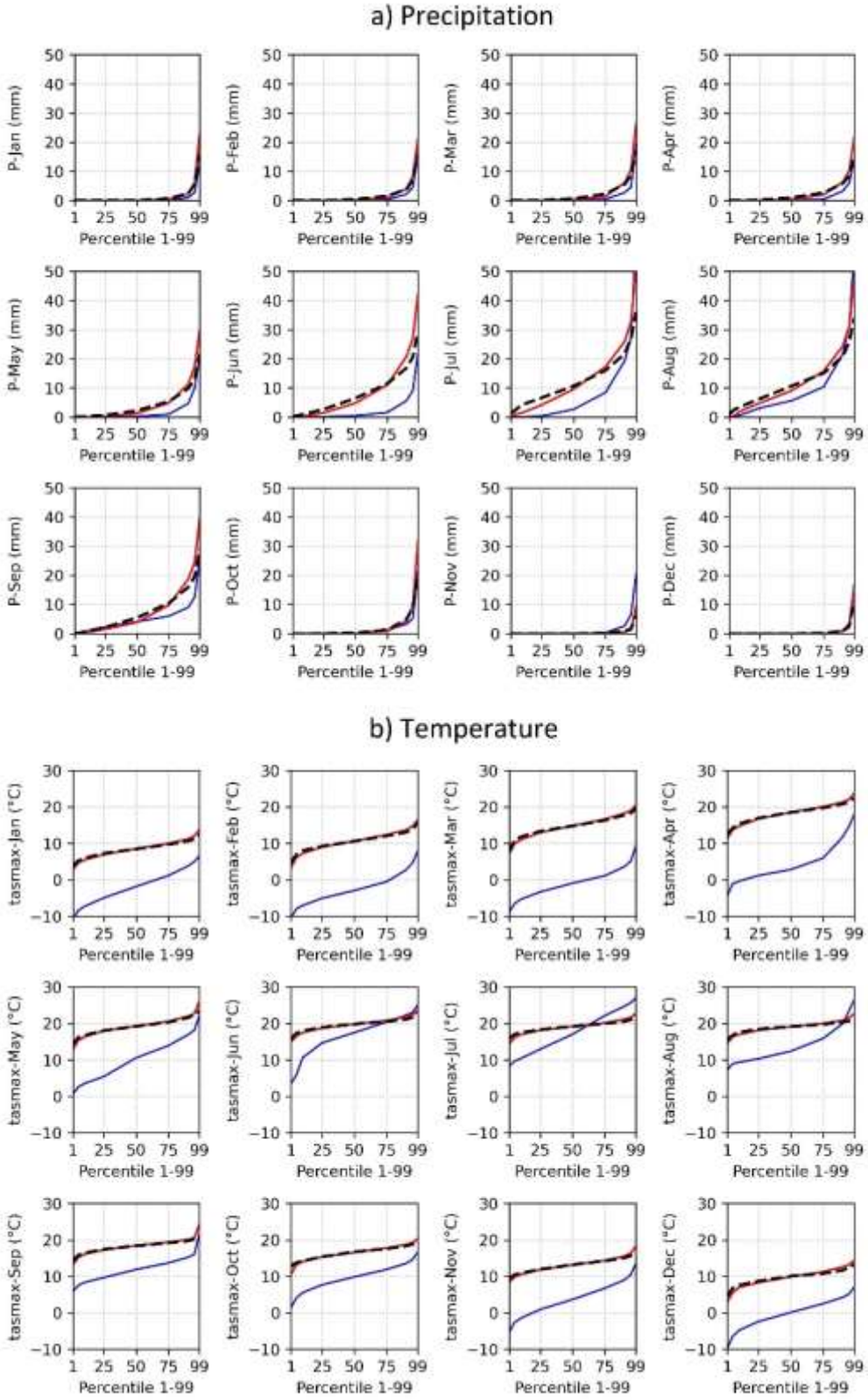

Figure 4.19: Monthly observed (black), uncorrected (blue) and bias-corrected (red) (a) precipitation and (b) mean temperature for RCP 4.5 of CanESM2

4.6.3 Climatology under different climate change scenarios

Percentage change in annual precipitation and temperature under two emission scenarios (RCPs 4.5 and 8.5) with respect to the baseline values are shown in Figure 4.20. Projected precipitation by all the GCMs for all time windows, immediate future (IF), mid future (MF), far future (FF), is most likely to increase in both RCPs except the MPI-ESM for MF and FF and HadGEM2 for IF in case of RCP 4.5, and HadGEM2 for IF and MF for RCP 8.5. The highest increase of about 9% and 20% from baseline values are found for RCP 4.5 in IF and RCP 8.5 in FF, respectively, projected by the CanESM2 model. Lowest projected precipitation by the HadGEM2 is found in IF time window. Their values are ~5% and 7% lower than the base case for RCPs 4.5 and 8.5, respectively. It can be seen from the figure that the precipitation is expected to increase with time, i.e. IF<MF<FF in RCP 8.5. However, in case of RCP 4.5, the response is mixed i.e., increasing trend for HadGEM2 (Cold-dry) and GFDL_ESM2G (Cold-wet) and decreasing in other two cases (Warm -wet and Warm- dry). This characteristic is illustrated in Figure 4.21 i.e., projected long term precipitation in RCP 8.5 shows a clear increasing trend, whereas there is no clear trend for RCP 4.5.

Both the maximum and minimum temperature projection by all the selected GCMs (in all climatic conditions) are found increasing while moving from IF to FF in both emission scenarios, which is expected. The rate of increase of temperature is higher by all projections for RCP 8.5 than that of RCP 4.5 (Figures 4.20 and 4.21**)**. It can also be observed that the increase in minimum temperature is higher compared to maximum temperature in all time windows for both emission scenarios and in all conditions except cold-wet condition (GFDL-ESM2G of RCP 4.5). However, the projected temperatures of selected models are found different. The maximum increase is found for minimum temperature projected by MIROC-ESM-CHEM (warm-dry/FF) of RCP 8.5 i.e., 6.5 ^{o}C. The minimum increase is found to be 0.6 ^{o}C projected by GFDL-ESM2G model in IF (Figure 4.20).

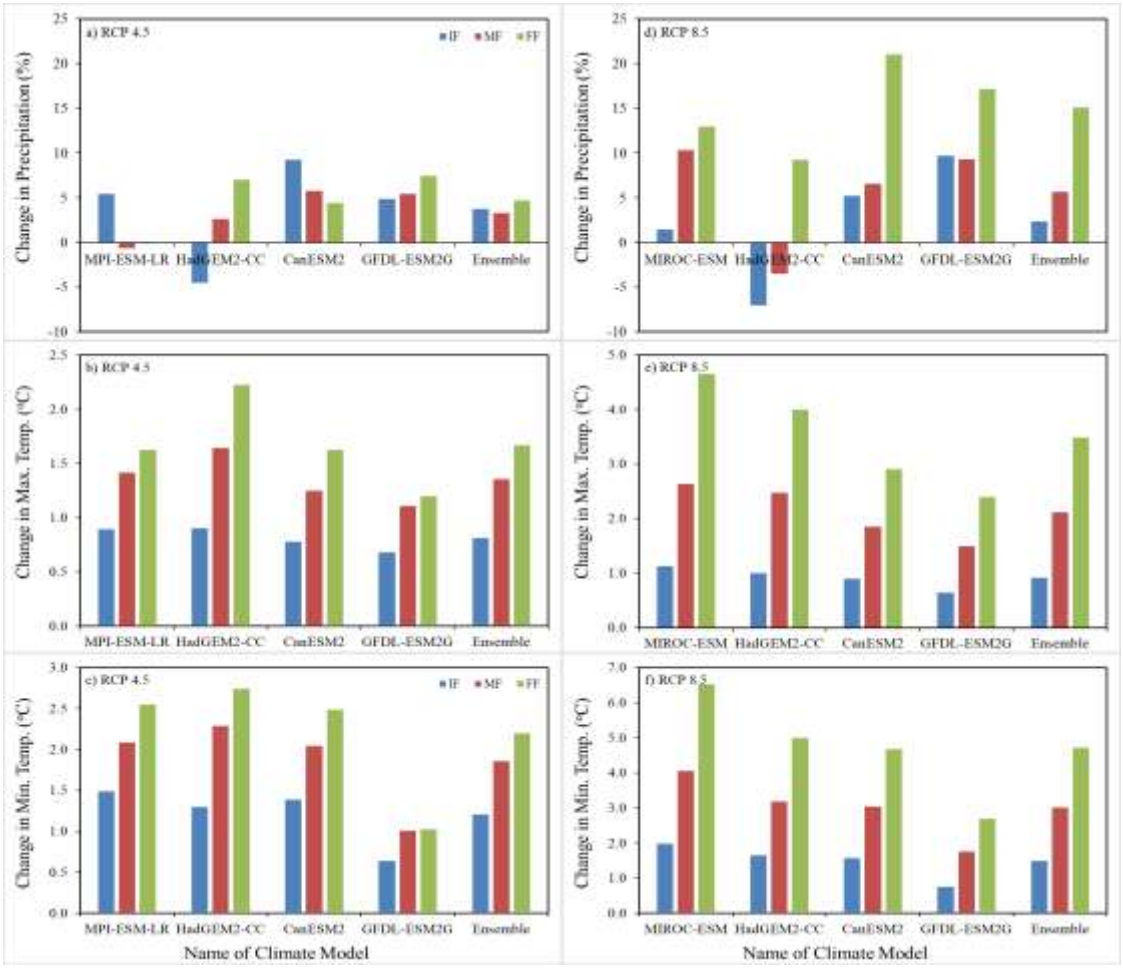

Figure 4.20: Change in precipitation (a and d); maximum temperature (b and e); minimum temperature (c and f) pattern of the four selected GCMs and ensemble of RCPs 4.5 (left) and 8.5 (right) with their respective time window: Blue (IF), Red (MF) and Gray (FF)

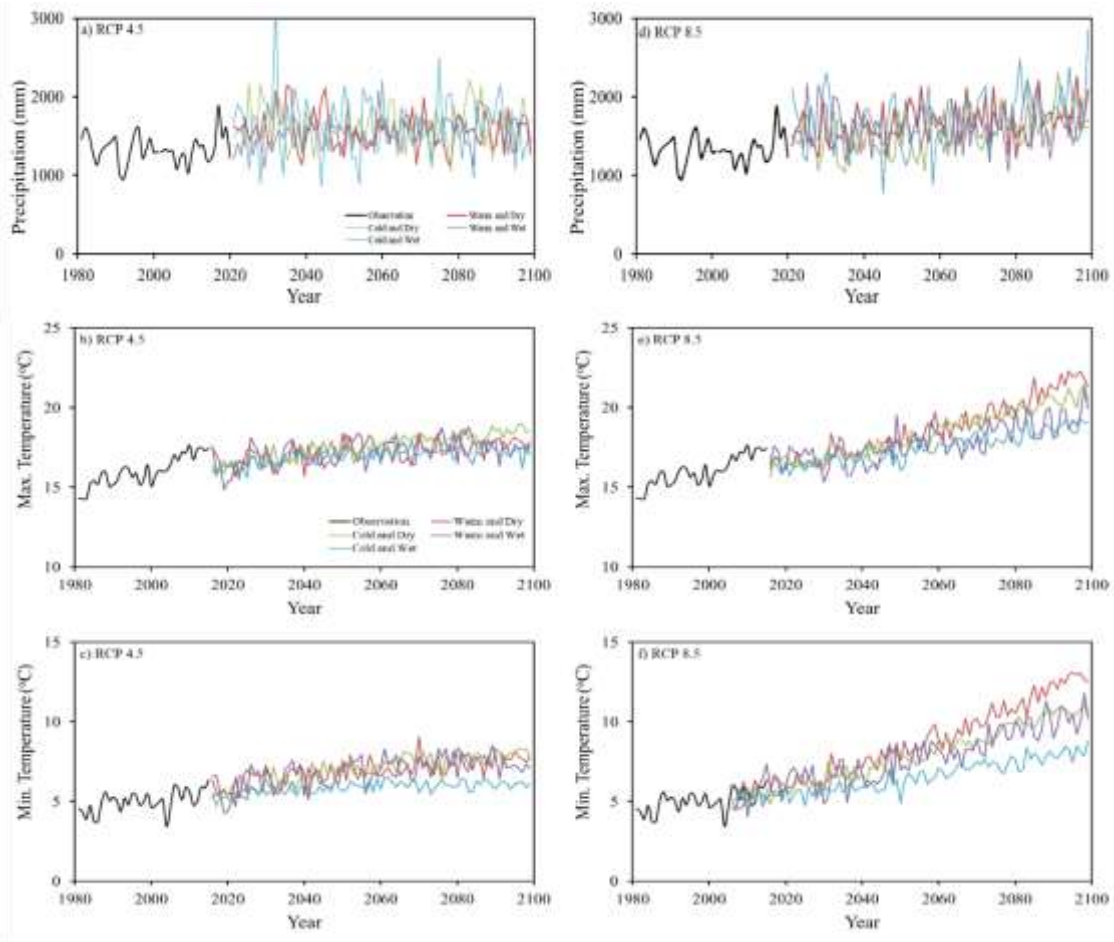

Figure 4.21: Precipitation and temperature (observed, bias corrected) of RCP 4.5 (a, b and c) and 8.5 (d, e and f) of the selected GCMs; Black (baseline), Red (MIROC/MPI), Blue (GFDL), Green (HadGEM) and Purple (CanESM2)

4.6.4 Variations of mean annual flow

The simulated average annual discharge at BRB for the baseline period is 240 m^3/s (Marahatta et al., 2021b). Table 4.11 presents the predicted flow and corresponding percentage changes in flow estimated by the selected GCMs for the four climatic conditions (warm wet: projected by CanESM2; warm-dry: MPI (RCP 4.5/MIRCO (RCP 8.5), cold-wet: GFDL and cold-dry: by HadGEM2) for all time windows capered to baseline flow.

The maximum increase of annual flow in RCP 4.5 is more than 30% in cold-dry condition of FF and the minimum increase is about 10% in IF for the same condition predicted by HadGEM2 model. It shows that the HadGEM2 predicted flow has more variation than other GCMs in terms of annual averages. The increased flow of long-term annual average is almost same for warm-wet condition projected by CanESM2

(IF: 29%, MF:30% and FF 28%) whereas it is in decreasing trend for warm-dry condition projected by MPI model (IF: 26%, MF: 20% and FF: 17%). Flow of other remaining two conditions are in increasing trend while moving from IF to FF [GFDL: 18% (IF), 20% (MF) and 24% (FF); and HadGEM2: 10% (IF), 24% (MF) and 31% (FF)].

The long-term average annual flow predicted by all GCMs for all time windows in RCP 8.5 are also more than the baseline flow; in increasing order from IF to FF for all climatic conditions similar to RCP 4.5. The increase in annual projected flow is in between 5% (cold-dry/IF) and 57% (warm-wet /FF). Thus, the increase in long-term mean annual discharge is expected in the future for considered climate scenarios for both RCPs. Increment of ensembled flow is in between 21% and 25% in RCP 4.5 and 20% and 48% in RCP 8.5. It shows that the magnitude of increment of future flow is expected to be is more for higher emission scenario.

Table 4.11: Impact of climate change on long-term mean annual discharge

Conditions	**Time Window**	**RCP 4.5**		**RCP 8.5**	
		Flow (m^3/s)	**% Change**	**Flow (m^3/s)**	**% Change**
Baseline		240	-	240	-
Cold Wet (GFDL-ESM2G)	IF	283	18	304	27
	MF	287	20	317	33
	FF	297	24	358	49
Warm Wet (CanESM2)	IF	309	29	311	30
	MF	311	30	315	32
	FF	306	28	377	57
Cold Dry (HadGEM)	IF	263	10	251	5
	MF	297	24	272	14
	FF	314	31	331	38
Warm Dry (MPI-ESM-LR/ MIROC-ESM)	IF	301	26	287	20
	MF	288	20	334	39
	FF	281	17	350	46
Ensemble	IF	289	21	288	20
	MF	296	23	310	29
	FF	299	25	354	48

4.6.5 Variation of mean monthly flows

Knowledge on the monthly variability under CC is useful for risk assessment of water resources development projects such as hydroelectricity, irrigation and municipal water supply. The monthly baseline and predicted ensembled flows as well as corresponding percentage changes due to CC for both RCPs are given in Figure 4.22. However, long-term monthly flow of three-time windows projected by four GCMs representing four climatic conditions of RCP 4.5 and RCP 8.5 emission scenarios are given in Appendix (Table A2 and Table A3) respectively. The data shows that the range of change in monthly projected flow in RCP 4.5 is from -17% (June/MF/cold-dry) to 68% (March/FF/warm-wet) with respect to baseline flows. It is noted here that only four out of 144 cases (12 months * 3 times windows * 4 climatic condition) have more than 5% decrease in monthly flow. In almost sixty percent of the cases, flows are in the range of +10% to +25% of the baseline flows. Monthly flows more than 25% of the baseline flows are found to be in one fourth of the total months. In general, in three climatic conditions (warm-wet, cold-wet and warm-dry), more than 25% increase is found in the month of March. Even for cold-dry condition, the increased percentage is high (>15%). The monsoon flow is projected to increase considerably high in considered time-windows except for cold-dry condition in June. Magnitude of the projected monthly maximum flow in all time windows for all climatic conditions are found to occur in August similar to baseline except far-future of cold wet condition. In this case the flow value is maximum in July.

In case of RCP 8.5, the range of change of monthly flow is nearly -50% (July/MF/cold-dry) to 200% (October & November/MF/cold-dry). Almost two-thirds of the predicted monthly flows are more than 25% of the baseline values for all climatic conditions. Almost one fourth of the cases are in between 10 to 25% increase in monthly flows. The decrease in predicted flow was found only for cold-dry conditions. It is noteworthy to mention that this decrease is mainly observed in monsoon season (June, July and August) and in May. The rate of increase is found to be higher in post-monsoon season (October and November).

The projected mean monthly flow are expected to increase in March, August, September, October and November for all scenarios except during May in MF for RCP 4.5 (2021-2099). However, in RCP 8.5, all the ensembles of projected monthly flow increase in all time windows. The relative change in projected mean monthly discharge

under RCP4.5 is +11 to +28%, -1 to +36% and +5 to +43% for IF, MF and FF, respectively. These figures range from +3 to +52%, + 6 to + 77% and +18 to + 82% for IF, MF and FF respectively in case of RCP 8.5. Ensembled flows are found to be greater in RCP 8.5 than in RCP 4.5, except from May - August in IF, and July - August in MF. The maximum increase of 43% for RCP 4.5 and 82% in RCP 8.5 occurs during September.

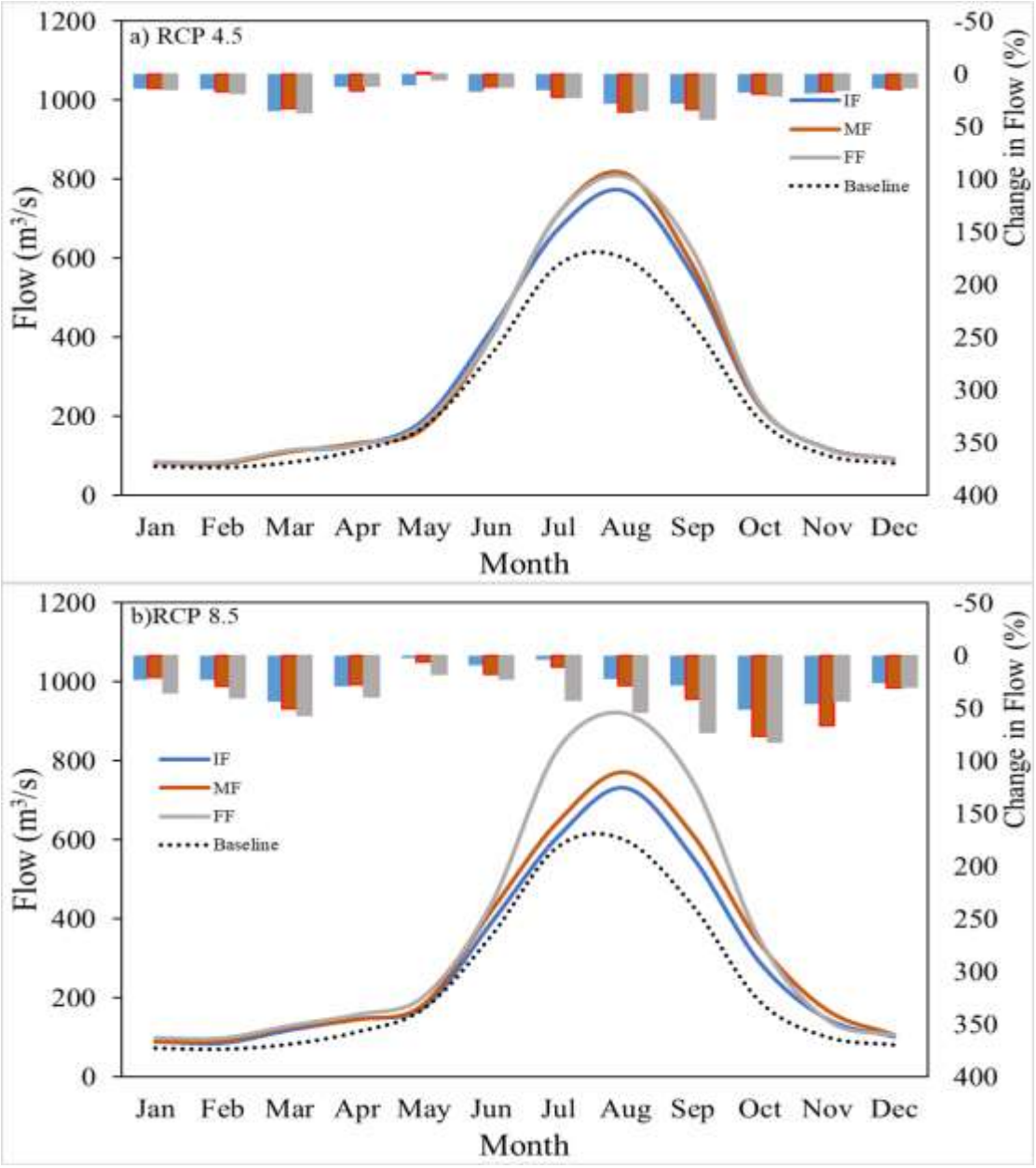

Figure 4.22: Hydrographs of monthly ensembled and baseline discharge and their changes

4.6.6 Variation in high and low flows

The 10^{th} percentile (Q_{10}, high flow) and 90^{th} percentile (Q_{90}, low flow) values were derived from corresponding baseline and flow duration curves predicted by all four GCMs for the considered time windows. Their ratios (Q_{10}:Q_{90}) were calculated separately for each case. The 10^{th} and 90^{th} percentiles of baseline flow are respectively 598 m^3/s and 64 m^3/s. It means this ratio of the baseline flow is 9. For RCP 4.5, the ratios of ensembled flow are found to be 11, 12 and 12 for IF, MF and FF respectively. However, such ensemble values for RCP 8.5 are respectively 14, 17 and 18 for IF, MF and FF. This result shows that variability is expected to increase with time and be of higher magnitude in RCP 8.5 than in RCP 4.5.

Analysis was made to see the number of days > Q_{10} and < Q_{90} flows to assess the frequency of incidence of high flow and low flow. The number of days exceeding Q_{10} or non-exceeding Q_{90} was 1098 for the baseline period (10% of the total number of the data). The number of days (for all the four GCMs) that is expected to have flow exceeding Q_{10} are more than 1098 days and non-exceeding Q_{90} are less than 1098 days except for one case (FF-low flow-warm dry-RCP 4.5). The increase in these days for IF, MF and FF are respectively 58%, 66% and 71% for RCP 4.5 and 43%, 62% and 97% for RCP 8.5 respectively. On the other hand, the percentage of decreased number of days in which the discharge is expected to be less than Q_{90} are 29%, 26% and 14% for RCP 4.5 and 43%, 20% and 42% for IF, MF and FF, respectively. The findings indicate that the likelihood of the number of flooding days would increase during the high flow season while the number of firm flow days in the low flow season would decrease.

4.6.7 Frequency analysis of Flow

In this study, frequency analysis of annual one day maximum and minimum discharge at the outlet of the BRB was carried out by Gumbel Method with and without CC impact as discussed below.

4.6.7.1 One day maximum flow

Maximum instantaneous flows are, generally, used to estimate the design floods (Chow et al., 1988; Devkota and Gyawali, 2015). Annual maximum one day flood and instantaneous flood are positively correlated (Chen et al., 2017; Devkota and Gyawali,

2015; Devkota et al., 2020). Therefore, it is assumed that the impact of CC on instantaneous flows is same as that in annual one-day-maximum flow.

The change in one-day-maximum flood for the emission scenarios RCP 4.5 and 8.5 and return periods are depicted in Table 4.12, including the baseline values. The baseline floods for 100, 500 and 1,000 years return period are respectively 1544, 1801, 1911 m^3/s. Table 4.12 also shows that the one-day-maximum flood resulting from CC is higher than the baseline floods for all climatic conditions and in all time windows for considered return periods. However, the predicted values differ among GCMs. The increase in the frequency for RCP 4.5 ranges from 66 % (warm-dry/IF/100 years) to 226% (warm-wet/MF/1000 years). Similarly, the increase for RCP 8.5 ranges from 69% (cold-dry/IF/100 years) to 317% (cold-wet/FF/1000 years). The flood frequency analysis also shows that the ensemble flood magnitudes are larger in the RCP 8.5 than in RCP 4.5 for all the return periods. However, cold and dry for IF and warm and wet for MF show smaller increase in the RCP 8.5 than for RCP 4.5. The change in ensembled projected flood is around 110%, 125% and 140% of baseline floods, respectively for IF, MF and FF time windows in case of RCP 4.5. These changes are 140%, 160% and 180% for IF, MF and FF, respectively for the three-time windows in RCP 8.5.

Table 4.12: One-day-maximum flood frequency analysis

Time window	Return Period (Years)	Baseline Flow (m^3/s)	% Change in flow (RCP 4.5)					% Change in flow (RCP 8.5)				
			Warm Dry	Cold Dry	Warm Wet	Cold Wet	Ensembled	Warm Dry	Cold Dry	Warm Wet	Cold Wet	Ensembled
IF	100	1,544	66	101	153	102	106	204	69	159	137	142
	500	1,801	67	109	163	106	111	226	72	171	145	154
	1000	1,911	68	111	166	108	113	234	73	175	148	158
MF	100	1,544	71	126	205	79	120	215	167	180	200	190
	500	1,801	72	131	220	79	125	228	183	189	217	204
	1000	1,911	72	133	226	78	127	233	188	192	223	209
FF	100	1,544	114	141	183	97	134	238	175	269	285	242
	500	1,801	123	149	197	98	142	254	183	280	309	256
	1000	1,911	126	151	202	98	144	260	186	283	317	262

4.6.7.2 One-day-minimum flow

One-day-minimum simulated flows for the different conditions are given in Table 4.13. Results showed that range of change in one-day-minimum flow due to CC with respect to the baseline condition is in between -27% (warm-dry/FF/20 years) to +9% (warm-wet/IF/2 years) for RCP 4.5 while it is in between -20% (warm-wet/MF/20 years) to +16% warm-wet/FF/2 years) for RCP 8.5 scenario. Almost half of the flow values in RCP 4.5 are expected to decrease by more than 10%. This phenomenon is mainly observed in MF and FF. Similar results are obtained in RCP 8.5, i.e., almost fifty percent of the low flows are lower than the base case values. It is more prominent in MF. Such decrease is mainly clustered for 10 and 20 years return period flows. Maximum decrease in predicted ensembled one-day-low flows are observed in FF in case of RCP 4.5 and MF in case of RCP 8.5.

Table 4.13: One-day-minimum flow frequency analysis

Time window	Return Period (Years)	Baseline Flow (m^3/s)	% Change in flow (RCP 4.5)					% Change in flow (RCP 8.5)				
			Warm Dry	Cold Dry	Warm Wet	Cold Wet	Ensembled	Warm Dry	Cold Dry	Warm Wet	Cold Wet	Ensembled
IF	2	56	7	0	9	4	5	5	2	9	7	6
	10	47	2	0	-9	-4	-3	6	-2	-4	4	1
	20	45	0	0	-13	-7	-5	7	-2	-7	4	1
MF	2	56	-4	5	4	-7	0	0	-2	4	-2	0
	10	47	-11	0	-11	-15	-9	-11	-15	-15	-15	-14
	20	45	-13	-2	-16	-16	-12	-13	-20	-20	-18	-18
FF	2	56	-13	2	-2	-5	-4	-5	4	16	4	4
	10	47	-23	-4	-17	-15	-15	-15	-13	2	-2	-7
	20	45	-27	-7	-20	-18	-18	-18	-18	-2	-4	-11

4.8 Impact of climate change on river flow

This study found that the projected annual flows by all GCMs and for all time windows greater than the base case, indicating that the CC is expected to increase the mean annual flow. Similar trend are reported in other studies made in Nepalese rivers basins, for example, Indrawati (Shrestha et al., 2016b), in Bagmati (Dahal et al., 2016), Kaligandaki (Bajracharya et al., 2018), Bheri (Mishra et al., 2018), Karnali (Dahal et al., 2020) and Koshi (Bharati et al., 2019; Devkota and Gyawali, 2015; Kaini et al., 2020) except (Bhatta et al., 2019) in Tamor. The increase in ensembled future flows are found similar to that of Koshi river in eastern Nepal (Kaini et al., 2020). The percentage

change in flow due to climate change in IF/MF/FF of this study and Koshi river are respectively 21/23/25 and 16/22/28 for RCP 4.5; and 20/29/48 and 18/31/57 for RCP 8.5. From the results presented above, we can see that the range of increase in annual flow is more in RCP 8.5 (5%-57%) than in RCP 4.5 (10%-30%), except IF and MF of cold-dry and IF of warm-dry conditions. The larger increase in RCP 8.5 indicates that the larger increase in the temperature causes overall increase in the river discharge. Lower value of the predicted flows in RCP 8.5 are attributed to less precipitation in RCP 8.5 in these GCMs. Although the overall trend of projected flow is found increasing, the individual scenarios show differences in the magnitude of changes in flows. Depending on the GCM used and location of the studied catchments, the magnitude (in some cases even direction) of changes in flow as the impact of CC are reported differently in previous studies (Kaini et al., 2020; Pandey et al., 2020a; Phi Hoang et al., 2016; Wang et al., 2019; Zhou et al., 2017). For examples, in the study by (Zhou et al., 2017) using SWAT model, they found that annual runoff of the Yinma River Basin (China) in the future (2021-2050) would increase by 88% for RCP 4.5 and by 48% for RCP 8.5 in comparison to baseline period (1981-2010). On the other hand, decreases of mean annual runoff are projected by VIC model in all future time windows of 2010–2039, 2040–2069 and 2070–2099 in a similar study by Wang et al. (2019) conducted in Upper Yangtz river basin of China (the decrease in mean annual flow were 7.84% under RCP 8.5 and 9.81% under RCP 4.5). Phi Hoang et al. (2016) found that the ensemble flow due to climate change shows increases in annual river flows between +5 and +16 %, in the Mekong River. Results from these studies highlight the need of localized prediction of future flows for water resource management considering the uncertainties.

Except May and June, future flows predicted by all GCMs are likely to increase in all other months of the year for all time windows. This is similar to the results of Koshi Basin in Nepal (Kaini et al., 2020). As in the case of annual flows, the range of predicted changes in future flows shows high level of uncertainty depending on the choice of GCM. Such variation is quite high in RCP 8.5 (–50% to +200%). However, similar monthly variations in flow between -70% and +190% are found in Wagener et al. (2004). Similarly, the maximum monthly flow increases by 143% and 99%, respectively for RCP 4.5 and 8.5 were reported in (Zhou et al., 2017). On the other hand, (Kingston et al., 2011) found that the mean monthly river flow varies from −16

% to +55 %, with highest decrease in July and August, and greatest increases in May and June.

Our results predict higher increase in high flows than that of low flows. The average increases (predicted by all GCMs for all time windows) of high flow (Q_{10}) are 23 and 26 %; and decrease of low flow (Q_{90}) are 14 and 17 percentage with respect to the baseline for RCP 4.5 and RCP 8.5, respectively. It shows that the negative impacts of climate change can be expected in both the high flows (increasing) and low flows (decreasing). Similar results are reported for Ljubljanica river of Slovenia in all three investigated future time windows i.e., 2011-2040, 2041-2070, 2071-2100 under RCP 4.5 (Sapač et al., 2019). Such projected impacts of climate change should be taken into consideration while planning and designing water resources development projects.

The highest change in one-day-maximum flood is expected in warm-wet climatic condition for case of RCP 4.5 in all time windows. However, for RCP 8.5, warm-wet of IF predicts higher values of flood while cold-wet in other two time periods (MF and FF). Projected flood values are different depending on the GCMs indicating the uncertainty in the results. Consequently, increased predicted floods by all GCMs show that the flood disposal structure should be designed at higher capacity than the one designed based on baseline flood values to achieve climate resilience. Further the results of this study show that one-day-minimum flow is expected to decrease in the future as an impact of CC. It shows the need of storage over RoR projects for optimal water use planning.

4.9 Impact of CC in hydro electricity production and revenue generation

4.9.1 Reservoir operating rules

A reservoir operating rule is a categorization of release decisions in operational periods, specified as a function of the reservoir storage at the beginning of a period and the inflow to the reservoir during the period. The reservoir operating rules adopted here is such that the dry season (December-May) energy is maximized and evenly distributed for this whole period, based on terrain data, live storage and long term monthly inflow data; and assumptions discussed in (Devkota et al., 2022; Marahatta et al., 2022). The operating rules were used to generate the available discharge and head of a particular month. Further, maximum energy at monthly timestep for the baseline was generated

(Table 4.14). The available discharge is the lowest (102 m^3/s) in November but it increases by three times in May (353 m^3/s).

October and November are the months with the maximum available head (215 m) which occurs when the reservoir is at its full supply level (FSL: 540 masl). Minimum head is in May (152 m), in which month the water level reaches to the minimum operating level (MOL: 470 masl). Utilizing the available head and discharge, power (P) has been calculated, as given in Table 4.14, for all the months, ranging from 491 MW (dry season: December to May) – 198 MW (June and November). The maximum power production in the dry season is attributed to the operating rule of maximizing dry season power/energy. The minimum power production in June is because of the utilization of the water of this month in filling the reservoir and in November because of the low flow in the river itself. Higher values of Q_{max} is available in April (322 m^3/s), May (354), June (351) and July (310) while it ranges from 251 to 297 m^3/s in the remaining months. The maximum possible power (P_{max}) is 491 MW throughout the year. The corresponding maximum possible monthly energy generation (E_{max}) ranges from 330-365 GWh with the annual total of 4301 GWh. These values have been enforced into the power and energy generation calculations for the baseline as well as future CC cases as boundary conditions.

Table 4.14: Monthly base case reservoir operating rule variables

Base Case Variables	Months											
	Jan	**Feb**	**Mar**	**Apr**	**May**	**Jun**	**Jul**	**Aug**	**Sep**	**Oct**	**Nov**	**Dec**
Q_{LTMA} (m^3/s)	73	71	83	114	171	354	577	593	429	191	102	81
Q_T (m^3/s)	266	280	297	322	354	141	231	238	172	191	102	255
H (m)	202	192	181	167	152	153	173	194	209	215	215	211
P (MW)	491	491	491	491	491	198	365	421	328	374	198	491
E(GWh)	365	330	365	353	365	142	272	313	236	278	143	365
Q_{max} (m^3/s)	266	280	297	322	354	351	310	277	257	251	251	255
P_{max} (MW)	491	491	491	491	491	491	491	491	491	491	491	491
E_{max} (GWh)	365	330	365	354	365	354	365	365	354	365	354	365

Q_{LTMA}: long-term mean monthly flow of the baseline period; Q_T: monthly discharge; P: Power; H: the available net head; Q_{max}: maximum allowable discharge; P_{max} and E_{max} are the maximum possible power and energy generation utilizing Q_{max} and H.

4.9.2 Baseline energy generation

The monthly variability in energy generation of the BGHP for the baseline period of 30 years is shown in Figure 4.23(a). For the months of December-May, the mean energy generation is ~350 GWh while the wet months show high variability in energy generation (~145 GWh: November – ~280: August). There are some months with zero energy generation even in the monsoon, particularly in the dry years because the flow during these dry years do not exceed the required storage needed for the dry period. Figure 4.23(b) shows the distribution of energy generation during the baseline period. It can be seen that energy generation is in the range of 350-400 GWh for about 38% of the time (135 months out of total 360 months). Similarly, 87 months (~27% of the time) generate 300-350 GWh while six months (< 2%) generate 50-100 GWh.

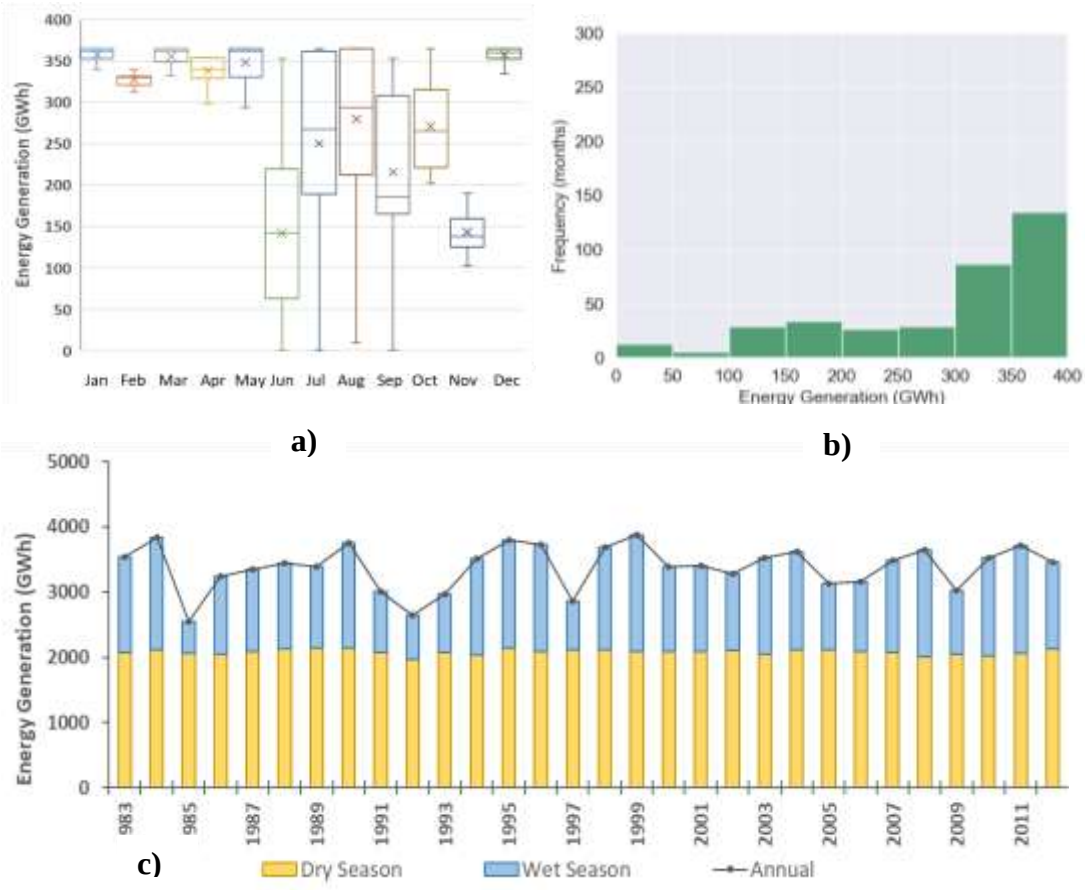

Figure 4.23: Monthly variability, frequency histogram and seasonal and annual variation of energy generation of the BGHP for the baseline period

The average annual energy generation for the baseline period is 3385 GWh. Because of the operating rules, approximately 2000 GWh is constantly generated in the dry season (Figure 4.23(c)). The small variations are because of the relatively drier monsoon with

insufficient storage. However, the variation during the monsoon and post monsoon seasons is mainly determined by the flow characteristics during the wet season, causing significantly larger variations in energy generation. Figure 4.23 (c) shows a fluctuation of 484 GWh (1985) to 1782 (1999) in the monsoon season. As a result, the total annual energy generation is determined by the energy generated during the wet season.

4.9.3 Future energy generation

It is projected that BGHP shall annually generate 3871, 3861 and 3877 GWh on an average in the IF, MF and FF respectively which indicates an increase of about 14% compared to the baseline. Figure 4.16 presents the energy distribution for the future scenarios. It can be seen that the project is likely to generate 350 to 400 GWh for >61% of the considered time duration in RCP 4.5 (Figure: 4.24 top) for all the time-windows. This is a pronounced increase compared to the baseline in which 350-400 GWh generation was possible only 38% of the time. In the cases of IF, MF and FF, 66, 64 and 68 months (~18% of the considered duration) respectively are expected to generate 300-350 GWh energy. The combined count of months with energy generation below 300 GWh is expected to reduce to 72 (~20% of the time) which is about half the value for the baseline (138 months) for all the considered time windows.

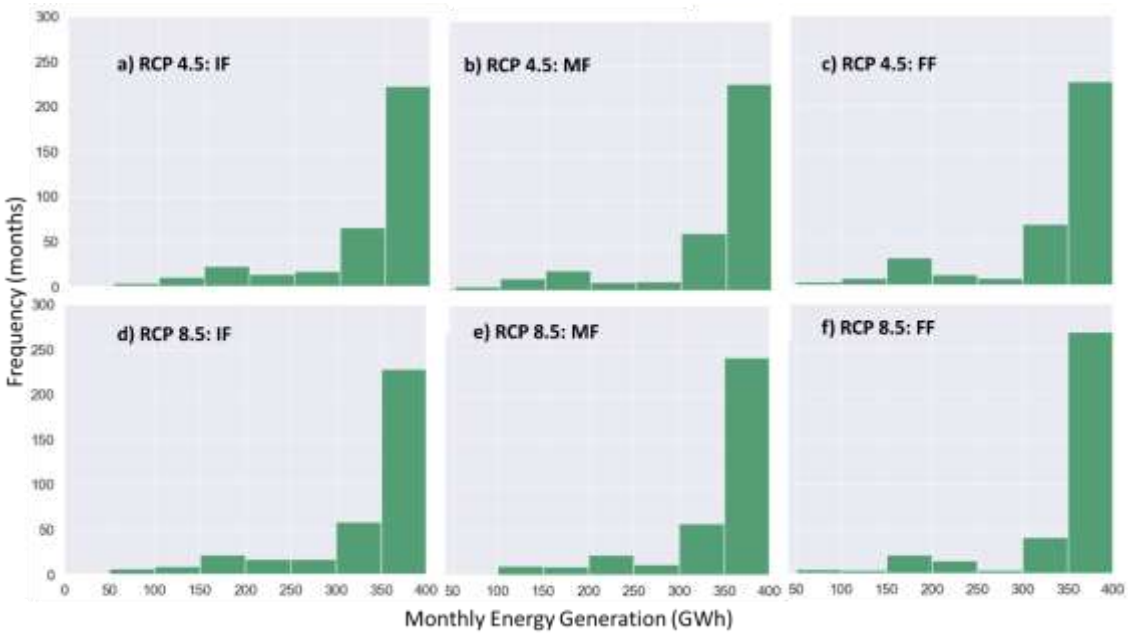

Figure 4.24: Distribution of monthly energy generation for RCP 4.5 and RCP 8.5 and three-time windows

The trend of energy generation in the case of RCP 8.5 (Figure 4.24 bottom) is similar to the RCP 4.5 case. Energy generation in the range of 350 to 400 GWh is projected from 228 (63% of the time duration), 242 (67%) and 269 (75%) months respectively for IF, MF and FF. Similarly, 300 to 350 GWh energy generation is expected from 59 (16%), 58 (16%) and 41 (11%) for IF, MF and FF respectively. A slight decrease in the number of months (20; 6%) expected to generate 250 to 300 GWh is projected for all the three time-windows. Energy generation up to 50 GWh is projected by less than two months for all the time windows – a considerable decrease (13 months) from the baseline. The expected average energy generation is 3864 (IF), 3949 (MF) and 3999 GWh (FF) annually which are 14%, 17% and 18% increments respectively compared to the baseline. The projected energy generation separated for dry and wet seasons as a function of time is shown in Figure 4.25. Dry season energy generation is almost constant at ~2000 GWh in all the scenarios. This constant value indicates that the total annual flow exceeds the minimum storage capacity. Similarly, due to the increased flow in the two climate change scenarios, the variations during the wet seasons is smaller than the baseline. However, a significant variation in the monsoon season is observed ranging from 1377 GWh (RCP 4.5-IF) to 2095 GWh (RCP 8.5-MF). As a result, the annual energy generation varies from 3520 GWh (RCP 4.5: IF) to 4239 GWh (RCP 8.5: MF).

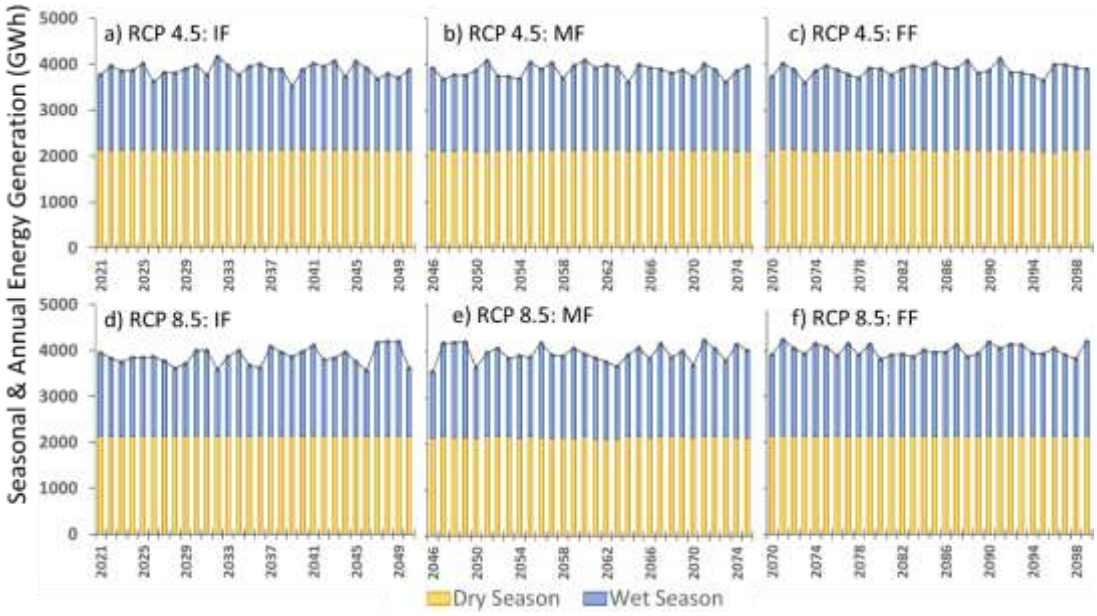

Figure 4.25: Seasonal and annual energy generation for considered climate scenarios

4.9.4 Change in future energy production

Monthly, seasonal and annual energy production for all climate scenarios were compared with the baseline (Table 4.15). Slight change is projected in the dry season while it is considerable in the monsoon. December-March shows no change while a small decrease is expected in April-May. Significant change is projected in November (MF; RCP 8.5) with 64.4% increase compared to the baseline. Annual energy production varies from 9.4 to 9.9 % for RCP 4.5 and 9.5 to 13.3% for RCP 8.5.

Table 4.15: Average energy generation for the baseline, RCPs 4.5 and 8.5 scenarios

Energy (GWh)	**Jan**	**Feb**	**Mar**	**Apr**	**May**	**Jun**	**Jul**	**Aug**	**Sep**	**Oct**	**Nov**	**Dec**	**Annual**
Base case	365	330	365	353	365	142	272	313	236	278	143	365	3528
						RCP 4.5							
IF	365	330	365	354	359	201	349	365	333	319	168	365	3871
% change	0.0	0.0	0.0	0.0	-1.7	41.0	28.2	**16.6**	40.8	14.8	17.2	0.0	9.7
MF	365	330	365	353	350	179	352	365	353	318	166	365	3861
% change	0.0	0.0	0.0	-0.3	**-4.2**	26.1	29.3	**16.6**	**49.4**	14.4	16.4	0.0	9.4
FF	365	333	365	349	353	192	352	365	353	321	165	365	3877
% change	0.0	**0.87**	0.0	**-1.2**	-3.4	34.9	29.3	**16.6**	**49.4**	15.5	15.1	0.0	9.9
						RCP 8.5							
IF	365	330	365	353	358	179	283	365	336	356	207	365	3864
% change	0.0	0.0	0.0	-0.3	-1.9	26.1	4.2	**16.6**	42.3	28.1	45.1	0.0	9.5
MF	365	330	365	351	356	200	300	365	353	365	235	365	3949
% change	0.0	0.0	0.0	-0.8	-2.5	40.8	10.2	**16.6**	**49.4**	**31.1**	**64.4**	0.0	11.9
FF	365	330	365	353	360	210	365	365	353	365	203	365	3999
% change	0.0	0.0	0.0	-0.3	-1.5	**47.8**	**34.2**	**16.6**	**49.4**	**31.1**	42.2	0.0	**13.3**

IF: Immediate Future; MF: Mid Future; and FF: Far Future; highest values of each column are bold-faced.

4.9.5 Change in future revenue generation

The total revenue of the base case is 306 billion USD. The monsoon share is approximately 27% ($ 83 million) whereas the dry season contributes the remaining 73% (223 million USD calculated using the PPA rates (NEA, 2018) (Figure 4.26). A notable increase in the monsoon season as well as annual revenue is expected in the considered climate scenarios (Figure 4.25). Revenue in the monsoon season of RCP 4.5 of all time windows and IF of RCP 8.5 is projected to increase by approximately 20 million USD annually. However, for the MF (26 million USD) and FF (28 million USD) of RCP 8.5, the changes are more significant. The dry season revenue is projected to decrease with a very little amount (approximately 1 million USD) in all the climate scenarios. The cumulative increase in revenue of each time window is approximately 600 million USD for RCP 4.5. When accumulated over 30 years, the increase in revenue are 590, 740 and 835 million USD for IF, MF and FF of RCP 8.5 respectively.

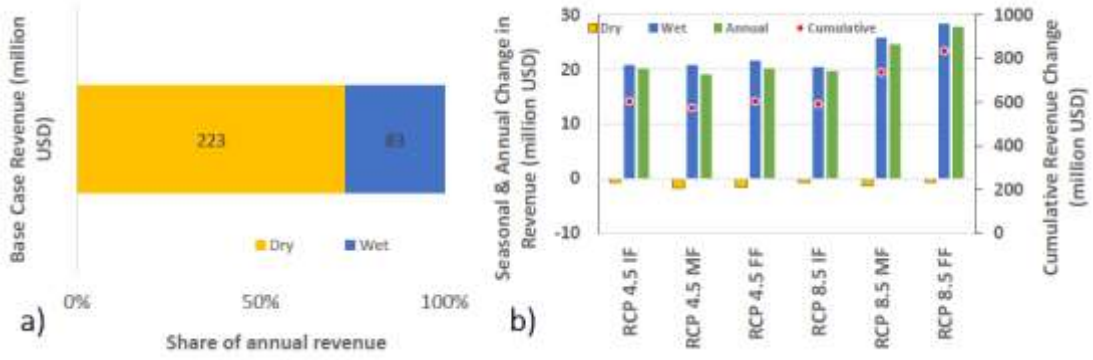

Figure 4.26: Revenue generation and their contribution to the annual value for the a) base case; b) climate change scenarios

Because of the differences in the geo-physical characteristics of the hydroelectricity projects, results from other studies are not directly comparable. Moreover, the scale and type of the project in addition to the used reservoir operating rules play a vital role in energy production (Chang et al., 2018). Therefore, we have compared the results of this study with other cases in the Hindu Kush Himalayan region. For example, an increase up to 45% in the streamflow and 25% in the electricity generation is estimated in the Ganga Basin (Ali et al., 2018). In the Tamakoshi basin of Nepal, hydroelectricity is expected to increase by 14% (Shrestha et al., 2016a). An increase of 1.7% in hydroelectricity potential is projected for Kabul River (Afghanistan) (Shirsat et al., 2021) while the Upper Indus basin is projected to face a change of -5 to +40% in

hydroelectricity generation (Casale et al., 2020). However, expected decrease (for instance, up to 13% in Kulekhani Basin of Nepal) in hydroelectricity generation is also reported by past studies because of decrease in runoff (Shrestha et al., 2021). Therefore, the values of projected change (9 to 13% increase) in future electricity production of the study basin can be considered comparable with the findings of the above-mentioned studies.

The total capital cost of the BGHP was estimated at 2550 million USD in 2015 (BGHP 2015). It can be observed that climate change positively impacts the earning potential of the BGHP with an additional revenue generation sufficient to construct an additional hydroelectricity project with approximately 30% generation capacity (~1015 GWh annually) of the proposed BGHP. The annual energy consumption of Nepal was 14.5 Mote (169 TWh) for the fiscal year 2019/020 (MoF, 2021). Contribution of liquified petroleum gas (LPG) was 449,063 Metric tonnes[2] (equivalent to 6295 GWh). LPG has a nearly 3.7% share of the total energy consumption of Nepal. Thus, the results show that nearly 16% of the current national LPG consumption can be replaced by additional revenue generated from the additional discharge because of climate change. The estimated additional revenue generation due to climate change from the BGHP alone in the RCP 8.5 is capable of replacing 28 million USD (more than 1.5 percent) of the national fuel import (1.8 billion USD which is nearly 16% of the total trade deficit for 2019/20) (MoF, 2021). These values can be considered as valuable contribution to the national economy, particularly for a developing country like Nepal. If this analysis is upscaled to the national level incorporating all the planned hydroelectricity projects in Nepal, the additional revenue from hydroelectricity due to climate change has the potential to replace current fossil fuel consumption.

Moreover, the economic status and availability of resources within a country largely governs the harnessing of its hydroelectricity potential. For instance, the Scandanavian countries, Australia, New Zealand, Japan and Canada are exploring other forms of renewable energy because their hydropower potential has already been harnessed (Gunturu and Hallgren 2017; Amir Jabbari and Nazemi 2019; Wagner et al. 2019; Poletti and Staffell 2021). Therefore, hydroelectricity generation of these countries are expected to be less impacted by CC. China has generated about 3000 GW of

[2] http://noc.org.np/import; accessed on 28 July 2021

hydroelectricity because of its strong economy, availability of resources, increasing demand and latest technology (Liu et al. 2016; IEA 2020; Qin et al. 2020b). On the other hand, in spite of tremendous hydropower potential, Africa has generated only less than 3% of its total hydroelectricity potential because of weak economy (Hamududu and Killingtveit 2016; Mtilatila et al. 2020; Uamusse et al. 2020), a condition very similar to Nepal (Jha, 2011). Brazil has generated significant hydroelectricity capable of supplying 30% of the total hydroelectricity use in Latin America. Therefore, Brazil faces a very large risk in hydroelectricity generation and trade in the future due to adverse impacts of CC (Caceres et al., 2021; de Faria and Jaramillo, 2017; de Jong et al., 2021, 2018; de Oliveira et al., 2017; de Queiroz et al., 2019; Donk et al., 2018). Therefore, it is seen that the impacts of CC on energy security and economy are likely to be severe in countries heavily reliant on hydroelectricity. Moreover, greenhouse gas reduction and additional revenue from hydroelectricity due to climate change are strong reasons for developing countries like Nepal to exploit its tremendous hydroelectricity potential in the future.

CHAPTER 5

CONCLUSION AND RECOMMENDATIONS

This study assessed the interannual variability of hydroclimatic condition of the Budhigandaki River Basin (BRB) using daily hydrological and meteorological data for the period from 1983 to 2012. The well-established hydrological model, Soil Water Assessment Tool (SWAT) is utilized to simulate the Budhigandaki River flow. Moreover, other approaches for the flow estimation are also tested and a new evaluation statistical index, naming Global Performance Index (GPI) is established and compared the performance of empirical methods with observational and SWAT model data. Budhigandaki River flow is also projected utilizing SWAT model for the warmer climate considering two RCPs (Representative Concentration Pathways) using bias corrected future climate data. This study further assessed the impact of climate change on flow and hydro-energy generation considering three 30-years' time windows, to analyze the energy economics associated with the climate change induced flow. The following conclusions and recommendation were drawn based on the results of this study.

5.1 Conclusions

Historical hydroclimatic data shows that there is a large variation in daily, monthly, seasonal and interannual flow in the study basin. The BRB receives nearly 1530 mm of annual precipitation with 74 % of rainfall in monsoon season. The stations; Jagat, Arughat, Gorkha and Dhading shows the slightly decreasing trends in precipitation while maximum 24 hours rainfall is in increasing trend however it is not statistically significant. The spatial variation of precipitation is quite high, the high-altitude stations received 50-60% of the annual precipitation in monsoon season. Windward side of the mountain barrier receives high annual precipitation (~ 2500 mm) while the leeward side remains relatively dry received less than 700 mm. Significant positive trends in historical maximum temperature is observed. Minimum temperature also observed positive trends however, there is no significant trends in the case of minimum temperature.

Calibration and validation of the model was carried out using daily flow data of 20 and 10 years (two-third and one-third period) at calibration station. Further validation at three supplementary points (two upstream and one downstream) at which the researcher collected primary river flow data and prepared rating curves. Long duration along with supplementary validation further added confidence to the model performance, the model performed well and was ranked "very good". This study estimated the mean annual flow at BRB outlet to be 240 m^3/s with annual precipitation 1495 mm and AET approximately 26% of the precipitation with distinct seasonal variability. Snowmelt contributes 20% of the total flow at the basin outlet during the pre-monsoon period and 8% in the post monsoon period. This study provides additional evidence to the SWAT diaspora of its applicability to simulate the rainfall-runoff characteristics of complex mountainous basin.

This study evaluated the performance of flow estimation using different empirical methods that are generally used to predict the monthly flow in Nepal; namely, DAR, GT, DHM/WECS 1990, NEA 1997, DHM 2004. The estimated flow was compared with the SWAT hydrological model using Global Performance Index (GPI) that was introduced to evaluate the flow estimation from methods. Based on the ranking of GPI, SWAT model is the best method considered for the monthly flow estimation in BRB.

Four GCMs representing cold-dry, warm-dry, cold-wet, and warm-wet conditions for two emission scenarios, i.e., RCPs 4.5 and 8.5, projected by the selected GCMs predict an increase in annual precipitation and temperature for RCP 4.5. In the case of RCP 8.5, most of the GCMs predict higher annual precipitation and temperature compared with the baseline condition, while some project a decrease in annual precipitation. The projected precipitation by almost all GCMs for all time windows (IF, MF, and FF) is most likely to increase in both RCPs. Both the maximum and minimum temperature projections by all the selected GCMs (in all climatic conditions) are found increasing while moving from IF to FF in both emission scenarios. The increasing temperature and variation in precipitation patterns in the BRB resulting from CC will impact the water resource availability in the future.

The long-term average annual flow from both RCPs scenarios is projected to increase continuously in future warming climate. The relative change in the mean monthly flow under RCP 4.5 and 8.5 is also projected to increase for IF, MF, and FF. Ensembled

flows are projected to be higher in RCP 8.5 than in RCP 4.5. The monsoon flow is expected to increase significantly for all time windows in both RCPs. While the variation in the monthly flows from the baseline values of RCP 8.5 is projected to be higher than that of RCP 4.5, and the rate of increase is found to be more in the post-monsoon season. The greatest magnitude of the projected monthly maximum flow in all time windows for all climatic conditions except FF of the cold–wet condition is found to occur in August, similar to the baseline condition. Moreover, the number of days exceeding the 10^{th} percentile and not exceeding the 90^{th} percentile is predicted to be more by all the GCMs. Likewise, the one-day-maximum floods (minimum flow) of different return periods are projected to be higher (lower) than those of the baseline floods (flow) for all climatic conditions and for all time windows in both RCPs. However, there is larger uncertainty in different ensembles of selected GCMs.

This research further evaluated the impacts of CC on energy production of a storage type hydro-electric project and extended the analysis further to assess the energy economics considering an ensemble of different CC scenarios for such two RCPs for three 30-year time windows. A set of operating rules for use in the reservoir simulation of the BGHP was derived considering the baseline flows, terrain data and other site constraints such that dry season (December - May) energy was maximized. Utilizing the derived operating rules and monthly average flows for the baseline as well as future time-windows, power (and energy) for the different scenarios were compared with the baseline value at monthly, seasonal and annual timescales. Besides, the corresponding seasonal and annual revenues for the above-mentioned scenarios were then calculated and also compared with the base case. Results show that future annual energy is expected to increase considerably by about 9 to 13% of the baseline values. Expected larger changes in energy generation with higher variability in the positive direction for almost all the scenarios indicate an optimistic picture of the future for the hydropower sector as a result of CC. Additionally, projected increment in future revenue generation is in the range of 20 to 28 million USD annually. Overall increase in the dry season revenue and significant gain in the wet season as well as annual revenue due to additional energy generation is an anticipated positive economic impact of CC which is capable of contributing to the reduction of greenhouse gases and minimizing fossil-fuel laden trade deficit.

The possibility of considerable economic gains in the future due to CC are strong reasons which should lure developing countries like Nepal with a high hydroelectricity potential to invest in and develop the clean renewable energy technology for sustainable energy security and environment protection. The findings of this research will be useful for hydrologists, economist and planners to utilize the available water rationally in the times to come and particularly, to harness the hydroelectric potential by considering the climate change in the complex mountainous basin like BRB.

5.2 Recommendations

The increase in future predicted floods implies the designing of flood disposal structures at a higher capacity than those designed based on historical data. Furthermore, the decrease in projected firm flows in the future suggests that storage-type water resource projects are preferred over run-of-river projects for optimal water use planning from the perspective of climate resilience. During the process of this study, some of the limitations had surfaced, which could be addressed in the future studies. Some recommendations for policy and researchers/academia are as follows:

5.2.1 Policy recommendation

Based on the assumptions and the results of this study, the following policy recommendations are prescribed to confront the impacts of CC on hydroelectricity:

- In areas where future flow and hydroelectricity generation are expected to increase, operating rules based on the historical baseline conditions are likely to turn out to be inefficient. Hence, provision of flexible operating rules in the energy/ hydro-electricity policy considering future hydro-climatic conditions is strongly recommended.
- Huge amount of resources are required for energy sector in Nepal, proper mobilization of adequate financial resources (both internal as well as external) and utilizing them effectively for making rapid progress in water resources management and energy security in terms of renewable energy; like hydroelectricity are of utmost importance.
- Regions where decreasing flow and/or hydroelectricity generation are expected in the future, other alternative sources of renewable energy like wind, solar and geothermal are to be explored for attaining a state of future energy security. Relying only on hydro-electricity might be extremely risky.

- Revenue aspects such as the power purchasing rates, rebates and subsidies, penalties, among others, should be revised accordingly considering future projected conditions for the sustainability of the hydro-electric projects.
- This study recommends that: STPs with the provision of flexible operating rules are desirable for climate resiliency in hydroelectricity;
- Alternative sources of renewable energy in the generation mix; and the policy instruments pertaining to the financial aspects should be continuously updated considering future conditions.

CHAPTER 6

SUMMARY

6.1 General overview

This study targeted five objectives to address the main research questions. I completed the research publishing five papers that address each research questions and this chapter summarizes the finding based on these five peer reviewed research papers.

Climate change has become a major challenge and threat to the planet particularly, after World War II. Although alteration in the Earth's climate has been going on forever, we have started acknowledging its impacts on humans and the current environment only in the second half of the twentieth century. An understanding of the nexus of climate change, river hydrology and energy economics can have policy implications in the developing countries like Nepal.

This study thus carried out to identify the impacts of climate change on river hydrology and energy economics at different scales; mainly continental, river basin and national level by establishing the hydrological model and the climate change analysis and their economic implication in terms of revenue generation. Available literatures, the secondary hydro-climatic data, energy table of the hydro-electricity projects and projected climate data from GCMs were considered for the analysis. DHM provided the hydroclimatic data mainly rainfall and temperature along with flow data from all its stations in and around the Budhigandaki River Basin from 1964 to 2017, while data from planed hydropower projects in the BRB were used to analyze at project level analysis from the Department of Electricity Development (DoED), Budhigandaki Hydroelectricity Project (BGHP) and private hydroelectricity developer. Similarly, hydro-electricity production and all types of energy used data of the whole country is collected from Nepal Electricity Authority and Water and Energy Commission Secretariat. Besides, the primary data generated by the author have also been used as the supplementary validation in this research for the validation of the reference hydrological station. The brief summary of analysis and results are presented here according to objectives of this study;

i. Identify historical variation in precipitation, temperature and runoff patterns,

ii. Evaluate the empirical method and hydrological simulation for flow estimation in ungauged basins.

iii. Simulate the historical river flow using SWAT hydrological model.

iv. Project the hydro-climatic patterns under different climate change scenarios for this century.

v. Analyze the hydroelectric power production and energy economics particularly change in revenue generation under the different climate change scenarios.

6.2 Summary related to 'specific objective i' of the study

The first objective of this study is to analyze the variation of hydroclimatic condition of the BRB, mainly focusing on the river hydrology and the result has been published in (Marahatta et al., 2021d). Daily flow data from 1964 to 2015 of Budhigandaki River at Arughat were considered to analyze the interannual flow variation of the RoR type of hydroelectric projects. The data show very high variation in all daily, monthly and seasonal flows. The long term annual average flow at Arughat is 160 m^3/s that varies from 120 to 210 m^3/s. The flow ratio between high 20% (Q_{20}) and lower 20% (Q_{80}) of exceedance flows was found to be about 14. The long-term averages of loss in flow for both dry and wet seasons based on daily flows for three design discharges at Q_{90}, Q_{60} and Q_{40} are -0.72, -1.76 and -1.54 m^3/s for dry season and 0.0, -0.27 and -2.26 m^3/s for wet season, respectively. Although long term average loss is small, uncertainty increases with the increase in design discharge. This study found that the long-term dry season power loss is ~3% for the RoR projects of the basin. However, its annual variation is large, i.e., there is a probability of losing the quantum of energy generation by nearly 40% in some years and gaining by about 30% in some other years in dry season. The impact of flow variation on power production is negative in both dry and wet seasons for RoR projects of BRB. This study concludes that uncertainty arising from daily flow variation should be assessed while estimating energy generation in hydroelectric projects.

6.3 Summary related to 'specific objective ii' of the study

The second objective of this study is to simulate the historical river flow using hydrological model and the result has been published in (Marahatta et al., 2021a) The soil and water assessment tool hydrological was used to characterize the rainfall-runoff behaviour of a complex transboundary mountainous BRB. The BRB was divided into 16 sub-basins and 344 hydrological response units. The calibration and validation were carried out at Arughat station using daily flow data of 20 years and 10 years, respectively. Additionally, this study also carried out validation at three supplementary stations at which the primary river flow data were collected. Four statistical indicators: NSE, PBIAS, KGE and ratio of the root mean square error to the standard deviation of measured data (RSR) were used to evaluate the model performance. Calibration and validation results rank the model performance as "very good". This study estimated the snowmelt contributes 20% of the total flow during the pre-monsoon and 8% in the post monsoon period. The 90%, 40% and 10% exceedance flows were calculated to be 39, 126 and 453 m^3/s respectively.

6.4 Summary related to 'specific objective iii' of the study

The third objective of this research is to evaluate the empirical method and hydrological simulation for flow estimation in ungauged basins and the result has been published (Marahatta et al., 2021c). Information and data on streamflow hydrology is crucial for different water management projects. However, availability of measured flow data in many cases is either inadequate or not available at all. When there is no gauging station available at the site of interest, various empirical methods are generally used to estimate the flow. This study aimed to estimate the monthly average flows using empirical methods and compare the results with hydrological simulation. This study found that hydrological modeling is the best among the considered methods of flow estimation for ungauged catchments.

6.5 Summary related to 'specific objective iv' of the study

The fourth objective of this research is to project the hydro-climatic condition of BRB under different climate change scenarios and the result has been published in (Marahatta et al., 2021b). A relatively new approach of selecting global climate models (GCMs) for two emission scenarios, RCP 4.5 and RCP 8.5, representing four extreme cases (warm-wet, cold-wet, warm-dry, and cold-dry conditions). The bias-corrected

GCM data were used to simulate the SWAT model one at a time to evaluate the future flows of BRB for three 30-year time windows that are Immediate Future (2021–2050), Mid Future (2046–2075), and Far Future (2070–2099). The results showed that future long-term average annual flows are expected to increase in all climatic conditions for both RCPs compared to the baseline. However, the range of predicted changes in future monthly, seasonal, and annual flows shows high uncertainty. The comparative frequency analysis of the annual one-day-maximum and -minimum flows shows increased high flows and decreased low flows in the future. These results can be implied for design modifications in hydraulic structures as well as the preference of storage over run-of-river water resources development projects in BRB from the perspective of climate resilience.

6.6 Summary related to 'specific objective v' of the study

The fifth and last objective of this study is to analyze the hydroelectric power production and energy economics particularly change in revenue generation under the different climate change scenarios and the result has been published in (Marahatta et al., 2022). The impact assessment was conducted considering an ensemble flow of different CC scenarios derived for the proposed 1200 MW Budhigandaki Storage Hydroelectric Project. We found that future energy is expected to increase by about 9 to 13% compared to the baseline values and projected increment in future revenue generation is in the range of 20 to 28 million USD annually. This overall gain in the revenue due to additional energy generation is an anticipated positive impact of CC which is capable of contributing to the reduction of greenhouse gases and minimizing trade deficit.

REFERENCES

Aawar, T., Khare, D., 2020. Assessment of climate change impacts on streamflow through hydrological model using SWAT model: a case study of Afghanistan. Model. Earth Syst. Environ. 6, 1427–1437. https://doi.org/10.1007/s40808-020-00759-0

Abbaspour, K.C., Rouholahnejad, E., Vaghefi, S., Srinivasan, R., Yang, H., Kløve, B., 2015. A continental-scale hydrology and water quality model for Europe: Calibration and uncertainty of a high-resolution large-scale SWAT model. J. Hydrol. 524, 733–752. https://doi.org/10.1016/j.jhydrol.2015.03.027

Aboelnour, M., Gitau, M.W., Engel, B.A., 2020. A comparison of streamflow and baseflow responses to land-use change and the variation in climate parameters using SWAT. Water (Switzerland) 12. https://doi.org/10.3390/w12010191

Adynkiewicz-Piragas, M., Miszuk, B., 2020. Risk analysis related to impact of climate change on water resources and hydropower production in the Lusatian Neisse River Basin. Sustain. 12. https://doi.org/10.3390/su12125060

Ahmad, A., El-Shafie, A., Mohd Razali, S.F., Mohamad, Z.S., 2014. Reservoir optimization in water resources: A review. Water Resour. Manag. 28, 3391–3405. https://doi.org/10.1007/s11269-014-0700-5

Akhtar, M., Ahmad, N., Booij, M.J., 2008. The impact of climate change on the water resources of Hindukush–Karakorum–Himalaya region under different glacier coverage scenarios. J. Hydrol. 355, 148–163.

Akoko, G., Kato, T., Tu, L.H., 2020. Evaluation of irrigation water resources availability and climate change impacts-a case study of Mwea irrigation scheme, Kenya. Water (Switzerland) 12. https://doi.org/10.3390/W12092330

Akoko, G., Le, T.H., Gomi, T., Kato, T., 2021. A review of swat model application in africa. Water (Switzerland) 13. https://doi.org/10.3390/w13091313

Alam, F., Alam, Q., Reza, S., Khurshid-ul-alam, S.M., Saleque, K., 2017. A review of hydropower projects in Nepal. Energy Procedia 110, 581–585. https://doi.org/10.1016/j.egypro.2017.03.188

Alford, D., 1992. Annual Runoff from Glaciers of the Nepal Himalaya, ICIMOD. Kathmandu, Nepal.

Alford, D., Armstrong, R., 2010. The role of glaciers in stream flow from the Nepal Himalaya. Cryosph. Discuss. 4, 469–494. https://doi.org/10.5194/tcd-4-469-2010

Alford, D., Armstrong, R., Racoviteanu, A., 2011. Glacier Retreat in the Nepal Himalaya: The role of glaciers in stream flow from the Nepal Himalaya.

Ali, S.A., Aadhar, S., Shah, H.L., Mishra, V., 2018. Projected Increase in Hydropower Production in India under Climate Change. Sci. Rep. 8, 1–12. https://doi.org/10.1038/s41598-018-30489-4

Amir Jabbari, A., Nazemi, A., 2019. Alterations in Canadian Hydropower Production Potential Due to Continuation of Historical Trends in Climate Variables. Resources 8, 163. https://doi.org/10.3390/resources8040163

Andrianaki, M., Shrestha, J., Kobierska, F., Nikolaidis, N.P., Bernasconi, S.M., 2019. Assessment of SWAT spatial and temporal transferability for a high-altitude glacierized catchment. Hydrol. Earth Syst. Sci. 23, 3219–3232. https://doi.org/10.5194/hess-23-3219-2019

Anghileri, D., Botter, M., Castelletti, A., Weigt, H., Burlando, P., 2018. A Comparative Assessment of the Impact of Climate Change and Energy Policies on Alpine Hydropower. Water Resour. Res. 54, 9144–9161. https://doi.org/10.1029/2017WR022289Anthwal, A., Disaster, U., Joshi, V., Sharma, A., 2006. Retreat of Himalayan Glaciers - Indicator of Climate Change. Nat. Sci. 4, 53–59.

Arnold, J.G., Srinivasan, R., Muttiah, R.S., Williams, J.R., Ramanarayanan, T.S., Arnold, J.G., Bednarz, S.T., Srinivasan, R., Muttiah, R.S., Williams, J.R., 1998. Large area hydrologic modeling and assessment part I: model development 1. JAWRA J. Am. Water Resour. Assoc. 34, 73–89.

Arriagada, P., Dieppois, B., Sidibe, M., Link, O., 2019. Impacts of climate change and climate variability on hydropower potential in data-scarce regions subjected to multi-decadal variability. Energies 12. https://doi.org/10.3390/en12142747

Aslan, A., 2014. Causality between electricity consumption and economic growth in Turkey: An ARDL bounds testing approach. Energy Sources, Part B Econ. Planning, Policy 9, 25–31.Asurza-Véliz, F.A., Lavado-Casimiro, W.S., 2020. Regional parameter estimation of the SWAT model: Methodology and application to river basins in the Peruvian pacific drainage. Water (Switzerland) 12, 1–25. https://doi.org/10.3390/w12113198

Athira, P., Sudheer, K.P., 2021. Calibration of distributed hydrological models considering the heterogeneity of the parameters across the basin: a case study of SWAT model. Environ. Earth Sci. 80, 1–18. https://doi.org/10.1007/s12665-021-09434-8

Awojobi, O., Jenkins, G.P., 2015. Were the hydro dams financed by the World Bank from 1976 to 2005 worthwhile? Energy Policy 86, 222–232. https://doi.org/10.1016/j.enpol.2015.06.040

Aznarez, C., Jimeno-Sáez, P., López-Ballesteros, A., Pacheco, J.P., Senent-Aparicio, J., 2021. Analysing the impact of climate change on hydrological ecosystem services in laguna del sauce (Uruguay) using the swat model and remote sensing data. Remote Sens. 13. https://doi.org/10.3390/rs13102014

Babel, M.S., Bhusal, S.P., Wahid, S.M., Agarwal, A., 2013. Climate change and water resources in the Bagmati River Basin, Nepal. Theor. Appl. Climatol. 115, 639–654. doi.org/10.1007/s00704-013-0910-4

Bahadori, A., Zahedi, G., Zendehboudi, S., 2013. An overview of Australia's hydropower energy: Status and future prospects. Renew. Sustain. Energy Rev. 20, 565–569. https://doi.org/10.1016/j.rser.2012.12.026

Bajracharya, A.R., Bajracharya, S.R., Shrestha, A.B., Maharjan, S.B., 2018. Climate change impact assessment on the hydrological regime of the Kaligandaki Basin, Nepal. Sci. Total Environ. 625, 837–848. https://doi.org/10.1016/j.scitotenv.2017.12.332

Bajracharya, S., Maharjan, S., Shrestha, F., Bajracharya, O., Baidya, S., 2014. Glacier status in Nepal and decadal change from 1980 to 2010 based on landsat data. International Centre for Integrated Mountain Development, Kathmandu, Nepal.

Bajracharya, S.R., Shrestha, M.S., Shrestha, A.B., 2017. Assessment of high-resolution

satellite rainfall estimation products in a streamflow model for flood prediction in the Bagmati basin, Nepal. J. Flood Risk Manag. 10, 5–16. https://doi.org/10.1111/jfr3.12133

Baris, K., Kucukali, S., 2012. Availibility of renewable energy sources in Turkey: Current situation, potential, government policies and the EU perspective. Energy Policy 42, 377–391.

Barnett, T.P., Adam, J.C., Lettenmaier, D.P., 2005. Potential impacts of a warming climate on water availability in snow-dominated regions. Nature 438, 303–309. https://doi.org/10.1038/nature04141

Barreto, R.A., 2018. Fossil fuels , alternative energy and economic growth. Econ. Model. 75, 196–220. https://doi.org/10.1016/j.econmod.2018.06.019

Bastola, S., Ishidaira, H., Takeuchi, K., 2008. Regionalisation of hydrological model parameters under parameter uncertainty: A case study involving TOPMODEL and basins across the globe. J. Hydrol. 357, 188–206. https://doi.org/10.1016/j.jhydrol.2008.05.007

Baurzhan, S., Jenkins, G.P., Olasehinde-Williams, G.O., 2021. The economic performance of hydropower dams supported by the world bank group, 1975–2015. Energies 14. https://doi.org/10.3390/en14092673

Beasley, D.B., Huggins, L.F., Monke, E.J., 1980. ANSWERS : A Model for Watershed Planning. Am. Soc. Agric. Eng. https://doi.org/10.13031/2013.34692

Belfiori, M.E., 2020. Fossil fuel subsidies, the green paradox and the Fiscal paradox. Econ. Energy Environ. Policy 10, 183–193. https://doi.org/10.5547/2160-5890.10.1.MBEL

Best, R., 2017. Switching towards coal or renewable energy? The effects of financial capital on energy transitions. Energy Econ. 63, 75–83. https://doi.org/10.1016/j.eneco.2017.01.019

Beven, K., 2019. How to make advances in hydrological modelling. Hydrol. Res. 1969, 1481–1494. https://doi.org/10.2166/nh.2019.134

Beven, K., 2001. How far can we go in distributed hydrological modelling? Hydrol. Earth Syst. Sci. 5, 1–12. https://doi.org/10.5194/hess-5-1-2001

Beven, K.J., 2011. Rainfall-runoff modelling: the primer. John Wiley & Sons.

Beven, K.J., Kirkby, M.J., 2009. A physically based , variable contributing area model of basin hydrology / Un modèle à base physique de zone d ' appel variable de l ' hydrologie du bassin versant 6936. https://doi.org/10.1080/02626667909491834

Beven, K.J., Kirkby, M.J., 1976. Toward a simple physicallybased variable contributing area of catchment hydrology, Vol. 154.

BGHEP, 2015. Feasibility Study and Detailed Design of Budhigandaki Hydropower Project Part 1. Budhigandaki Hydroelectric Project Development Committee, Government of Nepal, Kathmandu, Nepal.

BGHP, 2015. Feasibility Study and Detailed Design of Budhigandaki Hydropower Project Part 1. Kathmandu, Nepal.

Bharati, L., Bhattarai, U., Khadka, A., Gurung, P., Neumann, L.E., Penton, D.J., Dhaubanjar, S., Nepal, S., 2019. From the mountains to the plains: Impact of climate change on water resources in the Koshi River Basin. International Water Management Institute (IWMI).

Bharati, L., Gurung, P., Maharjan, L., Bhattarai, U., 2016. Past and future variability in the hydrological regime of the Koshi Basin , Nepal. Hydrol. Sci. J. 61, 79–93. https://doi.org/10.1080/02626667.2014.952639

Bhatta, B., Shrestha, S., Shrestha, P.K., Talchabhadel, R., 2020. Modelling the impact of past and future climate scenarios on streamflow in a highly mountainous watershed: A case study in the West Seti River Basin, Nepal. Sci. Total Environ. 740, 140156. https://doi.org/10.1016/j.scitotenv.2020.140156

Bhatta, B., Shrestha, S., Shrestha, P.K., Talchabhadel, R., 2019. Evaluation and application of a SWAT model to assess the climate change impact on the hydrology of the Himalayan River Basin. Catena 181, 104082. https://doi.org/10.1016/j.catena.2019.104082

Bhattarai, B.C., Burkhart, J.F., Tallaksen, L.M., Xu, C.Y., Matt, F.N., 2020. Evaluation of global forcing datasets for hydropower inflow simulation in Nepal. Hydrol. Res. 51, 202–225. https://doi.org/10.2166/nh.2020.079

Bhattarai, S., Zhou, Y., Shakya, N.M., Zhao, C., 2018. Hydrological modelling and climate change impact assessment using HBV light model: A case study of Narayani river basin, Nepal. Nat. Environ. Pollut. Technol. 17, 691–702.

Bierkens, M.F.P., 2015. Global hydrology 2015: State, trends, and directions. Water Resour. Res. 15, 4923–4947. https://doi.org/10.1002/ 2015WR017173

Bilgili, M., Bilirgen, H., Ozbek, A., Ekinci, F., Demirdelen, T., 2018. The role of hydropower installations for sustainable energy development in Turkey and the world. Renew. Energy 126, 755–764. https://doi.org/10.1016/j.renene.2018.03.089

Bocchiola, D., Bombelli, G.M., Camin, F., Ossi, P.M., 2020a. Field study of mass balance, and hydrology of the West Khangri Nup glacier (Khumbu, Everest). Water (Switzerland) 12, 1–23. https://doi.org/10.3390/w12020433

Bocchiola, D., Manara, M., Mereu, R., 2020b. Hydropower potential of run of river schemes in the himalayas under climate change: A case study in the dudh koshi basin of Nepal. Water (Switzerland) 12. https://doi.org/10.3390/W12092625

Bogdanov, D., Ram, M., Aghahosseini, A., Gulagi, A., Oyewo, A.S., Child, M., Caldera, U., Sadovskaia, K., Farfan, J., De Souza Noel Simas Barbosa, L., Fasihi, M., Khalili, S., Traber, T., Breyer, C., 2021. Low-cost renewable electricity as the key driver of the global energy transition towards sustainability. Energy 227, 120467. https://doi.org/10.1016/j.energy.2021.120467

BP, 2020. Statistical Review of World Energy, 69th ed. British Petroleum, London, UK.

Brouziyne, Y., Abouabdillah, A., Chehbouni, A., Hanich, L., Bergaoui, K., McDonnell, R., Benaabidate, L., 2020. Assessing hydrological vulnerability to future droughts in a Mediterranean watershed: Combined indices-based and distributed modeling approaches. Water (Switzerland) 12. https://doi.org/10.3390/W12092333

Budhathoki, A., Babel, M.S., Shrestha, S., Meon, G., Kamalamma, A.G., 2021. Climate change impact on water balance and hydrological extremes in different physiographic regions of the West Seti River Basin, Nepal. Ecohydrol.

Hydrobiol. 21, 79–95. https://doi.org/10.1016/j.ecohyd.2020.07.001

Bui, M.T., Lu, J., Nie, L., 2020. A review of hydrological models applied in the permafrost-dominated Arctic region. Geosci. 10, 1–27. https://doi.org/10.3390/geosciences10100401

Caceres, A.L., Jaramillo, P., Matthews, H.S., Samaras, C., Nijssen, B., 2021. Hydropower under climate uncertainty: Characterizing the usable capacity of Brazilian, Colombian and Peruvian power plants under climate scenarios. Energy Sustain. Dev. 61, 217–229. https://doi.org/10.1016/j.esd.2021.02.006

Casale, F., Bombelli, G.M., Monti, R., Bocchiola, D., 2020. Hydropower potential in the Kabul River under climate change scenarios in the XXI century. Theor. Appl. Climatol. 139, 1415–1434. https://doi.org/10.1007/s00704-019-03052-y

Chang, J., Wang, X., Li, Y., Wang, Y., Zhang, H., 2018. Hydropower plant operation rules optimization response to climate change. Energy 160, 886–897. https://doi.org/10.1016/j.energy.2018.07.066

Chawanda, C.J., Arnold, J., Thiery, W., van Griensven, A., 2020. Mass balance calibration and reservoir representations for large-scale hydrological impact studies using SWAT+. Clim. Change 163, 1307–1327. https://doi.org/10.1007/s10584-020-02924-x

Chen, B., Krajewski, W.F., Liu, F., Fang, W., Xu, Z., 2017. Estimating instantaneous peak flow from mean daily flow. Hydrol. Res. 48, 1474–1488. https://doi.org/10.2166/nh.2017.200

Chen, J., Chang, H., 2021. Relative impacts of climate change and land cover change on streamflow using SWAT in the Clackamas River Watershed, USA. J. Water Clim. Chang. 12, 1454–1470. https://doi.org/10.2166/wcc.2020.123

Chen, M., Gassman, P.W., Srinivasan, R., Cui, Y., Arritt, R., 2020. Analysis of alternative climate datasets and evapotranspiration methods for the Upper Mississippi River Basin using SWAT within HAWQS. Sci. Total Environ. 720, 137562. https://doi.org/10.1016/j.scitotenv.2020.137562

Chiang, J., Yang, H., Chen, Y., Lee, M., 2013. European Geosciences Union General Assembly 2013 , EGU Division Energy , Resources & the Environment , ERE

Potential Impact of Climate Change on Hydropower Generation in Southern Taiwan. Energy Procedia 40, 34–37. https://doi.org/10.1016/j.egypro.2013.08.005

Chinnasamy, P., Sood, A., 2020. Estimation of sediment load for Himalayan Rivers: Case study of Kaligandaki in Nepal. J. Earth Syst. Sci. 129. https://doi.org/10.1007/s12040-020-01437-6

Chow, V.T., Maidment, D.R., Mays, L.W., 1988. Applied Hydrology. TATA McGrawHill Inc., New York.

Chylek, P., Li, J., Dubey, M.K., Wang, M., Lesins, G., 2011. Observed and model simulated 20th century Arctic temperature variability: Canadian Earth System Model CanESM2. Atmos. Chem. Phys. Discuss. 11, 22893–22907. https://doi.org/10.5194/acpd-11-22893-2011

Clarke, R.T., 1973. A review of some mathematical models used in hydrology, with observations on their calibration and use. J. Hydrol. 19, 1–20. https://doi.org/10.1016/0022-1694(73)90089-9

Collins, W.J., Bellouin, N., Doutriaux-Boucher, M., Gedney, N., Halloran, P., Hinton, T., Hughes, J., Jones, C.D., Joshi, M., Liddicoat, S., Martin, G., O'Connor, F., Rae, J., Senior, C., Sitch, S., Totterdell, I., Wiltshire, A., Woodward, S., 2011. Development and evaluation of an Earth-System model - HadGEM2. Geosci. Model Dev. 4, 1051–1075. https://doi.org/10.5194/gmd-4-1051-2011

Coron, L., Andréassian, V., Perrin, C., Lerat, J., Vaze, J., Bourqui, M., Hendrickx, F., 2012. Crash testing hydrological models in contrasted climate conditions: An experiment on 216 Australian catchments. Water Resour. Res. 48, 1–17. https://doi.org/10.1029/2011WR011721

Crawford, N.H., Linsley, R.K., 1966. Digital Simulation in Hydrology'Stanford Watershed Model. Singapore: McGraw-Hill Palo Alto, CA.

Dahal, P., Lall, M., Panthi, J., Pradhananga, D., 2020. Modeling the future impacts of climate change on water availability in the Karnali River Basin of Nepal Himalaya. Environ. Res. 185, 109430. https://doi.org/10.1016/j.envres.2020.109430

Dahal, V., Shakya, N.M., Bhattarai, R., 2016. Estimating the impact of climate change on water availability in Bagmati Basin, Nepal. Environ. Process. 3, 1–17.

Daniel, E.B., Camp, J. V, LeBoeuf, E.J., Penrod, J.R., Dobbins, J.P., Abkowit, M.D., 2011. Watershed modeling and its applications: A state-of-the-art review, Open Hydrol. J 5, 26–50.

Davis, M., Moronkeji, A., Ahiduzzaman, M., Kumar, A., 2020. Assessment of renewable energy transition pathways for a fossil fuel-dependent electricity-producing jurisdiction. Energy Sustain. Dev. 59, 243–261. https://doi.org/10.1016/j.esd.2020.10.011

de Faria, F.A.M., Jaramillo, P., 2017. The future of power generation in Brazil: An analysis of alternatives to Amazonian hydropower development. Energy Sustain. Dev. 41, 24–35. https://doi.org/10.1016/j.esd.2017.08.001

de Jong, P., Barreto, T.B., Tanajura, C.A.S., Oliveira-Esquerre, K.P., Kiperstok, A., Andrade Torres, E., 2021. The Impact of Regional Climate Change on Hydroelectric Resources in South America. Renew. Energy 173, 76–91. https://doi.org/10.1016/j.renene.2021.03.077

de Jong, P., Tanajura, C.A.S., Sánchez, A.S., Dargaville, R., Kiperstok, A., Torres, E.A., 2018. Hydroelectric production from Brazil's São Francisco River could cease due to climate change and inter-annual variability. Sci. Total Environ. 634, 1540–1553. https://doi.org/10.1016/j.scitotenv.2018.03.256

de Oliveira Fagundes, H., Cauduro Dias de Paiva, R., Mainardi Fan, F., Costa Buarque, D., César Fassoni-Andrade, A., 2020. Sediment modeling of a large-scale basin supported by remote sensing and in-situ observations. Catena 190, 104535. https://doi.org/10.1016/j.catena.2020.104535

de Oliveira Serrão, E.A., Silva, M.T., Ferreira, T.R., de Paulo Rodrigues da Silva, V., de Salviano de Sousa, F., de Lima, A.M.M., de Ataide, L.C.P., Wanzeler, R.T.S., 2020. Land use change scenarios and their effects on hydropower energy in the Amazon. Sci. Total Environ. 744, 140981. https://doi.org/10.1016/j.scitotenv.2020.140981

de Oliveira, V.A., de Mello, C.R., Viola, M.R., Srinivasan, R., 2017. Assessment of climate change impacts on streamflow and hydropower potential in the

headwater region of the Grande river basin, Southeastern Brazil. Int. J. Climatol. 37, 5005–5023. https://doi.org/10.1002/joc.5138

de Queiroz, A.R., Faria, V.A.D., Lima, L.M.M., Lima, J.W.M., 2019. Hydropower revenues under the threat of climate change in Brazil. Renew. Energy 133, 873–882. https://doi.org/10.1016/j.renene.2018.10.050

Devi, G.K., Ganasri, B.P., Dwarakish, G.S., 2015. A Review on Hydrological Models 4, 1001–1007. https://doi.org/10.1016/j.aqpro.2015.02.126

Devkota, L.P., Bhattarai, U., Khatri, P., Marahatta, S., Shrestha, D., 2022. Resilience of hydropower plants to flow variation through the concept of flow elasticity of power: Theoretical development. Renew. Energy 184, 920–932. https://doi.org/10.1016/j.renene.2021.11.051

Devkota, L.P., Gyawali, D.R., 2015. Impacts of climate change on hydrological regime and water resources management of the Koshi River Basin, Nepal. J. Hydrol. Reg. Stud. 4, 502–515. https://doi.org/10.1016/j.ejrh.2015.06.023

Devkota, R., Bhattarai, U., Devkota, L., Maraseni, T.N., 2020. Assessing the past and adapting to future floods: a hydro-social analysis. Clim. Change 163, 1065–1082.

Devkota, R.P., Bhattarai, U., 2018. Assessment of climate change impact on floods from a techno- social perspective. J. Flood Risk Manag. 11, S186–S196.

Devkota, R.P., Maraseni, T., 2018. Flood risk management under climate change: a hydro-economic perspective. Water Sci. Technol. Water Supply 18, 1832–1840.

Devkota, R.P., Pandey, V.P., Bhattarai, U., Shrestha, H., Adhikari, S., Dulal, K.N., 2017. Climate change and adaptation strategies in Budhi Gandaki River Basin, Nepal: a perception-based analysis. Clim. Change 140, 195–208.

Devkota, R.P., Pandey, V.P., Bhattarai, U., Shrestha, H., Adhikari, S., Dulal, K.N., 2016. Climate change and adaptation strategies in Budhi Gandaki River Basin, Nepal: a perception-based analysis. Clim. Change. https://doi.org/10.1007/s10584-016-1836-5

Dhami, B., Kumar, S., Ashish, H., Amar, P., Gautam, K., 2018. Evaluation of the

SWAT model for water balance study of a mountainous snowfed river basin of Nepal. Environ. Earth Sci. https://doi.org/10.1007/s12665-017-7210-8

DHM, 2018. Streamflow Summary (1962-2015). Department of Hydrology and Meteorology, Government of Nepal, Kathmandu, Nepal.

DHM, 2017. Observed Climate Trend Analysis in the Districts and Physiographic Regions of Nepal (1971-2014). Department of Hydrology and Meteorology, Government of Nepal, Kathmandu, Nepall, Kathmandu, Nepal.

Dietzenbacher, E., Kulionis, V., Capurro, F., 2020. Measuring the effects of energy transition: A structural decomposition analysis of the change in renewable energy use between 2000 and 2014. Appl. Energy 258, 114040. https://doi.org/10.1016/j.apenergy.2019.114040

Dis, M.O., Anagnostou, E., Zac, F., Vergara, H., Hong, Y., 2015. Evaluating Multi-Scale Flow Predictions for the Connecticut River Basin 6. https://doi.org/10.4172/2157-7587.1000208

Dixit, A., 2002. Basic Water Science, 1st ed. Nepal Water Conservation Foundation.

Dobriyal, P., Badola, R., Tuboi, C., Hussain, S.A., 2017. A review of methods for monitoring streamflow for sustainable water resource management. Appl. Water Sci. 7, 2617–2628. https://doi.org/10.1007/s13201-016-0488-y

DOED, 2020. Design Guidelines for Headworks of Hydropower Projects. Department of Electricity Development, Ministry of Energy, Water Resource and Irrigation, Government of Nepal, Kathmandu.

DOED, 2018a. Hydrological, Sedimentation and GLOF Study Report for Feasibility and Environmental Impact Assessment Study of Arun-4 Hydropower Project. Department of Electricity Development, Kathmandu, Nepal.

DOED, 2018b. Guidelines for Study of Hydropower Projects. Water Resources and Irrigation, Department of Electricity Development, Kathmandu, Nepal.

Donk, P., Van Uytven, E., Willems, P., Taylor, M.A., 2018. Assessment of the potential implications of a 1.5 °C versus higher global temperature rise for the Afobaka hydropower scheme in Suriname. Reg. Environ. Chang. 18, 2283–2295. https://doi.org/10.1007/s10113-018-1339-1

Dooge, J.C., 1957. The rational method for estimating flood peaks. Engineering 184, 311–313.

dos Santos, M.A., Damázio, J.M., Rogério, J.P., Amorim, M.A., Medeiros, A.M., Abreu, J.L.S., Maceira, M.E.P., Melo, A.C., Rosa, L.P., 2017. Estimates of GHG emissions by hydroelectric reservoirs: The Brazilian case. Energy 133, 99–107. https://doi.org/10.1016/j.energy.2017.05.082

Duan, Y., Liu, T., Meng, F., Luo, M., Frankl, A., 2018. Inclusion of Modified Snow Melting and Flood. Water. https://doi.org/10.3390/w10121715

Edwards, P.N., 2011. History of climate modeling. Wiley Interdiscip. Rev. Clim. Chang. 2, 128–139. https://doi.org/10.1002/wcc.95

Eeckman, J., Nepal, S., Chevallier, P., Camensuli, G., Delclaux, F., Boone, A., De Rouw, A., 2019. Comparing the ISBA and J2000 approaches for surface flows modelling at the local scale in the Everest region. J. Hydrol. 569, 705–719. https://doi.org/10.1016/j.jhydrol.2018.12.022

Emerson, D.G., Vecchia, A. V, Dahl, A.L., 2005. Evaluation of drainage-area ratio method used to estimate streamflow for the Red River of the North Basin, North Dakota and Minnesota, Scientific Investigation Report.

Ergen, K., Kentel, E., 2016. An integrated map correlation method and multiple-source sites drainage-area ratio method for estimating streamflows at ungauged catchments: A case study of the Western Black Sea Region, Turkey. J. Environ. Manage. 166, 309–320.

Fagundes, H.O., Fan, F.M., Paiva, R.C.D., Siqueira, V.A., Buarque, D.C., Kornowski, L.W., Laipelt, L., Collischonn, W., 2021. Sediment Flows in South America Supported by Daily Hydrologic-Hydrodynamic Modeling. Water Resour. Res. 57, 1–26. https://doi.org/10.1029/2020WR027884

Fan, J.L., Hu, J.W., Zhang, X., Kong, L.S., Li, F., Mi, Z., 2020. Impacts of climate change on hydropower generation in China. Math. Comput. Simul. 167, 4–18. https://doi.org/10.1016/j.matcom.2018.01.002

Fan, W., Meng, M., Lu, J., Dong, X., Wei, H., Wang, X., Zhang, Q., 2020. Decoupling elasticity and driving factors of energy consumption and economic development

in the Qinghai-Tibet plateau. Sustain. 12, 1–22. https://doi.org/10.3390/su12041326

Feldman, A.D., 1981. HEC models for water resources system simulation: theory and experience Vol. 12. , 1981. Adv. Hydrosci. 12, 297–423.

Flint, R.W., 2004. The sustainable development of water resources. Water Resour. Updat. 127, 48–59.

Fuchs, G. (1982): Geologic-Tectonic Map of the Himalaya 1:2,000,000. – Geol. B.-A., Wien.

Gabiri, G., Diekkrüger, B., Näschen, K., Leemhuis, C., van der Linden, R., Mwanjalolo Majaliwa, J.G., Obando, J.A., 2020. Impact of Climate and Land Use / Land Cover Change on the Water Resources of a Tropical Inland Valley. Climate 83, 1–25.

García-olivares, A., Turiel, A., Ballabrera-poy, J., Sol, J., 2018. Renewable transitions and the net energy from oil liquids : A scenarios study 116, 258–271. https://doi.org/10.1016/j.renene.2017.09.035

Getachew, B., Manjunatha, B.R., Bhat, H.G., 2021. Modeling projected impacts of climate and land use/land cover changes on hydrological responses in the Lake Tana Basin, upper Blue Nile River Basin, Ethiopia. J. Hydrol. 595, 125974. https://doi.org/10.1016/j.jhydrol.2021.125974

Ghosh, S., 2002. Electricity consumption and economic growth in India. Energy Policy 30, 125–129. https://doi.org/10.1016/S0301-4215(01)00078-7

Glavan, M., White, S., Holman, I.P., 2011. Evaluation of River Water Quality Simulations at a Daily Time Step-Experience with SWAT in the Axe Catchment, UK. Clean - Soil, Air, Water 39, 43–54. https://doi.org/10.1002/clen.200900298

Gök, E., Kentel Erdoğan, E. 2015. Hydropower versus Other Renewable Energy Sources. World Water Congress XV (25th to 29th May 2015), Edinburgh, Scotland. https://hdl.handle.net/11511/72773.

Gomes, L.C., Bianchi, F.J.J.A., Cardoso, I.M., Schulte, R.P.O., Fernandes, R.B.A., Fernandes-Filho, E.I., 2021. Disentangling the historic and future impacts of

land use changes and climate variability on the hydrology of a mountain region in Brazil. J. Hydrol. 594, 125650. https://doi.org/10.1016/j.jhydrol.2020.125650

Granata, F., Gargano, R., Marinis, G. De, 2016. Support Vector Regression for Rainfall-Runoff Modeling in Urban Drainage : A Comparison with the EPA ' s Storm Water Management Model. https://doi.org/10.3390/w8030069

Green, H., Ampt, G.A., 1912. Studies on soil physics: Part II — the permeability of an ideal soil to air and water. J. Agric. Sci. 5, 1–26. https://doi.org/10.1017/S0021859600001751

Green, W.H., Ampt, G.A., 1911. Studies on soil physics. J. Agric. Sci. 4, 1–24.

Grusson, Y., Wesström, I., Svedberg, E., Joel, A., 2021. Influence of climate change on water partitioning in agricultural watersheds: Examples from Sweden. Agric. Water Manag. 249. https://doi.org/10.1016/j.agwat.2021.106766

Gudmundsson, L., Bremnes, J.B., Haugen, J.E., Engen-Skaugen, T., 2012. Technical Note: Downscaling RCM precipitation to the station scale using statistical transformations – A comparison of methods. Hydrol. Earth Syst. Sci. 16, 3383–3390. https://doi.org/10.5194/hess-16-3383-2012

Guevara-Ochoa, C., Medina-Sierra, A., Vives, L., 2020. Spatio-temporal effect of climate change on water balance and interactions between groundwater and surface water in plains. Sci. Total Environ. 722, 137886. https://doi.org/10.1016/j.scitotenv.2020.137886

Gumbel, E.J., 1941. Return Period of Flood Flows. Ann. Math. Stat 12, 163–190.

Gunturu, U.B., Hallgren, W., 2017. Asynchrony of wind and hydropower resources in Australia. Sci. Rep. 7, 1–9. https://doi.org/10.1038/s41598-017-08981-0

Gupta, A., Kayastha, R.B., Ramanathan, A., Dimri, A.P., 2019. Comparison of hydrological regime of glacierized Marshyangdi and Tamor river basins of Nepal. Environ. Earth Sci. 78, 1–15. https://doi.org/10.1007/s12665-019-8443-5

Gupta, C., Kulkarni, A. V., Taloor, A.K., 2021. Streamflow modeling and contribution of snow and glacier melt runoff in glacierized Upper Indus Basin. Environ.

Monit. Assess. 193. https://doi.org/10.1007/s10661-021-09537-6

Gupta, H. V, Kling, H., Yilmaz, K.K., Martinez, G.F., 2009. Decomposition of the mean squared error and NSE performance criteria : Implications for improving hydrological modelling. J. Hydrol. 377, 80–91. https://doi.org/10.1016/j.jhydrol.2009.08.003

Hajihosseini, M., Hajihosseini, H., Morid, S., Delavar, M., Booij, M.J., 2020. Impacts of land use changes and climate variability on transboundary hirmand river using swat. J. Water Clim. Chang. 11, 1695–1711. https://doi.org/10.2166/wcc.2019.100

Hall, C.A.S., Lambert, J.G., Balogh, S.B., 2014. EROI of different fuels and the implications for society 64, 141–152.

Hamududu, B.H., Killingtveit, Å., 2016. Hydropower production in future climate scenarios; the case for the Zambezi River. Energies 9, 1–18. https://doi.org/10.3390/en9070502

Hanif, I., Muhammad, S., Raza, F., Gago-de-santos, P., Abbas, Q., 2019. Fossil fuels , foreign direct investment , and economic growth have triggered CO 2 emissions in emerging Asian economies : Some empirical evidence. Energy 171, 493–501. https://doi.org/10.1016/j.energy.2019.01.011

Hargreaves, G.H., Samani, Z.A., 1982. Estimating potential evapotranspiration. J. Irrig. Drain. Div. 108, 225–230.

Hasan, M.M., Wyseure, G., 2018. Impact of climate change on hydropower generation in Rio Jubones Basin, Ecuador. Water Sci. Eng. 11, 157–166. https://doi.org/10.1016/j.wse.2018.07.002

Havrylenko, S.B., Bodoque del Pozo, J.M., Srinivasan, R., Zucarelli, G. V., Mercuri, P., 2016. Assessment of the soil water content in the Pampas region using SWAT. Catena 137, 298–309. https://doi.org/10.1016/j.catena.2015.10.001

Hawkins, E., Osborne, T.M., Kit, C., Challinor, A.J., 2013. Agricultural and Forest Meteorology Calibration and bias correction of climate projections for crop modelling : An idealised case study over Europe. Agric. For. Meteorol. 170, 19–31. https://doi.org/10.1016/j.agrformet.2012.04.007

Hazen, 1914. Storage to be provided in inpounding reservoirs for municipal water supply. Trans. Am.Soc.Civ.Eng. 77, 1539–1640.

Hishinuma, S., Takeuchi, K., Magome, J., 2014. Défis de l'analyse hydrologique pour le développement des ressources en eau dans les régions montagneuses semi-arides: Étude de cas en Iran. Hydrol. Sci. J. 59, 1718–1737. https://doi.org/10.1080/02626667.2013.853879

Horton, R.E., 1945. Erosional development of streams and their drainage basins; Hydrophysical approach to quantitative morphology. Bull. Geol. Soc. Am. 56, 275–370.

Horton, R.E., 1933. The role in infiltration in the hydrological cycle. Trans. Am. Geophys. Union 14, 446–460.

Hosseini, S.H., Khaleghi, M.R., 2020. Application of SWAT model and SWAT-CUP software in simulation and analysis of sediment uncertainty in arid and semi-arid watersheds (case study: the Zoshk–Abardeh watershed). Model. Earth Syst. Environ. 6, 2003–2013. https://doi.org/10.1007/s40808-020-00846-2

Houghton, E., 1996. Climate change 1995: The science of climate change: contribution of working group I to the second assessment report of the Intergovernmental Panel on Climate Change. Cambridge University Press.

Huang, Y., Ma, Y., Liu, T., Luo, M., 2020. Climate change impacts on extreme flows under IPCC RCP scenarios in the mountainous Kaidu watershed, Tarim River Basin. Sustain. 12, 1–23. https://doi.org/10.3390/su12052090

Huggins, L.F., 1966. The mathematical simulation of the hydrology of small watersheds. Purdue University.

ICIMOD, 2011. Glacial lakes and glacial lake outburst floods in Nepal. International Centre for Integrated Mountain Development, Kathmandu, Nepal.

IEA, 2020. Key World Energy Statistics 2020. International Energy Agency.

IEA, 2019. World Energy Outlook 2019. International Energy Agency.

IPCC, 2015. Drivers, Trends and Mitigation. Clim. Chang. 2014 Mitig. Clim. Chang. 351–412. https://doi.org/10.1017/cbo9781107415416.011

IPCC, 2014. Climate Change 2014 Synthesis Report Summary Chapter for Policymakers. Ipcc 31. https://doi.org/10.1017/CBO9781107415324

IPCC, 2007. Climate Change 2007: Impacts, Adaptation and Vulnerability, Contribution of Working Group II to the Fourth Assessment Report of the Intergovernmental Panel on Climate Change. Cambridge University Press, Cambridge, UK.

IRENA, 2020. Renewable Energy Statistics 2020. Renewable hydropower (including mixed plants).

IRENA, 2012. Renewable Energy Techlogies: Cost Analysis Series, Hydropower. Int. Renew. Energy Agency 1, 5.

Jain, Sharad K., Jain, Sanjay K., Jain, N., Xu, C.-Y., 2017. Hydrologic modeling of a Himalayan mountain basin by using the SWAT model. Hydrol. Earth Syst. Sci. 1–26. https://doi.org/10.5194/hess-2017-100

Janssen, A.B.G., Droppers, B., Kong, X., Teurlincx, S., Tong, Y., Kroeze, C., 2021. Characterizing 19 thousand Chinese lakes, ponds and reservoirs by morphometric, climate and sediment characteristics. Water Res. 202, 117427. https://doi.org/10.1016/j.watres.2021.117427

Jha, R., 2011. Total Run-of-River type Hydropower Potential of Nepal. Hydro Nepal J. Water, Energy Environ. 7, 8–13. https://doi.org/10.3126/hn.v7i0.4226

Jiang, T., Chen, Y.D., Xu, C. yu, Chen, Xiaohong, Chen, Xi, Singh, V.P., 2007. Comparison of hydrological impacts of climate change simulated by six hydrological models in the Dongjiang Basin, South China. J. Hydrol. 336, 316–333. https://doi.org/10.1016/j.jhydrol.2007.01.010

Johnston, R., Smakhtin, V., 2014. Hydrological Modeling of Large river Basins : How Much is Enough ? Water Resour. Manag. 28, 2695–2730. https://doi.org/10.1007/s11269-014-0637-8

Joorabian Shooshtari, S., Shayesteh, K., Gholamalifard, M., Azari, M., López-Moreno, J.I., 2021. Responses of surface water quality to future land cover and climate changes in the Neka River basin, Northern Iran. Environ. Monit. Assess. 193.

https://doi.org/10.1007/s10661-021-09184-x

Kaini, S., Nepal, S., Pradhananga, S., Gardner, T., Sharma, A.K., 2020. Impacts of climate change on the flow of the transboundary Koshi River, with implications for local irrigation. Int. J. Water Resour. Dev. 00, 1–26. https://doi.org/10.1080/07900627.2020.1826292

Kamaludin, M., 2013. Electricity consumption in developing countries. Asian J. Res. Soc. Sci. Humanit. 2, 84–90.Kaushal, R.K., Sarkar, A., Mishra, K., Sinha, R., Nepal, S., Jain, V., 2020. Spatio-temporal variability in stream power distribution in the Upper Kosi River basin, Central Himalaya: Controls and geomorphic implications. Geomorphology 350, 106888. https://doi.org/10.1016/j.geomorph.2019.106888

Kayastha, R.B., Steiner, N., Kayastha, R., Mishra, S.K., Forster, R.R., 2020. Comparative Study of Hydrology and Icemelt in Three Nepal River Basins Using the Glacio-Hydrological Degree-Day Model (GDM) and Observations From the Advanced Scatterometer (ASCAT) 7, 1–13. https://doi.org/10.3389/feart.2019.00354

Khadka, D., Babel, M.S., Shrestha, S., Tripathi, N.K., 2014. Climate change impact on glacier and snow melt and runoff in Tamakoshi basin in the Hindu Kush Himalayan (HKH) region. J. Hydrol. 511, 49–60. https://doi.org/10.1016/j.jhydrol.2014.01.005

Khadka, M., Kayastha, R.B., Kayastha, R., 2020. Future projection of cryospheric and hydrologic regimes in Koshi River basin, Central Himalaya, using coupled glacier dynamics and glacio-hydrological models. J. Glaciol. 66, 831–845. https://doi.org/10.1017/jog.2020.51

Khanal, S., Lutz, A.F., Kraaijenbrink, P.D.A., van den Hurk, B., Yao, T., Immerzeel, W.W., 2021. Variable 21st Century Climate Change Response for Rivers in High Mountain Asia at Seasonal to Decadal Time Scales. Water Resour. Res. 57, 1–26. https://doi.org/10.1029/2020WR029266

Khaniya, B., Priyantha, H.G., Baduge, N., Azamathulla, H.M., Rathnayake, U., 2020. Impact of climate variability on hydropower generation: A case study from Sri Lanka. ISH J. Hydraul. Eng. 26, 301–309.

https://doi.org/10.1080/09715010.2018.1485516

Kingston, D.G., Thompson, J.R., Kite, G., 2011. Uncertainty in climate change projections of discharge for the Mekong River Basin. Hydrol. Earth Syst. Sci. 15, 1459–1471. https://doi.org/10.5194/hess-15-1459-2011

Kiprotich, P., Wei, X., Zhang, Z., Ngigi, T., Qiu, F., Wang, L., 2021. Assessing the impact of land use and climate change on surface runoff response using gridded observations and swat+. Hydrology 8, 1–29. https://doi.org/10.3390/hydrology8010048

Knightes, C., 2017. An Overview of Rainfall-Runoff Model Types An Overview of Rainfall-Runoff Model Types 0–29.

Knisel, W.G., 1980. CREAMS: A field scale model for chemicals, runoff, and erosion from agricultural management systems. Department of Agriculture, Science and Education Administration.

Knoben, J.M.W., Freer, J.E., Woods, R.A., 2019. Technical note : Inherent benchmark or not ? Comparing Nash- Sutcliffe and Kling-Gupta efficiency scores. Hydrol. Earth Syst. Sci. 1–7.

Knoben, W.J.M., Freer, J.E., Woods, R.A., 2019. Technical note : Inherent benchmark or not ? Comparing Nash – Sutcliffe and Kling – Gupta efficiency scores 4323–4331.

Kokkonen, T., Koivusalo, H., Karvonen, T., 2001. A semi-distributed approach to rainfall-runoff modelling — a case study in a snow affected catchment 16, 481–493.

Kong, B., Yu, H., Deng, W., Wang, Q., 2021. Simulating glacier mass balance in the cross-border Poiqu/Bhotekoshi Basin, China and Nepal. J. Water Clim. Chang. 12, 1515–1531. https://doi.org/10.2166/wcc.2020.024

Kundu, D., Vervoort, R.W., van Ogtrop, F.F., 2017. The value of remotely sensed surface soil moisture for model calibration using SWAT. Hydrol. Process. 31, 2764–2780. https://doi.org/10.1002/hyp.11219

Lamichhane, S., Shakya, N.M., 2019. Integrated assessment of climate change and land use change impacts on hydrology in the Kathmandu Valley watershed, Central

Nepal. Water 11, 2059.

Le Treut, H., Cubasch, U., Allen, M., 2005. Historical Overview of Climate Change Science, in: Notes.

Leander, R., Buishand, T.A., 2007. Resampling of regional climate model output for the simulation of extreme river flows 487–496. https://doi.org/10.1016/j.jhydrol.2006.08.006

Lee, D.K., Cha, D.H., 2020. Regional climate modeling for Asia. Geosci. Lett. 7. https://doi.org/10.1186/s40562-020-00162-8

Lenderink, G., Buishand, A., Deursen, W. Van, 2007. Estimates of future discharges of the river Rhine using two scenario methodologies : direct versus delta approach 11, 1145–1159.

Leta, O.T., El-Kadi, A.I., Dulai, H., Ghazal, K.A., 2016. Assessment of climate change impacts on water balance components of Heeia watershed in Hawaii. J. Hydrol. Reg. Stud. 8, 182–197. https://doi.org/10.1016/j.ejrh.2016.09.006

Li, C., Fang, H., 2021. Assessment of climate change impacts on the streamflow for the Mun River in the Mekong Basin, Southeast Asia: Using SWAT model. Catena 201, 105199. https://doi.org/10.1016/j.catena.2021.105199

Li, M., Di, Z., Duan, Q., 2021. Effect of sensitivity analysis on parameter optimization: Case study based on streamflow simulations using the SWAT model in China. J. Hydrol. 603, 126896. https://doi.org/10.1016/j.jhydrol.2021.126896

Li, S., Bush, R.T., Santos, I.R., Zhang, Q., Song, K., Mao, R., Wen, Z., Lu, X.X., 2018. Large greenhouse gases emissions from China's lakes and reservoirs. Water Res. 147, 13–24. https://doi.org/10.1016/j.watres.2018.09.053

Li, Y., DeLiberty, T., 2020. Assessment of Urban Streamflow in Historical Wet and Dry Years Using SWAT across Northwestern Delaware. Environ. Process. 7, 597–614. https://doi.org/10.1007/s40710-020-00428-5

Liao, C., Erbaugh, J.T., Kelly, A.C., Agrawal, A., 2021. Clean energy transitions and human well-being outcomes in Lower and Middle Income Countries: A systematic review. Renew. Sustain. Energy Rev. 145, 111063. https://doi.org/10.1016/j.rser.2021.111063

Liu, L., Yang, Z.J., Delwiche, K., Long, L.H., Liu, J., Liu, D.F., Wang, C.F., Bodmer, P., Lorke, A., 2020. Spatial and temporal variability of methane emissions from cascading reservoirs in the Upper Mekong River. Water Res. 186, 116319. https://doi.org/10.1016/j.watres.2020.116319

Liu, M., Xie, H., He, Y., Zhang, Qianru, Sun, X., Yu, C., Chen, L., Zhang, W., Zhang, Qianggong, Wang, X., 2019. Sources and transport of methylmercury in the Yangtze River and the impact of the Three Gorges Dam. Water Res. 166, 115042. https://doi.org/10.1016/j.watres.2019.115042

Liu, X., Tang, Q., Voisin, N., Cui, H., 2016. Projected impacts of climate change on hydropower potential in China. Hydrol. Earth Syst. Sci. 20, 3343–3359. https://doi.org/10.5194/hess-20-3343-2016

Liu, Z., Herman, J.D., Huang, G., Kadir, T., Dahlke, H.E., 2021. Identifying climate change impacts on surface water supply in the southern Central Valley, California. Sci. Total Environ. 759, 143429. https://doi.org/10.1016/j.scitotenv.2020.143429

Lorde, T., Waithe, K., Francis, B., 2010. The importance of electrical energy for economic growth in Barbados. Energy Econ. 32, 1411–1420.Loukas, A., Vasiliades, L., 2014. Streamflow simulation methods for ungauged and poorly gauged watersheds. Nat. Hazards Earth Syst. Sci. 14, 1641–1661. https://doi.org/10.5194/nhess-14-1641-2014

Lucas-Borja, M.E., Carrà, B.G., Nunes, J.P., Bernard-Jannin, L., Zema, D.A., Zimbone, S.M., 2020. Impacts of land-use and climate changes on surface runoff in a tropical forest watershed (Brazil). Hydrol. Sci. J. 65, 1956–1973. https://doi.org/10.1080/02626667.2020.1787417

Luo, L., Zhou, Q., He, H.S., Duan, L., Zhang, G., Xie, H., 2020. Relative importance of land use and climate change on hydrology in agricultural watershed of southern China. Sustain. 12. https://doi.org/10.3390/SU12166423

Lutz, A.F., ter Maat, H.W., Biemans, H., Shrestha, A.B., Wester, P., Immerzeel, W.W., 2016. Selecting representative climate models for climate change impact studies: an advanced envelope-based selection approach. Int. J. Climatol. 36, 3988–4005. https://doi.org/10.1002/joc.4608

Ma, D., Xu, Y.P., Xuan, W., Gu, H., Sun, Z., Bai, Z., 2020. Do model parameters change under changing climate and land use in the upstream of the Lancang River Basin, China? Hydrol. Sci. J. 1894–1908. https://doi.org/10.1080/02626667.2020.1782915

Magaju, D., Cattapan, A., Franca, M., 2020. Identification of run-of-river hydropower investments in data scarce regions using global data. Energy Sustain. Dev. 58, 30–41. https://doi.org/10.1016/j.esd.2020.07.001

Maharjan, M., Aryal, A., Talchabhadel, R., Thapa, B.R., 2021. Impact of climate change on the streamflow modulated by changes in precipitation and temperature in the north latitude watershed of Nepal. Hydrology 8. https://doi.org/10.3390/hydrology8030117

Malagó, A., Bouraoui, F., Vigiak, O., Grizzetti, B., Pastori, M., 2017. Modelling water and nutrient fluxes in the Danube River Basin with SWAT. Sci. Total Environ. 603–604, 196–218. https://doi.org/10.1016/j.scitotenv.2017.05.242

Manandhar, S., Pandey, V.P., Ishidaira, H., Kazama, F., 2013. Perturbation study of climate change impacts in a snow-fed river basin. Hydrol. Process. 27, 3461–3474. https://doi.org/10.1002/hyp.9446

Mapes, K.L., Pricope, N.G., 2020. Evaluating SWAT model performance for runoff, percolation, and sediment loss estimation in low-gradientwatersheds of the Atlantic Coastal Plain. Hydrology 7. https://doi.org/10.3390/HYDROLOGY7020021

Marahatta, S., 2015. Post April 25, 2015 Earthquake and Ramche Landslide Dam in Kali Gandaki.

Marahatta, S., Devkota, L.P., Aryal, D., 2021a. Application of swat in hydrological simulation of complex mountainous river basin (Part I: Model Development). Water (Switzerland) 13. https://doi.org/10.3390/w13111546

Marahatta, S., Aryal, D., Devkota, L.P., Bhattarai, U., Shrestha, D., 2021b. Application of swat in hydrological simulation of complex mountainous river basin (Part II: Climate Change Impact Assessment). Water (Switzerland) 13. https://doi.org/10.3390/ w13111548

Marahatta, S., Bhattarai, U., Devkota, L.P., Aryal, D., 2022. Unravelling the water-energy-economics-continuum of hydroelectricity in the face of climate change. Int. J. Energy Water Resour.

Marahatta, S., Devkota, L., Aryal, D., 2021c. Hydrological Modeling: A Better Alternative to Empirical Methods for Monthly Flow Estimation in Ungauged Basins. J. Water Resour. Prot. 13, 254–270. https://doi.org/10.4236/jwarp.2021.133015

Marahatta, S., Devkota, L.P., Aryal, D., 2021d. Impact of Flow Variation on Hydropower Projects in Budhigandaki River Basin of Nepal. J. Inst. Sci. Technol. 26, 89–98. https://doi.org/10.3126/jist.v26i1.37831

Marahatta, S., Dongol, B.S., Gurung, G., 2009. Temporal and Spatial Variability of Climate Change over Nepal (1976 - 2005), First. ed. Practical Action Nepal, Kathmandu, Nepal.

Maraseni, T., An-Vo, D.-A., Mushtaq, S., Reardon-Smith, K., 2021. Carbon smart agriculture: An integrated regional approach offers significant potential to increase profit and resource use efficiency, and reduce emissions. J. Clean. Prod. 282, 124555.

Maraun, D., 2016. Bias Correcting Climate Change Simulations - a Critical Review. Curr. Clim. Chang. Reports 211–220. https://doi.org/10.1007/s40641-016-0050-x

Maraun, D., Widmann, M., 2018. Cross-validation of bias-corrected climate simulations is misleading 4867–4873.

Marcinkowski, P., Mirosław-Świątek, D., 2020. Modelling of climate change impact on flow conditions in the lowland anastomosing river. PeerJ 2020. https://doi.org/10.7717/peerj.9275

Marhaento, H., Booij, M.J., Rientjes, T.H.M., Hoekstra, A.Y., 2017. Attribution of changes in the water balance of a tropical catchment to land use change using the SWAT model. Hydrol. Process. 31, 2029–2040. https://doi.org/10.1002/hyp.11167

Marin, M., Clinciu, I., Tudose, N.C., Ungurean, C., Adorjani, A., Mihalache, A.L.,

Davidescu, A.A., Davidescu, Șerban O., Dinca, L., Cacovean, H., 2020. Assessing the vulnerability of water resources in the context of climate changes in a small forested watershed using SWAT: A review. Environ. Res. 184. https://doi.org/10.1016/j.envres.2020.109330

Marras, P.A., Lima, D.C.A., Soares, P.M.M., Cardoso, R.M., Medas, D., Dore, E., De Giudici, G., 2021. Future precipitation in a Mediterranean island and streamflow changes for a small basin using EURO-CORDEX regional climate simulations and the SWAT model. J. Hydrol. 603, 127025. https://doi.org/10.1016/j.jhydrol.2021.127025

Martínez-Retureta, R., Aguayo, M., Abreu, N.J., Stehr, A., Duran-Llacer, I., Rodríguez-López, L., Sauvage, S., Sánchez-Pérez, J.M., 2021. Estimation of the climate change impact on the hydrological balance in basins of south-central chile. Water (Switzerland) 13. https://doi.org/10.3390/w13060794

Martínez-Salvador, A., Millares, A., Eekhout, J.P.C., Conesa-García, C., 2021. Assessment of streamflow from euro-cordex regional climate simulations in semi-arid catchments using the swat model. Sustain. 13. https://doi.org/10.3390/su13137120

Martins, F., Felgueiras, C., Smitková, M., 2018. Fossil fuel energy consumption in European countries. Energy Procedia 153, 107–111. https://doi.org/10.1016/j.egypro.2018.10.050

Mattmann, M., Logar, I., Brouwer, R., 2016. Hydropower externalities: A meta-analysis. Energy Econ. 57, 66–77. https://doi.org/10.1016/j.eneco.2016.04.016

Mauritsen, et al., 2019. Developments in the MPI-M Earth System Model version 1.2 (MPI-ESM1.2) and Its Response to Increasing CO_2. J. Adv. Model. Earth Syst. 11, 998–1038. https://doi.org/10.1029/2018MS001400

MCTCA, 2014. Mountaineering in Nepal Facts & Figures. Ministry of Culture, Tourism & Civil Aviation, Kathmandu, Nepal.

Meng, F., Sa, C., Liu, T., Luo, M., Liu, J., Tian, L., 2020. Improved model parameter transferability method for hydrological simulation with SWAT in ungauged mountainous catchments. Sustain. 12, 1–19. https://doi.org/10.3390/SU12093551

Meng, Y., Liu, J., Leduc, S., Mesfun, S., Kraxner, F., 2017. Hydropower Production Bene fi ts More From 1 . 5 ° C than 2 ° C Climate Scenario Water Resources Research 1–16. https://doi.org/10.1029/2019WR025519

Meng, Y., Liu, J., Leduc, S., Mesfun, S., Kraxner, F., Mao, G., Qi, W., Wang, Z., 2020. Hydropower Production Benefits More From 1.5 °C than 2 °C Climate Scenario. Water Resour. Res. 55, 1–16. https://doi.org/10.1029/2019WR025519

Meng, Y., Liu, J., Wang, Z., Mao, G., Wang, K., Yang, H., 2021. Undermined co-benefits of hydropower and irrigation under climate change. Resour. Conserv. Recycl. 167, 105375. https://doi.org/10.1016/j.resconrec.2020.105375

Milewski, A., Seyoum, W.M., Elkadiri, R., Durham, M., 2020. Multi-scale hydrologic sensitivity to climatic and anthropogenic changes in northern Morocco. Geosci. 10, 1–22. https://doi.org/10.3390/geosciences10010013

Miller, J.D., Immerzeel, W.W., Rees, G., 2012. Climate change impacts on glacier hydrology and river discharge in the Hindu Kush–Himalayas. Mt. Res. Dev. 32, 461–467.

Mimeau, L., Esteves, M., Jacobi, H.W., Zin, I., 2019. Evaluation of gridded and in situ precipitation datasets on modeled glacio-hydrologic response of a small glacierized himalayan catchment. J. Hydrometeorol. 20, 1103–1121. https://doi.org/10.1175/JHM-D-18-0157.1

Miquel, J., Roche, P.A., 1986. Reservoir Operation. Houille Blanche 41, 409–425. https://doi.org/10.1051/lhb/1986043

Mishra, S.K., Hayse, J., Veselka, T., Yan, E., Kayastha, R.B., LaGory, K., McDonald, K., Steiner, N., 2018. An integrated assessment approach for estimating the economic impacts of climate change on River systems: An application to hydropower and fisheries in a Himalayan River, Trishuli. Environ. Sci. Policy 87, 102–111. https://doi.org/10.1016/j.envsci.2018.05.006

Mishra, S.K., Veselka, T.D., Prusevich, A.A., Grogan, D.S., Lammers, R.B., Rounce, D.R., Ali, S.H., Christian, M.H., Watson, C.S., 2020. Differential Impact of Climate Change on the Hydropower Economics of Two River Basins in High Mountain Asia. Front. Environ. Sci. 8, 1–22.

https://doi.org/10.3389/fenvs.2020.00026

Mishra, V., Lilhare, R., 2016. Hydrologic sensitivity of Indian sub- continental river basins to climate change. Glob. Planet. Chang. J. 139, 78–96. https://doi.org/10.1016/j.gloplacha.2016.01.003

Mishra, Y., Babel, M.S., Nakamura, T., Mishra, B., 2021. Impacts of climate change on irrigation water management in the babai river basin, Nepal. Hydrology 8, 1–21. https://doi.org/10.3390/hydrology8020085

Mishra, Y., Nakamura, T., Babel, M.S., Ninsawat, S., Ochi, S., 2018. Impact of climate change on water resources of the Bheri River Basin, Nepal. Water (Switzerland) 10. https://doi.org/10.3390/w10020220

Moazami Goudarzi, F., Sarraf, A., Ahmadi, H., 2020. Prediction of runoff within Maharlu basin for future 60 years using RCP scenarios. Arab. J. Geosci. 13. https://doi.org/10.1007/s12517-020-05634-x

MoEWRI, 2019. National Energy Efficiency Strategy , 2075. Kathmandu, Nepal.

MoF, 2021. Economic Survey 2077/78. Kathmandu, Nepal.

MoFE, 2019. Climate change scenarios for Nepal for National Adaptation Plan (NAP). Kathmandu, Nepal.

Mohajan, H.K., 2019. The First Industrial Revolution: Creation of a New Global Human Era. J. Soc. Sci. Humanit. 5, 377–387.

Molden, D.J., Shrestha, A.B., Nepal, S., Immerzeel, W.W., 2016. Downstream implications of climate change in the Himalayas. Water Secur. Clim. Chang. Sustain. Dev. 65–82.

Momiyama, S., Sagehashi, M., Akiba, M., 2020. Assessment of the climate change risks for inflow into sagami dam reservoir using a hydrological model. J. Water Clim. Chang. 11, 367–379. https://doi.org/10.2166/wcc.2018.256

Moriasi, D.N., Arnold, J.G., Liew, M.W. Van, Bingner, R.L., Harmel, R.D., Veith, T.L., 2007. Model Evaluation Guidelines for Systematic Quantification of Accuracy in Watershed Simulations. Am. Soc. Agric. Biol. Eng. 50, 885–900.

Moriasi, D.N., Gitau, M.W., Pai, N., Daggupati, P., 2015. Hydrologic and water quality

models: Performance measures and evaluation criteria. Trans. ASABE 58, 1763–1785. https://doi.org/10.13031/trans.58.10715

MoWR, 2010. Report on 20 Years Hydropower Development Plan Task Force -2010 [Nepali]. Kathmandu, Nepal.

MoWR, 2009. Report on 10 Years Hydropower Development Plan Task Force -2009 [Nepali]. Ministry of Water Resources, Government of Nepal, Kathmandu.

Mtilatila, L., Bronstert, A., Shrestha, P., Kadewere, P., Vormoor, K., 2020. Susceptibility of water resources and hydropower production to climate change in the tropics: The case of Lake Malawi and Shire River Basins, SE Africa. Hydrology 7. https://doi.org/10.3390/HYDROLOGY7030054

Muhammad, A., Evenson, G.R., Unduche, F., Stadnyk, T.A., 2020. Climate change impacts on reservoir inflow in the Prairie Pothole Region: Awatershed model analysis. Water (Switzerland) 12, 1–18. https://doi.org/10.3390/w12010271

Müller, et al., 2018. A Higher-resolution Version of the Max Planck Institute Earth System Model (MPI-ESM1.2-HR). J. Adv. Model. Earth Syst. 10, 1383–1413. https://doi.org/10.1029/2017MS001217

Mutezo, G., Mulopo, J., 2021. A review of Africa ' s transition from fossil fuels to renewable energy using circular economy principles. Renew. Sustain. Energy Rev. 137, 110609. https://doi.org/10.1016/j.rser.2020.110609

Mutsindikwa, T.C., Yira, Y., Bossa, A.Y., Hounkpè, J., Salack, S., Saley, I.A., Rabani, A., 2020. Modeling climate change impact on the hydropower potential of the Bamboi catchment. Model. Earth Syst. Environ. https://doi.org/10.1007/s40808-020-01052-w

Mwakalila, S., 2003. Estimation of stream flows of ungauged catchments for river basin management. Phys. Chem. Earth, Parts A/B/C 28, 935–942.

Naderi, M., 2020. Assessment of water security under climate change for the large watershed of Dorudzan Dam in southern Iran. Hydrogeol. J. 28, 1553–1574. https://doi.org/10.1007/s10040-020-02159-1

Nash, J.E., Sutcliffe, J.V., 1970. River flow forecasting through conceptual models part I — A discussion of principles. J. Hydrol. 10, 282–290.

https://doi.org/doi.org/10.1016/0022-1694(70)90255-6.

NEA, 2021. Nepal Electricity Authority A Year in Review Fiscal Year 2020/2021. Kathmandu, Nepal.

NEA, 2019. Annual Report of Nepal Electricity Authority. Nepal Electricity Authority, Kathmandu, Nepal.

NEA, 2017. NEA Board Decisions on the Power Purchase Rates and Associated Rules for PPA of RoR / PRoR / Storage.

NEA, JICA, 2003. The Basic Study for the Rural Electrification through Small Hydropower Development in Rural Hilly Areas in Nepal, Final Report, 1., Kathmandu, Nepal.

Negewo, T.F., Sarma, A.K., 2021. Estimation of Water Yield under Baseline and Future Climate Change Scenarios in Genale Watershed, Genale Dawa River Basin, Ethiopia, Using SWAT Model. J. Hydrol. Eng. 26, 05020051. https://doi.org/10.1061/(asce)he.1943-5584.0002047

Neitsch, S.L., Arnold, J.G., Kiniry, J.R., Williams, J.R., 2011. Soil and water assessment tool theoretical documentation version 2009. Texas Water Resources Institute.

Nepal, S., 2016. Impacts of climate change on the hydrological regime of the Koshi river basin in the Himalayan region. J. Hydro-Environment Res. 10, 76–89. https://doi.org/10.1016/j.jher.2015.12.001

Nepal, S., Chen, J., Penton, D.J., Neumann, L.E., Zheng, H., Wahid, S., 2017. Spatial GR4J conceptualization of the Tamor glaciated alpine catchment in Eastern Nepal: evaluation of GR4JSG against streamflow and MODIS snow extent. Hydrol. Process. 31, 51–68. https://doi.org/10.1002/hyp.10962

Nerantzaki, S.D., Hristopulos, D.T., Nikolaidis, N.P., 2020. Estimation of the uncertainty of hydrologic predictions in a karstic Mediterranean watershed. Sci. Total Environ. 717. https://doi.org/10.1016/j.scitotenv.2020.137131

Ngo, L.A., Masih, I., Jiang, Y., Douven, W., 2018. Impact of reservoir operation and climate change on the hydrological regime of the Sesan and Srepok Rivers in the Lower Mekong Basin. Clim. Change 149, 107–119.

https://doi.org/10.1007/s10584-016-1875-y

Nguyen, V.T., Dietrich, J., Uniyal, B., Tran, D.A., 2018. Verification and correction of the hydrologic routing in the soil and Water Assessment Tool. Water (Switzerland) 10. https://doi.org/10.3390/w10101419

NPC, 2020. The Fifteenth Plan (Fiscal Year 2019/20 – 2023/24). National Planning Commission, Government of Nepal,Singha Durbar, Kathmandu.

O'Connor, P.A., Cleveland, C.J., 2014. U.S. energy transitions 1780-2010. Energies 7, 7955–7993. https://doi.org/10.3390/en7127955

Oceanic, N., Brunswick, N., Oceanic, N., Survey, U.S.G., Oceanic, N., Biology, E., 2006. GFDL ' s CM2 Global Coupled Climate Models . Part I : Formulation and 643–674.

Odoni, N.A., Lane, S.N., 2010. Knowledge-theoretic models in hydrology. Prog. Phys. Geogr. Earth Environ. 34, 151–171. https://doi.org/10.1177/0309133309359893

Omani, N., Srinivasan, R., Karthikeyan, R., Smith, P.K., 2017. Hydrological modeling of highly glacierized basins (Andes, Alps, and Central Asia). Water (Switzerland) 9. https://doi.org/10.3390/w9020111

Oñate-Valdivieso, F., Bosque-Sendra, J., Sastre-Merlin, A., Ponce, V.M., 2016. Calibration, validation and evaluation of a lumped hydrologic model in a mountain area in Southern Ecuador. Agrociencia 50, 945–963.

Orlińska-Wozniak, P., Szalińska, E., Wilk, P., 2020. Do land use changes balance out sediment yields under climate change predictions on the sub-basin scale? The carpathian basin as an example. Water (Switzerland) 12. https://doi.org/10.3390/w12051499

Padhiary, J., Patra, K.C., Dash, S.S., Uday Kumar, A., 2020. Climate change impact assessment on hydrological fluxes based on ensemble gcm outputs: A case study in Eastern Indian river basin. J. Water Clim. Chang. 11, 1676–1694. https://doi.org/10.2166/wcc.2019.080

Pakhtigian, E.L., Jeuland, M., Dhaubanjar, S., Pandey, V.P., 2020. Balancing intersectoral demands in basin-scale planning: The case of Nepal's western river

basins. Water Resour. Econ. 30, 100152. https://doi.org/10.1016/j.wre.2019.100152

Palazzoli, I., Maskey, S., Uhlenbrook, S., Nana, E., Bocchiola, D., 2014. Impact of prospective climate change on water resources and crop yields in the Indrawati basin, Nepal. Agric. Syst. https://doi.org/10.1016/j.agsy.2014.10.016

Pandey, B.K., Khare, D., Kawasaki, A., Meshesha, T.W., 2021. Integrated approach to simulate hydrological responses to land use dynamics and climate change scenarios employing scoring method in upper Narmada basin, India. J. Hydrol. 598, 126429. https://doi.org/10.1016/j.jhydrol.2021.126429

Pandey, V.P., Dhaubanjar, S., Bharati, L., Thapa, B.R., 2020a. Spatio-temporal distribution of water availability in Karnali-Mohana Basin, Western Nepal: Hydrological model development using multi-site calibration approach (Part-A). J. Hydrol. Reg. Stud. 29, 100690. https://doi.org/10.1016/j.ejrh.2020.100690

Pandey, V.P., Dhaubanjar, S., Bharati, L., Thapa, B.R., 2020b. Journal of Hydrology : Regional Studies Spatio-temporal distribution of water availability in Karnali-Mohana Basin , Western Nepal : Climate change impact assessment. J. Hydrol. Reg. Stud. 29, 100691. https://doi.org/10.1016/j.ejrh.2020.100691

Pandey, V.P., Dhaubanjar, S., Bharati, L., Thapa, B.R., 2020c. Spatio-temporal distribution of water availability in Karnali-Mohana Basin, Western Nepal: Climate change impact assessment (Part-B). J. Hydrol. Reg. Stud. 29, 100691.

Pandey, V.P., Dhaubanjar, S., Bharati, L., Thapa, B.R., 2019. Hydrological response of Chamelia watershed in Mahakali Basin to climate change. Sci. Total Environ. 650, 365–383. https://doi.org/10.1016/j.scitotenv.2018.09.053

Pechlivanidis, I., Jackson, B., Mcintyre, N., Wheater, H.S., 2011. Catchment Scale Hydrological Modelling: A Review of Model Types, Calibration Approaches and Uncertainty Analysis Methods in The Context of Recent Developments in Technology and Applications. Glob. NEST 13, 193–214.

Peker, I.B., Sorman, A.A., 2021. Application of SWAT using snow data and detecting climate change impacts in the mountainous eastern regions of Turkey. Water (Switzerland) 13. https://doi.org/10.3390/w13141982

Peng, S., Wang, C., Eguchi, S., Kuramochi, K., Kohyama, K., Yoshikawa, S., Itahashi, S., Igura, M., Ohkoshi, S., Hatano, R., 2021. Response of hydrological processes to climate and land use changes in Hiso River watershed, Fukushima, Japan. Phys. Chem. Earth 123, 103010. https://doi.org/10.1016/j.pce.2021.103010

Petpongpan, C., Ekkawatpanit, C., Visessri, S., Kositgittiwong, D., 2021. Projection of hydro-climatic extreme events under climate change in yom and nan river basins, thailand. Water (Switzerland) 13, 1–20. https://doi.org/10.3390/w13050665

Phi Hoang, L., Lauri, H., Kummu, M., Koponen, J., Vliet, M.T.H.V., Supit, I., Leemans, R., Kabat, P., Ludwig, F., 2016. Mekong River flow and hydrological extremes under climate change. Hydrol. Earth Syst. Sci. 20, 3027–3041. https://doi.org/10.5194/hess-20-3027-2016

Piani, C., Haerter, J.O., Coppola, E., 2010a. Statistical bias correction for daily precipitation in regional climate models over Europe. Theor Appl Clim. 99, 187–192. https://doi.org/10.1007/s00704-009-0134-9

Piani, C., Weedon, G.P., Best, M., Gomes, S.M., Viterbo, P., Hagemann, S., Haerter, J.O., 2010b. Statistical bias correction of global simulated daily precipitation and temperature for the application of hydrological models. J. Hydrol. 395, 199–215. https://doi.org/10.1016/j.jhydrol.2010.10.024

Pokhrel, B.K., Chevallier, P., Andréassian, V., Tahir, A.A., Arnaud, Y., Neppel, L., Bajracharya, O.R., Budhathoki, K.P., 2014. Comparison of two snowmelt modelling approaches in the Dudh Koshi basin (eastern Himalayas, Nepal). Hydrol. Sci. J. 59, 1507–1518. https://doi.org/10.1080/02626667.2013.842282

Poletti, S., Staffell, I., 2021. Understanding New Zealand ' s wind resources as a route to 100 % renewable electricity. Renew. Energy 170, 449–461. https://doi.org/10.1016/j.renene.2021.01.053

Pool, S., Vis, M., Seibert, J., 2018. Evaluating model performance : towards a non-parametric variant of the Kling-Gupta efficiency Kling-Gupta efficiency. Hydrol. Sci. J. 63, 1941–1953. https://doi.org/10.1080/02626667.2018.1552002

Priya, Y.R., Manjula, R., 2020. A review for comparing SWAT and SWAT coupled models and its applications. Mater. Today Proc. 45, 7190–7194. https://doi.org/10.1016/j.matpr.2021.02.414

Pulighe, G., Lupia, F., Chen, H., Yin, H., 2021. Modeling climate change impacts on water balance of a mediterranean watershed using swat+. Hydrology 8, 1–14. https://doi.org/10.3390/hydrology8040157

Pun, S.B., 2017. Reflections on India's' Guidelines on Cross Border Trade of Electricity'Vis-a-vis Nepal's' Electricity Development Decade 2016/'026'and'2017/'018 Budget'. Hydro Nepal J. Water, Energy Environ. 21.

Qi, J., Li, S., Li, Q., Xing, Z., Bourque, C.P.A., Meng, F.R., 2016. A new soil-temperature module for SWAT application in regions with seasonal snow cover. J. Hydrol. 538, 863–877. https://doi.org/10.1016/j.jhydrol.2016.05.003

Qi, J., Zhang, X., Yang, Q., Srinivasan, R., Arnold, J.G., Li, J., Waldholf, S.T., Cole, J., 2020. SWAT ungauged: Water quality modeling in the Upper Mississippi River Basin. J. Hydrol. 584. https://doi.org/10.1016/j.jhydrol.2020.124601

Qin, P., Xu, H., Liu, M., Xiao, C., Forrest, K.E., Samuelsen, S., Tarroja, B., 2020. Assessing concurrent effects of climate change on hydropower supply, electricity demand, and greenhouse gas emissions in the Upper Yangtze River Basin of China. Appl. Energy 279, 115694. https://doi.org/10.1016/j.apenergy.2020.115694

Rafee, S.A.A., Uvo, C.B., Martins, J.A., Domingues, L.M., Rudke, A.P., Fujita, T., Freitas, E.D., 2019. Large-scale hydrological modelling of the Upper Paraná River Basin. Water (Switzerland) 11. https://doi.org/10.3390/w11050882

Rafiei, V., Ghahramani, A., An-Vo, D.A., Mushtaq, S., 2020. Modelling hydrological processes and identifying soil erosion sources in a tropical catchment of the great barrier reef using SWAT. Water (Switzerland) 12. https://doi.org/10.3390/W12082179

Rahimpour, M., Tajbakhsh, M., Memarian, H., Aghakhani Afshar, A., 2021. Impact assessment of climate change on hydro-climatic conditions of arid and semi-arid watersheds (case study: Zoshk-Abardeh watershed, Iran). J. Water Clim. Chang. 12, 580–595. https://doi.org/10.2166/wcc.2020.224

Rani, S., Sreekesh, S., 2021. Flow regime changes under future climate and land cover scenarios in the Upper Beas basin of Himalaya using SWAT model. Int. J. Environ. Stud. 78, 382–397. https://doi.org/10.1080/00207233.2020.1811574

Ranzani, A., Bonato, M., Patro, E.R., Gaudard, L., Michele, C. De, 2018. Hydropower Future : Between Climate Change , Renewable Deployment , Carbon and Fuel Prices 10, 1–17. https://doi.org/10.3390/w10091197

Ravazzani, G., Valle, F.D., Gaudard, L., Mendlik, T., Gobiet, A., Mancini, M., 2016. Assessing climate impacts on hydropower production: The case of the Toce river basin. Climate 4, 1–15. https://doi.org/10.3390/cli4020016

Razavi, T., Coulibaly, P., 2016. Improving streamflow estimation in ungauged basins using a multi-modelling approach. Hydrol. Sci. J. 61, 2668–2679.

Reddy, P.J., 2001. A Text Book of Hydrology. Laxmi Publications P. Ltd., New Delhi, India.

Refsgaard, J.C., 1997. Parameterisation, calibration and validation of distributed hydrological models. J. Hydrol. 198, 69–97.

Refsgaard, J.C., 1990. Terminology, modelling protocol and classification of hydrological model codes, in: Abbott, M.B., Refsgaard, C. (Eds.), Distributed Hydrological Modelling. Springer, Dordrecht, pp. 17–39.

Rehman, A., Ma, H., Chishti, M.Z., Ozturk, I., Irfan, M., Ahmad, M., 2021. Asymmetric investigation to track the effect of urbanization , energy utilization , fossil fuel energy and CO 2 emission on economic efficiency in China : another outlook 17319–17330. https://doi.org/https://doi.org/10.1007/s11356-020-12186-w

Ricci, G.F., De Girolamo, A.M., Abdelwahab, O.M.M., Gentile, F., 2018. Identifying sediment source areas in a Mediterranean watershed using the SWAT model. L. Degrad. Dev. 29, 1233–1248. https://doi.org/10.1002/ldr.2889

Richards, L.A., 1931. Capillary conduction of liquids through porous mediums. J. Gen. Appl. Phys. 1, 318–333.

Ridwansyah, I., Yulianti, M., Apip, Onodera, S. ichi, Shimizu, Y., Wibowo, H., Fakhrudin, M., 2020. The impact of land use and climate change on surface

runoff and groundwater in Cimanuk watershed, Indonesia. Limnology 21, 487–498. https://doi.org/10.1007/s10201-020-00629-9

Ridwansyah, I., Yulianti, M., Wibowo, H., 2019. Soil Water Analysis Tools (SWAT) hydrology modelling as a basis for spatial planning: A case study in Cimandiri Watershed, West Java Province. IOP Conf. Ser. Earth Environ. Sci. 380, 1–10. https://doi.org/10.1088/1755-1315/380/1/012017

Robock, A., Turco, R.P., Harwell, M.A., Ackerman, T.P., Andressen, R., Chang, H.S., Sivakumar, M.V.K., 1993. Use of general circulation model output in the creation of climate change scenarios for impact analysis. Clim. Change 23, 293–335. https://doi.org/10.1007/BF01091621

Rodrigues, A.L.M., Reis, G.B., dos Santos, M.T., da Silva, D.D., dos Santos, V.J., de Siqueira Castro, J., Calijuri, M.L., 2019. Influence of land use and land cover's change on the hydrological regime at a Brazilian southeast urbanized watershed. Environ. Earth Sci. 78, 1–13. https://doi.org/10.1007/s12665-019-8601-9

Ross, B.B., Contractor, D.N., Shanholtz, V.O., 1977. Finite element simulation of overland and channel flow. Trans. ASAE 20, 705–0712.

Ruan, H., Zou, S., Yang, D., Wang, Y., Yin, Z., Lu, Z., Li, F., Xu, B., 2017. Runoff Simulation by SWAT Model Using High-Resolution Gridded Precipitation in the Upper Heihe River Basin, Northeastern Tibetan Plateau. Water (Switzerland) 9, 1–22. https://doi.org/10.3390/w9110866

Salari, M., Javid, R.J., Noghanibehambari, H., 2021. The nexus between CO 2 emissions , energy consumption , and economic growth in the U . S . Econ. Anal. Policy 69, 182–194. https://doi.org/10.1016/j.eap.2020.12.007

Samimi, M., Mirchi, A., Moriasi, D., Ahn, S., Alian, S., Taghvaeian, S., Sheng, Z., 2020. Modeling arid/semi-arid irrigated agricultural watersheds with SWAT: Applications, challenges, and solution strategies. J. Hydrol. 590, 125418. https://doi.org/10.1016/j.jhydrol.2020.125418

Samuel, J., Coulibaly, P., Metcalfe, R.A., 2011. Estimation of continuous streamflow in Ontario ungauged basins: comparison of regionalization methods. J. Hydrol. Eng. 16, 447–459.

Sapač, K., Medved, A., Rusjan, S., Bezak, N., 2019. Investigation of low- and high-flow characteristics of karst catchments under climate change. Water (Switzerland) 11, 3–7. https://doi.org/10.3390/w11050925

Satpathy, M., 2015. Importance of energy and power sector in economic development An Indian perspective. Int. Res. J. Manag. Sci. Technol. 6, 41–45.

Shah, M.I., Khan, A., Akbar, T.A., Hassan, Q.K., Khan, A.J., Dewan, A., 2020. Predicting hydrologic responses to climate changes in highly glacierized and mountainous region Upper Indus Basin:. R. Soc. Open Sci. 7. https://doi.org/10.1098/rsos.191957rsos191957

Shankar, K., 1969. Landslides in Burhi Gandaki at Labu Bensi. J. Nepal Eng. Assoc. I, 47–49.

Sharannya, T.M., Mudbhatkal, A., Mahesha, A., 2018. Assessing climate change impacts on river hydrology–A case study in the Western Ghats of India. J. Earth Syst. Sci. 127, 1–11.

Sharma, K.D., Sorooshian, S., Wheater, H., 2008. Hydrological Modelling in Arid and Semi-Arid Areas. Cambridge University Press, New York.

Sharma, K.P., Adhikari, N.R., 2004. Hydrological Estimation in Nepal,. Department of Hydrology and Meteorology, Government of Nepal, Kathmandu, Nepal.

Sharma, N., Zakaullah, M., Tiwari, H., Kumar, D., 2015. Runoff and sediment yield modeling using ANN and support vector machines: a case study from Nepal watershed. Model. Earth Syst. Environ. 1, 1–8. https://doi.org/10.1007/s40808-015-0027-0

Shea, J.M., Immerzeel, W.W., Wagnon, P., Vincent, C., Bajracharya, S., 2015. Modelling glacier change in the Everest region, Nepal Himalaya. Cryosphere 9, 1105–1128. https://doi.org/10.5194/tc-9-1105-2015

Shelton, S., 2021. Evaluation of the Streamflow Simulation by SWAT Model for Selected Catchments in Mahaweli River Basin, Sri Lanka. Water Conserv. Sci. Eng. 6, 233–248. https://doi.org/10.1007/s41101-021-00117-w

Sherman, L.K., 1932. The Relation Of Hydrographs of Runoff to Size and Character of Drainage-Basins. Am. Geophys. Union 332–339.

Shin, S., Pokhrel, Y.., Talchabhadel, R., Panthi, J., 2021. Spatio-temporal dynamics of hydrologic changes in the Himalayan river basins of Nepal using high-resolution hydrological-hydrodynamic modeling. J. Hydrol. 598.

Shirsat, T.S., Kulkarni, A. V., Momblanch, A., Randhawa, S.S., Holman, I.P., 2021. Towards climate-adaptive development of small hydropower projects in Himalaya: A multi-model assessment in upper Beas basin. J. Hydrol. Reg. Stud. 34, 100797. https://doi.org/10.1016/j.ejrh.2021.100797

Shrestha, A., Shrestha, S., Tingsanchali, T., Budhathoki, A., Ninsawat, S., 2021. Adapting hydropower production to climate change: A case study of Kulekhani Hydropower Project in Nepal. J. Clean. Prod. 279, 123483. https://doi.org/10.1016/j.jclepro.2020.123483

Shrestha, A.B., Wake, C.P., Mayewski, P.A., Dibb, J.E., 1999. Maximum Temperature Trends in the Himalaya and Its Vicinity : An Analysis Based on Temperature Records from Nepal for the Period 1971 – 94. J. Clim. 12, 2775–2786.

Shrestha, H.M., 1966. Cadastre of Potential Water Power Resources of less studied High Mountainous Regions (with special reference to Nepal). Moscow Technical University.

Shrestha, J.P., Pahlow, M., Cochrane, T.A., 2020. Development of a SWAT hydropower operation routine and its application to assessing hydrological alterations in the mekong. Water (Switzerland) 12. https://doi.org/10.3390/W12082193

Shrestha, M., Wang, L., Koike, T., Xue, Y., Hirabayashi, Y., 2012. Modeling the spatial distribution of snow cover in the Dudhkoshi Region of the Nepal Himalayas. J. Hydrometeorol. 13, 204–222. https://doi.org/10.1175/JHM-D-10-05027.1

Shrestha, S., Bajracharya, A.R., Babel, M.S., 2016a. Assessment of risks due to climate change for the Upper Tamakoshi Hydropower Project in Nepal. Clim. Risk Manag. 14, 27–41. https://doi.org/10.1016/j.crm.2016.08.002

Shrestha, S., Khatiwada, M., Babel, M.S., Parajuli, K., 2014. Impact of Climate Change on River Flow and Hydropower Production in Kulekhani Hydropower Project of Nepal. Environ. Process. 1, 231–250. https://doi.org/10.1007/s40710-014-0020-z

Shrestha, S., Sattar, H., Khattak, M.S., Wang, G., Babur, M., 2020. Evaluation of adaptation options for reducing soil erosion due to climate change in the Swat River Basin of Pakistan. Ecol. Eng. 158, 106017. https://doi.org/10.1016/j.ecoleng.2020.106017

Shrestha, S., Shrestha, M., Babel, M.S., 2017. Assessment of climate change impact on water diversion strategies of Melamchi Water Supply Project in Nepal. Theor. Appl. Climatol. 128, 311–323. https://doi.org/10.1007/s00704-015-1713-6

Shrestha, S., Shrestha, M., Babel, M.S., 2016b. Modelling the potential impacts of climate change on hydrology and water resources in the Indrawati River Basin, Nepal. Environ. Earth Sci. 75, 1–13.

Shrestha, S., Shrestha, M., Shrestha, P.K., 2018. Evaluation of the SWAT model performance for simulating river discharge in the Himalayan and tropical basins of Asia Sangam Shrestha , Manish Shrestha and Pallav Kumar Shrestha. Hydrol. Res. 49, 846–860. https://doi.org/10.2166/nh.2017.189

Shukla, S., Jain, S.K., Kansal, M.L., 2021. Hydrological modelling of a snow/glacier-fed western Himalayan basin to simulate the current and future streamflows under changing climate scenarios. Sci. Total Environ. 795, 148871. https://doi.org/10.1016/j.scitotenv.2021.148871

Singh, L., Saravanan, S., 2020. Comparison of different efficiency criteria for hydrological model assessment. J. Hydrol. Reg. Stud. 3, 95–105. https://doi.org/10.5194/adgeo-5-89-2005

Singh, V.P., 2018. Hydrologic modeling: progress and future directions. Geosci. Lett. 5, 1–18.

Singh, V.P., 1995. Computer models of watershed hydrology. Water Resources Publications.

Singh, V.P., Frevert, D.K. (Eds.), 2010. Watershed models. CRC press.

Sinha, R.K., Eldho, T.I., Subimal, G., 2020. Assessing the impacts of land use/land cover and climate change on surface runoff of a humid tropical river basin in Western Ghats, India. Int. J. River Basin Manag. 0, 1–12. https://doi.org/10.1080/15715124.2020.1809434

Siri, R., Mondal, S.R., Das, S., 2021. Alternative Energy Resources, in: Pathak, P., Srivastava, R.R. (Eds.), Alternative Energy Resources: The Way to Sustainable Modern Society. Springer Nature, Switzerland., Switzerland, pp. 93–114. https://doi.org/10.1007/698_2020_635

Solaun, K., Cerdá, E., 2017. The impact of climate change on the generation of hydroelectric power-a case study in southern Spain. Energies 10. https://doi.org/10.3390/en10091343

Soncini, A., Bocchiola, D., Confortola, G., Minora, U., Vuillermoz, E., Salerno, F., Viviano, G., Shrestha, D., Senese, A., Smiraglia, C., Diolaiuti, G., 2016. Future hydrological regimes and glacier cover in the Everest region: The case study of the upper Dudh Koshi basin. Sci. Total Environ. 565, 1084–1101. https://doi.org/10.1016/j.scitotenv.2016.05.138

Sood, A., Smakhtin, V., 2015. Revue des modèles hydrologiques globaux. Hydrol. Sci. J. 60, 549–565. https://doi.org/10.1080/02626667.2014.950580

Sorooshian, S., Gupta, V.K. (Eds.), 1995. Model calibration. Computer Models of Watershed Hydrology. Water Resour Publications, Highlands Ranch, Colorado, USA.

Stern, D.I., Burke, P.J., Bruns, S.B., 2019. The impact of electricity on economic development: a macroeconomic perspective. UC Berkeley: Center for Effective Global Action.Schmidli, J., Frei, C., Vidale, P.L., 2006. Downscaling from GCM precipitation: A benchmark for dynamical and statistical downscaling methods. Int. J. Climatol. 26, 679–689. https://doi.org/10.1002/joc.1287Stern, D.I., 2012. The Role of Energy in Economic Growth,. SSRN Electron. J. https://doi.org/10.2139/ssrn.1878863

Stern, N., Peters, S., Bakhshi, V., Bowen, A., Cameron, C., Catovsky, S., Zenghelis, D., 2006b. Stern Review: The economics of climate change.

Tallaksen, L.M., 1995. A review of baseflow recession analysis. J. Hydrol. 165, 349–370.

Tan, M.L., Gassman, P.W., Liang, J., Haywood, J.M., 2021a. A review of alternative climate products for SWAT modelling: Sources, assessment and future directions. Sci. Total Environ. 795, 148915.

https://doi.org/10.1016/j.scitotenv.2021.148915

Tan, M.L., Gassman, P.W., Srinivasan, R., Arnold, J.G., Yang, X.Y., 2019. A review of SWAT studies in Southeast Asia: Applications, challenges and future directions. Water (Switzerland) 11, 1–25. https://doi.org/10.3390/w11050914

Tan, M.L., Gassman, P.W., Yang, X., Haywood, J., 2020. A review of SWAT applications, performance and future needs for simulation of hydro-climatic extremes. Adv. Water Resour. 143, 103662. https://doi.org/10.1016/j.advwatres.2020.103662

Tan, M.L., Liang, J., Samat, N., Chan, N.W., Haywood, J.M., Hodges, K., 2021b. Hydrological extremes and responses to climate change in the kelantan river basin, malaysia, based on the CMIP6 highresmip experiments. Water (Switzerland) 13. https://doi.org/10.3390/w13111472

Tangtham, N., 1978. An Application of a Modified Universal Soil Loss Equation in Predicting Suspended-Sediment Yield from a Small Agricultural Watershed. The Pennsylvania State University.

Tanteliniaina, M.F.R., Rahaman, M.H., Zhai, J., 2021. Assessment of the future impact of climate change on the hydrology of the mangoky river, madagascar using ann and swat. Water (Switzerland) 13. https://doi.org/10.3390/w13091239

Tapiador, Francisco, Navarro, A., Moreno, R., Sánchez, J.L., García-Ortega, E., 2020. Regional climate models: 30 years of dynamical downscaling. Atmos. Res. 235, 104785. https://doi.org/10.1016/j.atmosres.2019.104785

Tapiador, F., Navarro, A., Moreno, R., Sánchez, J.L., García-Ortega, E., 2020. Regional climate models: 30 years of dynamical downscaling. Atmos. Res. 235, 104785.

Taylor, K.E., 2001. Summarizing multiple aspects of model performance in a single diagram. J. Geophys. Res. 106, 7183–7192.

Tegegne, G., Park, D.K., Kim, Y., 2017. Journal of Hydrology : Regional Studies Comparison of hydrological models for the assessment of water resources in a data-scarce region , the Upper Blue Nile River Basin. J. Hydrol. Reg. Stud. 14, 49–66. https://doi.org/10.1016/j.ejrh.2017.10.002

Tehsome, H.H., Engida, A.N., Gebrie, G.S., 2021. Effect of Watershed Delineation on

SWAT Model Performance for Daily Streamflow Simulation , in Blue Nile , East Africa.

Terink, W., Hurkmans, R.T.W.L., Torfs, P.J.J.F., Uijlenhoet, R., 2021. Evaluation of a bias correction method applied to downscaled precipitation and temperature reanalysis data for the Rhine basin 687–703.

Teutschbein, C., Seibert, J., 2013. Is bias correction of regional climate model (RCM) simulations possible for non-stationary conditions ? 5061–5077. https://doi.org/10.5194/hess-17-5061-2013

Thapa, G., Basnett, Y., 2015. Using Hydroelectricity to Power Economic Transformation in Nepal, Supporting Economic Transformation: Overseas Development Institute (ODI).

Thapa, S., Zhang, F., Zhang, H., Zeng, C., Wang, L., Xu, C.Y., Thapa, A., Nepal, S., 2021. Assessing the snow cover dynamics and its relationship with different hydro-climatic characteristics in Upper Ganges river basin and its sub-basins. Sci. Total Environ. 793, 148648. https://doi.org/10.1016/j.scitotenv.2021.148648

Thatcher, M., McGregor, J., Dix, M., Katzfey, J., 2015. A new approach for coupled regional climate modeling using more than 10, 000 cores. IFIP Adv. Inf. Commun. Technol. 448, 599–607. https://doi.org/10.1007/978-3-319-15994-2_61

Themeßl, M.J., Gobiet, A., Heinrich, G., 2012. Empirical-statistical downscaling and error correction of regional climate models and its impact on the climate change signal 449–468. https://doi.org/10.1007/s10584-011-0224-4

Theron, S.N., Weepener, H.L., Le Roux, J.J., Engelbrecht, C.J., 2021. Modelling potential climate change impacts on sediment yield in the Tsitsa river catchment, South Africa. Water SA 47, 67–75. https://doi.org/10.17159/wsa/2021.v47.i1.9446

Thiessen, A.H., 1911. Precipitation averages for large areas. Mon. Weather 39, 1082–1089.

Thiha, S., Shamseldin, A.Y., Melville, B.W., 2021. Assessment of the Myitnge River

flow responses in Myanmar under changes in land use and climate. Model. Earth Syst. Environ. 7, 1393–1415. https://doi.org/10.1007/s40808-020-00926-3

Tobin, I., Jerez, S., Greuell, W., Ludwig, F., Vautard, R., van Vliet, M.T.H., Breon, F.-M., 2018. Vulnerabilities and resilience of European power OPEN ACCESS Vulnerabilities and resilience of European power. Environ. Res. Lett.

Todini, E., 1988. Rainfall-Runoff Modeling Past, Prestent and Future. J. Hydrol. 100, 341–352.

Tomczyk, P., Wiatkowski, M., 2020. Challenges in the development of hydropower in selected european countries. Water (Switzerland) 12. https://doi.org/10.3390/w12123542

Touseef, M., Chen, L., Masud, T., Khan, A., Yang, K., Shahzad, A., Ijaz, M.W., Wang, Y., 2020. Assessment of the future climate change projections on Streamflow Hydrology and water availability over upper Xijiang River Basin, China. Appl. Sci. 10. https://doi.org/10.3390/app10113671

Touseef, M., Chen, L., Yang, W., 2021. Assessment of surfacewater availability under climate change using coupled SWAT-WEAP in hongshui river basin, China. ISPRS Int. J. Geo-Information 10. https://doi.org/10.3390/ijgi10050298

Troin, M., Vallet-Coulomb, C., Piovano, E., Sylvestre, F., 2012. Rainfall-runoff modeling of recent hydroclimatic change in a subtropical lake catchment: Laguna Mar Chiquita, Argentina. J. Hydrol. 475, 379–391. https://doi.org/10.1016/j.jhydrol.2012.10.010

Turner, S.W.D., Hejazi, M., Kim, S.H., Clarke, L., Edmonds, J., 2017a. Climate impacts on hydropower and consequences for global electricity supply investment needs. Energy 141, 2081–2090. https://doi.org/10.1016/j.energy.2017.11.089

Turner, S.W.D., Ng, J.Y., Galelli, S., 2017b. Examining global electricity supply vulnerability to climate change using a high-fidelity hydropower dam model. Sci. Total Environ. 590–591, 663–675. https://doi.org/10.1016/j.scitotenv.2017.03.022

Uamusse, M.M., Aljaradin, M., Nilsson, E., Persson, K.M., 2017. Climate Change observations into Hydropower in Mozambique. Energy Procedia 138, 592–597. https://doi.org/10.1016/j.egypro.2017.10.165

Uamusse, M.M., Tussupova, K., Persson, K.M., 2020. Climate change effects on hydropower in Mozambique. Appl. Sci. 10. https://doi.org/10.3390/app10144842

UNDP, 2020. Pathways To Sustainable. United Nations Development Programme.

UNEP, 2012. The UN-Water Status Report on the Application of Integrated Approaches to Water Resources Management. United Nations Development Programme.

UNESCO, 1978. U.S.S.R. National Committee for the International Hydrological Decade, World water balance and water resources of the earth, English translation, Studies and Reports in Hydrology. Paris.

UNFCCC, 2016. Conference of the Parties Report of the Conference of the Parties on its twenty-first session , held in Paris from 30 November to 13 December 2015 Paragraphs 01192.

UNFCCC, 2010. Report of the Conference of the Parties on its fifteenth session, held in Copenhagen from 7 to 19 December 2009.

United Nations, 1998. Kyoto Protocol to the United Nations Framework Convention on Climate Change, United Nations.

United Nations, 1992. Report of the United Nations Conference on Environment and Development, Rio de Janeiro.

United Nations, 1973. United Nations Conference on the Human Environment, United Nations. https://doi.org/10.1051/epn/19720307006

Upadhyay, S.N., Gaudel, P., 2018. Water Resources Development in Nepal: Myths and Realities. Hydro Nepal J. Water, Energy Environ. 23, 22–29.

USDA, 1972. National engineering handbook, section 4: Hydrology. Washington, DC.

Van Liew, M.W., Arnold, J.G., Bosch, D.D., 2005. Problems and potential of autocalibrating a hydrologic model. Trans. ASAE 48, 1025–1040.

Vanderkelen, I., Van Lipzig, N.P.M., Thiery, W., 2018. Modelling the water balance of Lake Victoria (East Africa)-Part 1: Observational analysis. Hydrol. Earth Syst. Sci. 22, 5509–5525. https://doi.org/10.5194/hess-22-5509-2018

Vanegas Cantarero, M.M., 2020. Of renewable energy, energy democracy, and sustainable development: A roadmap to accelerate the energy transition in developing countries. Energy Res. Soc. Sci. 70, 101716. https://doi.org/10.1016/j.erss.2020.101716

Vaze, J., Jordan, P., Beecham, R., Frost, A., Summerell, G., 2012. Guidelines for rainfall–runoff modelling: towards best practice model application, eWater CRC. Bruce, Australia.

Venetsanou, P., Anagnostopoulou, C., Loukas, A., Voudouris, K., 2020. Hydrological impacts of climate change on a data-scarce Greek catchment. Theor. Appl. Climatol. 140, 1017–1030. https://doi.org/10.1007/s00704-020-03130-6

Vilaysane, B., Takara, K., Luo, P., Akkharath, I., Duan, W., 2015. Hydrological Stream Flow Modelling for Calibration and Uncertainty Analysis Using SWAT Model in the Xedone River Basin, Lao PDR. Procedia Environ. Sci. 28, 380–390. https://doi.org/10.1016/j.proenv.2015.07.047

Villamizar, S.R., Pineda, S.M., Carrillo, G.A., 2019. The effects of land use and climate change on the water yield of a watershed in Colombia. Water (Switzerland) 11. https://doi.org/10.3390/w11020285

Viviroli, D., Archer, D.R., Buytaert, W., Fowler, H.J., Greenwood, G.B., Hamlet, A.F., Huang, Y., Koboltschnig, G., Litaor, M.I., López-Moreno, J.I., 2011. Climate change and mountain water resources: overview and recommendations for research, management and policy. Hydrol. Earth Syst. Sci. 15, 471–504.

Viviroli, D., Dürr, H.H., Messerli, B., Meybeck, M., Weingartner, R., 2007. Mountains of the world, water towers for humanity: Typology, mapping, and global significance. Water Resour. Res. 43, 1–13. https://doi.org/10.1029/2006WR005653

Vliet, M.T.H. Van, Wiberg, D., Leduc, S., Riahi, K., 2016. Power-generation system vulnerability and adaptation to changes in climate and water resources 6. https://doi.org/10.1038/NCLIMATE2903

Vuuren, D.P. Van, Edmonds, J., Kainuma, M., Riahi, K., Nakicenovic, N., Smith, S.J., Rose, S.K., 2011. The representative concentration pathways : an overview 5–31. https://doi.org/10.1007/s10584-011-0148-z

Wagener, T., Wheater, H., Gupta, H.V., 2004. Rainfall-runoff modelling in gauged and ungauged catchments. World Scientific.

Wagner, B., Hauer, C., Habersack, H., 2019. Current hydropower developments in Europe. Curr. Opin. Environ. Sustain. 37, 41–49. https://doi.org/10.1016/j.cosust.2019.06.002

Wang, Y., Yang, X., Zhang, M., Zhang, L., Yu, X., Ren, L., Liu, Y., Jiang, S., Yuan, F., 2019. Projected effects of climate change on future hydrological regimes in the upper Yangtze River basin, China. Adv. Meteorol. 2019.

WECS, 2013. National Energy Strategy of Nepal. Water and Energy Commission Secretariat Singha Durbar, Kathmandu.

WECS, 2011. Water resources of Nepal in the context of climate change. Water and Energy Commission Secretariat, Kathmandu, Nepal.

WECS, 2005. National Water Plan. Water and Energy Commission Secretariat Singha Durbar, Kathmandu.

WECS, 1990. Methodology for Estimating Hydrological Characteristics of Ungauged Locations in Nepal. His Majesty's Government of Nepal, Ministry of Water Resources, Seq. No. 331, Water and Energy Commission Secretariat and Department of Hydrology and Meteorology, Kathmandu, Nepal.

Wheater, H.S., 1993. Progress and Directions in Rainfall-Runoff Modelling: Modelling Change in Environmental Systems. Wiley and Sons, Southampton, UK, UK.

William W-G. Yeh, 1985. Reservoir Management and Operations Models: A State- of-the Art Review. Water Resour. Res. 21, 1797–1818.

Williams, J.R., Hann, R.W., 1972. Hymo, A problem- oriented computer language for building hydrologic models. Water Resour. Res. 8, 79–86. https://doi.org/10.1029/WR008i001p00079.

WMO, 1989. Calculation of Monthly and Annual 30-Year Standard Normals.

Washington, D.C, USA.

Worku, T., Khare, D., Tripathi, S.K., 2017. Modeling runoff–sediment response to land use/land cover changes using integrated GIS and SWAT model in the Beressa watershed. Environ. Earth Sci. 76, 1–14. https://doi.org/10.1007/s12665-017-6883-3

World Bank, 2020. Energy Use [WWW Document]. URL https://data.worldbank.org/indicator/EG.USE.PCAP.KG.OE

World Bank, 2017. Water Resources Management.

Wrigley, E.A., 2013. Energy and the english industrial revolution. Philos. Trans. R. Soc. A Math. Phys. Eng. Sci. 371. https://doi.org/10.1098/rsta.2011.0568

Yan, Y., Xue, B., Yinglan, A., Sun, W., Zhang, H., 2020. Quantification of climate change and land cover/use transition impacts on runoff variations in the upper Hailar Basin, NE China. Hydrol. Res. 51, 976–993. https://doi.org/10.2166/nh.2020.022

Yasir, M., Hu, T., Hakeem, S.A., 2021. Impending hydrological regime of lhasa river as subjected to hydraulic interventions-a SWAT model manifestation. Remote Sens. 13. https://doi.org/10.3390/rs13071382

Yeo, M.H., Chang, A., Pangelinan, J., 2021. Application of a SWAT model for supporting a ridge- to- reef framework in the Pago Watershed in Guam. Water (Switzerland) 13. https://doi.org/10.3390/w13233351

Yilmaz, M.U., Onoz, B., 2020. A Comparative Study of Statistical Methods for Daily Streamflow Estimation at Ungauged Basins in Turkey. Water 12, 459.

Yoro, K.O., Daramola, M.O., 2020. CO2 emission sources, greenhouse gases, and the global warming effect, Advances in Carbon Capture. Elsevier Inc. https://doi.org/10.1016/b978-0-12-819657-1.00001-3

Young, A.R., 2006. Stream flow simulation within UK ungauged catchments using a daily rainfall-runoff model. J. Hydrol. 320, 155–172.

Zamoum, S., Souag-Gamane, D., 2019. Monthly streamflow estimation in ungauged catchments of northern Algeria using regionalization of conceptual model

parameters. Arab. J. Geosci. 12, 1–14.

Zare, M., Azam, S., Sauchyn, D., 2022. Evaluation of Soil Water Content Using SWAT for Southern Saskatchewan, Canada. Water (Switzerland) 14. https://doi.org/10.3390/w14020249

Zhang, Q., Knowles, J.F., Barnes, R.T., Cowie, R.M., Rock, N., Williams, M.W., 2018. Surface and subsurface water contributions to streamflow from a mesoscale watershed in complex mountain terrain. Hydrol. Process. 32, 954–967. https://doi.org/10.1002/hyp.11469

Zhong, R., Zhao, T., He, Y., Chen, X., 2019. Hydropower change of the water tower of Asia in 21st century: A case of the Lancang River hydropower base, upper Mekong. Energy 179, 685–696. https://doi.org/10.1016/j.energy.2019.05.059

Zhou, Q., Hanasaki, N., 2018. Economic consequences of global climate change and mitigation on future hydropower generation 77–90.

Zhou, Y., Xu, Y.J., Xiao, W., Wang, J., Huang, Y., Yang, H., 2017. Climate change impacts on flow and suspended sediment yield in headwaters of high-latitude regions-A case study in China's far Northeast. Water (Switzerland) 9. https://doi.org/10.3390/w9120966

APPENDICES

APPENDIX -1 PUBLICATION OF RESEARCH ARTICLES

Journal of Institute of Science and Technology, 26(1), 89-98 (2021)
ISSN: 2469-9062 (print), 2467-9240 (e)
https://doi.org/10.3126/jist.v26i1.37831

Research Article

IMPACT OF FLOW VARIATION ON HYDROPOWER PROJECTS IN BUDHIGANDAKI RIVER BASIN OF NEPAL

Suresh Marahatta[1*], **Laxmi Prasad Devkota**[2,3], **Deepak Aryal**[1]

[1]*Central Department of Hydrology ad Meteorology, Tribhuvan University, Kathmandu, Nepal*
[2]*Nepal Academy of Science and Technology (NAST), Kathmandu, Nepal*
[3]*Water Modeling Solutions Pvt. Ltd. (WMS), Kathmandu, Nepal*
[*]*Corresponding author: suresh.marahatta@cdhm.tu.edu.np*

(***Received**: March 10, 2021; **Revised**: May 14, 2021; **Accepted**: June 04, 2021)*

ABSTRACT

Daily flow data from 1964 to 2015 of Budhigandaki River at Arughat were analyzed to assess the impact of flow variation at different time scales to the run of the river (RoR) type of hydropower projects. The data show very high inter-annual variation in daily, monthly and seasonal flows. The long term annual average flow at Arughat was 160 m^3/s and varies from 120 to 210 m^3/s. The long-term averages of loss in flow for both dry and wet seasons based on daily flows for three design discharges (Q_{90}, Q_{60} and Q_{40}) were found to be respectively -0.72, -1.76 and -1.54 m^3/s for dry season and 0.0, -0.27 and -2.26 m^3/s for wet season. Although long-term average loss is small, uncertainty increases with the increase in design discharge. The long-term dry season power loss is about 3 % for the RoR projects of the basin however, its annual variation is large. There is a probability of losing the quantum of energy generation by nearly 40% in some years and gaining by about 30 % in some other years in dry season. The impact of flow variation on power production was negative in both dry and wet seasons for RoR projects of Budhigandaki basin. This study concludes that uncertainty arising from daily flow variation should be assessed while estimating energy generation in hydropower projects. Intra-annual flow variation is, thus, to be taken into consideration while calculating the power generated by the RoR plants; and it should be reflected in power purchase agreement.

Keywords: Design discharges, Energy, Fractional difference, Monthly flows, Runoff the river

INTRODUCTION

Nepal is one of the 47 least developed countries in the world at present (United Nations, 2020). The government of Nepal has put priority on the hydropower generation as the backbone of economic development in its endeavor to advance from its Least Developed Country status to Developing Country by 2022 and to reach to the middle income country level by 2030 has put its endeavor to graduate from its Least Developed Country status to Developing Country in 2022 and to upgrade middle income country level by 2030 (NPC, 2020). In order to realize these goals, Nepal has to achieve high growth in all sectors of economic development.

Electricity is one of the key drivers among these factors for overall development of the country. Number of past studies showed that economic development of a country was strongly correlated with the access of electricity and its consumption (Aslan, 2014; Devkota, 2020; Kamaludin, 2013; Lorde *et al.*, 2010; Stern *et al.*, 2019). It is because electricity brings higher agricultural productivity through powering irrigation, food and seed preservations, and contributes to effective running of industrial and service sectors. Similarly, it enhances productivity of education efforts and health services, and helps to improve clean water supply and sanitation. It also helps to create opportunities in the application of new technologies and ease access to information (Satpathy, 2015). Previous empirical studies have revealed the bidirectional causality between economic growth and electricity consumption, i.e., greater electricity consumption brings about higher economic growth and higher economic growth creates demands for greater electricity consumption (Ogundipe & Apata, 2013). However, this relationship was not linear and depends on the stages of development (Hirsh & Koomey, 2015). Some of the other studies found unidirectional causality between economic growth and electricity consumption, i.e., electricity consumption leads to economic growth or vice versa, depending on the stage of development (Bayar & Özel, 2014; Zhang *et al.*, 2017).

Per capita energy consumption in Nepal is low, i.e., 434 kg oil equivalent for the year 2014 when the world average was 1,922 kg oil equivalent (World Bank, 2020). More than 77 % of the energy consumed comes from traditional and inefficient sources, e.g., wood, cow dung and agricultural residue, and about 17 % from petroleum product and coal. The share of electricity in total energy use is only 3.4 % (WECS, 2013). The per capita electricity consumption of Nepal was 146 KWh in 2014, less than 5 % of the world average of 3,132 KWh. Nepal's electricity consumption is less than 4 % and 18 % compared to China and India, respectively (World Bank, 2020).

Recognizing the importance of energy for socio-economic development, the Government of Nepal plans to increase

per capita energy consumption in its finer form, i.e., electricity. Nepal has set hydropower development as a priority (WECS, 2013) using its annual available water of 225 km^3 (WECS, 2005) and its unique topography, vast abundance of rivers and streams for hydropower development. Hydropower development can contribute to national development through reduced imports of fossil fuels, expand the area of land under irrigation and diversify the economy in which poor households are more integrated in the economy. Increase in greater electricity generation is expected to promote industrialization, generate foreign currency reserves through export of electricity to reduce Nepal's trade deficit (Alam et al., 2017; MoWR, 2009; Thapa & Basnett, 2015).

Hydropower development in Nepal started in 1911 with a 500 KW plant in Pharping near Kathmandu (Dixit, 2002). At present, total hydropower production in Nepal is around 1,278 MW (NEA, 2020), of which storage plant produces 104 MW (DOED, 2020). After the People's Movement of 2006 that transformed the country's political structure into federal republic, the Government of Nepal (GoN) has taken new policy and project level initiatives for hydropower development. A task force was formed in December 2008 to formulate programs for developing 10,000 MW in 10 years for overcoming the energy crisis (MoWR, 2009).

This task force has provided the list of storage and run-off the river projects with a time-line for development. Similarly, GoN has also proposed a plan of development of 25,000 MW in 20 years in 2009 (MoWR, 2010). The government has announced plans for developing 3,000 MW of hydropower in three years, 5,000 in five years and 15,000 MW in ten years, raising per capita energy consumption of 245 KWh to 700 KWh in 2022 (NEA, 2019). It includes both storage projects: (16, Total Capacity: 9,000 MW) and peaking run-of the river (PRoR) projects (16, Total Capacity: 6,000 MW) (MoWR, 2010).

The above shows a shift in the government's priority to hydropower development and focus on storage projects. This shift is useful because a storage project addresses the seasonal variation of river hydrology by storing water during high flow period (monsoon season) for power generation during lean flow period when the demand of electricity is higher in Nepal. Further they can act as a multipurpose water resources projects by having provisions for water supplies for drinking, irrigation and industrial uses; recreation; navigation and flood control. To have year-round irrigation mainly in the Terai region (Indo-Gangetic plain), the irrigation policy of Nepal foresees the need of reservoir projects. Reservoir projects are not only beneficial to Nepal but also to India in terms of irrigation and flood control (Pun, 2017; Upadhyay & Gaudel, 2018). Although stored water of a reservoir can be used for various purposes, in Nepal they are meant for hydropower generation.

Production of electricity (hydropower) is a function of flow and head. The capacity of a power plant depends on the river discharge in RoR types of projects. In a storage hydropower plant, the operation is based on the reservoir volume, inflow characteristics and purpose of its use, such as if a plant is operated for generating electricity to meet the daily demand or to meet peak hours' demand (Liu *et al.*, 2016). Whatever the cases, river hydrology plays an important role in hydropower generation.

Rivers supply water for drinking, industries, irrigation, hydropower generation, transport and sustaining ecosystems services to the people in downstream (Akhtar *et al.*, 2008; Miller *et al.*, 2012; Molden *et al.*, 2011; Viviroli *et al.*, 2011), however climate change is impacting river hydrology (Devkota & Gyawali, 2015; Pandey *et al.*, 2020). Variation in flow in rivers is high (BGHEP, 2015; DHM, 2018) and the impact of variation in meeting daily, monthly or seasonal water requirements is seldom studied. This understanding of river hydrology is important from a technical point of view of generation and operation of hydropower plants and from an investment portfolio as investment is substantial. The knowledge of the magnitude of such variations is crucial to the private investors because the developer has to pay penalty if the project cannot supply the agreed amount of energy to NEA (NEA, 2017). In 2020, private producers contribute almost 55 % of power to Nepal's integrated power system (NEA: 582 MW, IPPs: 696 MW) (NEA, 2020).

Energy generation by a hydropower project is calculated on the basis of the long-term monthly average flow (Q_{LTMA}) of the river (DOED, 2018). However, the flow of a given month of a particular year varies significantly from Q_{LTMA}. Such variations have implications on power production of the plant but the developer has to pay penalty if the project cannot supply the agreed amount of energy to NEA (NEA, 2017). The main objective of this study was to assess the impact of flow variation in the Budhigandaki river basin on power production of RoR type of hydropower projects. The specific objectives of the study were (i) to estimate the flow available for power production of each month based on long term monthly flow and design discharge, and (ii) to calculate the change in power production due to monthly variation in flows.

MATERIALS AND METHODS

Study area

The location map of the Budhigandaki river basin is given in Fig. 1. It is a part of the Narayani river basin, bordered in the north by the Tibetan Plateau, in the south and east by the Trishuli river basin, and in the west by the Marsyangdi river basin. The flow gauging station of this

basin is located at Arughat (#445) of which the catchment area is 3,863 km^2. The total catchment area at the confluence of the river with the Trishuli river is 4,988 km^2 (Marahatta *et al.*, 2021).

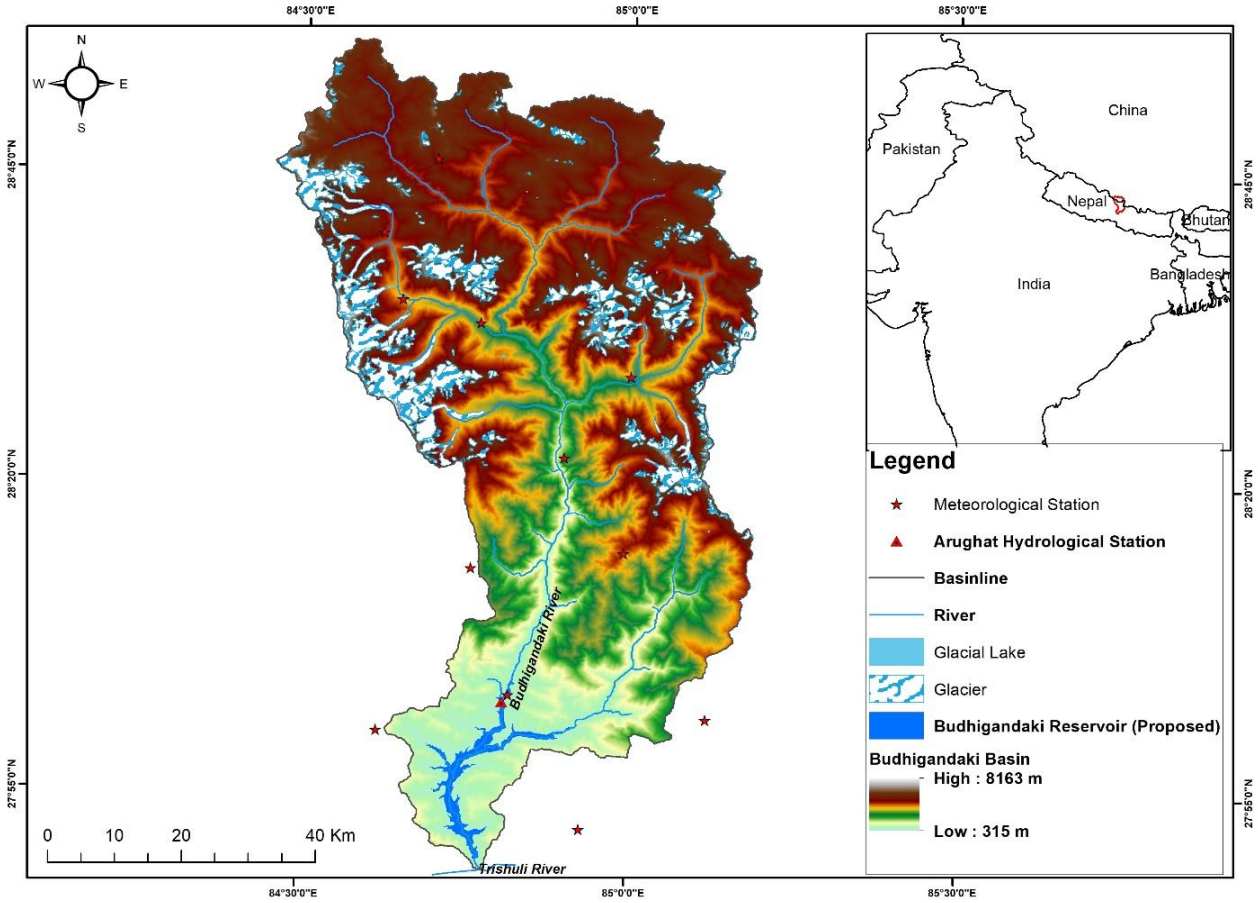

Fig. 1. Location map of Budhigandaki basin

The database of the Department of Electricity Development (http://www.doed.gov.np) shows that 35 hydropower projects (total capacity ~ 3000 MW) are ranging from 0.5 to 1200 MW at various stages of development in the Budhigandaki basin. Budhigandaki storage hydro-electric project (1200 MW) is one proposed.

Theoretical background; the impact of flow variation in power generation

The power that can be generated in a hydroelectric power plant is given as in equation (1)

$$P = \eta\gamma QH \quad (1)$$

Where, P represents the power (KW), η is the efficiency of the plant, γ is the unit weight of water (9.8 KN/m^3), Q flows through the turbine (m^3/s), and H is the net head (m).

A power plant is either storage or the run of the river (RoR) type depending on the availability of storage reservoir in a river and the generation system. The RoR type of project uses the instantaneous flow of the river which governs the capacity of the RoR plant. In Nepal, the RoR plants are generally designed for Q_{40} (Q_x: the flow having x percent exceedance probability) using historic daily flow data (DOED, 2018). Energy generated by such plants is estimated based on the long-term monthly average flows. Department of Electricity Development, of the Government of Nepal, grants survey and generation license to the private/public developers (DOED, 2018) based on the calculated energy. A power purchase agreement (PPA) is signed between the developers and the Nepal Electricity Authority (NEA), the sole buyer of electric energy in the country. The price of electricity depends on the season of the year (dry or wet). It is more for dry season energy than for wet one. If a producer cannot supply a committed amount of electricity to NEA in the dry period of a given year, a penalty is imposed on the producer. The flow variation in the river (daily, monthly, annual) affects the power generation by a power plant affecting the price. The variation besides

affecting power planning for NEA brings in uncertainty for the producers in terms of revenue and the danger of a penalty.

Using equation (1), the change in power (*dP*) generated can be expressed as equation (2). In RoR projects, change in head, *dH* of equation (2) is negligible. Thus, the change in power generation by RoR plants for a given day or month is dependent on the change in the flow (*dQ*) of the river entering into the system as given by equation (3).

$$dP = \eta\gamma[QdH + HdQ] \quad (2)$$

$$dP = \eta\gamma HdQ \quad (3)$$

Possible case of flow and implication of flow variation in RoR project

The flow in a river at a particular month can be divided into 6 types with respect to the long-term mean monthly (Q_{LTMA}) and design flows (Q_{design}) as given in Table 1. These flows are clustered into two cases. Case 1 can be taken as a flow in the wet season (June-November) in which Q_{LTMA} is, generally, higher than the design discharge. Case 2 resembles dry season (December -May) flow in which season Q_{LTMA} is generally lower than Q_{design}. The flow at a particular day can be higher or lower than both Q_{design} and Q_{LTMA} or in between them. Such deviation of flow ($\pm dQ$)) from Q_{LTMA} can be advantageous, disadvantageous or neutral for the project as shown in Table 1.

Daily flow data at Arughat gauging station (#445) from January 1, 1964 to December 31, 2015 were collected from the Department of Hydrology and Meteorology (DHM) of Nepal (DHM, 2018). An exceptionally high flood of July 5, 1968 washed away the gauging station (Shankar, 1969), and DHM could not collect the data for the remaining days of that year. The flow data of 1968 was, therefore, not included in the analysis. The methodology followed to assess the impact of flow variation on power production is as follows:

Table 1. The implication of flow variation for a run of the river power plant

Case/Flow	Condition	Loss/gain amount inflow (***dQ***)	Power loss or gain to design value	Remarks Spill: resource loss
Case 1: Q1-1	$Q > Q_{LTMA}$ & $Q > Q_{design}$	0	No	Water Spill ($Q - Q_{design}$)
Case 1: Q1-2	$Q < Q_{LTMA}$ & $Q > Q_{design}$	0	No	Water Spill ($Q - Q_{design}$)
Case 1: Q1-3	$Q < Q_{LTMA}$ & $Q < Q_{design}$	$Q-Q_{design}$	Loss (-)	No Spill
Case 2: Q2-1	$Q > Q_{LTMA}$ & $Q > Q_{design}$	$Q_{design}-Q_{LTMA}$	Gain (+)	Water Spill ($Q - Q_{design}$)
Case 2: Q2-2	$Q > Q_{LTMA}$ & $Q < Q_{design}$	$Q-Q_{LTMA}$	Gain (+)	No Spill
Case 2: 2-3	$Q < Q_{LTMA}$ & $Q < Q_{design}$	$Q-Q_{LTMA}$	Loss (-)	No Spill

Annual and monthly flow estimation: The annual average flow, monthly average flow for each year, and long-term monthly flows were calculated from daily data.

Seasonal flow estimation: Average flows for the monsoon season (June-September), post-monsoon season (October and November), winter season (December-February), Pre-monsoon season (March-May) flows, and dry season (December-May) and wet season (June-November) flows for each year from monthly flows were calculated.

Design discharge estimation: Three design discharges viz. Q_{90}, Q_{60}, and Q_{40} were estimated from the flow duration curve.

Estimation of change in available flow (dQ) for power production: Based on long-term mean monthly flow (Q_{LTMA}) and design flows (Q_x) as discussed in the theoretical section, the change in available flow for power production in a particular month was calculated.

Estimation of change in power production (dP): Change in power production for each month was calculated using equation (3).

RESULTS AND DISCUSSION

Annual flow characteristics

Annual average, an average of the upper 20 % and lower 20 % of the flows, and their mean values are plotted in Fig. 2 to examine if there is any trend in those flows. A few ups and downs can, noticeably, be seen in an interval of certain years, mainly on high and average flow. However, they were found decreasing since 2000 for about 15 years.

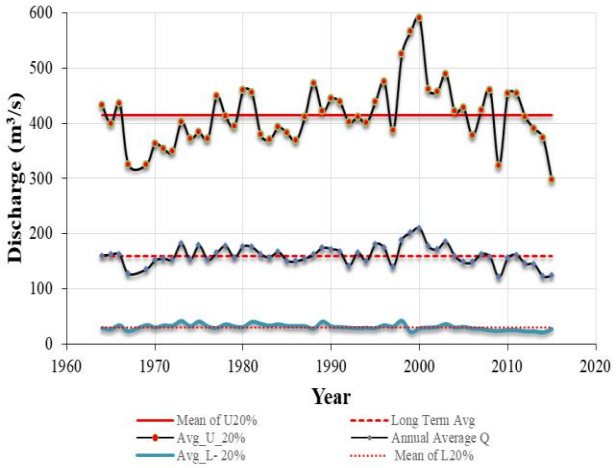

Fig. 2. Annual average, mean of upper 20 % and lower 20 % flow at Arughat

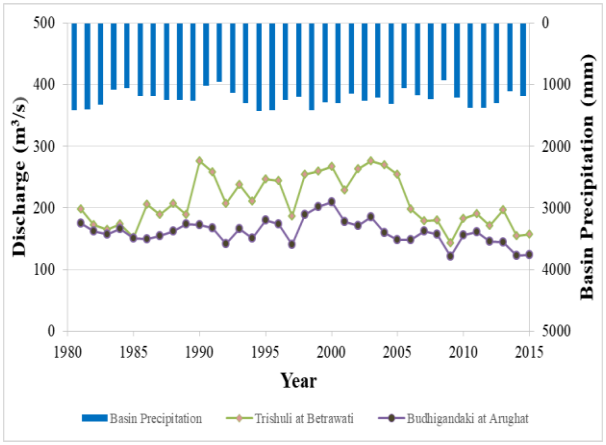

Fig. 3. Comparison of annual average flow at Arughat with the rainfall and flow at nearby Gauging station, Betrawati

To cross-check if the observed flow data of this period at Arughat are correct, the annual average flow of this station was plotted along with annual total rainfall at Arughat rain-gauge station and annual average flow observed at nearby gauging station (Betrawati of Trishuli river) in Fig. 3. Similar variability and decreasing trend after the year 2000 both inflows and rainfall can be seen in this figure. It depicts that the observed flow data used in the analysis can be safely said to be reliable and the decrease in flow after 2000 is mainly attributed to rainfall decrease in this period. However, it is too early to say that the flow at Arughat station has started to decrease as a result of climate change.

Long term average of annual, upper 20 %, and lower 20 % flows are given in Table 2. It shows that the long-term average flow at Arughat was 160 m^3/s with an annual variation between 121 and 210 m^3/s. Similarly, long-term averages of the highest 20 % and lowest 20 % flows were respectively 416 and 31 m^3/s. Data showed that the annual variation was more in higher flows (298-591 m^3/s) and less for low flows (21-42 m^3/s). The fractional difference between upper 20 % and lower 20 % flows is about 14 for the study period. However, in some years this fractional difference was quite above 20 (26 in 1999 and 21 in 2000). It showed a great variation between high and low flows that occur in this river.

Table 2. Flow characteristics of Budhigandaki River at Arughat

Particulars	No. of data	Average flow (m^3/s)	Standard deviation (m^3/s)	Minimum flow (m^3/s)	Maximum flow (m^3/s)
Annual flow	51	160	18	121	210
Monthly flow	612	160	148	20	597
Daily flow	18,627	160	157	18	1,457
Upper 20 %	51	416	57	298	591
Lower 20 %	51	31	5	21	42

Daily and monthly flow characteristics

Data presented in Table 2 show that the observed daily flow varied from 18 m^3/s to 1,457 m^3/s whereas monthly averages vary from 20 to 597 m^3/s in the study period (1964-2015). It shows that the fractional difference between maximum to minimum of daily and monthly flows were 80 and 30 respectively. A higher fractional difference of maximum to minimum flow with decreasing period reveals the need for a storage facility in this river to utilize its water to the maximum extent possible, in the present case for hydropower generation. At the same time, it indicates high uncertainty on the availability of water for the run of the river schemes proposed in this basin.

Seasonal variation

In Nepal southwest monsoon becomes active from June to September when rainfall is heavy. The river flow is, consequently, high during these months (monsoon season). In the next two months, October and November (post-monsoon season), the flow is less than monsoon season but substantially high. The months of December, January, and February are called the winter season in which river flow is low. During the remaining three

months (March, April, and May) called pre-monsoon season temperature starts to rise and the snow starts to melt. The flow in Nepalese rivers during monsoon and post-monsoon (considered wet) seasons is high and enough to meet various needs including hydropower generation.

The remaining two seasons categorized as dry season (NEA, 2019) flow in the rivers is not sufficient to meet the required water demand, for hydropower generation. The long-term average, minimum and maximum flows calculated for these seasons at the Arughat Gauging station are depicted in Fig. 4. The flow during monsoon, post-monsoon, winter, and pre-monsoon seasons were respectively 72 %, 12 %, 6 %, and 10 % of the total annual flow. These figures show the six months of the dry season has only 16 % of the annual total whereas the wet season has as high as 84 % of the total flow. The fractional difference between seasonal maximum to minimum flows lies between 2 and 3 (Fig. 4).

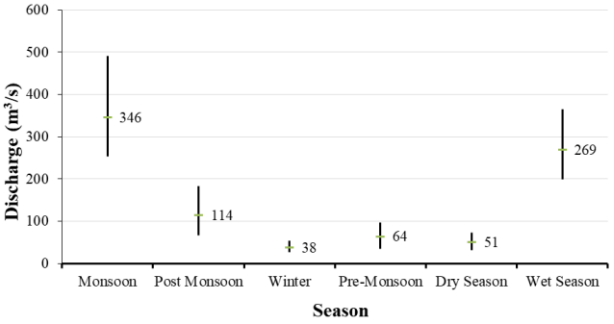

Fig. 4. Seasonal variation of flow at Arughat station

Monthly variation

Month-wise long-term average flows and their variation are given in Table 3. In hydropower projects, these long-term monthly average flows are used to calculate the energy generation for the RoR plants. We can see from Table 3 that the highest value of long-term monthly average flow occurs in August (436 m^3/s) and the lowest (30 m^3/s) in February.

The intra-month variation in those 51 years' data is high, i.e., more than three times in four months (April, May, June, and October) and not that much high (less than two) in August while in other months it is in between 2 and 3. The number of months in which flow was greater than the long-term average is also given in Table 3. Except for February, in all other months, these numbers were less than 50 %. In some months (April, September, and October) it was around 40-45 %. It means there is a high probability of having less energy generation than the calculated ones based on long-term monthly average flows. The consequence has a revenue implication for the project. It clearly shows that the chances of penalty to be paid by the developers are more likely as stipulated in NEA (NEA, 2017). To be fair to developers, this issue of uncertainty needs to be considered while devising PPA.

Table 3. Long term monthly flow at Arughat

Month	Data No.	Average flow (m^3/s)	Stdev (m^3/s)	Min flow (m^3/s)	Max flow (m^3/s)	No. of months with $Q > Q_{avg}$
Jan	51	35.1	5.4	23.9	48.3	25
Feb	51	**29.9**	4.8	21.2	43.0	24
Mar	51	34.4	7.3	20.2	53.2	26
Apr	51	56.2	14.9	27.2	96.7	22
May	51	101.6	30.1	50.0	189.3	25
Jun	51	221.8	54.3	111.8	390.0	24
Jul	51	408.6	58.6	290.6	570.1	24
Aug	51	**436.2**	65.3	330.2	597.2	25
Sep	51	313.6	58.4	207.9	459.8	20
Oct	51	150.0	34.8	85.8	257.8	22
Nov	51	76.8	16.7	47.5	114.3	23
Dec	51	47.7	8.7	30.7	74.3	25

Design flows

The Run of the River Power Plants can be designed for any design flow. However, it is, generally, designed for Q_{40} (40 % of the days in a year, the flow in the river is more than the design flow value) in Nepal (DOED, 2018). Flow duration curve (FDC) constructed from historical daily flow data is utilized to estimate the design flow which is given in Fig. 5 for the Arughat station. The analysis shows that the Q_{10}, Q_{40}, Q_{50}, Q_{60}, and Q_{90} for Arughat were 413, 125, 84, 59, and 30 m^3/s, respectively.

However, values of Q_{40} (design flow for RoR), Q_{60} (an intermediate value), and Q_{90} (sustained flow) were used to see the impact of flow variation on power generation hereunder.

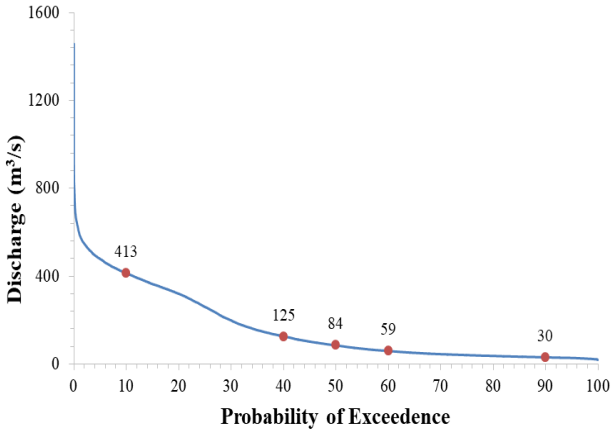

Fig. 5. Flow duration curve of Arughat Gauging site

Impact of flow variation

As stated above, energy calculation of the power plant was made, and PPA was done with NEA by power producer based on the long-term monthly average flows (Q_{LTMA}) and the designed flow (Qx where x represents probability of exceedance of flow, i.e., flow equal or greater the x percentage of days of the year). However, inter-annual variation in daily flow in a particular month can be more than the considered Q_{LTMA} in some years and less in other years. If the flow on a particular day is more than the design flow, it will spill. On the other hand, if it is less than the design flow, less power will be produced. The PPA rate was different for two seasons, i.e., Rs 8.40 and 4.50 per KWh for the dry season and wet season respectively for RoR Project (NEA, 2019). The impact assessment for RoR plants was, therefore, made separately for the dry and wet seasons. Three design flows were considered in the analysis: Q_{90} (sustained flow), Q_{60} (intermediate value), and Q_{40} (popular design Q for power plants).

Impact of flow variation on RoR projects

The long-term averages of loss/gain inflow for both dry and wet seasons for three design flows (Q_{90}, Q_{60}, and Q_{40}) are given in Fig. 6. They were respectively -0.72, -1.76, and -1.54 m^3/s for the dry season, and 0.0, -0.27, and -2.26 m^3/s for the wet season based on daily flow analysis. These results show that the impact of flow variation was found to be negative, i.e., there will be less flow available for power generation in RoR projects in all cases except in the wet season for the Q_{90} scenario where there is neither loss nor gain. This result unveiled the necessity of energy calculation based on daily flow while assessing the full extent of uncertainty in energy generation by a RoR project.

Since Q_{90} flow is quite small (30.1 m^3/s) and all daily flows of the wet season exceed this value, no loss situation occured for this case. In other cases, daily flows were either more than both Q_x and Q_{LTMA} of the considered month or less than these flows or in between these two values. It has resulted in either flow gains in some years and lost in other years with a net loss inflow. In Fig. 6, the range in which the variation in loss or gain inflow values for these cases occurs is also shown. From this figure, we can see that the extent is more on the losing side than on the gain side in all cases. The range is becoming wider for higher Q_x. Although long-term average loss is small, uncertainty increases with the increase in Q_x. For example, the loss in flow for Q_{90} in one year reaches -4.37 but for Q_{40} it is -18.93 m^3/s while the gains for these scenarios are 0.02 and 16.0 m^3/s, respectively, for Q_{90} and Q_{40}. This is happening in the dry season. Similarly, the extent of gain and loss of flow in wet seasons for design discharge as Q_{40} were respectively 12.5 and 5.6 m^3/s.

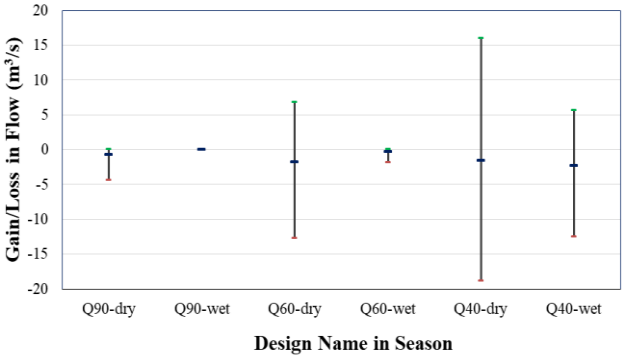

Fig. 6. Long term average loss of flow due to flow variation in the river, Q_x-dry: considered design flow is Q_x and season is dry, $Q_x$wet: considered design flow is Q_x and season is wet (x: 90, 60, 40)

Out of 51 years, the number of years in which the flow less than the anticipated values (Q_{LTMA} for dry season and Q_{design} for wet season) is depicted in Fig. 7. From the figure, we can see that the number of years in which the flow is less than 50% in all cases except the Q_{90}-wet season. The numbers of years in which both wet and dry seasons lose the flow were respectively 27 and 24 for Q_{60} and Q_{40}. The above figures clearly show that the current basis of PPA is not in the favor of the energy producer as the probability of losing years is more likely than gaining years. As per (DOED, 2020) the application for survey and construction licenses is more than 15,000 MW and 7,000 MW respectively. Even now the production of hydropower by private developers is almost 10% more than that of the government (NEA, 2020). If the private developers are not getting a profit, their contribution to the hydropower sector will go down and the aspiration of the Government of Nepal of developing hydropower will be jeopardized.

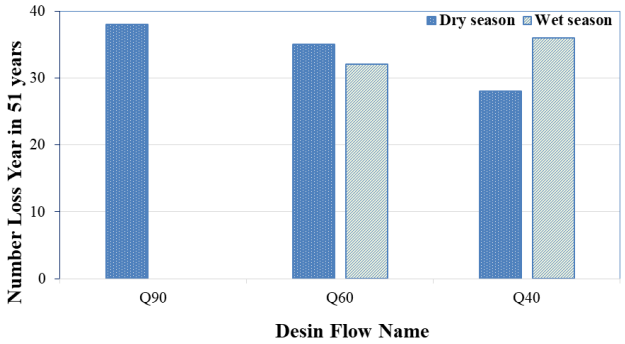

Fig. 7. Number of loss years in different scenarios, Q_x: considered design flow is Q_x (x: 90, 60, 40)

Impact of flow variation on power production of RoR projects

As per equation (3), the gain or loss of flow due to flow variation in a river has a direct impact on power generation i.e., y % reduction or augmentation inflow results in the y % loss or gain in power generation in RoR projects. During the dry season the daily flow in the river governs the power generation as it is generally less than design discharge, and in wet season design discharge governs power generation as it is less than the daily flow. The flow was less than the anticipated long-term monthly flow by 1.54 m^3/s (~3 %) for the dry season while it was 2.26 m^3/s (~ 2 %) for design flow for the wet season. It implies that the expected value of the dry season power loss is about 3 % and 2 % for the RoR projects proposed in the Budhigandaki basin. However, the annual variation in power production is quite high. The graph shows that the probability of losing and gaining power generation in a year are respectively 40 % and 30 % in the dry season (Fig. 8). Similarly, the probability of losing and gaining in power generation was about 10 % and 5 % respectively in the wet season.

Fig. 8 also depicts that there is a probability of producing less power than the estimated one for 11 consecutive years (> 20 %) in the dry season and 27 consecutive years (>50 %) for the wet season. It is noted here that the production will be less than the estimated for 11 consecutive years in both seasons. It indicates that the revenue generated by the developers of RoR projects in the Budhigandaki basin is likely to be less than the calculated one. The flow characteristics of other rivers of Nepal are also somewhat similar to that of the Bhudhigandaki River if we look at the data of DHM (2018). It implies that the private power producer is more likely to suffer if the current system of analysis continues.

Electricity helps to increase the productivity of all three major sectors of productions (agriculture, industry, and service sectors). It enhances the quality of education, health services and access to information, etc. (Satpathy, 2015) Economic development of a country was, thus, positively and strongly correlated with access to electricity and its consumption (Aslan, 2014; Kamaludin, 2013; Stern *et al.*, 2019). Hydropower is a clean, renewable, and environmentally friendly source of energy that helps to reduce greenhouse gas production and consequent climate change. The CO_2 emissions per GWh are 3-4 tonnes for run-of-the-river hydropower, and 10-33 tonnes for hydropower with a reservoir (WEC, 2004). These values are about 100 times less than the emissions from traditional thermal power (Berga, 2016).

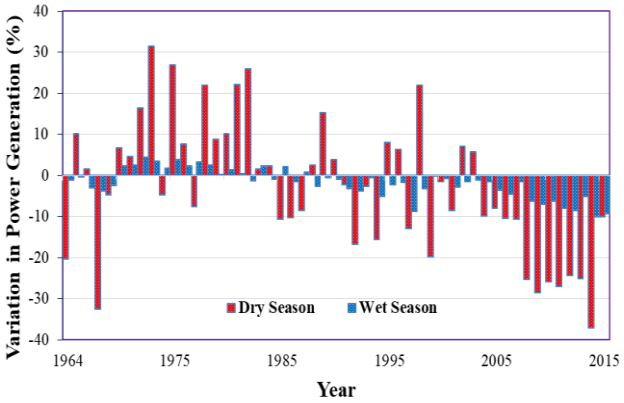

Fig. 8. Impact of flow loss/gain in power production from RoR plants in Budhigandaki basin

The demand for LPG gas is rapidly increasing as an alternative option for kerosene in the urban area and firewood in the rural area of Nepal. However, the high import of LPG is challenging for the sustainability and energy security of the country. In the Medium Growth Scenario, substituting LPG with electricity could save the country from $21.8 million (2016) to $70.8 million (2035) each year (Bhandari & Pandit, 2018). It all shows that Nepal should prioritize hydropower development for its prosperity as envisioned in its constitution (GoN, 2015) and private power producers are to be encouraged in this national endeavor. The analysis of this study found that the inter-annual flow variation issue should be dealt with rationally not to discourage RoR hydropower development in Nepal.

CONCLUSIONS

The long-term annual average flow at Arughat is 160 m^3/s. However, it varied from 120 to 210 m^3/s in the study period. The flow at this gauging station during monsoon, post-monsoon, winter, and pre-monsoon seasons were respectively 72 %, 12 %, 6 %, and 10 % of the total flow. It implies that the dry season has only 16 % whereas the wet season has as high as 84 % of the total flow. The fractional difference of upper 20 % to lower 20 % flows amounted to 14. The relatively high ratio and long-term monthly average flow ranging from 30 m^3/s in February to 436 m^3/s in August show high inter and intra annual variation in Budhigandaki River flow.

This study found that the flow was less than the anticipated long-term monthly flow by 1.54 m^3/s (~3 %) for the dry season while it was 2.26 m^3/s (~ 2 %) with respect to design flow for the wet season. In other words, the expected value of the dry season power loss was about 3 % and 2 % for the RoR projects proposed in the Budhigandaki River basin. Nevertheless, these figures are not so high; the probability of less production of power in a year may go up to 40 % for the dry season and 10 % in the wet season. Further, there is a probability of producing less power than the estimated one for 11 consecutive years (> 20 %) in the dry season and 27 consecutive years (> 50 %) for the wet season. The flow characteristics of other rivers of Nepal are also somewhat similar to that of the Bhudhigandaki River. This study concludes that uncertainty arising from daily flow variation should be assessed while estimating energy generation in hydropower projects, and it should be reflected in the power purchase agreement.

REFERENCES

Akhtar, M., Ahmad, N., & Booij, M. J. (2008). The impact of climate change on the water resources of the Hindukush–Karakorum–Himalaya region under different glacier coverage scenarios. *Journal of Hydrology*, *355*(1-4), 148-163.

Alam, F., Alam, Q., Reza, S., Khurshid-ul-Alam, S. M., Saleque, K., & Chowdhury, H. (2017). A review of hydropower projects in Nepal. *Energy Procedia*, *110*, 581-585.

Aslan, A. (2014). Causality between electricity consumption and economic growth in Turkey: An ARDL bounds testing approach. *Energy Sources, Part B: Economics, Planning, and Policy*, *9*(1), 25-31.

Bayar, Y., & Özel, H. A. (2014). Electricity consumption and economic growth in emerging economies. *Journal of Knowledge Management, Economics and Information Technology*, *4*(2), 1-18.

Berga, L. (2016). The role of hydropower in climate change mitigation and adaptation: a review. *Engineering*, *2*(3), 313-318.

BGHEP. (2015). *Feasibility study and detailed design of Budhigandaki hydropower project part 1*. Budhigandaki Hydroelectric Project Development Committee, Government of Nepal, Kathmandu, Nepal.

Bhandari, R., & Pandit, S. (2018). Electricity as cooking means in Nepal− a modelling tool approach. *Sustainability*, *10*(8), 2841. https://doi.org/10.3390/su10082841

Devkota, L. (2020). Development of water resources in Nepal: Conditions and dimensions of utilization [Nepali]. *Smarika*, 15-23.

Devkota, L. P., & Gyawali, D. R. (2015). Impacts of climate change on hydrological regime and water resources management of the Koshi River Basin, Nepal. *Journal of Hydrology: Regional Studies*, *4*, 502-515.

DHM. (2018). *Streamflow summary (1962-2015)*. Department of Hydrology and Meteorology, Government of Nepal, Kathmandu, Nepal.

Dixit, A. (2002). *Basic water science* (1st ed.). Nepal Water Conservation Foundation.

DOED. (2018). *Guidelines for study of hydropower projects*. Water Resources and Irrigation, Department of Electricity Development. Retrieved from http://www.doed.gov.np

DOED. (2020). *Design Guidelines for Headworks of Hydropower Projects*. Department of Electricity Development, Ministry of Energy, Water Resource and Irrigation, Government of Nepal, Kathmandu.

GoN. (2015). *Constitution of Nepal*. Government of Nepal, Kathmandu. Retrieved from http://www.moljpa.gov.np/wp-content/uploads/2017/11/Constitution-of-Nepal-_English_-with-1st-Amendment_2.pdf

Hirsh, R. F., & Koomey, J. G. (2015). Electricity consumption and economic growth: a new relationship with significant consequences? *The Electricity Journal*, *28*(9), 72-84.

Kamaludin, M. (2013). Electricity consumption in developing countries. *Asian Journal of Research in Social Sciences and Humanities*, *2*(2), 84-90.

Liu, X., Tang, Q., Voisin, N., & Cui, H. (2016). Projected impacts of climate change on hydropower potential in China. *Hydrology and Earth System Sciences*, *20*(8), 3343-3359.

Lorde, T., Waithe, K., & Francis, B. (2010). The importance of electrical energy for economic growth in Barbados. *Energy Economics*, *32*(6), 1411-1420.

Marahatta, S., Devkota, L., & Aryal, D. (2021). *Hydrological Modeling : A Better Alternative to Empirical Methods for Monthly Flow Estimation in Ungauged Basins*. 254-270. https://doi.org/10.4236/jwarp.2021.133015

Miller, J. D., Immerzeel, W. W., & Rees, G. (2012). Climate change impacts on glacier hydrology and river discharge in the Hindu Kush–Himalayas. *Mountain Research and Development*, *32*(4), 461-467.

Molden, D. J., Shrestha, A. B., Nepal, S., & Immerzeel, W. W. (2016). Downstream implications of climate change in the Himalayas. *Water Security, Climate Change and Sustainable Development* (pp. 65-82).

MoWR. (2009). *Report on 10 years hydropower development plan task force -2009* [Nepali]. Ministry of Water Resources, Government of Nepal, Kathmandu. Retrieved from https://moewri.gov.np/storage/listies/May2020/taskforce-report-parti.pdf

MoWR. (2010). *Report on 10 years hydropower development plan task force -2010* [Nepali]. Retrieved from https://moewri.gov.np/storage/listies/May2020/twenty-year-task-force-report-merged.pdf

NEA. (2017). *The Power Purchase Rates and Associated Rules for PPA of RoR/PRoR/Storage Project Effective from April 27, 2017*.

NEA. (2019). *Annual report of Nepal Electricity Authority*. Nepal Electricity Authority. Retrieved from Nepal Electricity Authority website: https://www.nea.org.np/annual_report

NEA. (2020). *Annual report of Nepal Electricity Authority*. Nepal Electricity Authority. Retrieved from Nepal Electricity Authority website: https://www.nea.org.np/annual_report

NPC. (2020). *The Fifteenth Plan (Fiscal Year 2019/20 - 2023/24)*. National Planning Commission, Government of Nepal, Singha Durbar, Kathmandu.

Ogundipe, A. A., & Apata, A. (2013). Electricity consumption and economic growth in Nigeria. *Journal of Business Management and Applied Economics*, *11*(4). http://eprints.covenantuniversity.edu.ng/id/eprint/1777

Pandey, V. P., Dhaubanjar, S., Bharati, L., & Thapa, B. R. (2020). Spatio-temporal distribution of water availability in Karnali-Mohana Basin, Western Nepal: Hydrological model development using multi-site calibration approach (Part-A). *Journal of Hydrology: Regional Studies*, *29*, 100690. https://doi.org/10.1016/j.ejrh.2020.100690

Pun, S. B. (2017). Reflections on India's guidelines on cross border trade of electricity'vis-a-vis Nepal's electricity development decade 2016/'026'and'2017/'018 budget'. *Hydro Nepal: Journal of Water, Energy & Environment*, *21*, 5-10.

Satpathy, M. (2015). Importance of energy and power sector in economic development an Indian perspective. *International Research Journal of Management Science & Technology*, *6*(8), 41-45.

Shankar, K. (1969). Landslides in Burhi Gandaki LabuBensi. *Journal of Nepal Engineers' Association*, *1* (February).

Stern, D. I., Burke, P. J., & Bruns, S. B. (2019). *The impact of electricity on economic development: a macroeconomic perspective*. UC Berkeley: Center for Effective Global Action. Retrieved from https://escholarship.org/uc/item/7jb0015q

Thapa, G., & Basnett, Y. (2015). Using Hydroelectricity to Power Economic Transformation in Nepal. In *Supporting Economic Transformation: Overseas Development Institute (ODI)*. Retrieved from https://set.odi.org/wp-content/uploads/2015/07/Using-hydroelectricity-to-power-economic-transformation-in-Nepal_19-May-2015.pdf

United Nations. (2020). *The least developed countries report 2020 productive capacities for the new decade*. United Nations.

Upadhyay, S. N., & Gaudel, P. (2018). Water resources development in Nepal: myths and realities. *Hydro Nepal: Journal of Water, Energy, and Environment*, *23*, 22-29.

Viviroli, D., Archer, D. R., Buytaert, W., Fowler, H. J., Greenwood, G. B., Hamlet, A. F., … López-Moreno, J. I. (2011). Climate change and mountain water resources: overview and recommendations for research, management, and policy. *Hydrology and Earth System Sciences*, *15*(2), 471-504.

WEC. (2004). *Comparison of energy systems using life cycle assessment: a special report of the world energy council*. World Energy Council, London, UK.

WECS. (2005). *National water plan*. Water and Energy Commission Secretariat Singha Durbar, Kathmandu.

WECS. (2013). *National energy strategy of Nepal*. Water and Energy Commission Secretariat Singha Durbar, Kathmandu. Retrieved from https://www.wecs.gov.np/storage/listies/October2020/national-energy-strategy-of-nepal-2013.pdf

World Bank. (2020). *Energy use*. Retrieved from https://data.worldbank.org/indicator/EG.USE.PCAP.KG.OE

Zhang, C., Zhou, K., Yang, S., & Shao, Z. (2017). On electricity consumption and economic growth in China. *Renewable and Sustainable Energy Reviews*, *76*, 353-368.

water

MDPI

Article

Application of SWAT in Hydrological Simulation of Complex Mountainous River Basin (Part I: Model Development)

Suresh Marahatta [1,*], Laxmi Prasad Devkota [2,3] and Deepak Aryal [1]

[1] Central Department of Hydrology and Meteorology, Tribhuvan University, Kathmandu 44600, Nepal; deepak.aryal@cdhm.tu.edu.np
[2] Nepal Academy of Science and Technology (NAST), Kathmandu 44600, Nepal; lpdevkota1@gmail.com
[3] Water Modeling Solutions Pvt. Ltd. (WMS), Kathmandu 44600, Nepal
* Correspondence: suresh.marahatta@cdhm.tu.edu.np

Abstract: The soil and water assessment tool (SWAT) hydrological model has been used extensively by the scientific community to simulate varying hydro-climatic conditions and geo-physical environment. This study used SWAT to characterize the rainfall-runoff behaviour of a complex mountainous basin, the Budhigandaki River Basin (BRB), in central Nepal. The specific objectives of this research were to: (i) assess the applicability of SWAT model in data scarce and complex mountainous river basin using well-established performance indicators; and (ii) generate spatially distributed flows and evaluate the water balance at the sub-basin level. The BRB was discretised into 16 sub-basins and 344 hydrological response units (HRUs) and calibration and validation was carried out at Arughat using daily flow data of 20 years and 10 years, respectively. Moreover, this study carried out additional validation at three supplementary points at which the study team collected primary river flow data. Four statistical indicators: Nash–Sutcliffe efficiency (NSE), percent bias (PBIAS), ratio of the root mean square error to the standard deviation of measured data (RSR) and Kling Gupta efficiency (KGE) have been used for the model evaluation. Calibration and validation results rank the model performance as "very good". This study estimated the mean annual flow at BRB outlet to be 240 m^3/s and annual precipitation 1528 mm with distinct seasonal variability. Snowmelt contributes 20% of the total flow at the basin outlet during the pre-monsoon and 8% in the post monsoon period. The 90%, 40% and 10% exceedance flows were calculated to be 39, 126 and 453 m^3/s respectively. This study provides additional evidence to the SWAT diaspora of its applicability to simulate the rainfall-runoff characteristics of such a complex mountainous catchment. The findings will be useful for hydrologists and planners in general to utilize the available water rationally in the times to come and particularly, to harness the hydroelectric potential of the basin.

Keywords: hydrological simulation; SWAT; water balance; complex mountain; Budhigandaki

Citation: Marahatta, S.; Devkota, L.P.; Aryal, D. Application of SWAT in Hydrological Simulation of Complex Mountainous River Basin (Part I: Model Development). *Water* **2021**, *13*, 1546. https://doi.org/10.3390/w13111546

Academic Editor: Raghavan Srinivasan

Received: 8 April 2021
Accepted: 24 May 2021
Published: 31 May 2021

1. Introduction

Complex interactions between the atmospheric system and the underlying topography determine river discharge. It is a part of rainfall that appears in a stream and represents the total response of a basin. Surface flow, subsurface flow, base flow and precipitation that directly falls on the stream constitutes the total discharge in the river [1,2]. Time series of flow data is one of the most important requirements for planning, operation and control of all water resources projects [3–5]. However, measured flow data are not available in most of the cases in such project sites [5]. It is because of the lack of sufficient flow gauging stations in most river basins. The situation is more severe in mountainous basins [6] because of the inaccessibility of most of these sites for local observations. It is the reason why water budget analyses in such basins are not as easy as in other gauged basins [7,8]. However, most of the large rivers (e.g., the Ganga, the Indus, the Sutlej, the Brahmaputra, the Mekong, the Yellow) in the world originate from the mountains and are

perennial in nature as they are constantly fed by snow and glaciers. Mountain basins might have, thus, been considered as the water towers of the world [7,9].

The characteristics of the river basins are usually controlled by the geo-physical environment and hydro-climatic conditions [10]. In central Himalaya, high relief with steep topography along with tectonic activities, climate-driven erosional process and high sediment yield, among many other factors, make the basins complex [11]. Precipitation in Nepalese mountainous river basins, including the Budhigandaki River Basin (BRB), are mostly influenced by orography, aspect and physiography, with more amount of precipitation in the windward side than in leeward side [12–18]. The challenge is further exacerbated due to limited data availability in these regions because of difficult access.

To address the challenge of non-availability of observed data at local level for water resources planning and utilization in the river basin, hydrologic simulation method has been widely used in recent years [19–23]. Simulation models provide excellent platforms for evaluating various options for water resources as well as environmental planning [24,25]. In hydrological simulation, a hydrologic model which is a simplified software representation of the hydrological process within a basin boundary, is used to generate the flow at required locations of the river basin.

Based on spatial discretization, three types of model are in practice: lumped, semi-distributed and fully-distributed. For example, Hydrologiska Byråns Vattenbalansavdelning (HBV), GR4J (Génie Rural à four paramètres Journalier), hydrological model (HYMOD), artificial neural network (ANN) based data-driven hydrological models, simplified version of the HYDROLOG (SIMHYD), Snowmelt Runoff Model (SRM) and TANK are lumped models while the Soil and Water Assessment Tool (SWAT), topographic hydrologic model (TOPMODEL), Variable Infiltration Capacity (VIC) and Hydrologic Engineering Center—Hydrologic Modeling System (HEC-HMS), are semi distributed ones. Variant of Système Hydrologique Européen (MIKE SHE) and Visualizing Ecosystem Land Management Assessments (VELMA) are fully distributed models [25–28]. These are either event-based (e.g., Runoff Analysis and Fow Training, RAFT) or continuous (e.g., MIKE SHE, SWAT) flow generating models [29,30].

The SWAT model [30,31] has been chosen among many hydrological models for this study. Several studies have been carried out to assess the water availability and impacts of climate change; land use and land cover changes around the world using SWAT model [21,32–34]. Studies in the Nile Basin by Griensven et al. [35], Itapemirim River basin (Brazil) by Fukunaga et al. [36], Ganga Basin by Anand et al. [37], and Mekong Basin by Tang et al. [38] are some of them. Details on the use of SWAT for various purposes can be found in [39]. Shrestha et al. [40] has evaluated the hydrological responses of SWAT models for 11 basins in two contrasting climatic regions (Himalayan and Tropical) of Asia. Their result reveals that SWAT is a suitable tool for modelling hydrological responses in both regions including four snow-fed basins of Nepal. SWAT model has successfully been used in other Nepalese catchments too; Koshi [27,41] Narayani [42], West Rapti [43] and Karnali [25,44–46]. There are a number of similar studies that used SWAT model in other river basins of Nepal to assess the river hydrology and the impact of climate change [47] in Kaligandaki basin; [48,49] in Bagmati basin; [50] in Karnali basin; [51] in Tamor basin, and [52] in Koshi basin. SWAT being a freely available public domain hydrological model capable of simulating complex hydrological processes might have made it popular for hydrological simulation around the world.

The Budhigandaki River Basin (BRB) was selected for this study. Altitudinal variation in precipitation pattern is remarkable in this basin [53–55] including Tibet. Furthermore, precipitation is quite high (>75% of the total) during the monsoon season (June–September) as compared to other months of the year [56,57]. The main objective of this study is to apply SWAT model to simulate the river hydrology of BRB. The specific objectives are to: (i) assess the applicability of SWAT model in data scarce and complex mountainous river basin using well-established performance indicators; and (ii) generate spatially distributed flows and evaluate the water balance at the sub-basin level. Further, the model was used to

assess the impact of climate change in the hydrology of the basin (Part II—accompanied paper).

2. Materials and Methods

2.1. Study Area

The BRB is a transboundary river basin of which about one-fourth of the basin area lies in Tibetan plateau of People's Republic of China and the remaining part lies in Federal Democratic Republic of Nepal (Figure 1). The basin area at the confluence of Trishuli River is 4988 km^2, with an average elevation of 3723 masl (range: 315 m–8163 m). Physiographically, the basin falls in the Middle Mountains and the Himalayas. It is noted here that Mount Manaslu, the eighth highest peak in the world, is situated in this basin [58]. Long-term annual rainfall of the BRB is 1495 mm with an extremely high spatial variability within the basin. Rainfall intensities vary throughout the basin with maximum intensity occurring on the south facing slopes of the mountains. The station Arughat receives an annual precipitation of greater than 2500 mm while the Tibetan part of the basin receives less than 700 mm [57,59]. The mean annual flow of the Budhigandaki river near the Budhigandaki Hydroelectric Project (BGHEP) dam site is estimated at 222 m^3/s [53]. The temperature varies from −2.0 °C in winter to 33.0 °C in summer in the study basin [60].

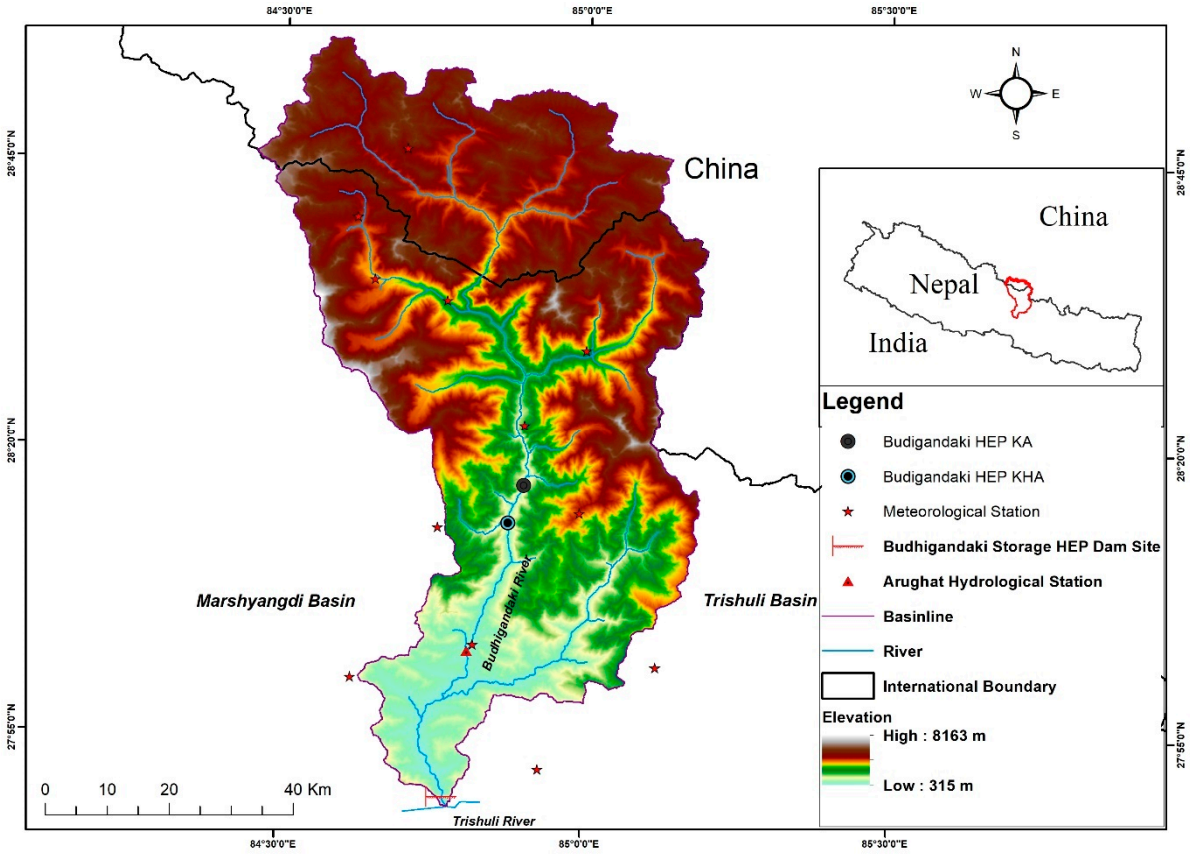

Figure 1. Location map of the Budhigandki River Basin.

2.2. Data Used

The hydro-meteorological data that has been used for the SWAT model in this study are precipitation, minimum and maximum air temperature. Besides, Digital Elevation Model (DEM), land use and soil map data are the spatial data required (Table 1).

Table 1. Sources of Data.

Data	Data Source
River flow	[53,61–63]
Precipitation and temperature	Nepal- Department of Hydrology and Meteorology (DHM), Tibet—[64] https://data.tpdc.ac.cn/, assessed on 24 July 2020
Digital elevation model (DEM)-30 m resolution	Shuttle Radar Topography Mission (SRTM) (www.earthexplorer.usgs.gov, accessed on 25 July 2020)
Soil	SOTER (2019) for Tibet (http://www.isric.org/data/data-download, assessed on 24 July 2020) Nepal—[65]
Land use	[65,66]

2.2.1. Meteorological Data

Meteorological data from eight stations in and around the study basin (1981–2015) were used as input to the model (Figure 1). Two stations have both observed precipitation and temperature data while the remaining six stations have only precipitation data. Gridded data of precipitation and temperature for the Tibet part of the basin was also used in the study. Quality checking of the data was done through various methods: homogeneity test, outliers checking, inter parameter consistency checking, spatial checking and double mass curve analysis. The average areal precipitation over the catchment was calculated by the Thiessen polygon method [67] using geographic information system (GIS).

2.2.2. Flow Data

Long term daily flow data (1983–2012) of Budhigandaki river at Arughat gauging station has been used for calibration and validation of the model. Similarly, short term flow data available at the damsite of the proposed Budhigandaki Storage Hydropower Project (2013–2014) lying downstream of the Arughat station and headwork sites of two proposed run of the river hydropower projects, viz., Budhigandaki KA and KHA (2009) lying upstream of Arughat (Figure 1) were also used for additional validation of the model.

2.2.3. Spatial Data

Shuttle Radar Topography Mission (SRTM; 1 arc second horizontal resolution) DEM was used to delineate the river network and sub-basins. Landuse and land cover (LULC) data were obtained from [65]. Soil data of the Tibetan part of the basin was taken from Soil Terrain Database Programme (SOTER) which is at 1:1 million scale whereas soil data for Nepal was obtained from [65]. LULC and soil maps of the basin are shown in Figure 2a and b respectively. LULC data was categorized into nine classes while soil data was segregated into 17 classes. BRB is covered by snow and glaciers (SNGL-29%), followed by forest (FORS-23%), barren (BARN-21%), shrub and grassland (SHGR-18%) and agriculture (AGVT, AGST, AGLT-8%). River (RIVR) and residential built-up area (RESI) covers the least portion (~1%) of the total area. It can be seen from Figure 2b that hard rock mass in mountainous terrain (RockRock) covers a significant part (~33%) of the basin while inceptisols with loamy sand texture (IncSand) covers about 21% of the basin area. Gelic leptosols with rocky texture (LpiRock-13%) and gelic leptosols with loamy skeletal texture (LpiSkel-10%) are also found in different parts of BRB. Entisols with sandy texture (EntSand-7%), spodosols with sandy texture (SpoSand-5%), inceptisols with loamy texture (IncLoam-3%), alfisols with loamy texture (AlfLoam-3%) and eutric leptosols with rocky texture (LpeRock-3%) are also found in small patches. Inceptisols with loamy skeletal texture (IncSkel-1%), eutric leptosols with sandy texture (LpeSand-1%), entisols with loamy skeletal texture (EntSkel-0.5%), haplic luvisols with loamy texture (LvhLoam-0.4%), mollisols with sandy texture (MolSand-0.2%), leptosols with loamy texture (LpLoam < 0.1%), leptosols with loamy

skeletal texture (LpmSkel < 0.1%) and entisols with loamy texture (Entloam < 0.1%) are found in traces.

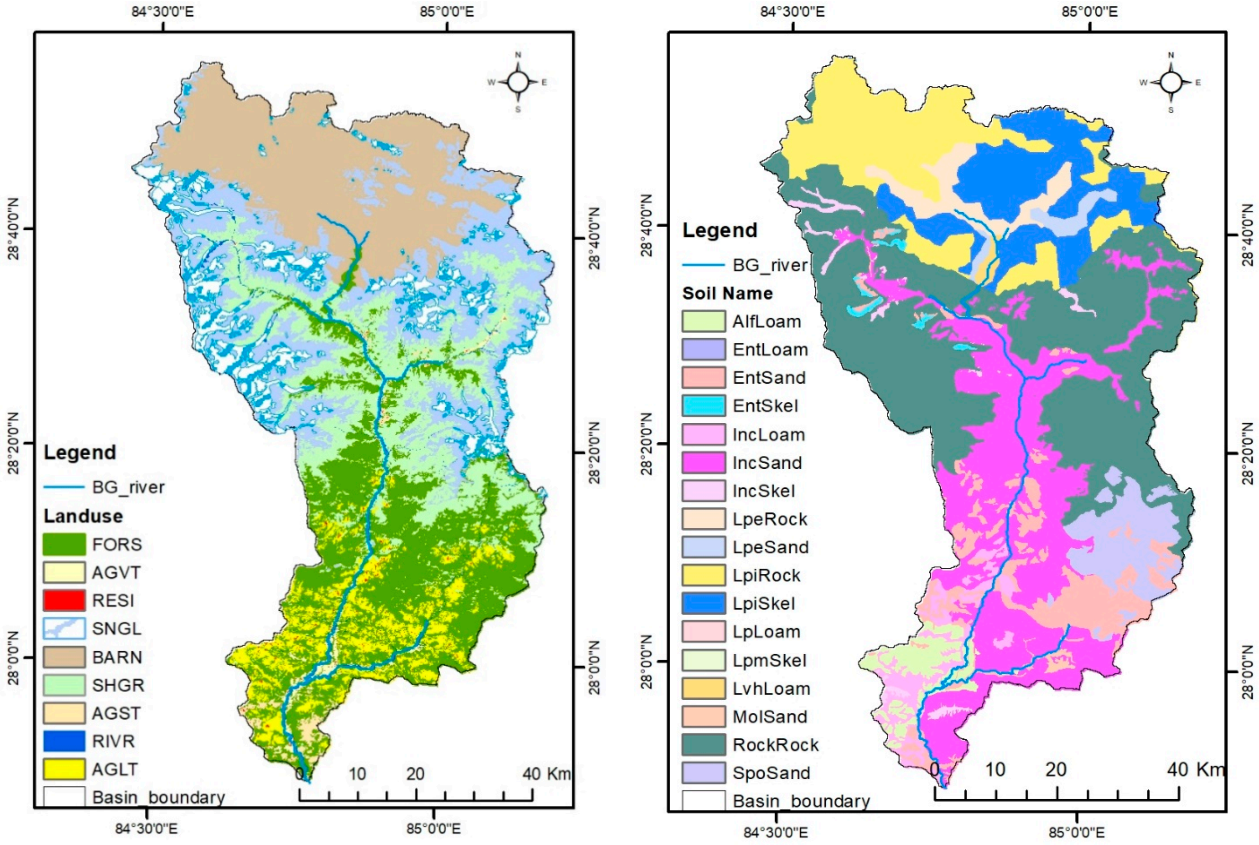

(**a**) (**b**)

Figure 2. (**a**) Landuse and Land Cover, (**b**) Soil Map.

2.3. SWAT Model

The Soil Water Assessment Tool (SWAT model) is a continuous-time, semi-distributed, process-based river basin simulation model operating on a daily or sub-daily time steps [68–70]. The basin is partitioned into a number of subbasins. Each sub-basin is further discretised into a number of hydrologic response units (HRUs), which are unique combinations of soil-landuse-slope exceeding a certain user defined threshold. Processes are simulated at HRU level and aggregated for each sub-basin, which are then routed through the river system using the variable storage or Muskingum method. SWAT facilitates an assortment of parameters defined at HRU, subbasin or basin level. The SWAT model simulates the various hydrological processes occurring in the river basin based on water balance within the basin as given by Equation (1).

$$SW_t = SW_0 + \sum_{i=1}^{t}(R_{day} - Q_{surf} - E_a - W_{seep} - Q_{gw}) \quad (1)$$

where SW_t is the final soil water content (mm), SW_0 is the initial soil water content (mm), t is the time in days, R_{day} is the amount of precipitation on day i (mm), Q_{surf} is the amount of surface runoff on day i (mm), E_a is the amount of evapotranspiration on day i (mm), W_{seep} is the amount of water entering the vadose zone from soil profile on day i (mm), Q_{gw} is the amount of return flow on day i (mm).

SWAT uses the climate data from the station nearest to the centroid of each sub-basin. A given precipitation is classified as solid (snow) and liquid (rainfall) based on a

user-defined threshold value of mean air temperature. Snow melts when the maximum temperature on a given day exceeds the user defined threshold level. In snow covered areas, a fraction of the estimated daily potential evapotranspiration occurs by sublimation. Evaporation from soils and plants is computed separately by the model. Details of the SWAT model can be found in [30,70,71].

2.4. Model Setup and Simulation

The BRB was divided into 16 sub-basins and five slope classes (0–30, 30–50, 50–70, 70–90 and >90 percent). A threshold value of 10% each for land use and land cover, soil (Figure 2) and slopes were used to divide the subbasin into unique 344 HRUs. Further, to account for orographic effects, we generated 500 m range elevation band in each sub basin. The methodological framework for model setup and simulation is given in Figure 3.

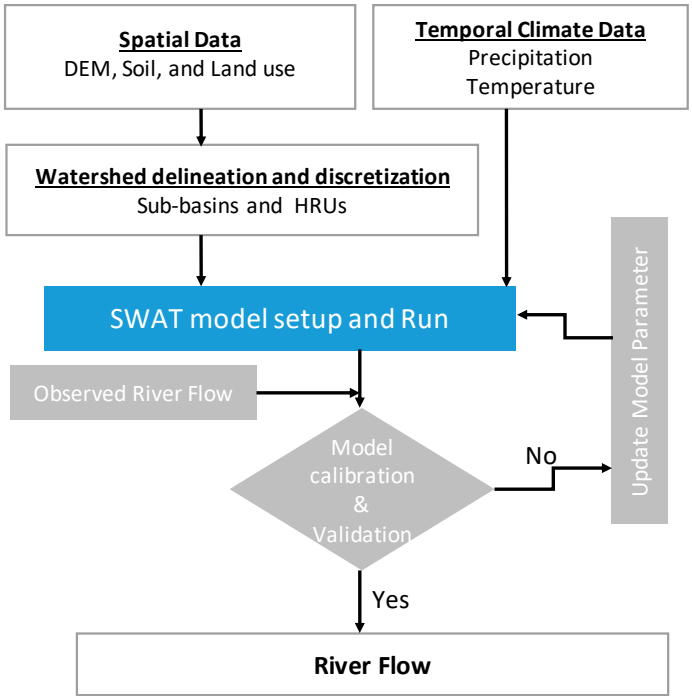

Figure 3. Methodological framework for application of SWAT hydrological model.

Precipitation and temperature data were fed into the model. Having a large number of missing flow data of years 2013 and 2014 at Arughat station and having 30 years [19,72–74] of relatively better data before 2013, observed flow data of Arughat station from 1981–2012 were used in the study. A warm up period (to stabilize the model initially) of 2 years (1981–1982) was excluded from the analysis. The model was calibrated using 20 years (two-thirds) of the study period (1983–2002) and validated using the remaining one-third i.e., 10 years (2003–2012). Based on the modeling experience in Nepalese basins and judgement of the study team, manual method was used for calibrating the model.

Surface runoff was estimated by the SCS curve number (SCS-CN) [75] method. The potential evapotranspiration was computed using Hargreaves method [76]. The computed runoff from each sub-basin was routed through the river network to the main basin outlet by using variable storage method.

Performance Evaluation Criteria

Moriasi et al. [77] has discussed various graphical and statistical model evaluation techniques. Among them, three well-established statistical indicators: Nash–Sutcliffe efficiency (NSE), percent bias (PBIAS), and ratio of the root mean square error to the standard deviation of measured data (RSR) were used in this study for model evaluation [69,77,78].

In addition to these three, Kling Gupta efficiency (KGE) prescribed by [79–82] has also been used for the purpose of evaluation.

Nash–Sutcliffe efficiency (NSE) is a normalized statistic that determines the relative magnitude of the residual variance ("noise") compared to the measured data variance ("information"). NSE indicates how well the plot of observed versus simulated data fits the 1:1 line [83]. NSE is computed using Equation (2):

$$NSE = 1 - \left[\frac{\sum_{i=1}^{12}(Q_{0i} - Q_{ei})^2}{\sum_{i=1}^{12}(Q_{0i} - \overline{Q_o})^2}\right] \quad (2)$$

where, Q_{0i} and Q_{ei} are respectively observed and estimated discharge of day i, $\overline{Q_0}$ is the mean of the observed discharges. The optimum value is 1.0, with higher value indicating better model performance.

Percent bias (PBIAS) measures the average tendency of the simulated data to be larger or smaller than their observed counterparts. The optimal value of PBIAS is 0.0, with low-magnitude values indicating accurate model simulation. Positive values indicate model underestimation bias, and negative values indicate model overestimation bias [77]. PBIAS is, generally, expressed in percentage and is calculated using Equation (3).

$$PBIAS = \frac{\sum_{i=1}^{n} V_o - \sum_{i=1}^{n} V_e}{\sum_{i=1}^{n} V_o}\% \quad (3)$$

where V_o and V_e are respectively the observed and simulated volumes of water for day i.

The root mean square error (RMSE) and the standard deviation of observed flow (σ_o) can be expressed as a ratio (RSR). It is commonly accepted that the lower the RMSE the better the model performance. RSR varies from the optimal value of 0, which indicates zero residual variation and therefore perfect model simulation, to a large positive value that indicates poorer model performance [77]. RSR is calculated using Equation (4).

$$RSR = \frac{RMSE}{\sigma_o} = \frac{\sqrt{\sum (Q_{oi} - Q_{ei})^2}}{\sqrt{\sum (Q_{oi} - \overline{Q}_o)^2}} \quad (4)$$

The Kling–Gupta efficiency (KGE) that incorporates correlation, variability bias and mean bias [80] is increasingly used for model calibration and evaluation. It is expressed using Equation (5).

$$KGE = 1 - \sqrt{(r-1)^2 + \left(\frac{\sigma_e}{\sigma_o} - 1\right)^2 + \left(\frac{\overline{Q_e}}{\overline{Q_o}} - 1\right)^2} \quad (5)$$

where, r is the correlation coefficient between the observed and simulated flows, σ_o and σ_e are standard deviations of observed and simulated flows respectively.

3. Results

3.1. Observed Rainfall-Runoff Characteristics

Long term monthly average precipitation and observed flow (1983–2012) based on Department of Hydrology and Meteorology (DHM) at Arughat gauging station is depicted in Figure 4. The figure shows that the flow closely follows the precipitation pattern of the basin. Long term annual basin precipitation has been calculated as 1301 mm (maximum 278 mm in July and minimum 11 mm in November). Similarly, the long-term average and standard deviation of the monthly flows are 163 m^3/s and 156 m^3/s, respectively.

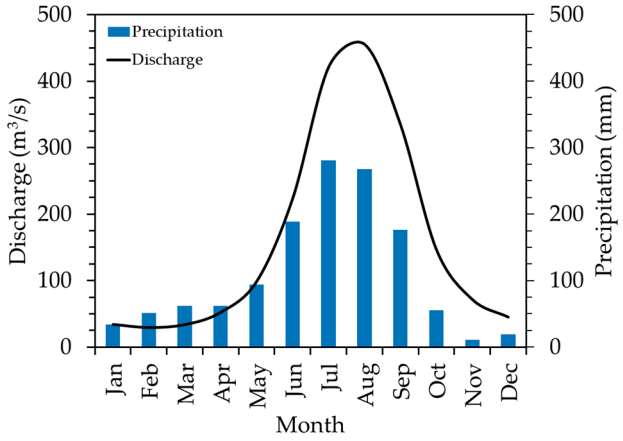

Figure 4. Long term rainfall-runoff pattern of the Budhigandaki River Basin at Arughat.

3.2. SWAT Model Performance

The SWAT model was calibrated and validated manually for a simulation period of 30 years (1983–2012). The 15 most sensitive parameters were selected for calibration. The final adopted values of the parameters (in alphabetical order) are shown in Table 2. It can be seen that two different sets of parameters directly influence the surface runoff (CN2 and OV_N) and lateral flow (LAT_TIME and SURLAG) whereas five parameters (ALPHA_BF, GWDELAY, GWQMIN, SOL_AWC and SOL_Z) impact the baseflow from the basin. It is interesting to note that there are six snow related parameters (snowfall temperature (SFTMP), snowmelt temperature (SMTMP), snow cover (SNOCOVMX), degree-day factors (SMFMX, SMFMN) and temperature lapse rate (TLAPS)) which are used to calculate the snow component of the total flow. Thus, it is seen that the basin demonstrates a high degree of complexity among the different interacting components of the hydrological cycle.

Table 2. Selected SWAT parameters and their calibrated values.

Parameter	Unit	Final Value	Allowable Range *	Impacted Component of Flow
ALPHA_BF	day	0.01	0–1	Baseflow
CN2		50–93	35–98	Surface runoff
GW_DELAY	day	55	0–500	Baseflow
GWQMIN	mm	200	0–5000	Baseflow
LAT_TIME	day	18	0–180	Lateral flow
OV_N	$s/m^{1/3}$	0.5	0.01–0.41	Surface runoff
SFTMP	°C	4.5	−5–5	Snow
SMFMN	mm/°C/day	2.5	1.7–6.5	Snow
SMFMX	mm/°C/day	4.5	1.7–6.5	Snow
SMTMP	°C	2.5	−5–5	Snow
SNOCOVMX	mm	400	0–1.0	Snow
SOL_AWC	mm/mm	0–0.3	0–1.0	Baseflow
SOL_Z	mm	0–50	0–3500	Baseflow
SURLAG	day	0.1	1–10	Lateral flow
TLAPS	°C/km	−6.5	−10–10	Snow

* Reference [84].

Simulated and observed hydrographs for the calibration and the validation periods at Arughat on daily and monthly time steps are shown in Figure 5. The mean and standard deviation of the observed (and simulated) flows are 168 (170) m^3/s and 167 (168) m^3/s, respectively for the calibration period and 154 (181) m^3/s and 163 (180) m^3/s, respectively for the validation period (Table 3). It can be seen from Figure 5 that the model simulates the flow pattern very well and the hydrographs are in good agreement with the rainfall pattern

at daily and monthly timescales even for this length of time (20 years for calibration and 10 years for validation). It is also evident from the scatter plots of simulated vs. observed daily flows of these periods (Figure 6a,b). The difference in cumulative volume between the simulated and observed flow is very small for the calibration period (Figure 6c), however, the model has over-estimated the flow in the validation period (Figure 6d).

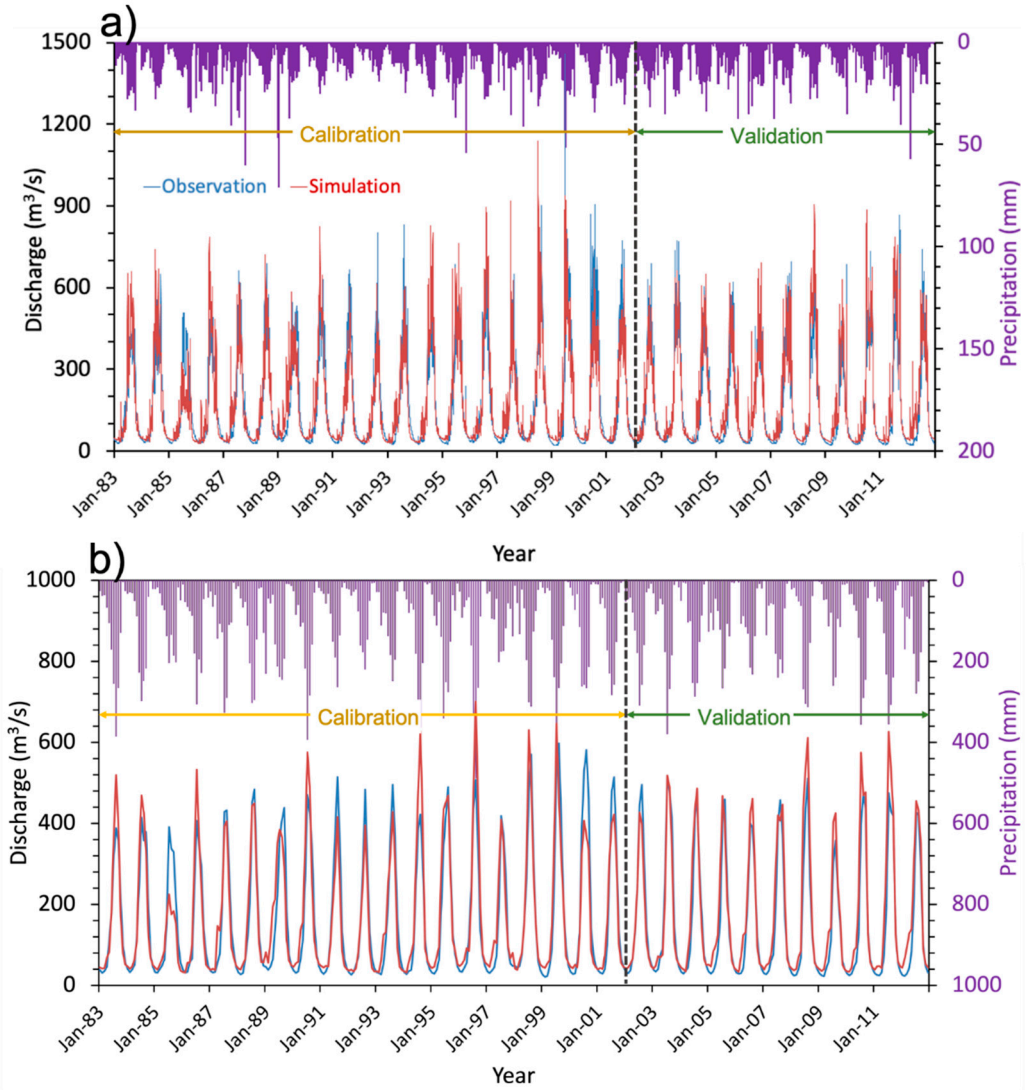

Figure 5. Simulated (red line) and observed (blue line) hydrograph for calibration (1983–2002) and validation period (2003–2012) at Arughat Station. Upper panel (**a**) shows the daily and lower panel; (**b**) shows the monthly simulation results. Precipitation data are shown in the inverted secondary *y*-axis as purple bars.

Table 3. Model calibration and validation statistics at Arughat station in daily timestep.

Statistic (Years)	Mean Flow (m^3/s)		Standard Deviation (m^3/s)		Performance Indicators			
	Observed	Simulated	Observed	Simulated	NSE	PBIAS	RSR	KGE
Calibration (1983–2002)	168	170	167	168	0.78	−1.46%	0.47	0.89
Validation (2003–2012)	154	181	163	180	0.81	−17.1%	0.44	0.79
Entire Simulation (1983–2012)	163	174	166	172	0.79	−6.38%	0.46	0.88

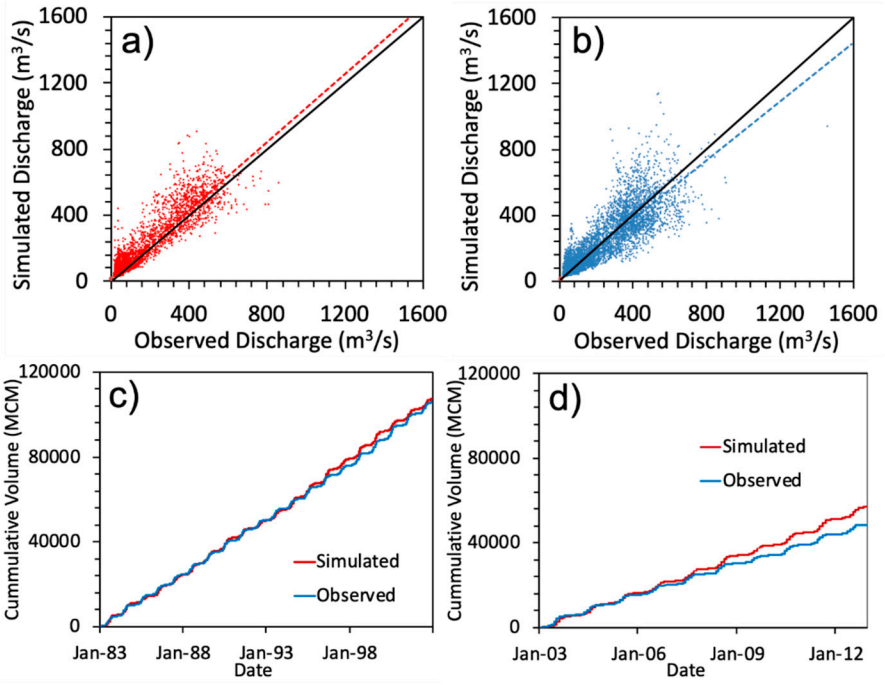

Figure 6. Scattered plots for daily flow in (**a**) calibration and; (**b**) validation; cumulative volume balance in the (**c**) calibration period; and the (**d**) validation period.

The NSE, PBIAS, RSR and KGE values for the calibration period are, respectively, 0.78, −1.46%, 0.47 and 0.89. Similarly, for the validation period, the values of NSE, PBIAS, RSR and KGE are 0.81, −17.1%, 0.44 and 0.79, respectively (Table 3). Based on the criteria prescribed by [77,80], all these indices fall in the 'very good' category except PBIAS in the validation period ('satisfactory' range). The graphical comparison (Figures 4–6) and the performance rating (Table 3) show that the SWAT model is well calibrated and validated for the BRB at Arughat.

The monthly flows, both observed and simulated, for the period 1983–2012 are depicted in Figure 5b. The model performance parameters for monthly flows are 0.88 (NSE), −6.5% (PBIAS), 0.35 (RSR) and 0.91 (KGE). The graph and the performance statistics show that the calibrated SWAT model is capable of simulating the monthly flows well which is required for water availability studies in the BRB.

3.3. Additional Validation of SWAT at Supplementary Stations

Previous studies, e.g., [25,85] have used multi-site approach to calibrate the SWAT model. In the current study, the model is calibrated at a single point and validated at three supplementary points upstream and downstream of Arughat: (i) intake site of Budhigandaki KA (BG KA), (ii) intake site of Budhigandaki KHA (BG KHA) and (iii) 1200 MW Budhigandaki Hydroelectric Project (BGHEP) dam site (see Figure 1). It is to be noted that the study team carried out rigorous discharge measurements and prepared rating curves at these three locations during 2009–2010 (BG KA and BG KHA) and 2013–2014 (BGHEP damsite) which has been used for the additional validation. The results of the validation have been shown in Figure 7. The NSE, RSR, PBIAS and KGE values for BG KA are 0.66, 0.58, 21% and 0.59 and 0.58, 0.65, 13% and 0.54 for BG KHA, respectively. Similarly, their respective values for the BGHEP damsite are 0.91, 0.31, 7.88% and 0.81. As per the rating criteria by [77,80], the model performance is "very good" at the BGHEP dam site, "good" at BG KA and "satisfactory" at BG KHA. This independent validation at supplementary sites reveals that the calibrated model at Arughat can simulate the flow well for the Budhigandaki Basin up to the Trishuli confluence, although the performance is better in the downstream reach compared to the upstream reach.

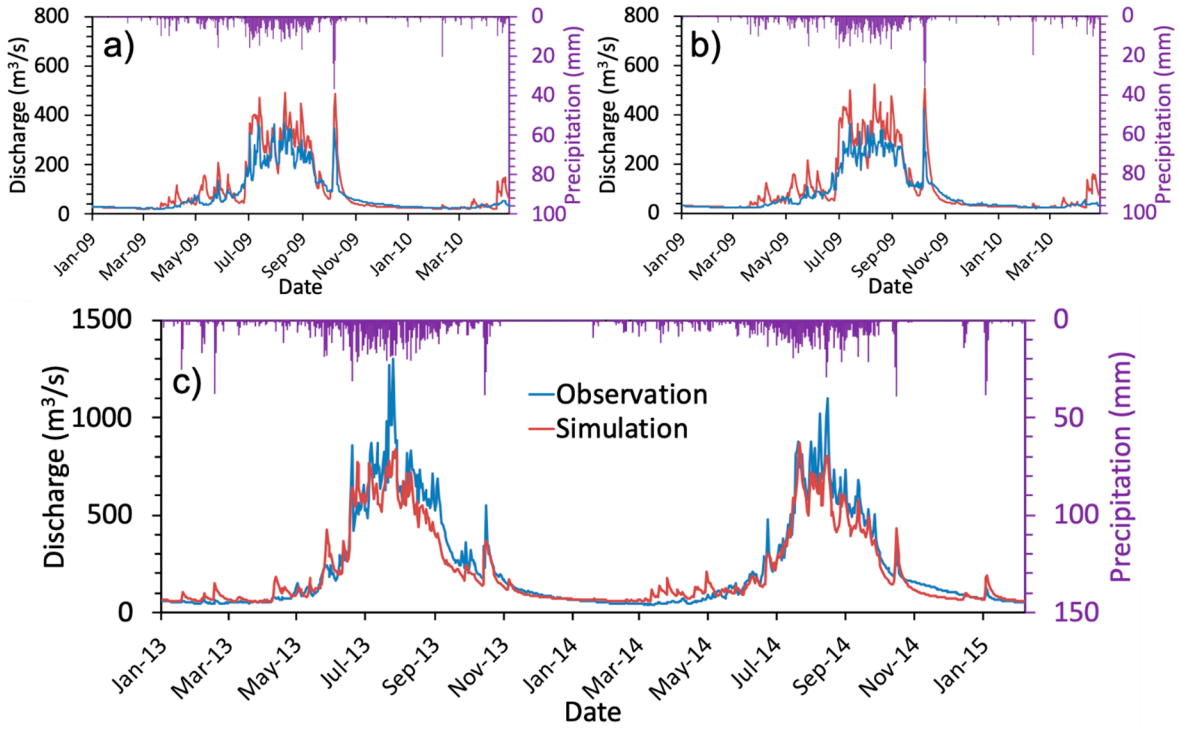

Figure 7. Additional validation of flows at supplementary stations in daily time step: (**a**) Budhigandaki KA, (**b**) Budhigandaki KHA and (**c**) BGHEP dam site. Precipitation data are shown in the inverted secondary *y*-axis as purple bars.

3.4. Flow Duration Curve

The flow-duration curve (FDC) is a probability discharge curve that shows the percentage of time in which a particular flow is equaled or exceeded [1]. FDC was prepared from the observed as well as simulated daily flow data at Arughat (Figure 8a). From the figure, it can be seen that the magnitude of the observed flows at 10%, 40% and 90% exceedance probabilities are 431, 118 and 29 m^3/s respectively. Similarly, the exceedance probabilities are respectively 453, 126 and 39 m^3/s for simulated flows. This indicates that the fractional difference between the corresponding values of the two flow-series are 5%, 7%, and 33%, respectively. The relationship between the simulated and observed values at 10 percentile exceedance intervals are plotted in Figure 8b. A very good linear correlation is found between these two series as indicated by the R^2 value of 0.998.

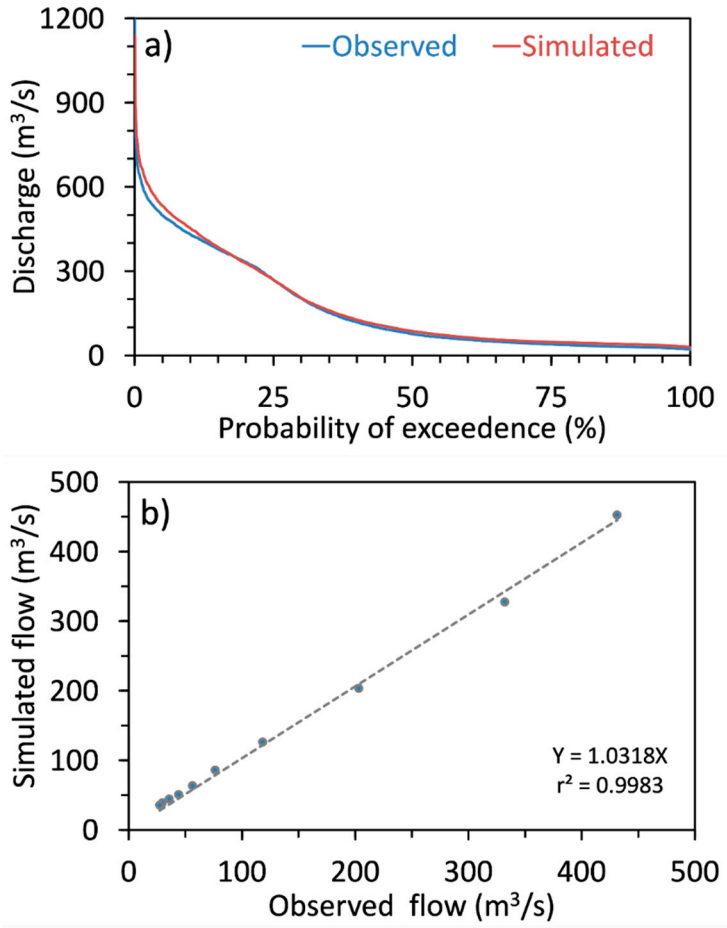

Figure 8. (**a**) FDC of observed and simulated flows, and (**b**) relationship between observed and simulated exceedance flow at 10 percentile intervals.

3.5. Water Balance of the Budhigandaki Basin

Monthly water balance of the BRB is shown in Figure 9. The figure depicts the distribution of water balance components, namely, precipitation (P), actual evapotranspiration (AET) and the net water yield (WY) of the study basin. The WY refers to the total flow coming as surface runoff, lateral flow, and groundwater flow minus transmission losses and pond abstractions [30]. Change in storage is defined as ΔStorage = −[(Precipitation (P) − Net Water Yield (WY) − Evapotranspiration (ET)]. It implies that if P > (WY + ET), the excess water infiltrates and is stored, as soil moisture and GW storages, of the basin. On the other hand, if (WY + ET) > P, the water deficit is met by soil and GW storages of the basin. For example, in January, some water is released from the basin to meet the WY and ET while it is stored in the soil and GW storage in July. It is noted here that Δstorage accounts for model errors too. It can be seen from the results that precipitation across the SWAT sub-basins varies from less than 700 mm (leeward side of northern Trans-Himalayan region) to above 2500 mm (foothills of the Himalayas). The average annual precipitation over the entire basin is 1528 mm. Here precipitation has been taken as the sum of annual rainfall and snowmelt (318 mm). The percentage of precipitation falling in pre-monsoon, monsoon, post monsoon and winter are respectively 16%, 74%, 4% and 6% of the total annual value. The average annual AET over the basin is 402 mm while WY is 1010 mm. The WY is about 56% during monsoon (June–September) while it is only 28% and 9% in pre-monsoon (March–May) and post-monsoon (October and November) seasons, respectively. It is only 7% of the total annual volume for the winter season (December–February). Delta storage for the entire simulation period has been calculated to be around 8%.

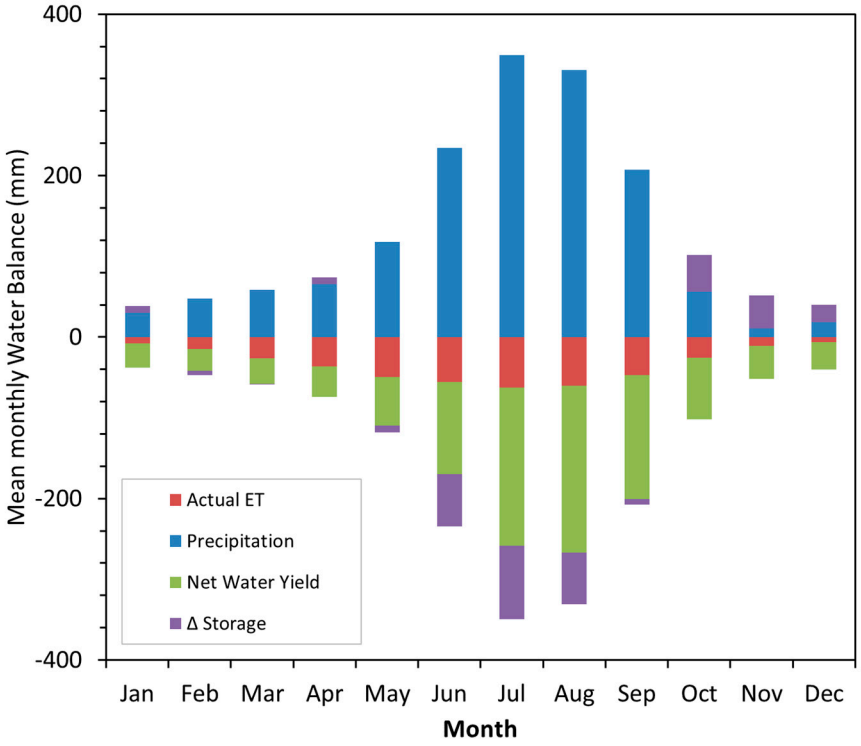

Figure 9. Mean monthly simulated (1983–2012) water balance in Budhigandaki basin.

4. Discussion

In the BRB, the monsoon season (June–September) contributes approximately 74% of the total annual flow while the flow during the other eight months is only 26%. The highest flow occurs in August (23% of the total annual flow) while the lowest flow occurs in February (1.5%). The fractional difference between these two months was calculated to be more than 15, showing high runoff variability in the study basin. This value is comparable with other large and medium size basins of Nepal, for example, West Seti, Karnali, Trishuli, Narayani, Dudhkoshi and Sapta Koshi. The fractional differences of these basins range from 13 (West Seti at Gopighat and Sapta Koshi at Chatara) to 18 (Dudhkoshi at Rabuwa); flow contribution in monsoon season ranges from 72% to 77%, respectively. Furthermore, the low flow contribution is relatively higher in Karnali, West Seti and Saptakoshi (approximately 2%) while this is less than 1.5% in Dudhkoshi. It is interesting to note that low flow contribution is higher in the basins with a significant drainage area of Tibet and lying in the western part of Nepal.

The SWAT model was calibrated using 20 years (two-thirds) of the study period (1983–2002) and validated using the remaining one-third 10 years (2003–2012) which is comparable with the time period taken by [24]. The performance indices of this study are found better or comparable to similar studies carried out in other Nepalese basins. For example, for Chameliya, Karnali, Bheri, Kaligandaki, Indrawati, Tamakoshi, Arun and Tamor basins of Nepal, NSE (and PBIAS) values are respectively 0.75 (+5.1%), 0.84 (−14.2%), 0.70 (−4.4%), 0.78 (−4.0%), 0.72 (-), 0.76 (−1.7%), 0.81 (−6.8%) and 0.85 (+4.3%) for calibration period while these values are 0.65 (-9.3%), 0.84 (−15.4%), 0.71 (−8.9%), 0.8 (+9.6%), 0.87 (-), 0.84 (+5.2%), 0.58 (+24.6%) and 0.89 (+5.5%) respectively for validation period [25,40,45,47,51,85–87]. Similarly, NSE (and PBIAS) values of Gilgelabay basin of Ethiopia, Gurupura basin of India and Tizinafu basin of Western China were found to be respectively 0.69 (+4.8%), 0.83 (+17.5%) and 0.71 (+5.79%) for calibration period while these values for validation period were 0.68 (+4.9%), 0.85 (−3.9%) and 0.64 (−18.0%), respectively [88–90]. Moreover, [42] used SWAT model to simulate five glacierized mountain river basins of the world that includes the Narayani (Nepal), Vakhsh (Central Asia), Rhone (Switzerland), Mendoza (Central Andes, Argentina), and Chile (Central Dry Andes,

Chile). The magnitudes of the statistical indicators of NSE, RSR and PBIAS of our study are comparable with this study.

Even though the model has simulated the flow very well in general, it has underestimated the high flow in some cases (e.g., 1992, 1993, 1999, 2000) while overestimated in some other cases (e.g., 1986, 2008) (Figure 5). The hydrographs in Figure 7a,b show the extended validation results which are based on the primary data collected at BG KA and BG KHA intake sites by the study team during 2009–2010. Figure 7c shows the simulated and observed hydrographs at BGHEP damsite for the year 2013–2014. The reference hydrological station (Arughat) is a few kilometers downstream and upstream from these points. It is to be noted here that the time of simulation for the Figure 7a–c are different. Data for the years 2013 and 2014 are not available at Arughat station for direct comparison. Nevertheless, it can be seen from Figure 5 that the flows for the years 2010, 2011 and 2012 are also overestimated by the model which is very much similar to the condition shown by Figure 7a,b. Further, the simulated flow data series in Figure 7c follows the precipitation pattern and as a result, the simulated hydrograph can be considered to be reasonable, although underestimated from the observed data. It is worth mentioning here that a longer simulation and observation period would add more confidence in the model performance at these locations. There are various factors that cause the difference in the observed and simulated flows that can be grouped into observation errors and model errors. Observation errors are attributed to (i) error in precipitation (human error while reading precipitation and instrumental error); (ii) inadequate rain-gauge stations to capture the spatial variation of precipitation including windward/leeward effect; (iii) error in water level reading; (iv) use of extrapolated stage-discharge relationship while calculating higher and lower flows; and (v) possible combinations of above [61,73,91–94]. In addition to observation errors discussed above, inherent limitations of SWAT flow calculation modules also affect simulated flows. Similarly, resolution of the DEM, land use and land cover, and soil types are only approximations of the real system. The differences between the observed and simulated flows at short timespans are found to be more compared to the long-term values. Despite these differences, the long-term values of the simulated and observed flows and their statistics are highly comparable.

In a water resources project, FDC is a useful tool to know the dependable flow while planning and designing engineering structures. For the BRB, the fractional difference between the simulated and observed low flows is seen to be high. However, the difference in the absolute values of the flows is considerably less compared to the high flows. Twenty-eight percent of the Budhigandaki River Basin is covered with snow and less than one percent (315 km^2) is covered with glaciers. In the upper subbasins, the contribution of the glacier melt might affect the total runoff to some extent [95–98] whereas our area of interest lies in the lower part of BRB near Arughat (elevation 540 masl), where the contribution of glacier melt is insignificant in the total runoff. Past studies have modeled glacier melt in high altitude catchments above 3000 masl (for e.g., [95,97]) in which the calibration stations are also located in high elevations (Langtang at 3670 masl; catchment area 353 km^2). Furthermore, from these studies it can be seen that the annual runoff quantified at the reference stations is around 9 m^3/s while it is about 160 m^3/s at Arughat. Thus, even a small contribution from glacier melt will have a huge impact on the high elevation stations while it will be less considerable at stations lying in lower elevations. There is some contribution of snowmelt flow during the pre-monsoon period whereas the base flow contribution is more in post monsoon period. It is to be noted that the precipitation contributes to net storage from May to September (wet period) and the storage depletes during most of the dry period from October to April. This causes the percentage of precipitation contribution to net water yield to be smaller during the monsoon period than the other three periods.

5. Conclusions

This study discretized the BRB into 16 sub-basins and 344 HRUs and developed a hydrological model in SWAT to characterize spatial and temporal distribution of water

availability. Calibration and validation of the model was carried out at Arughat using daily flow data of 20 years and 10 years respectively. Even in such a long duration, the model performed well and was ranked "very good". In addition to the conventional method of validation at the calibration station, this study further carried out validation at three supplementary points (two upstream and one downstream) at which the study team collected primary river flow data and prepared rating curves. Results of the supplementary validation further added confidence to the model performance.

This study estimated the mean annual flow at BRB outlet to be 240 m^3/s with annual precipitation 1528 mm and AET approximately 26% of the precipitation. However, distinct seasonal variability is noted in the basin with precipitation varying from 67 mm (post-monsoon) to 1122 mm (monsoon), AET from 28 mm (winter) to 225 mm (monsoon), and WY from 92 mm (winter) to 670 mm (monsoon). The monsoon season contribution is 73%, 56%, and 66% in the average annual precipitation, AET, and WY, respectively in the BRB. Snowmelt contributes 20% of the total flow at the basin outlet during the pre-monsoon period and 8% in the post monsoon period. The magnitude of the simulated flows at 10%, 40% and 90% exceedance probabilities are 453, 126 and 39 m^3/s respectively indicating high energy generation potential.

This study provides additional evidence to the SWAT diaspora of its applicability to simulate the rainfall-runoff characteristics of complex mountainous basin. Furthermore, the spatial and temporal variability in the available water of the BRB was estimated. The findings will be useful for hydrologists and planners in general to utilize the available water rationally in the times to come and particularly, to harness the hydroelectric potential of the basin.

Author Contributions: Conceptualization, S.M., D.A. and L.P.D.; methodology, S.M., D.A. and L.P.D.; software, validation, formal analysis, investigation, resources, data curation, writing—original draft preparation, S.M.; writing—review and editing, S.M., D.A. and L.P.D.; supervision, D.A. and L.P.D.; funding acquisition, D.A. All authors have read and agreed to the published version of the manuscript.

Funding: This research was funded by University Grants Commission (UGC), Nepal.

Institutional Review Board Statement: Not applicable.

Informed Consent Statement: Not applicable.

Data Availability Statement: The datasets used in this study can be accessed freely.

Acknowledgments: Authors would like to thank the Department of Hydrology and Meteorology, Government of Nepal for providing hydro-climatic data. The Budhigandaki Hydroelectric Project Development Committee is also acknowledged for providing hydrological data. The authors would like to thank three anonymous reviewers for constructive comments which helps to improve our manuscript substantially.

Conflicts of Interest: The authors declare no conflict of interest.

References

1. Chow, V.T.; Maidment, D.R.; Mays, L.W. *Applied Hydrology*; TATA McGrawHill Inc.: New York, NY, USA, 1988.
2. Zhang, Q.; Knowles, J.F.; Barnes, R.T.; Cowie, R.M.; Rock, N.; Williams, M.W. Surface and subsurface water contributions to streamflow from a mesoscale watershed in complex mountain terrain. *Hydrol. Process.* **2018**, *32*, 954–967. [CrossRef]
3. Tallaksen, L.M. A review of baseflow recession analysis. *J. Hydrol.* **1995**, *165*, 349–370. [CrossRef]
4. Dobriyal, P.; Badola, R.; Tuboi, C.; Hussain, S.A. A review of methods for monitoring streamflow for sustainable water resource management. *Appl. Water Sci.* **2017**, *7*, 2617–2628. [CrossRef]
5. Loukas, A.; Vasiliades, L. Streamflow simulation methods for ungauged and poorly gauged watersheds. *Nat. Hazards Earth Syst. Sci.* **2014**, *14*, 1641–1661. [CrossRef]
6. Shin, S.; Pokhrel, Y.; Talchabhadel, R.; Panthi, J. Spatio-temporal dynamics of hydrologic changes in the Himalayan river basins of Nepal using high-resolution hydrological-hydrodynamic modeling. *J. Hydrol.* **2021**, *598*, 126209. [CrossRef]
7. Alford, D.; Armstrong, R.; Racoviteanu, A. Glacier Retreat in the Nepal Himalaya: The role of glaciers in stream flow from the Nepal Himalaya. *World Bank Tech. Rep. Forthcom.* **2011**. [CrossRef]

8. Hishinuma, S.; Takeuchi, K.; Magome, J. Challenges of hydrological analysis for water resource development in semi-arid mountainous regions: Case study in Iran. *Hydrol. Sci. J.* **2014**, *59*, 1718–1737. [CrossRef]
9. Viviroli, D.; Dürr, H.H.; Messerli, B.; Meybeck, M.; Weingartner, R. Mountains of the world, water towers for humanity: Typology, mapping, and global significance. *Water Resour. Res.* **2007**, *43*. [CrossRef]
10. Horton, R.E. Drainage-basin characteristics. *EOS Trans. Am. Geophys. Union* **1932**, *13*, 350–361. [CrossRef]
11. Kale, V.S. Fluvial geomorphology of Indian rivers: An overview. *Prog. Phys. Geogr.* **2002**, *26*, 400–433. [CrossRef]
12. Higuchi, K.; Ageta, Y.; Yasunari, T.; Inoue, J. Characteristics of precipitation during the monsoon season in high-mountain areas of the Nepal Himalaya. *IAHS Publ.* **1982**, *138*, 21–30.
13. Shrestha, A.B.; Wake, C.P.; Dibb, J.E.; Mayewski, P.A. Precipitation fluctuations in the Nepal Himalaya and its vicinity and relationship with some large scale climatological parameters. *Int. J. Climatol. J. R. Meteorol. Soc.* **2000**, *20*, 317–327. [CrossRef]
14. Kansakar, S.R.; Hannah, D.M.; Gerrard, J.; Rees, G. Spatial pattern in the precipitation regime of Nepal. *Int. J. Climatol. J. R. Meteorol. Soc.* **2004**, *24*, 1645–1659. [CrossRef]
15. Putkonen, J.K. Continuous Snow and Rain Data at 500 to 4400 m Altitude near Annapurna, Nepal, 1999–2001. *Arct. Antarct. Alp. Res.* **2004**, *36*, 244–248. [CrossRef]
16. Ichiyanagi, K.; Yamanaka, M.D.; Muraji, Y.; Vaidya, B.K. Precipitation in Nepal between 1987 and 1996. *Int. J. Climatol. J. R. Meteorol. Soc.* **2007**, *27*, 1753–1762. [CrossRef]
17. Devkota, R.P.; Pandey, V.P.; Bhattarai, U.; Shrestha, H.; Adhikari, S.; Dulal, K.N. Climate change and adaptation strategies in Budhi Gandaki River Basin, Nepal: A perception-based analysis. *Clim. Chang.* **2017**, *140*, 195–208. [CrossRef]
18. Pokharel, B.; Wang, S.S.; Meyer, J.; Marahatta, S.; Nepal, B.; Chikamoto, Y.; Gillies, R. The east–west division of changing precipitation in Nepal. *Int. J. Climatol.* **2020**, *40*, 3348–3359. [CrossRef]
19. WMO. *Calculation of Monthly and Annual 30-Year Standard Normals, Prepared by a Meeting of Experts, Washington, DC, USA, March 1989*; WCDP-No. 10, WMO-TD/No. 341; World Meteorological Organization: Geneva, Switzerland, 1989.
20. Jain, S.K.; Jain, S.K.; Jain, N.; Xu, C.-Y. Hydrologic modeling of a Himalayan mountain basin by using the SWAT mode. *Hydrol. Earth Syst. Sci. Discuss.* **2017**, 1–26. [CrossRef]
21. Woolridge, D.D.; Niemann, J.D. *Mountain Basin Hydrologic Study*. 2018. Available online: https://dnrweblink.state.co.us/dwr/0/edoc/3377613/DWR_3377613.pdf?searchid=10250736-fd55-4a8f-a43f-b9270fad6e92 (accessed on 22 December 2020).
22. Meng, F.; Sa, C.; Liu, T.; Luo, M.; Liu, J.; Tian, L. Improved Model Parameter Transferability Method for Hydrological Simulation with SWAT in Ungauged Mountainous Catchments. *Sustainability* **2020**, *12*, 3551. [CrossRef]
23. Marahatta, S.; Devkota, L.; Aryal, D. Hydrological Modeling: A Better Alternative to Empirical Methods for Monthly Flow Estimation in Ungauged Basins. *J. Water Resour. Prot.* **2021**, 254–270. [CrossRef]
24. Abbaspour, K.C.; Rouholahnejad, E.; Vaghefi, S.; Srinivasan, R.; Yang, H.; Kløve, B. A continental-scale hydrology and water quality model for Europe: Calibration and uncertainty of a high-resolution large-scale SWAT model. *J. Hydrol.* **2015**, *524*, 733–752. [CrossRef]
25. Pandey, V.P.; Dhaubanjar, S.; Bharati, L.; Thapa, B.R. Spatio-temporal distribution of water availability in Karnali-Mohana Basin, Western Nepal: Hydrological model development using multi-site calibration approach (Part-A). *J. Hydrol. Reg. Stud.* **2020**, *29*, 100690. [CrossRef]
26. Zhou, X.; Helmers, M.; Qi, Z. Modeling of subsurface tile drainage using MIKE SHE. *Appl. Eng. Agric.* **2013**, *29*, 865–873.
27. Devkota, L.P.; Gyawali, D.R. Impacts of climate change on hydrological regime and water resources management of the Koshi River Basin, Nepal. *J. Hydrol. Reg. Stud.* **2015**, *4*, 502–515. [CrossRef]
28. Sitterson, J.; Knightes, C.; Parmar, R.; Wolfe, K.; Avant, B.; Muche, M. An Overview of Rainfall-Runoff Model Types. 2018. Available online: https://cfpub.epa.gov/si/si_public_record_report.cfm?dirEntryId=339328&Lab=NERL (accessed on 12 January 2021).
29. Hossain, S.; Hewa, G.A.; Wella-Hewage, S. A Comparison of continuous and event-based rainfall–runoff (RR) modelling using EPA-SWMM. *Water* **2019**, *11*, 611. [CrossRef]
30. Arnold, J.G.; Srinivasan, R.; Muttiah, R.S.; Williams, J.R.; Ramanarayanan, T.S.; Arnold, J.G.; Bednarz, S.T.; Srinivasan, R.; Muttiah, R.S.; Williams, J.R. Large area hydrologic modeling and assessment part I: Model development 1. *JAWRA J. Am. Water Resour. Assoc.* **1998**, *34*, 73–89. [CrossRef]
31. Williams, J.R.; Arnold, J.G.; Kiniry, J.R.; Gassman, P.W.; Green, C.H. History of model development at Temple, Texas. *Hydrol. Sci. J.* **2008**, *53*, 948–960. [CrossRef]
32. Douglas-Mankin, K.R.; Srinivasan, R.; Arnold, J.G. Soil and Water Assessment Tool (SWAT) model: Current developments and applications. *Trans. ASABE* **2010**, *53*, 1423–1431. [CrossRef]
33. Tan, M.L.; Gassman, P.W.; Srinivasan, R.; Arnold, J.G.; Yang, X. A review of SWAT studies in Southeast Asia: Applications, challenges and future directions. *Water* **2019**, *11*, 914. [CrossRef]
34. Das, B.; Jain, S.; Singh, S.; Thakur, P. Evaluation of multisite performance of SWAT model in the Gomti River Basin, India. *Appl. Water Sci.* **2019**, *9*, 1–10. [CrossRef]
35. Van Griensven, A.; Ndomba, P.; Yalew, S.; Kilonzo, F. Critical review of SWAT applications in the upper Nile basin countries. *Hydrol. Earth Syst. Sci.* **2012**, *16*, 3371–3381. [CrossRef]
36. Fukunaga, D.C.; Cecílio, R.A.; Zanetti, S.S.; Oliveira, L.T.; Caiado, M.A.C. Application of the SWAT hydrologic model to a tropical watershed at Brazil. *Catena* **2015**, *125*, 206–213. [CrossRef]

37. Anand, J.; Gosain, A.K.; Khosa, R.; Srinivasan, R. Regional scale hydrologic modeling for prediction of water balance, analysis of trends in streamflow and variations in streamflow: The case study of the Ganga River basin. *J. Hydrol. Reg. Stud.* **2018**, *16*, 32–53. [CrossRef]
38. Tang, X.; Zhang, J.; Gao, C.; Ruben, G.B.; Wang, G. Assessing the uncertainties of four precipitation products for swat modeling in Mekong River basin. *Remote Sens.* **2019**, *11*, 304. [CrossRef]
39. CARD (Center for Agricultural and Rural Development). *Swat Lit. Database Peer-Reviewed J. Artic*; Center for Agricultural and Rural Development—Iowa State University: Ames, IA, USA, 2020; Available online: https://www.card.iastate.edu/swatarticles (accessed on 13 January 2021).
40. Shrestha, S.; Shrestha, M.; Shrestha, P.K. Evaluation of the SWAT model performance for simulating river discharge in the Himalayan and tropical basins of Asia. *Hydrol. Res.* **2018**, *49*, 846–860. [CrossRef]
41. Bharati, L.; Gurung, P.; Jayakody, P.; Smakhtin, V.; Bhattarai, U. The projected impact of climate change on water availability and development in the Koshi Basin, Nepal. *Mt. Res. Dev.* **2014**, *34*, 118–130. [CrossRef]
42. Omani, N.; Srinivasan, R.; Karthikeyan, R.; Smith, P.K. Hydrological modeling of highly glacierized basins (Andes, Alps, and Central Asia). *Water* **2017**, *9*, 111. [CrossRef]
43. Talchabhadel, R.; Nakagawa, H.; Kawaike, K.; Yamanoi, K.; Aryal, A.; Bhatta, B.; Karki, S. SWAT modeling for assessing future scenarios of soil erosion in West Rapti River Basin of Nepal. In Proceedings of the EGU General Assembly Conference Abstracts, Online, 4–8 May 2020; p. 1853.
44. Dhami, B.; Himanshu, S.K.; Pandey, A.; Gautam, A.K. Evaluation of the SWAT model for water balance study of a mountainous snowfed river basin of Nepal. *Environ. Earth Sci.* **2018**, *77*. [CrossRef]
45. Mishra, Y.; Nakamura, T.; Babel, M.S.; Ninsawat, S.; Ochi, S. Impact of climate change on water resources of the Bheri River Basin, Nepal. *Water* **2018**, *10*, 220. [CrossRef]
46. Dahal, P.; Shrestha, M.L.; Panthi, J.; Pradhananga, D. Modeling the future impacts of climate change on water availability in the Karnali River Basin of Nepal Himalaya. *Environ. Res.* **2020**, *185*, 109430. [CrossRef]
47. Bajracharya, A.R.; Bajracharya, S.R.; Shrestha, A.B.; Maharjan, S.B. Climate change impact assessment on the hydrological regime of the Kaligandaki Basin, Nepal. *Sci. Total Environ.* **2018**, *625*, 837–848. [CrossRef]
48. Lamichhane, S.; Shakya, N.M. Integrated assessment of climate change and land use change impacts on hydrology in the Kathmandu Valley watershed, Central Nepal. *Water* **2019**, *11*, 2059. [CrossRef]
49. Dahal, V.; Shakya, N.M.; Bhattarai, R. Estimating the impact of climate change on water availability in Bagmati Basin, Nepal. *Environ. Process.* **2016**, *3*, 1–17. [CrossRef]
50. Pandey, V.P.; Dhaubanjar, S.; Bharati, L.; Thapa, B.R. Spatio-temporal distribution of water availability in Karnali-Mohana Basin, Western Nepal: Climate change impact assessment (Part-B). *J. Hydrol. Reg. Stud.* **2020**, *29*, 100691. [CrossRef]
51. Bhatta, B.; Shrestha, S.; Shrestha, P.K.; Talchabhadel, R. Evaluation and application of a SWAT model to assess the climate change impact on the hydrology of the Himalayan River Basin. *Catena* **2019**, *181*, 104082. [CrossRef]
52. Bharati, L.; Gurung, P.; Maharjan, L.; Bhattarai, U. Past and future variability in the hydrological regime of the Koshi Basin, Nepal. *Hydrol. Sci. J.* **2016**, *61*, 79–93. [CrossRef]
53. BGHEP. *Feasibility Study and Detailed Design of Budhigandaki Hydropower Project Part 1*; Budhigandaki Hydroelectric Project Development Committee, Government of Nepal: Kathmandu, Nepal, 2015.
54. Khatri, H.B.; Jain, M.K.; Jain, S.K. Modelling of streamflow in snow dominated Budhigandaki catchment in Nepal. *J. Earth Syst. Sci.* **2018**, *127*, 1–14. [CrossRef]
55. Pangali Sharma, T.P.; Zhang, J.; Khanal, N.R.; Prodhan, F.A.; Paudel, B.; Shi, L.; Nepal, N. Assimilation of snowmelt runoff model (SRM) using satellite remote sensing data in Budhi Gandaki River Basin, Nepal. *Remote Sens.* **2020**, *12*, 1951. [CrossRef]
56. Shrestha, M.L. Interannual variation of summer monsoon rainfall over Nepal and its relation to Southern Oscillation Index. *Meteorol. Atmos. Phys.* **2000**, *75*, 21–28. [CrossRef]
57. Marahatta, S.; Dangol, B.S.; Gurung, G.B. *Temporal and Spatial Variability of Climate Change over Nepal, 1976–2005*; Practical Action Nepal Office: Kathmandu, Nepal, 2009; ISBN 9937813522.
58. MoCTCA. *Mountaineering in Nepal Facts and Figures*; Ministry of Culture, Tourism and Civil Aviation (MoCTCA), Government of Nepal: Kathmandu, Nepal, 2014.
59. DHM. *Study of Climate and Climatic Variation over Nepal*; Technical Report; Department of Hydrology and Meteorology, Government of Nepal: Kathmandu, Nepal, 2015.
60. DHM. *Institutional Development of Department of Hydrology and Meteorology*; Technical Report No.7 (Basin Study); DHM: Kathmandu, Nepal, 2002.
61. DHM. *Streamflow Summary (1962–2015)*; Department of Hydrology and Meteorology, Government of Nepal: Kathmandu, Nepal, 2018.
62. NNH. *Hydrology, Hydraulics and Sediment Studies of Budhigandaki KA HEP*; Naulo Nepal Hydro-electric (P) Ltd.: Kaski District, Nepal, 2010.
63. NNH. *Hydrology, Hydraulics and Sediment Studies of Budhigandaki KHA HEP*; Naulo Nepal Hydro-electric (P) Ltd.: Kaski District, Nepal, 2010.
64. Yang, K.; He, J. China Meteorological Forcing Dataset (1979−2018). National Tibetan Plateau Data Center, 2019. Available online: https://doi:10.11888/AtmosphericPhysics.tpe.249369.file (accessed on 29 May 2021).

65. *DoWRI Irrigation Master Plan Preparation through Integrated River Basin Planning (Dataset), Water Resources Project Preparatory Facility*; Department of Water Resources and Irrigation, Ministry of Energy, Water Resources and Irrigation (MoEWRI): Kathmandu, Nepal, 2019.
66. ICIMOD. *Land Cover of Nepal 2010 [Dataset]*; International Center for Integrated Mountain Development (ICIMOD): Kathmandu, Nepal, 2010; Available online: http://rds.icimod.org/Home/DataDetail (accessed on 3 December 2020).
67. Thiessen, A.H. Precipitation averages for large areas. *Mon. Weather Rev.* **1911**, *39*, 1082–1089. [CrossRef]
68. Srinivasan, R.; Ramanarayanan, T.S.; Arnold, J.G.; Bednarz, S.T. Large area hydrologic modeling and assessment part II: Model application 1. *J. Am. Water Resour. Assoc.* **1998**, *34*, 91–101. [CrossRef]
69. Moriasi, D.N.; Wilson, B.N.; Douglas-Mankin, K.R.; Arnold, J.G.; Gowda, P.H. Hydrologic and water quality models: Use, calibration, and validation. *Trans. ASABE* **2012**, *55*, 1241–1247. [CrossRef]
70. Van Liew, M.W.; Arnold, J.G.; Bosch, D.D. Problems and potential of autocalibrating a hydrologic model. *Trans. ASAE* **2005**, *48*, 1025–1040. [CrossRef]
71. Neitsch, S.L.; Arnold, J.G.; Kiniry, J.R.; Williams, J.R. *Soil and Water Assessment Tool Theoretical Documentation Version 2009*; Texas Water Resources Institute: College Station, TX, USA, 2011.
72. WMO. *The Role of Climatological Normals in a Changing Climate*; WCDMP-No. 61, WMO-TD No. 1377; World Meteorological Organization: Geneva, Switzerland, 2007.
73. WMO. *Guide to Climatological Practices*; 2011 Edition, WMO Number 100; World Meteorological Organization: Geneva, Switzerland, 2011.
74. WMO. *Guidelines on the Calculation of Climate Normals*; 2017 Edition WMO-No. 1203; World Meteorological Organization: Geneva, Switzerland, 2017.
75. Mockus, V. *National Engineering Handbook*; Soil Conservation Service: Washington, DC, USA, 1964; Volume 4.
76. Hargreaves, G.H.; Samani, Z.A. Estimating potential evapotranspiration. *J. Irrig. Drain. Div.* **1982**, *108*, 225–230. [CrossRef]
77. Moriasi, D.N.; Arnold, J.G.; Van Liew, M.W.; Bingner, R.L.; Harmel, R.D.; Veith, T.L. Model evaluation guidelines for systematic quantification of accuracy in watershed simulations. *Trans. ASABE* **2007**, *50*, 885–900. [CrossRef]
78. Moriasi, D.N.; Gitau, M.W.; Pai, N.; Daggupati, P. Hydrologic and water quality models: Performance measures and evaluation criteria. *Trans. ASABE* **2015**, *58*, 1763–1785.
79. Schaefli, B.; Gupta, H.V. Do Nash values have value? *Hydrol. Process. An Int. J.* **2007**, *21*, 2075–2080. [CrossRef]
80. Gupta, H.V.; Kling, H.; Yilmaz, K.K.; Martinez, G.F. Decomposition of the mean squared error and NSE performance criteria: Implications for improving hydrological modelling. *J. Hydrol.* **2009**, *377*, 80–91. [CrossRef]
81. Knoben, W.J.M.; Freer, J.E.; Woods, R.A. Inherent benchmark or not? Comparing Nash–Sutcliffe and Kling–Gupta efficiency scores. *Hydrol. Earth Syst. Sci.* **2019**, *23*, 4323–4331. [CrossRef]
82. Pool, S.; Vis, M.; Seibert, J. Evaluating model performance: Towards a non-parametric variant of the Kling-Gupta efficiency. *Hydrol. Sci. J.* **2018**, *63*, 1941–1953. [CrossRef]
83. Nash, J.E.; Sutcliffe, J.V. River flow forecasting through conceptual models part I—A discussion of principles. *J. Hydrol.* **1970**, *10*, 282–290. [CrossRef]
84. Arnold, J.G.; Kiniry, J.R.; Srinivasan, R.; Williams, J.R.; Haney, E.B.; Neitsch, S.L. *Soil & Water Assessment Tool: Input/Output Documentation*; Version 2012; TR-439; Texas Water Resources Institute: Forney, TX, USA, 2013; p. 650.
85. Bharati, L.; Bhattarai, U.; Khadka, A.; Gurung, P.; Neumann, L.E.; Penton, D.J.; Dhaubanjar, S.; Nepal, S. *From the Mountains to the Plains: Impact of Climate Change on Water Resources in the Koshi River Basin*; International Water Management Institute (IWMI): Colombo, Sri Lanka, 2019; Volume 187, ISBN 9290908858.
86. Pandey, V.P.; Dhaubanjar, S.; Bharati, L.; Thapa, B.R. Hydrological response of Chamelia watershed in Mahakali Basin to climate change. *Sci. Total Environ.* **2019**, *650*, 365–383. [CrossRef]
87. Palazzoli, I.; Maskey, S.; Uhlenbrook, S.; Nana, E.; Bocchiola, D. Impact of prospective climate change on water resources and crop yields in the Indrawati basin, Nepal. *Agric. Syst.* **2015**, *133*, 143–157. [CrossRef]
88. Tegegne, G.; Park, D.K.; Kim, Y.-O. Comparison of hydrological models for the assessment of water resources in a data-scarce region, the Upper Blue Nile River Basin. *J. Hydrol. Reg. Stud.* **2017**, *14*, 49–66. [CrossRef]
89. Sharannya, T.M.; Mudbhatkal, A.; Mahesha, A. Assessing climate change impacts on river hydrology–A case study in the Western Ghats of India. *J. Earth Syst. Sci.* **2018**, *127*, 1–11. [CrossRef]
90. Duan, Y.; Liu, T.; Meng, F.; Luo, M.; Frankl, A.; De Maeyer, P.; Bao, A.; Kurban, A.; Feng, X. Inclusion of modified snow melting and flood processes in the swat model. *Water* **2018**, *10*, 1715. [CrossRef]
91. Le Coz, J. A Literature Review of Methods for Estimating the Uncertainty Associated with Stage-Discharge Relations. *WMO Rep. PO6a* **2012**, *21*. Available online: https://www.semanticscholar.org/paper/A-literature-review-of-methods-for-estimating-the-Coz-Cemagref/b685243d91acd17a64c3e31ecff08ea39d5b279d (accessed on 14 January 2021).
92. Subramanayam, K. *Engineering Hydrology*; TATA McGraw Hills Publications Ltd.: New Delhi, India, 1994; ISBN 0-07-462449-8.
93. Domeneghetti, A.; Castellarin, A.; Brath, A. Assessing rating-curve uncertainty and its effects on hydraulic model calibration. *Hydrol. Earth Syst. Sci.* **2012**, *16*, 1191–1202. [CrossRef]
94. Manfreda, S.; Pizarro, A.; Moramarco, T.; Cimorelli, L.; Pianese, D.; Barbetta, S. Potential advantages of flow-area rating curves compared to classic stage-discharge-relations. *J. Hydrol.* **2020**, *585*, 124752. [CrossRef]

95. Kayastha, R.B.; Steiner, N.; Kayastha, R.; Mishra, S.K.; Forster, R.R. Comparative Study of Hydrology and Icemelt in Three Nepal River Basins Using the Glacio-Hydrological Degree-Day Model (GDM) and Observations from the Advanced Scatterometer (ASCAT). *Front. Earth Sci.* **2020**, *7*, 354. [CrossRef]
96. Mishra, S.K.; Hayse, J.; Veselka, T.; Yan, E.; Kayastha, R.B.; LaGory, K.; McDonald, K.; Steiner, N. An integrated assessment approach for estimating the economic impacts of climate change on River systems: An application to hydropower and fisheries in a Himalayan River, Trishuli. *Environ. Sci. Policy* **2018**, *87*, 102–111. [CrossRef]
97. Pradhananga, N.S.; Kayastha, R.B.; Bhattarai, B.C.; Adhikari, T.R.; Pradhan, S.C.; Devkota, L.P.; Shrestha, A.B.; Mool, P.K. Estimation of discharge from Langtang River basin, Rasuwa, Nepal, using a glacio-hydrological model. *Ann. Glaciol.* **2014**, *55*, 223–230. [CrossRef]
98. Khadka, M.; Kayastha, R.B.; Kayastha, R. Future projection of cryospheric and hydrologic regimes in Koshi River basin, Central Himalaya, using coupled glacier dynamics and glacio-hydrological models. *J. Glaciol.* **2020**. [CrossRef]

Journal of Water Resource and Protection, 2021, 13, 254-270
https://www.scirp.org/journal/jwarp
ISSN Online: 1945-3108
ISSN Print: 1945-3094

Hydrological Modeling: A Better Alternative to Empirical Methods for Monthly Flow Estimation in Ungauged Basins

Suresh Marahatta[1*], Laxmi Devkota[2,3], Deepak Aryal[1]

[1]Central Department of Hydrology and Meteorology, Tribhuvan University, Kathmandu, Nepal
[2]Nepal Academy of Science and Technology (NAST), Kathmandu, Nepal
[3]Water Modeling Solutions Pvt. Ltd. (WMS), Lalitpur, Nepal
Email: *suresh.marahatta@cdhm.tu.edu.np

How to cite this paper: Marahatta, S., Devkota, L. and Aryal, D. (2021) Hydrological Modeling: A Better Alternative to Empirical Methods for Monthly Flow Estimation in Ungauged Basins. *Journal of Water Resource and Protection*, **13**, 254-270.
https://doi.org/10.4236/jwarp.2021.133015

Received: February 18, 2021
Accepted: March 22, 2021
Published: March 25, 2021

Abstract

Water resource is required for agricultural, industrial, and domestic activities and for environmental preservation. However, with the increase in population and growth of urbanization, industrialization, and commercial activities, planning and management of water resources have become a challenging task to meet various water demands globally. Information and data on streamflow hydrology are, thus, crucial for this purpose. However, availability of measured flow data in many cases is either inadequate or not available at all. When there is no gauging station available at the site of interest, various empirical methods are generally used to estimate the flow there and the best estimation is chosen. This study is focused on the estimation of monthly average flows by such methods popular in Nepal and assessment of how they compare with the results of hydrological simulation. Performance evaluation of those methods was made with a newly introduced index, Global Performance Index (GPI) utilizing six commonly used goodness-of-fit parameters viz. coefficient of determination, mean absolute error, root mean square error, percentage of volume bias, Nash Sutcliff Efficiency and Kling-Gupta Efficiency. This study showed that hydrological modeling is the best among the considered methods of flow estimation for ungauged catchments.

Keywords

Ungauged Basins, Modeling, Monthly Flows, Global Performance Index

1. Introduction

Water resources is required to perform agricultural, industrial, and domestic ac-

tivities and for environmental preservation [1]. With the increase in population and accelerated growth of urbanization, industrialization, and commercial development, demand for water resources of sufficient quantity and quality will continue to increase [2] [3] [4]. The design of all water related structures such as dams, highway bridges, embankments, among others, consists of three basic components: hydrologic design, hydraulic design and structural design. Hydrologic design deals with the estimation of the quantities of water to be handled at the site of the structure in terms of time distribution, time of occurrence and frequency of occurrence [5]. Streamflow time series is, therefore, one of the most important data required for the effective water resource planning and management at both local and national scales [6]. However, availability of measured flow data in many cases is either inadequate or not available at all [7] [8]. Such situations create challenges not only for the optimal use of water resources in ungauged river basins for various development works like domestic water supply and sanitation, irrigation, hydropower etc. but also in flood control works [9] [10]. Underestimation of the flows could lead to rejection of attractive projects whereas overestimation could have huge implications on the physical infrastructure and overall economic feasibility of the projects [4] [11]. Accurate flow estimates are, therefore, necessary at these basins where water resources projects are developed.

Although the global scientific community has put substantial efforts to resolve the issue of flow estimation in ungauged basins/sites, a universal solution method is not available till date [12]. Various methods are found in use in different parts of the world to deal with this issue. One of the oldest methods of generating flow data is the use of regression equation/s developed at the regional level [7] [13] [14] [15]. Razavi and Coulibaly [6] reviewed regional methods and highlighted that those methods making use of different combinations of physiographic information and meteorological attributes, among others, were found to predict streamflows in ungagged basins/sites better. They listed catchment area, elevation, slope of basin, rainfall and temperature as the main parameters used in those methods. Another popular method is transposition of gauged streamflow data to ungauged sites. One of them is the Drainage Area Ratio (DAR) method [16] [17]. It is based on the assumption that the streamflow at the ungauged site can be estimated by multiplying the ratio of the drainage area for this site and the drainage area for the gauging site by the streamflow of the gauging site [17]. As it needs only catchments areas and the observed streamflow of the gauged station, it is considered one of the easiest methods of flow prediction and therefore popularly used in the past [16]. One of the variants of the DAR method is MDAR (Multiple gauging stations Drainage Area Ratio). In the MDAR method, the weighted sum of more than one streamflow gauging stations is used to estimate the flow at the site of interest [18]. Incorporating the basin rainfall ratio of the ungauged basin to the gauged one as a multiplier to the DAR method has been considered as an improved version of the DAR method [17] [19]. This method can be called as a General Transposition (GT) method.

Hydrological simulation method is a numerical method in which a hydrologic model, a simplified software representation of the natural rainfall-runoff process within a catchment boundary, is used to generate streamflow data at the site of interest with known meteorological data. The hydrological model is first calibrated and validated at a gauged basin and then the model parameters are used appropriately at other ungauged sites within the modeling domain to simulate the flows using the calibrated model [8] [20]. Usually, several statistical indicators as well as visual inspection of the results (hydrographs and the water balance distribution in particular) are relied upon to determine the performance capacity and robustness of the model.

Since the simulation of the entire hydrologic cycle became a reality by Stanford Watershed Model as reported by Crawford and Linsley in 1966, modeling at large spatial scales and at small temporal scales [21] became possible with the recent development in hardware and software capabilities at an exponential rate in the last few decades [22]. Being able to use precise satellite data such as precipitation in hydrological models has further improved the performance and thus the overall applicability of hydrological models considerably around the globe. In recent years, application of hydrological models is becoming popular in Nepal, for assessment of water availability, planning purposes and to examine the impact of climate change in river hydrology [10] [23]-[28]. However, they are confined mainly to academic research studies. When the world is utilizing artificial intelligence as part of a data-driven approach to assist watershed modeling for stream flow generation [29], most of the project level studies in Nepal are still using coarse conventional methods in ungauged sites in Nepal, especially in the study of hydropower projects of different scales [19] [30] [31] [32]. As an awakening step, SWAT (Soil and Water Assessment Tool), a public domain hydrological model and capable for hydrological modeling in Nepalese catchments [23] [26] [27] [33] was used to estimate the flow at ungauged sites in this study and compared with other commonly used methods viz.WECS/DHM1990, NEA1997, DHM2004, DAR and its variant GT methods.

The Budhigandaki River Basin (BRB) of Nepal was chosen for the study. Six popular performance evaluation parameters viz. coefficient of determination (R^2), Mean Absolute Error (MAR), Root Mean Square Error (RMSE), Percentage of Volume Bias (PBIAS), Nash Sutcliff Efficiency (NSE) and Kling-Gupta Efficiency (KGE) [16] [34] were used to evaluate the considered flow estimation methods in this study. Global Performance Index (GPI) was introduced for overall evaluation of flow estimation methods. The assessed flow estimation methods in Nepal were ranked based on the GPI value. It was found that hydrological simulation ranked the best among the considered methods.

2. Study Area

The Budhidgandaki River Basin (BRB) is situated in the central part of Nepal, between 27˚50' and 29˚00'N latitudes and 84˚30' and 85˚10'E longitudes (**Figure**

1). It has an elongated shape with its main axis oriented north-south. Its length is about 113 km while the width is in the range of 15 and 30 km. The basin elevations range from 315 masl at Budhigandaki-Trishuli confluence to 8163 meters above sea level (masl) at Mount Manaslu (8th highest peak) of the world [35] with a mean basin elevation of 3723 m. The basin area, thus, falls in two physiographic regions; Middle Mountains and the Himalaya [36]. It is a part of the Narayani drainage system, bordered in the north by the vast Tibetan Plateau, in the south and east by the Trishuli River basin and in the west by the Marsyangdi River basin.

The reference flow gauging station is at Arughat (Department of Hydrology and Meteorology, DHM station #445) which is at an elevation of 485 masl. The catchment area of the BRB at this station is 3863 km^2 while it is 4985 km^2 for Budhigandaki-Dam site (**Figure 1**).

3. Theoretical Background

When any water resources development project is planned and implemented in an ungauged catchment, different methods are generally used to estimate the flow at the project sites. Among them, one set of values are chosen for the design purpose based on the prevailing site conditions and judgment of the hydrologist. The most popular methods used in the estimation of mean monthly flow at ungauged sites are given below.

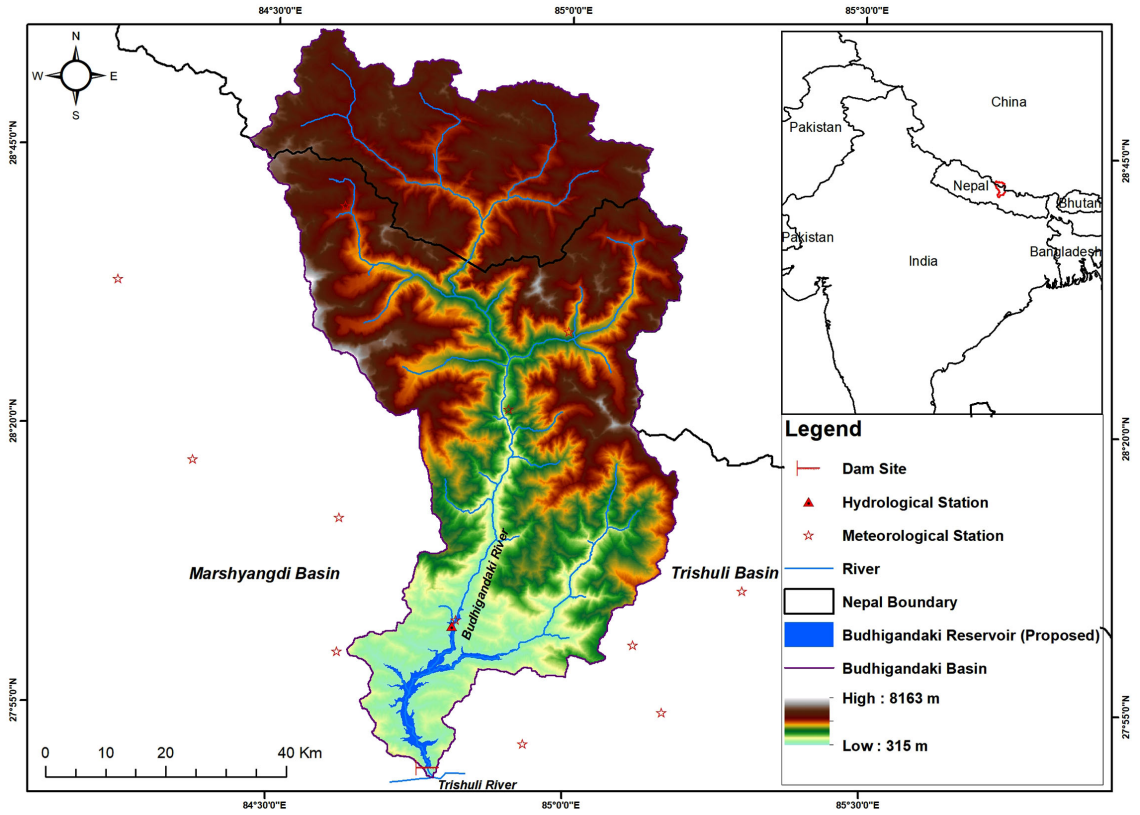

Figure 1. Location Map of the Budhigandki River Basin

3.1. Hydrological Simulation Method

Hydrological models have been broadly categorized depending on their spatial discretization (lumped, semi-distributed, fully-distributed), period of simulation (event-based or long term) and other complexities associated with the data requirement, governing equations and licensing issues. There is no doubt that they are gaining popularity in recent times. HEC-HMS, SWAT, MIKE SHE, MIKE NAM and VIC, among others, are some popular hydrological models used globally for assessing flows [29]. SWAT (Soil and Water Assessment Tool) model capable of simulating the hydrological process satisfactorily in Nepalese catchments [23] [26] [27] [33] was used for simulating the flows of the BRB in this study.

SWAT is a process-based semi-distributed hydrological model that is capable of simulating the impact of land management practices on flow, sediment and agricultural chemical yields in basins with varying soils, land use and management conditions [37]. Conceptually, SWAT divides a basin into sub-basins and further into Hydrological Response Units (HRUs). An HRU is a unique combination of land use, topographical and soil characteristics in a sub-watershed. SWAT simulates hydrology, vegetation growth and management practices at the HRU level [26]. SWAT simulates the hydrologic cycle based on the water balance equation as expressed in Equation (1).

$$SW_t = SW_0 + \sum_{i=1}^{t}\left[R_{day} - Q_{sur} - E_a - w_{seep} - Q_{gw}\right] \quad (1)$$

where:

SW_t is final soil water content (mm); SW_0 is initial soil water content on day i (mm); t is time (day); R_{day} is amount of precipitation on day i (mm); Q_{sur} is amount of surface runoff on day i (mm); E_a is amount of evapotranspiration on day i (mm); w_{seep} is amount of water entering into the vadose zone from the soil profile on day i (mm) and Q_{gw} is amount of return flow (from groundwater) on day i (mm).

3.2. WECS/DHM 1990 Method

The Water and Energy Commission Secretariat (WECS) and Department of Hydrology and Meteorology (DHM), Government of Nepal (GoN) [13] proposed a regression equation to estimate the long term mean monthly flow at an un-gauged site given in Equation (2).

$$Q_{mean} = CA_{total}^{\alpha} \cdot A_{<5k}^{\beta} \cdot \mathrm{MWI}^{\gamma} \quad (2)$$

where, Q_{mean} is the mean monthly flow (m^3/s); A_{total} is the total catchment area (km^2); $A_{<5k}$ is catchment area below 5000 masl elevation (km^2); MWI is monsoon wetness index (total rainfall of the catchment from June to September in mm); C is a regression constant; and α, β and γ are constants derived from the regression analysis for each month (supplementary, S-1).

3.3. NEA 1997 Method

Nepal Electricity Authority (NEA), GoN proposed another regression based

method to estimate the mean monthly flow for an un-gauged site [30]. It is given in Equation (3)

$$Q_{mean} = CA_{total}^{\alpha} \cdot \mathrm{MWI}^{\gamma} \tag{3}$$

where, constants C, α and γ for this method are given in S-2

3.4. DHM 2004 Method

The DHM developed Equations (4a and 4b) for the estimation of monthly flow [14]. For some months logarithmic transformation gave a better estimate while in the other months square root transformation performed better. Monthly flow estimation equation with logarithmic transformation takes the following form:

$$Q_{mean} = \exp\left[C + \varepsilon \cdot \ln(\mathrm{AvgElev}) + \rho \cdot \ln(\mathrm{AWI}) + \mu \cdot \ln(A_{<3k})\right] \tag{4a}$$

Monthly flow estimation equation with square root transformation takes the following form:

$$Q_{mean} = \left[C + \delta \cdot \sqrt{A_{<5k}}\right]^2 \tag{4b}$$

where, AvgElev is average elevation of the catchment (masl); AWI is annual wetness index (mm); $A_{<3k}$ is catchment area below 3000 masl elevation (km^2); and ε, ρ, μ and δ are the constants derived from regression analysis; their values are given in S-3. For March, April and May, square root transformation is better while for the other months, logarithmic transformation gives better estimates [14].

3.5. Drainage Area Ratio (DAR) Method

The DAR method is a simple method based on the assumption that the specific discharge calculated using the data from a flow gauging station remains constant within the basin [16] [17]. It is expressed as in Equation (5).

$$Q_{e\text{-}site} = \frac{Q_{gs}}{A_{gs}} A_{site} \tag{5}$$

where $Q_{e\text{-}site}$ is the estimated flow at the site of interest (m^3/s); Q_{gs} is the observed flow at gauging station (m^3/s); A_{gs} and A_{site} are the catchment areas (km^2) at the gauging station and site of interest respectively.

3.6. General Transposition (GT) Method

The GT method can be considered as an improved version of the DAR method, as it accounts the rainfall in addition to the drainage area. Although different variations of this method are found in application [19] [31], a simple form given in Equation (6) has been used in this study.

$$Q_{e\text{-}site} = \frac{Q_{gs}}{A_{gs}} \frac{P_{avg\text{-}site}}{P_{avg\text{-}gs}} A_{site} \tag{6}$$

where $P_{avg\text{-}site}$ and $P_{avg\text{-}gs}$ are the annual average precipitation values (mm) of the basin up to the site of interest and the gauging station respectively.

4. Data Collection and Analysis

Spatial data (digital elevation model, land use land cover map and soil map) and hydro-meteorological time series data (temperature, rainfall and discharge) are required for this study. The collected data types and their use are given in Table 1. The Digital Elevation Model (DEM) and soil map were downloaded from Shuttle Radar Topography Mission (SRTM) and SOTER soil map site respectively while Land Use and Land Cover (LULC) Map was obtained from International Center for Integrated Mountain Development (ICIMOD), Nepal, Department of Water Resources and Irrigation (DoWRI) and district soil map of Nepal Agriculture Research Council (NARC). Precipitation, maximum and minimum temperature and discharge of Budhigandaki river at Arughat (#445) was collected from the Department of Hydrology and Meteorology (DHM), GoN while discharge at Budhigandaki Hydroelectric Project (BGHEP) dam site was collected from BGHEP project office. Data collected by the BGHEP for two years during the feasibility study was only available at this site.

Total catchments area, area below 3000 masl and 5000 masl of Arughat gauging station and Budhigandaki Hydro-Electric Project (BGHEP) dam site were calculated using GIS. Annual wetness indexes, monsoon wetness index for the basin area were calculated from the available daily rainfall data. Mean monthly values of the observed flows of Arughat gauging station and BGHEP dam site were calculated from the available daily flow data.

The hydrological model was setup and calibrated using ArcSWAT and used to simulate the flow in the BRB. Model development was carried out by generating the river networks and sub-basins using the 30 m × 30 m SRTM DEM. Hydrological response units were generated from land use land cover, soil maps, and by providing slope ranges. The model was calibrated (1983-2002) and validated (2003-2012) at Arughat using 30 years flow data. However, simulation was done up to 2014 to see how the model performed at BGHEP dam site lying downstream of Arughat station (Figure 2). The model simulated flows were extracted at Arughat (1983-2012) and BGHEP dam site (2013-2014) and compared with the respective observed data.

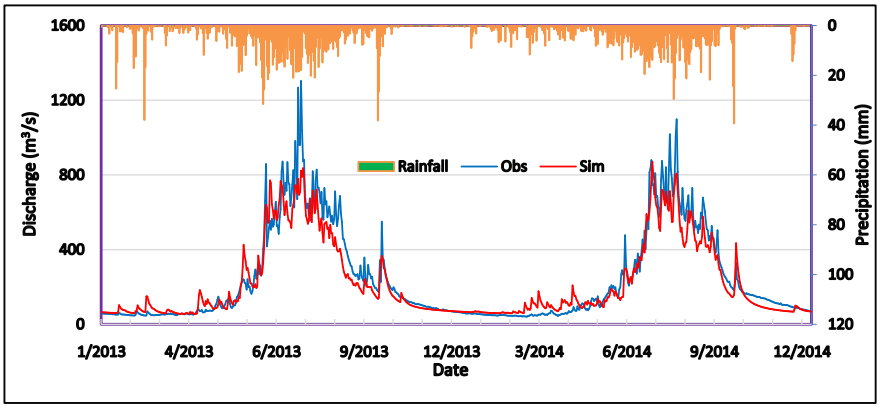

Figure 2. Hydrological simulation results at BGHEP dam site.

Table 1. Data used in the study.

SN	Data Type	Accessed Data/Available Period	Source	Application
		1. Spatial Data		
1.1	DEM (30 m resolution)	2019	Shuttle Radar Topography Mission (SRTM) DEM data [38]	Hydrological modeling/regression equations
1.2	LULC Map	2019	[39]	Hydrological modeling
1.3	Soil Map	2019	Soil and Terrain database system (SOTER) soil map of China and Nepal [38]	Hydrological modeling
		2. Time Series Data		
2.1	Temperature and Rainfall	1983-2014	DHM (daily) and Third Pole Environment (TPE)—3-hourly [40]	Hydrological modeling and use in flow estimation methods
2.2	Daily discharge at Arughat #445	1983-2014	DHM	Comparison with estimated value and to estimate discharge at BGHEP site

Mean monthly flows at Arughat and BGHEP dam site from WECS/DHM 1990, NEA 1997 and DHM 2004 methods were calculated using the equation given in Sections 3.2 to 3.4. Flows were transposed by DAR and GT methods to BGHEP dam site using observed monthly average flow data of Arughat station and vice versa.

5. Performance Evaluation

Performance of the various flow estimation methods explained above was evaluated objectively using goodness-of-fit measures by comparing the estimated and observed monthly flows. Performance evaluation of considered methods of the study at Arughat and BGHEP dam site were made using the following statistical parameters:

5.1. Coefficient of Determination (R^2)

Coefficient of Determination measures both the strength of the linear relationship between observed and estimated values. It is calculated by Equation (8).

$$R^2 = \left[\frac{\sum_{i=1}^{n} \left(Q_{0i} - \overline{Q_o}\right)\left(Q_{ei} - \overline{Q_e}\right)}{\sqrt{\sum_{i=1}^{n} \left(Q_{0i} - \overline{Q_o}\right)^2} \sqrt{\sum_{i=1}^{n} \left(Q_{ei} - \overline{Q_e}\right)^2}} \right]^2 \quad (8)$$

where, $\overline{Q_o}$ = Observed Annual Average Flow (m^3/s)

$\overline{Q_e}$ = Estimated Annual Average Flow (m^3/s)

Q_{0i} = Observed monthly average flow of month i

Q_{ei} = Estimated monthly average flow of month i

n = number of data. As number of months are 12, $n = 12$ in this case.

The coefficient of determination (R^2) is the square of the coefficient of correlation.

Criteria: Larger the value of R^2, better the performance.

5.2. Mean Absolute Error (MAE)

The MAE measures the average of the deviation of the estimated values with respect to the observed ones. It is calculated using Equation (9).

$$\text{MAE} = \frac{1}{n}\sum_{i=1}^{n}\left|Q_{0i} - Q_{ei}\right| \tag{9}$$

Criteria: Smaller the value of MAE, better the performance.

5.3. Root Mean Square Error (RMSE)

The RMSE measures the differences between the estimated and observed values. It is given as Equation (10).

$$\text{RMSE} = \sqrt{\frac{1}{n}\sum_{i=1}^{12}\left(Q_{0i} - \overline{Q_o}\right)^2} \tag{10}$$

Criteria: Smaller the value of RMSE, better the performance.

5.4. Percentage Volume Bias (PBIAS)

The PBIAS measures the degree of volume biasness between the observed and estimated values. It is given by Equation (11).

$$\text{PBIAS} = \frac{\sum_{i=1}^{n} V_o - \sum_{i=1}^{n} V_e}{\sum_{i=1}^{n} V_o}\% \tag{11}$$

where V_o = Observed total volume

V_e = Estimated total volume

Criteria: Smaller the absolute value of PBIAS, better the performance. The sign of the PBIAS value shows the direction towards which the estimated result is biased: +ve value is an indication of underestimation while −ve value shows overestimation.

5.5. Nash Sutcliff Efficiency (NSE)

The NSE is a normalized statistic that determines the relative magnitude of the residual variance compared to the observed value variance. It is calculated with Equation (12).

$$\text{NSE} = 1 - \left[\frac{\sum_{i=1}^{12}\left(Q_{0i} - Q_{ei}\right)^2}{\sum_{i=1}^{12}\left(Q_{0i} - \overline{Q_o}\right)^2}\right] \tag{12}$$

Criteria: Larger the value of NSE, better the performance.

5.6. Kling-Gupta Efficiency (KGE)

The KGE is considered as an improvement over the widely used NSE which considers different types of model/estimation errors, namely the error in the mean, the variability and the dynamics. The KGE is calculated using Equation (13).

$$\text{KGE} = 1 - \sqrt{\sum_{i=1}^{n}\left(r-1\right)^2 + \left(\frac{Q_{e\text{-}sd}}{Q_{0\text{-}sd}} - 1\right)^2 + \left(\frac{\overline{Q_e}}{\overline{Q_o}} - 1\right)^2} \tag{13}$$

where, r = correlation coefficient

$Q_{0\text{-}sd}$ = Standard deviation of observed flow

$Q_{e\text{-}sd}$ = Standard deviation of estimated flow

Criteria: Larger the value of KGE, better the performance.

5.7. Global Performance Index

A total of six performance evaluation criteria of the flow estimation methods are discussed above. However, assessment and comparison of the individual evaluation criteria and thus establishing the preference of one criterion over another is beyond the scope of this paper. Therefore, all the criteria are treated with equal weights while evaluating the overall performance of the flow estimation methods. To find the best method, the lowest performing method to the highest performing method with respect to a given parameter were assigned values from 1 to 6 in increments of one. If two/three values are equal, average of the two/three values are assigned for both/all of them. For example, if the NSE values calculated for Hydro-Sim, WECS1990, NEA1997, DHM2004, DAR and GT methods are 0.97, 0.67,0.95, 0.67, 0.74 and 0.92 respectively, then the respective numerical values these methods get are 6, 1.5, 5, 1.5, 3 and 4. The WECS1990 and DHM2004 methods have equal values of NSE *i.e.*, 0.67, and therefore both these methods are assigned 1.5 (average of 1 and 2). The mean value of performance of each method was then calculated as Global Performance Index (GPI) as given by Equation (14).

$$\mathrm{GPI}_j = \frac{\mathrm{R}_j^2 + \mathrm{MAE}_j + \mathrm{RMSE}_j + \mathrm{PBIAS}_j + \mathrm{NSE}_j + \mathrm{KGE}_j}{6} \tag{14}$$

where j represents the estimating method, say, for hydrological simulation method $j = 1$ while for DAR method, $j = 5$.

Based on the GPI value, the six considered methods are ranked from first to sixth such that higher the GPI value, better the method for monthly flow estimation.

6. Results and Discussion

6.1. Comparison of Average Flows at Arughat

The observed and estimated average monthly flows at Arughat gauging station are given in supplementary material (S-5) and depicted in Figure 3. Numerical figures of Goodness-of-fit of different flow estimation methods are presented in Table 2. It is to be noted here that performance evaluation of simulation results, WECS/DHM1990, NEA1997 and DHM2004 methods are made with respect to long term averages of observed flow (1983-2012: Obs-A) at Arughat. However, DAR and GT estimates are compared with the average of two years data (2013-2014: Obs-B) at BGHEP Dam site. This limitation is because measured data at BGHEP dam site is not available for the other years. It is assumed that such difference will have minimum impact on performance parameters.

Considering the monthly values, R^2 is almost the same for all the methods. All

the other calculated performance parameters except MAE show that the simulated flows obtained through SWAT hydrological modeling are found closer to the observed values. Even for MAE, the calculated value is very close to the NEA 1997 method. Thus, from the table, the overall performance ranking indicates that that hydrological simulation is the best among the methods considered in the study to estimate the flows for Arughat at monthly time steps. Further, the NEA 1997 and GT methods ranked second and third in terms of performance ranking.

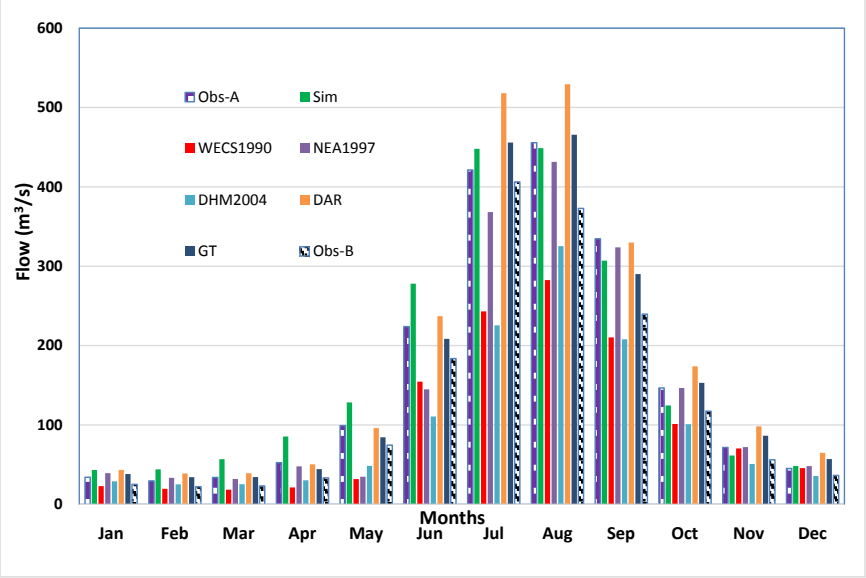

Figure 3. Comparison of monthly flows at arughat.

Table 2. Performance parameters of estimated methods at arughat.

Data Length	Obs-A: 30 years (1983-2012)						Obs-B: 2 years (2013-2014)
Parameters	**Hydro Sim**	**WECS1990**	**NEA1997**	**DHM2004**	**DAR**	**GT**	**Parameters**
R^2	0.98	0.97	0.97	0.96	0.99	0.99	**R^2**
MAE	21.6	60.6	20.9	61.0	52.4	30.2	**MAE**
RMSE	36.6	209.6	65.1	211.4	181.5	104.5	**RMSE**
PBIAS	−6.4	37.3	11.6	37.6	−39.5	−22.7	**PBIAS**
NSE	0.97	0.67	0.95	0.67	0.74	0.92	**NSE**
KGE	0.87	0.45	0.81	0.45	0.49	0.72	**KGE**
GPI	5.5	2.1	4.8	1.3	3.1	4.3	**GPI**
Performance Rank	**I**	**V**	**II**	**VI**	**IV**	**III**	**Performance Rank**

Obs-A: Observed flow data from DHM; Hydro Sim: Simulated flow using SWAT; WECS1990: Flow calculated using the WECS/DHM-1990 method; NEA1997: Flow calculated using the NEA-1997 method; DHM2004: Flow calculated using the DHM-2004 method; DAR: Flow calculated using drainage area ratio method; GT: Flow calculated using general transposition method; Obs-B: Observed flow data from BGHP at the dam site.

From the viewpoint of availability of flow for electricity production and demand of the electrical energy, three distinct seasons can be seen in Nepal [19]: Dry (December to May), Monsoon (June to September) and Post Monsoon (October and November). Seasonal evaluation at Arughat gauging site was also done following the methods discussed above to see whether the performance of each method differed from the monthly time steps. GPI based ranking in dry, monsoon and post-monsoon seasons are presented in Table 3. For dry and post-monsoon seasons, the GT and NEA 1997 methods respectively showed the best performance while hydrological simulation is next to these methods in both cases. However, its performance is better than the other methods in the monsoon season. This is particularly important in most Nepalese catchments where the runoff is largely rainfall driven. Based on weighted average GPI, the GT method ranks first in overall. Hydrological simulation and NEA 1997 methods rank second and third respectively. The remaining three methods are not found satisfactory in terms of seasonal performance.

6.2. Comparison of Average Flows at Budhigandaki Dam Site

The monthly observed and estimated flows by different methods at Budhigandaki Dam site are given in S-6 and shown in Figure 4. Values of the different performance parameters of those methods are presented in Table 4. They clearly indicate that the hydrological simulation method is the best by all criteria. The GT method ranked second as shown by the respective values while the DAR method ranked the last.

Seasonal performance of these methods at Budhigandaki dam site was also analyzed to see if it is consistent with the monthly and annual performance. The calculated seasonal GPI of the six performance parameters and its weightage average are given in Table 5. Although the dry season performance is found better for the GT method, hydrological simulation is found better for the other two seasons. The weighted GPI is the highest for hydrological modeling which is similar to the results of the whole year at this site (Table 4). Based on the overall GPI value, the hydrological simulation ranked first, GT the second and NEA 1997 the last.

Table 3. Seasonal Performance of flow estimation methods at Arughat.

GPI and Rank	Hydro Sim	WECS1990	NEA1997	DHM2004	DAR	GT
GPI-Dry Season	3.83	1.50	3.50	3.83	2.92	5.42
GPI-Monsoon	4.92	2.33	4.58	1.25	3.42	4.50
GPI Post Monsoon	4.67	3.08	5.58	2.42	1.92	3.33
GPI-Weighted Average	4.33	2.04	4.21	2.74	2.92	4.76
Rank	II	VI	III	V	IV	I

Table 4. Performance parameters of estimated methods at the budhigandaki dam site.

Data length	2 years (2013-2014)					
Parameters	**Hydro Sim**	**WECS1990**	**NEA1997**	**Q_DHM2004**	**DAR**	**GT**
R^2	0.99	0.97	0.96	0.95	0.99	0.99
MAE	38	52	54	51	68	44
RMSE	69	181	186	176	234	153
PBIAS	8.39	21.88	22.62	21.26	28.30	18.51
NSE	0.95	0.89	0.88	0.88	0.85	0.94
KGE	0.78	0.69	0.67	0.69	0.63	0.76
GPI	5.83	3.25	2.08	3.17	1.67	5.00
Performance Rank	I	III	V	IV	VI	II

Table 5. Seasonal performance of flow estimation methods at budhigandaki dam site.

GPI and Rank	**Hydro Sim**	**WECS1990**	**NEA1997**	**DHM2004**	**DAR**	**GT**
GPI-Dry Season	4.67	2.42	2.00	3.42	2.92	5.58
GPI-Monsoon	5.50	3.25	2.08	2.75	2.17	5.25
GPI Post Monsoon	5.50	4.83	3.17	3.83	1.42	2.25
GPI-Weighted Average	5.08	3.10	2.22	3.26	2.42	4.92
Rank	I	IV	VI	III	V	II

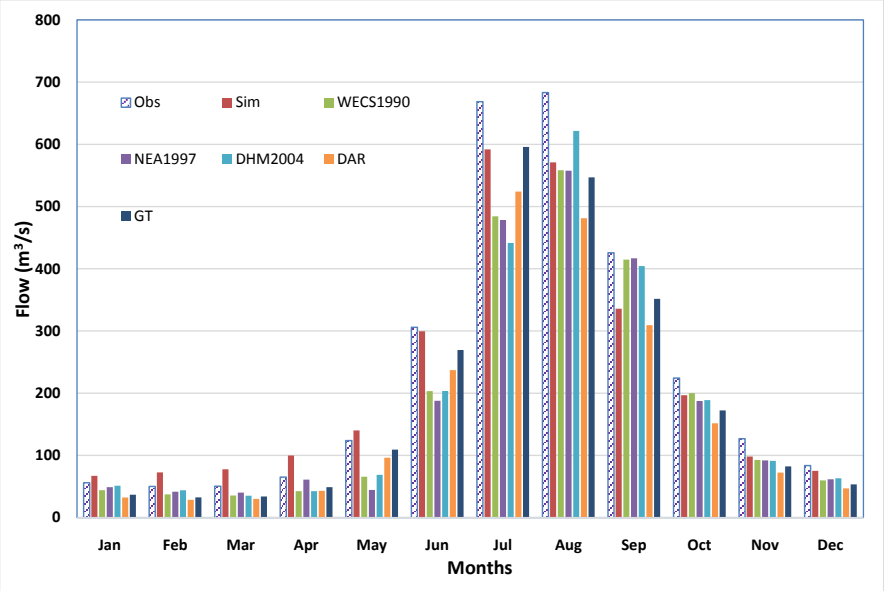

Figure 4. Comparison of monthly flow at budhigandaki dam site.

Based on the results presented above, it can be inferred that hydrological simulation method is the best among the other considered methods of flow estimation in the BRB. It is to be noted here that the WECS 1990, NEA 1997 and DHM 2004 are regional methods and their coefficients are average values which

have been established by regression analysis. Thus, these methods may perform better in some catchments while poorer in the others depending upon how well the coefficients represent the catchment characteristics. Since the DAR method does not account the rainfall variation, it might be better suited for in regions where rainfall variation is small. The GT method takes into account the rainfall, and therefore, it performs better than the regional and the DAR methods. However, it does not take into consideration the spatial variation in soil type and land use/land cover. Hydrological modeling takes all these factors into account and the flow estimated by this method is better than that by all the other considered regional methods for ungauged basins. Another advantage of the hydrological simulation method over others is that it provides continuous data at the site of interest which could be extremely useful for hydrological analysis required for any water resources project development works. However, it is extremely important that quality (length, accuracy and reliability) of the input data for model setup as well as calibration and validation is mandatory for the hydrological model to perform its best.

7. Conclusion

This study was carried out to evaluate the performance of different flow generation methods namely, DAR, GT, DHM/WECS 1990, NEA 1997, DHM 2004 and hydrological modeling using SWAT. The estimated flows from each method were compared with the observed flows at Arughat and BGHEP dam site of the Budhigandaki River Basin. Six performance parameters viz. R^2, MAE, RMSE, PBIAS, NSE and KGE were used to evaluate the considered flow estimation methods. For overall evaluation of these flow estimation methods, Global Performance Index (GPI) was introduced. Results show that hydrological modeling is the best among all considered methods for estimating flows at monthly timescales. Carrying out hydrological analyses using suitable hydrological model(s) for Nepalese river basins is recommended as a policy prescription to the Government of Nepal so that flow at the site of interest can be obtained when required for any water resources development project.

Conflicts of Interest

The authors declare no conflicts of interest regarding the publication of this paper.

References

[1] UNEP (2012) The UN-Water Status Report on the Application of Integrated Approaches to Water Resources Management. United Nations Development Programme.

[2] Flint, R.W. (2004) The Sustainable Development of Water Resources. *Water Resources Update*, **127**, 48-59.

[3] World Bank (2017) Water Resources Management. https://www.worldbank.org/en/topic/waterresourcesmanagement

[4] Devkota, R.P. and Maraseni, T. (2018) Flood Risk Management under Climate Change:

A Hydro-Economic Perspective. *Water Science and Technology*: *Water Supply*, **18**, 1832-1840. https://doi.org/10.2166/ws.2018.003

[5] Reddy, P.J. (2001) A Text Book of Hydrology. Laxmi Publications P. Ltd., New Delhi.

[6] Razavi, T. and Coulibaly, P. (2016) Improving Streamflow Estimation in Ungauged Basins Using a Multi-Modelling Approach. *Hydrological Sciences Journal*, **61**, 2668-2679. https://doi.org/10.1080/02626667.2016.1154558

[7] Young, A.R. (2006) Stream Flow Simulation within UK Ungauged Catchments Using a Daily Rainfall-Runoff Model. *Journal of Hydrology*, **320**, 155-172. https://doi.org/10.1016/j.jhydrol.2005.07.017

[8] Loukas, A. and Vasiliades, L. (2014) Streamflow Simulation Methods for Ungauged and Poorly Gauged Watersheds. *Natural Hazards and Earth System Sciences*, **14**, 1641-1661. https://doi.org/10.5194/nhess-14-1641-2014

[9] Mwakalila, S. (2003) Estimation of Stream Flows of Ungauged Catchments for River Basin Management. *Physics and Chemistry of the Earth*, *Parts A/B/C*, **28**, 935-942. https://doi.org/10.1016/j.pce.2003.08.039

[10] Devkota, R.P., Pandey, V.P., Bhattarai, U., Shrestha, H., Adhikari, S. and Dulal, K.N. (2017) Climate Change and Adaptation Strategies in Budhi Gandaki River Basin, Nepal: A Perception-Based Analysis. *Climatic Change*, **140**, 195-208. https://doi.org/10.1007/s10584-016-1836-5

[11] Devkota, R., Bhattarai, U., Devkota, L. and Maraseni, T.N. (2020) Assessing the Past and Adapting to Future Floods: A Hydro-Social Analysis. *Climatic Change*, **163**, 1065-1082. https://doi.org/10.1007/s10584-020-02909-w

[12] Zamoum, S. and Souag-Gamane, D. (2019) Monthly Streamflow Estimation in Ungauged Catchments of Northern Algeria Using Regionalization of Conceptual Model Parameters. *Arabian Journal of Geosciences*, **12**, Article No. 342. https://doi.org/10.1007/s12517-019-4487-9

[13] WECS (1990) Methodology for Estimating Hydrological Characteristics of Ungauged Locations in Nepal, His Majesty's Government of Nepal. Ministry of Water Resources, Seq. No. 331, Water and Energy Commission Secretariat and Department of Hydrology and Meteorology, Kathmandu.

[14] Sharma, K.P. and Adhikari, N.R. (2004) Hydrological Estimation in Nepal. Department of Hydrology and Meteorology, Government of Nepal, Kathmandu.

[15] Samuel, J., Coulibaly, P. and Metcalfe, R.A. (2011) Estimation of Continuous Streamflow in Ontario Ungauged Basins: Comparison of Regionalization Methods. *Journal of Hydrologic Engineering*, **16**, 447-459. https://doi.org/10.1061/(ASCE)HE.1943-5584.0000338

[16] Yilmaz, M.U. and Onoz, B. (2020) A Comparative Study of Statistical Methods for Daily Streamflow Estimation at Ungauged Basins in Turkey. *Water*, **12**, 459. https://doi.org/10.3390/w12020459

[17] Emerson, D.G., Vecchia, A.V. and Dahl, A.L. (2005) Evaluation of Drainage-Area Ratio Method Used to Estimate Streamflow for the Red River of the North Basin, North Dakota and Minnesota: Scientific Investigation Report 2005-5017. https://doi.org/10.3133/sir20055017

[18] Ergen, K. and Kentel, E. (2016) An Integrated Map Correlation Method and Multiple-Source Sites Drainage-Area Ratio Method for Estimating Streamflows at Ungauged Catchments: A Case Study of the Western Black Sea Region, Turkey. *Journal of Environmental Management*, **166**, 309-320. https://doi.org/10.1016/j.jenvman.2015.10.036

[19] BGHEP (2015) Feasibility Study and Detailed Design of Budhigandaki Hydropower Project Part 1 Budhigandaki Hydroelectric Project Development Committee. Government of Nepal, Kathmandu.

[20] Wagener, T., Wheater, H. and Gupta, H.V. (2004) Rainfall-Runoff Modelling in Gauged and Ungauged Catchments. World Scientific. https://doi.org/10.1142/p335

[21] Singh, V.P. (2018) Hydrologic Modeling: Progress and Future Directions. *Geoscience Letters*, **5**, Article No. 15. https://doi.org/10.1186/s40562-018-0113-z

[22] Maraseni, T., An-Vo, D.-A., Mushtaq, S. and Reardon-Smith, K. (2021) Carbon Smart Agriculture: An Integrated Regional Approach Offers Significant Potential to Increase Profit and Resource Use Efficiency, and Reduce Emissions. *Journal of Cleaner Production*, **282**, 124555. https://doi.org/10.1016/j.jclepro.2020.124555

[23] Devkota, L.P. and Gyawali, D.R. (2015) Impacts of Climate Change on Hydrological Regime and Water Resources Management of the Koshi River Basin, Nepal. *Journal of Hydrology*: *Regional Studies*, **4**, 502-515. https://doi.org/10.1016/j.ejrh.2015.06.023

[24] Shrestha, S., Shrestha, M. and Babel, M.S. (2016) Modelling the Potential Impacts of Climate Change on Hydrology and Water Resources in the Indrawati River Basin, Nepal. *Environmental Earth Sciences*, **75**, Article No. 280. https://doi.org/10.1007/s12665-015-5150-8

[25] Bajracharya, A.R., Bajracharya, S.R., Shrestha, A.B. and Maharjan, S.B. (2018) Climate Change Impact Assessment on the Hydrological Regime of the Kaligandaki Basin, Nepal. *Science of the Total Environment*, **625**, 837-848. https://doi.org/10.1016/j.scitotenv.2017.12.332

[26] Bharati, L., Bhattarai, U., Khadka, A., Gurung, P., Neumann, L.E., Penton, D.J., Dhaubanjar, S. and Nepal, S. (2019) From the Mountains to the Plains: Impact of Climate Change on Water Resources in the Koshi River Basin. IWMI Working Paper-187, International Water Management Institute (IWMI), Colombo. https://doi.org/10.5337/2019.205

[27] Lamichhane, S. and Shakya, N.M. (2019) Integrated Assessment of Climate Change and Land Use Change Impacts on Hydrology in the Kathmandu Valley Watershed, Central Nepal. *Water*, **11**, 2059. https://doi.org/10.3390/w11102059

[28] Pandey, V.P., Dhaubanjar, S., Bharati, L. and Thapa, B.R. (2020) Spatio-Temporal Distribution of Water Availability in Karnali-Mohana Basin, Western Nepal: Hydrological Model Development Using Multi-Site Calibration Approach (Part-A). *Journal of Hydrology*: *Regional Studies*, **29**, 100690. https://doi.org/10.1016/j.ejrh.2020.100690

[29] Daniel, E.B., Camp, J.V., LeBoeuf, E.J., Penrod, J.R., Dobbins, J.P. and Abkowit, M.D. (2011) Watershed Modeling and Its Applications: A State-of-the-Art Review. *The Open Hydrology Journal*, **5**, 26-50. https://doi.org/10.2174/1874378101105010026

[30] NEA and JICA (2003) The Basic Study for the Rural Electrification through Small Hydropower Development in Rural Hilly Areas in Nepal. Final Report, Kathmandu.

[31] DOED (2018) Hydrological, Sedimentation and GLOF Study Report for Feasibility and Environmental Impact Assessment Study of Arun-4 Hydropower Project. Department of Electricity Development, Kathmandu.

[32] DOED (2020) Design Guidelines for Headworks of Hydropower Projects. Department of Electricity Development, Ministry of Energy, Water Resource and Irrigation, Government of Nepal, Kathmandu.

[33] Pandey, V.P., Dhaubanjar, S., Bharati, L. and Thapa, B.R. (2020) Spatio-Temporal

Distribution of Water Availability in Karnali-Mohana Basin, Western Nepal: Climate Change Impact Assessment (Part-B). *Journal of Hydrology: Regional Studies*, **29**, 100691. https://doi.org/10.1016/j.ejrh.2020.100691

[34] Burgan, H.I. and Aksoy, H. (2020) Monthly Flow Duration Curve Model for Ungauged River Basins. *Water*, **12**, 338. https://doi.org/10.3390/w12020338

[35] MoCTCA (2014) Mountaineering in Nepal Facts and Figures Ministry of Culture, Tourism and Civil Aviation (MoCTCA), Government of Nepal.

[36] DHM (2017) Observed Climate Trend Analysis in the Districts and Physiographic Regions of Nepal (1971-2014). Department of Hydrology and Meteorology, Government of Nepal, Kathmandu.

[37] Srinivasan, R., Ramanarayanan, T.S., Arnold, J.G. and Bednarz, S.T. (1998) Large Area Hydrologic Modeling and Assessment Part II: Model Application. *Journal of the American Water Resources Association*, **34**, 91-101. https://doi.org/10.1111/j.1752-1688.1998.tb05962.x

[38] DoWRI (2019) Irrigation Master Plan Preparation through Integrated River Basin Planning (Dataset). Water Resources Project Preparatory Facility, Department of Water Resources and Irrigation, Ministry of Energy, Water Resources and Irrigation (MoEWRI), Nepal.

[39] ICIMOD (2010) Land Cover of Nepal 2010 [Dataset]. International Center for Integrated Mountain Development (ICIMOD), Kathmandu. http://rds.icimod.org/Home/DataDetail

[40] Yang, K. and He, J. (2019) China Meteorological Forcing Dataset (1979-2018). National Tibetan Plateau Data Center, Beijing.

water

MDPI

Article

Application of SWAT in Hydrological Simulation of Complex Mountainous River Basin (Part II: Climate Change Impact Assessment)

Suresh Marahatta [1,*], Deepak Aryal [1], Laxmi Prasad Devkota [2,3], Utsav Bhattarai [3,4] and Dibesh Shrestha [3]

1 Central Department of Hydrology and Meteorology, Tribhuvan University, Kathmandu 44600, Nepal; deepak.aryal@cdhm.tu.edu.np
2 Nepal Academy of Science and Technology (NAST), Kathmandu 44600, Nepal; lpdevkota1@gmail.com
3 Water Modeling Solutions Pvt. Ltd. (WMS), Kathmandu 44600, Nepal; utsav.bhattarai@wms.com.np (U.B.); dibeshshrestha@live.com (D.S.)
4 Institute for Life Sciences and the Environment, University of Southern Queensland, Toowoomba, QLD 4350, Australia
* Correspondence: suresh.marahatta@cdhm.tu.edu.np

Abstract: This study aims at analysing the impact of climate change (CC) on the river hydrology of a complex mountainous river basin—the Budhigandaki River Basin (BRB)—using the Soil and Water Assessment Tool (SWAT) hydrological model that was calibrated and validated in Part I of this research. A relatively new approach of selecting global climate models (GCMs) for each of the two selected RCPs, 4.5 (stabilization scenario) and 8.5 (high emission scenario), representing four extreme cases (warm-wet, cold-wet, warm-dry, and cold-dry conditions), was applied. Future climate data was bias corrected using a quantile mapping method. The bias-corrected GCM data were forced into the SWAT model one at a time to simulate the future flows of BRB for three 30-year time windows: Immediate Future (2021–2050), Mid Future (2046–2075), and Far Future (2070–2099). The projected flows were compared with the corresponding monthly, seasonal, annual, and fractional differences of extreme flows of the simulated baseline period (1983–2012). The results showed that future long-term average annual flows are expected to increase in all climatic conditions for both RCPs compared to the baseline. The range of predicted changes in future monthly, seasonal, and annual flows shows high uncertainty. The comparative frequency analysis of the annual one-day-maximum and -minimum flows shows increased high flows and decreased low flows in the future. These results imply the necessity for design modifications in hydraulic structures as well as the preference of storage over run-of-river water resources development projects in the study basin from the perspective of climate resilience.

Keywords: climate change; fractional difference; SWAT; quantile mapping; extreme flow

Citation: Marahatta, S.; Aryal, D.; Devkota, L.P.; Bhattarai, U.; Shrestha, D. Application of SWAT in Hydrological Simulation of Complex Mountainous River Basin (Part II: Climate Change Impact Assessment). *Water* **2021**, *13*, 1548. https://doi.org/10.3390/w13111548

Academic Editor: Raghavan Srinivasan

Received: 9 April 2021
Accepted: 24 May 2021
Published: 31 May 2021

1. Introduction

Traditional energy sources along with human labour and draught transport were replaced initially by coal and then by oil in the early 1900s for powering machines and transportation [1,2]. Access to cheaper fossil fuels has been a major milestone for modern development pathways [3]. Since the beginning of the industrial age, the ability to harness and use different forms of energy has led to global economic growth and an increase in production and consumption, which enabled people to perform increasingly productive tasks and to improve the living standards of billions of people [4,5]. However, scientific evidence indicates that huge emissions of CO_2 and other greenhouse gases (GHGs) in the atmosphere are associated with the increasing use of fossil fuel [6,7]. The era of the industrial revolution can, thus, be taken as the starting point of climate change (CC) as the scientific community has defined it today [8]. With the widespread use of fossil fuels and

human interventions after the first industrial revolution, global warming has emerged as an environmental issue that has captured the attention of the world [9].

CC has become a major challenge and threat to the planet, particularly after World War II. Although alteration to the Earth's climate has been going on forever, we have started acknowledging its impacts on humans and the current environment only in the second half of the 20th century [9]. The first world conference on the environment held in Stockholm in June 1972 [10] formally opened the doors for a dialogue between industrialized and developing countries on the link between economic growth; the pollution of the air, water, and oceans; and the wellbeing of people around the world. Moreover, the formation of the United Nations Environment Programme (UNEP) is one of the major achievements of the Stockholm conference. The UN World Meteorological Organization (WMO) and UNEP established the Intergovernmental Panel on Climate Change (IPCC) with the objective of conducting and disseminating the findings of scientific research on CC in 1988 [11]. The Second Earth Summit organized by the UN in Rio de Janeiro, Brazil, in June 1992 formed a mechanism for cooperation between states, sectors, and people on issues related to environmental protection and sustainable economic development [12]. Further, in 1997, the Kyoto Protocol set the first GHG emission reduction targets for industrialized nations. In this regard, a total of 192 nations of the world committed to reducing their emissions by an average of 5.2% by 2012, which is popularly referred to as Kyoto Protocol [13]. The United Nations Climate Change Conference held in December 2009 documented that CC is one of the greatest challenges of the present day and prescribed that actions be taken to keep temperature increases to below 2 °C [14]. The 2015 Paris COP 21, a global consensus, established that average global warming needs to be kept below 1.5 to 2 °C to avoid the irreversible threat to environmental, economic, social, and political challenges by CC for years and decades to come [15]. The IPCC reports that all currently available global climate models (GCMs) agree on an increase in global mean temperature over the 21st century. The latest assessment report by the IPCC (AR6) has recommended limiting global warming to 1.5 °C in order to significantly reduce the risks and impacts of CC [16].

The GCMs and regional climate models (RCMs) have been found to be effective tools in developing a better understanding of CC by predicting future climate projections [17,18]. Scientists of the Geophysical Fluid Dynamics Laboratory (GFDL), National Oceanic and Atmospheric Administration (NOAA), developed the first coupled ocean-atmosphere general circulation climate model (GCM) in the 1960s capable of simulating the temperatures and precipitation of the past 50 years [19,20]. Following GFDL, many other studies across the world have developed different climate models. For example, the Hadley Centre Global Environment Model (HadGEM) [21], the Canadian Earth System Model (CanESM) [22], and the Max Planck Institute for Meteorology (MPI) [23] are some notable GCMs, while the Seoul National University Regional Climate Model (SNURCM) [24], the Max Planck Institute for Meteorology—REMO2009 [25], and the Conformal Cubic Atmospheric Model (CCAM) [26] are popular RCMs. Lately, it has become very convenient to use these GCM/RCM datasets in hydrological models such as the Système Hydrologique Européen (MIKE SHE), the Soil and Water Assessment Tool (SWAT), and the Variable Infiltration Capacity (VIC), among others, for CC studies. Comparing future climate projections with the baseline period to reach meaningful conclusions has been a routine procedure in the hydrological modelling and CC domains. Water availability studies using the output of climate models have been carried out at global [27], regional [28], and local scales [29]. Several studies have been conducted to assess the water availability and impacts of CC in the Hindu Kush Himalayan region [30–33] that includes the Budhigandaki River Basin (BRB) [34–36]. Results of such studies vary considerably across the spatial and temporal scales, and thus a generic conclusion on the impact of CC in water availability cannot be reached deterministically. These studies suggest the SWAT model can be a useful tool to assess the flow and water balance and the impacts of CC on them.

The quantification of available water at the local scale and examining how it is impacted by CC is extremely important from a water management perspective at the river

basin level. The overarching objective of this study is to analyse the impact of CC on the hydrology of a complex mountainous river basin, namely the Budhigandaki River Basin (BRB) of Nepal. The well-calibrated and validated SWAT model (in Part I of this research) was used to simulate future flows using future CC data [37]. A relatively new approach of selecting climate models representing four different extreme cases (warm-wet, cold-wet, warm-dry, and cold-dry conditions) were applied in the study. Generally, analysis of the impact of CC was limited to annual, monthly, and seasonal flows and based on people's perceptions in most of the previous studies [32,34,38–40]. This study has extended the analyses further to compare with the baseline condition the results of the frequency analysis of the annual one-day-maximum and -minimum flows for three-time windows, i.e., immediate, mid, and far futures.

2. Methodology and Data

The methodological framework used in this study is depicted in Figure 1. Future data of different global climate models (GCMs) to assess the impact of climate change (CC) on the Budhigandaki River Basin (BRB) was projected for 79 years (2021–2099). These climate data were considered for two RCPs, 4.5 (stabilization scenario) and 8.5 (high emission scenario), of the Intergovernmental Panel on Climate Change Fifth Assessment Report (IPCC AR5) [41]. A brief description of the selected GCMs and their selection criteria, bias correction methods, impact of CC on climatic parameters and hydrology, and frequency analysis of extreme flows are given below.

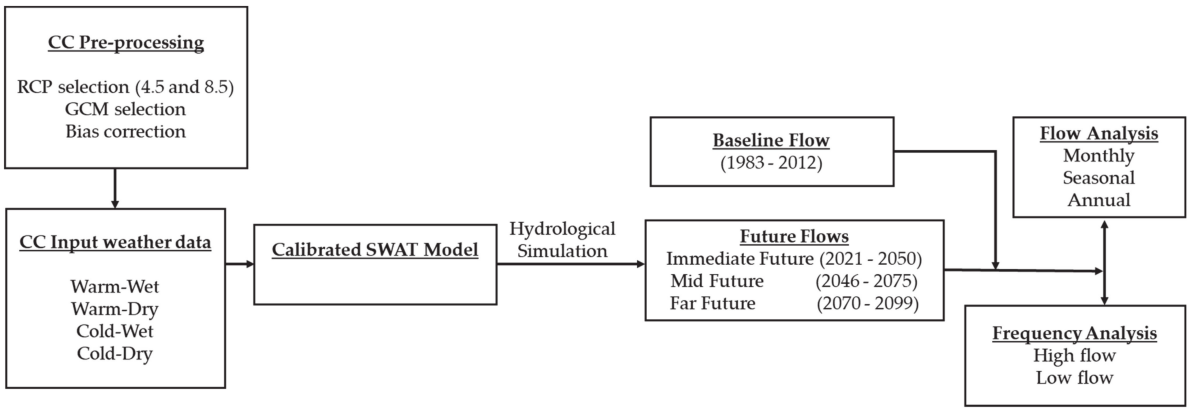

Figure 1. Overall methodological framework.

2.1. Hydrological Modelling

The Soil and Water Assessment Tool (SWAT), a continuous-time, semi-distributed, process-based river basin simulation model [42,43] capable of simulating hydrology and other environmental processes, was used in the study to examine the impact of CC on the basin hydrology. The Budhigandaki River Basin (BRB) was divided into 16 sub-basins and 344 hydrologic response units (HRUs) to capture the spatial heterogeneity across the basin. The model was calibrated and validated at the Arughat hydrological station. Moreover, supplementary validation of the model was done at three locations upstream and downstream of Arughat. The model performance was evaluated using four widely used statistical indicators: Nash–Sutcliffe efficiency (NSE), root mean square standard deviation ration (RSR), percent bias (PBIAS), and Kling–Gupta efficiency (KGE). Details of the SWAT hydrological model development and its evaluation are discussed in the first part of this study [37].

2.2. Selection of Climate Models

This study used the advanced envelop-based climate selection method to assess the projected future climates as described in Lutz et al. [28]. It is based on two general criteria for the selection of GCMs: (a) GCMs should be common to a pool of models with changes

in temperature and precipitation, and (b) they must be available on a continuous daily scale. Based on these two conditions, 105 models for RCP 4.5 and 78 models for RCP 8.5 scenarios were included in the initial pool of models. Climatic data (mean temperature and precipitation) were obtained from GCMs through the KNMI climate explorer interface (https://climexp.knmi.nl/start.cgi, accessed on 16 June 2020) for the study area. The applied method uses three steps connecting future projections with past performance (1981–2005), as shown in Figure 2.

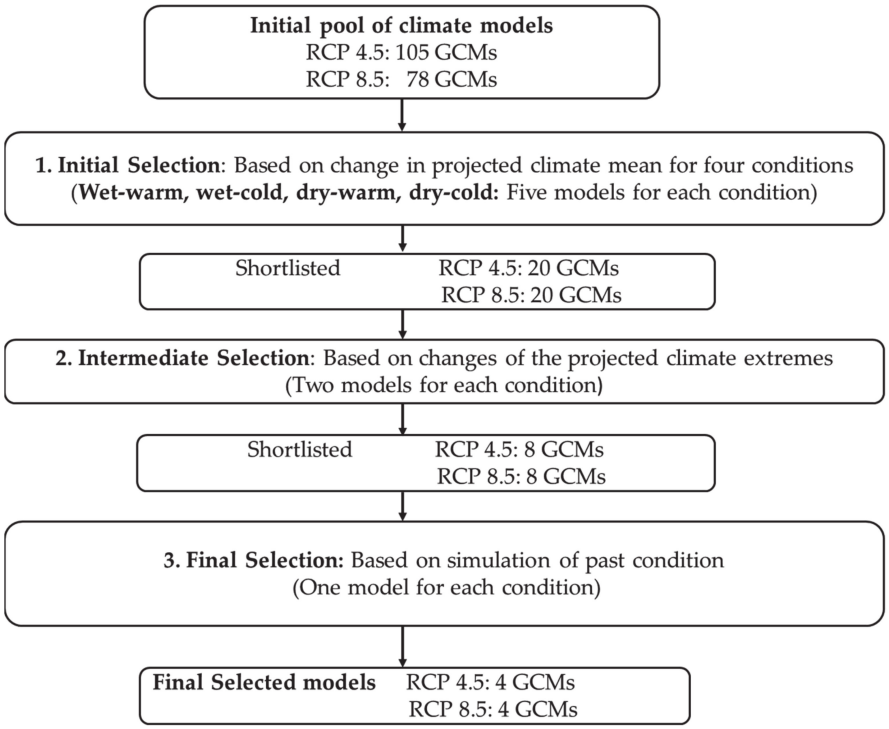

Figure 2. Climate model selection (adopted and modified from [28]).

Step 1: In the first step, the projected changes in future climate from the baseline period are computed for each GCM listed in the pool of models considering warm-dry, warm-wet, cold-wet, and cold-dry corners to form an envelope. The 10th and 90th percentile values for change in mean temperature (ΔT) and percentage change in annual precipitation (ΔP) for each scenario were determined. These values represent the four corners of the spectrum of the projections for temperature and precipitation change. The tenth percentile value of ΔT and tenth percentile value for ΔP are in the 'cold-dry' corner of the spectrum. Likewise, the tenth percentile value of ΔT and 90th percentile value for ΔP are in the 'cold-wet' corner, while the 90th percentile value of ΔT and 90th percentile value of ΔP are in the 'warm-wet' corner. Similarly, the 90th percentile value of ΔT and tenth percentile value of ΔP fall in the 'warm-dry' corner of the spectrum. The proximity of the model running to the 10th and 90th percentile values is derived using the distance metrics recommended by [28]. A total of 20 models (5 models in each four corners) were selected from this step.

Step 2: Two GCMs in each corner were selected in the intermediate step based on the projection of changes in climate extremes using four of the Expert Team on Climate Change Detection and Indices (ETCCDI), as mentioned by [28]. They are R_{95P} [Precipitation due to extremely wet days (> 95th percentile)], CDD [Consecutive dry days: maximum length of dry spell (p < 1 mm)], WSDI [Warm spell duration index: count of days in a span of at least 6 days where TX > 90th percentile (TX_{ij} is the daily T_{max} on day i in period j)], and CSDI [Cold spell duration index: count of days in a span of at least 6 days where TN < 10th percentile (TN_{ij} is the daily T_{min} on day i in period j)].

Step 3: In the final step, the ability of the selected GCMs to hindcast the past observation is evaluated between the selected two models in Step 2 of each of the four corners. In this step, the Taylor method [44] was used to evaluate the GCMs on the basis of three statistics: correlation coefficient, centred root mean squared error (RMS), and the standard deviation. The most reasonable GCM for each corner was selected as the one having the average of the highest Taylor score of the precipitation and temperature. In this way, four models, one in each corner with the highest Taylor score, were selected for each RCP.

2.3. Bias Correction

In order to apply GCM projections at the local scale, bias correction is necessary. This is because of the following reasons: (a) GCMs have inherent systematic biases which can be due to the model's representation of physical processes and their parameterization, initializations, or human judgement, and (b) they are often incompatible on scales (because of coarser resolution) that are necessary for local level hydrological impact studies [45]. Different methods for bias correction for climate variables like precipitation and temperature are discussed in the literature that range from simple corrections in the annual or monthly mean values to complex distribution fitting that corrects the entire distribution. For example, [46] used the delta change approach in crop modelling in Europe for both temperature and precipitation. Lenderink et al. [47] used the linear scaling approach for estimating the future discharges of the Rhine River. Local intensity scaling (LOCI) was applied by [48], while the power transformation method was used in other studies [47,49].

This study used the distribution mapping approach in which the mean, variance, and whole distribution is considered [50–52]. The projected climate data at the meteorological stations were then bias corrected using the quantile mapping (QM) method [51,53]. QM corrects the quantiles of GCM data to match those of observed data by creating suitable transfer functions explained in Equation (1):

$$X^{corr}_{future,t} = inverse\ ecdf\ ^{obs}_{baseline}\left(ecdf^{GCM}_{baseline}\left(X^{GCM}_{future,t}\right)\right) \quad (1)$$

where, *ecdf* is the empirical cumulative distribution function for the reference time period, $X^{GCM}_{future,t}$ is the raw GCM (projected value) at future time t, $ecdf^{GCM}_{baseline}$ is the empirical cumulative distribution function of GCM for the baseline period, and $inverse\ ecdf\ ^{obs}_{baseline}$ is the inverse empirical cumulative distribution function of observation for the baseline period. $X^{corr}_{future,t}$ is the corrected estimate of $X^{GCM}_{future,t}$. We used the frequency adaptation method as described in [54] for the correction of extra dry days when the frequency of dry days in the baseline period in GCM data is greater than the frequency of dry days in the observed data.

The bias-corrected times series climatic data from the selected GCMs for each meteorological station were averaged for each climate scenario. The projected future CC and associated impacts were analysed based on those individual climatic scenarios which were used as input to the SWAT hydrological model.

2.4. Climatology under Climate Change

The percentage change in annual average precipitation and mean temperature under CC were compared with the baseline data for both emission scenarios (RCPs 4.5 and 8.5).

2.4.1. Climate Change Impact Analysis of Future Flows

The SWAT model developed and discussed in Part I of this study [37] was applied to simulate the future flows by enforcing the projected GCMs'- CC data. Projected flows were divided into three 30-year time windows: Immediate Future (IF: 2021–2050), Mid Future (MF: 2046–2075), and Far Future (FF: 2070–2099). Projected flows were compared with corresponding monthly, seasonal, annual, and fractional differences of extreme flows (Q_{90} and Q_{10}) of the simulated baseline flows (1983–2012). Such comparisons were made for all four scenarios, three future time windows, and for both RCPs.

2.4.2. Frequency Analysis

Annual one-day-maximum and -minimum flow series were extracted for each time window of all four scenarios for both RCPs along with the baseline simulated flow. Gumbel distribution [55] was fitted to these time series in order to find the magnitude of high and low flows for the selected return periods. Interestingly, some flood-related studies have applied hydro-economic [56] and techno-social [57] perspective CC assessment methods.

3. Results

3.1. Climate Model Selection

The first selection was made by comparing the projected mean temperature and annual precipitation changes (%) of 2021–2050 with the baseline period of 1981–2005 for both RCPs shown as dots in Figure 3. In RCP 4.5, the projected changes in annual precipitation are in the range of −9% to +23%, while most models show an increase in precipitation. Similarly, the change in projected temperature ranges from +0.6 °C to +3.1 °C with the multi-model mean showing an increase by approximately +1.7 °C. Similarly, in RCP 8.5, most of the models indicate an increase in annual precipitation, while in some cases, it is decreases (range of change in precipitation: −11% to +21%). In the case of temperature, the changes are from +0.7 °C to +3.0 °C, with the mean value of +1.9 °C.

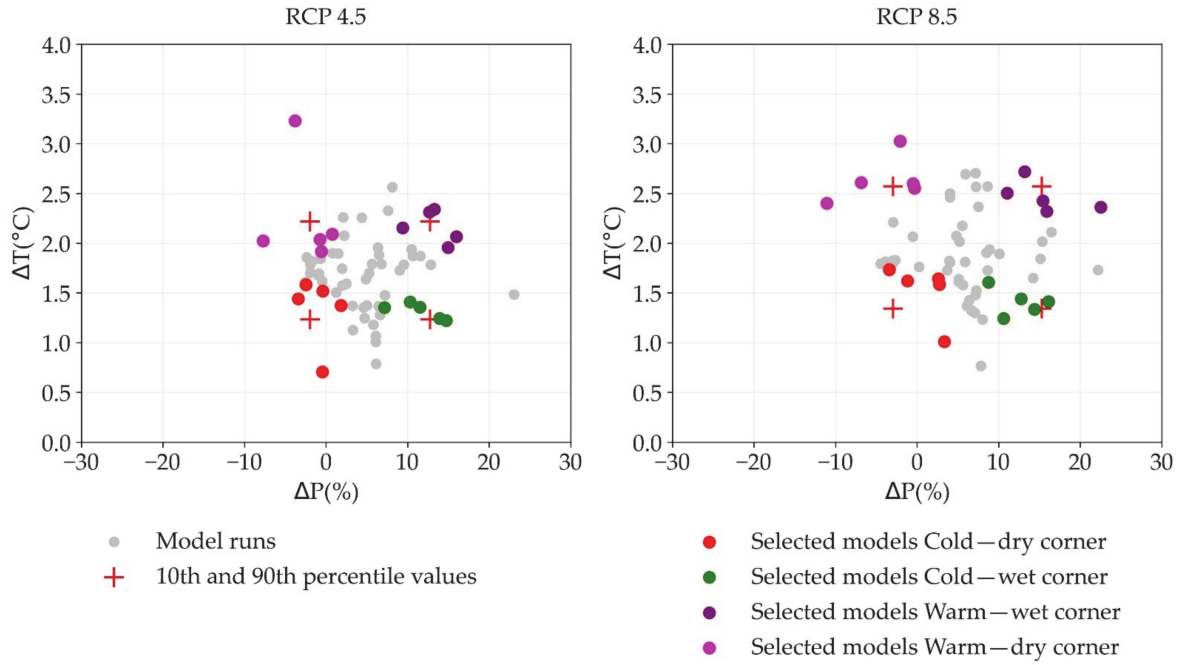

Figure 3. Projected changes in annual precipitation (ΔP %) and annual mean temperature (ΔT °C) for RCP 4.5 and RCP 8.5. Pink, violet, red, and green dots represent warm-dry, warm-wet, cold-dry, and cold-wet conditions, respectively.

ETCCDI extreme indices, viz. R_{95P}, CDD, WSDI, and CSDI, were used to filter GCMs from 20 to 8. The two GCMs that have the topmost combined scores for the changes in precipitation and temperature indices in each corner are selected in the intermediate selection steps given in Supplementary Tables S1 and S2. Using the Taylor method [44], four GCMs, one for each corner, are selected (Table 1). HadGEM2 was selected for cold and dry conditions, GFDL for cold and wet conditions, and CanESM2 for warm and wet conditions for both RCPs. However, in the case of warm and dry conditions, MPI-ESM for RCP 4.5 and MIROC-ESM for RCP 8.5 were selected.

3.2. Bias Correction

Monthly average precipitation and temperature (observed, uncorrected, and bias corrected) are given in Figure 4 for RCP 4.5 of CanESM2 as a representative graph. The graph shows that the climate data are well bias corrected.

Table 1. Summary of selected GCMs for RCPs 4.5 and 8.5.

Climatic Condition	GCMs for RCP 4.5	GCMs for RCP 8.5
Cold-dry (p_{10_10})	HadGEM2-CC_rcp45_r1i1p1	HadGEM2-ES_rcp85_r1i1p1
Cold-wet (p_{10_90})	GFDL-ESM2G_rcp45_r1i1p1	GFDL-ESM2M_rcp85_r1i1p1
Warm-wet (p_{90_90})	CanESM2_rcp45_r3i1p1	CanESM2_rcp85_r3i1p1
Warm-dry (p_{90_10})	MPI-ESM-LR_rcp45_r3i1p1	MIROC-ESM-CHEM_rcp85_r1i1p1

Note: p_{x_y}: xth and yth percentiles of temperature and precipitation.

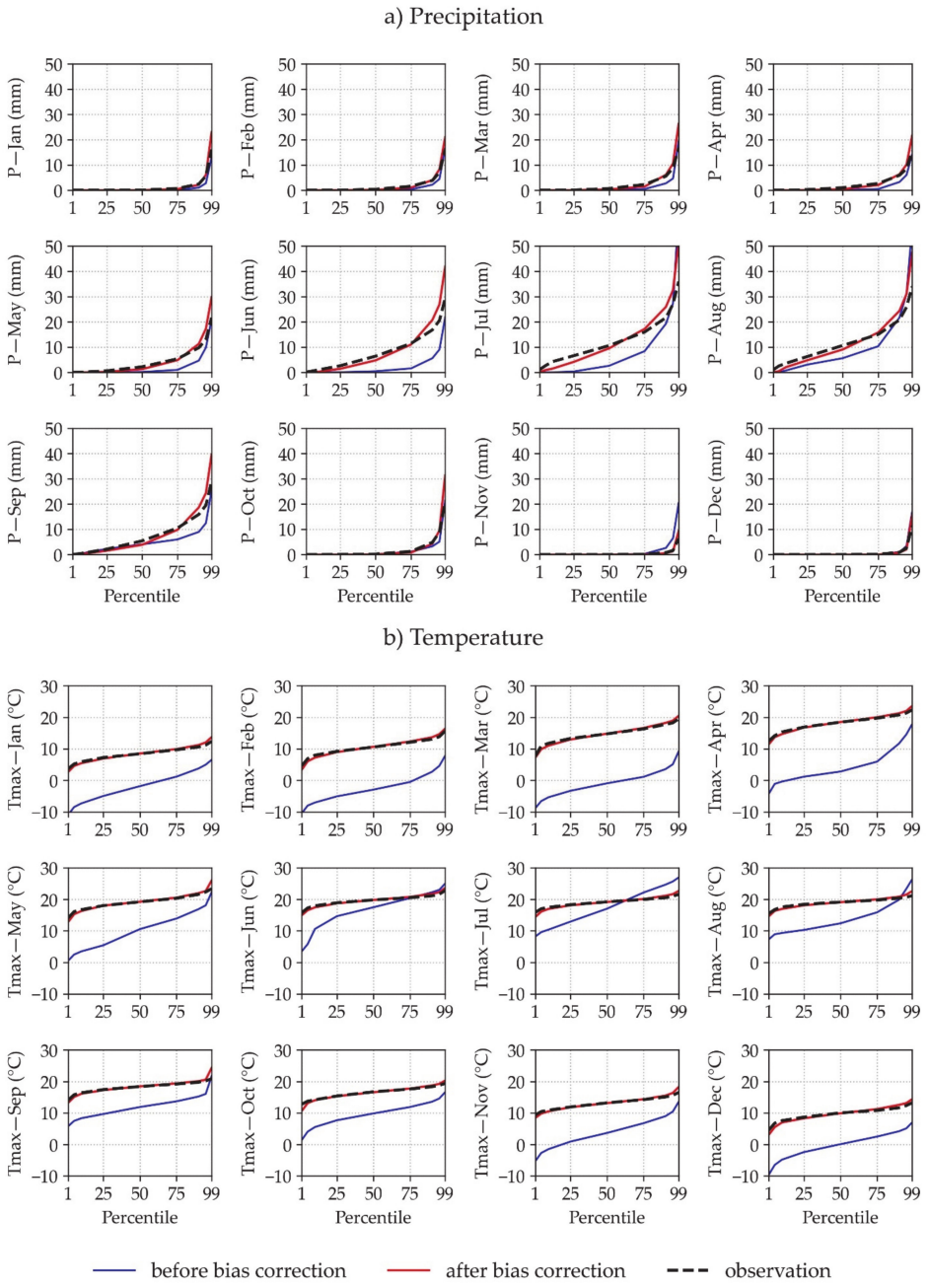

Figure 4. Observed (black), before bias correction (blue), and after bias correction (red) precipitation (top) and maximum temperature (bottom) monthly values for RCP 4.5 of CanESM2.

3.3. Climatology under Climate Change

The percentage changes in annual precipitation and temperature under the two emission scenarios (RCPs 4.5 and 8.5) with respect to the baseline values are depicted in Figure 5. The projected precipitation by all GCMs for all time windows (IF, MF and FF) is most likely to increase in both RCPs except MPI-ESM (MF, FF) and HadGEM2 (IF), in the case of RCP 4.5, and HadGEM2 (IF and MF) for RCP 8.5. The highest increase of about 9% and 20% from the baseline values are found for RCP 4.5 (in IF) and RCP 8.5 (in FF), respectively, projected by the CanESM2 model. The lowest projected precipitation by the HadGEM2 is found in the IF time window. Their values are about 5% and 7% lower than the base case, respectively, in RCPs 4.5 and 8.5. It can be seen from the figure that the precipitation is expected to increase with time (IF < MF < FF) in RCP 8.5. However, in the case of RCP 4.5, the response is mixed, i.e., an increasing trend for HadGEM2 (Cold-dry) and GFDL_ESM2G (Cold-wet) and a decreasing one in the other two cases (Warm-wet and Warm-dry). This characteristic is distinctly depicted in Figure 6, i.e., the projected long-term precipitation in RCP 8.5 shows a clear increasing trend which is not clear for RCP 4.5.

Both the maximum and minimum temperature projections by all the selected GCMs (in all climatic conditions) are found increasing while moving from IF to FF in both emission scenarios. The rate of increase of temperature is higher by all projections for RCP 8.5 than that of RCP 4.5, as expected (Figures 5 and 6). It can also be observed that the increase in minimum temperature is more than that of maximum temperature in all time windows for both emission scenarios and in all conditions except the cold-wet condition (GFDL-ESM2G of RCP 4.5). However, the projected temperatures of selected models are found to be different. The maximum increase is found for the minimum temperature projected by MIROC-ESM-CHEM (warm-dry/FF) of RCP 8.5, i.e., 6.5 °C. The minimum increase is found to be 0.6 °C projected by the GFDL-ESM2G model in IF (Figure 5).

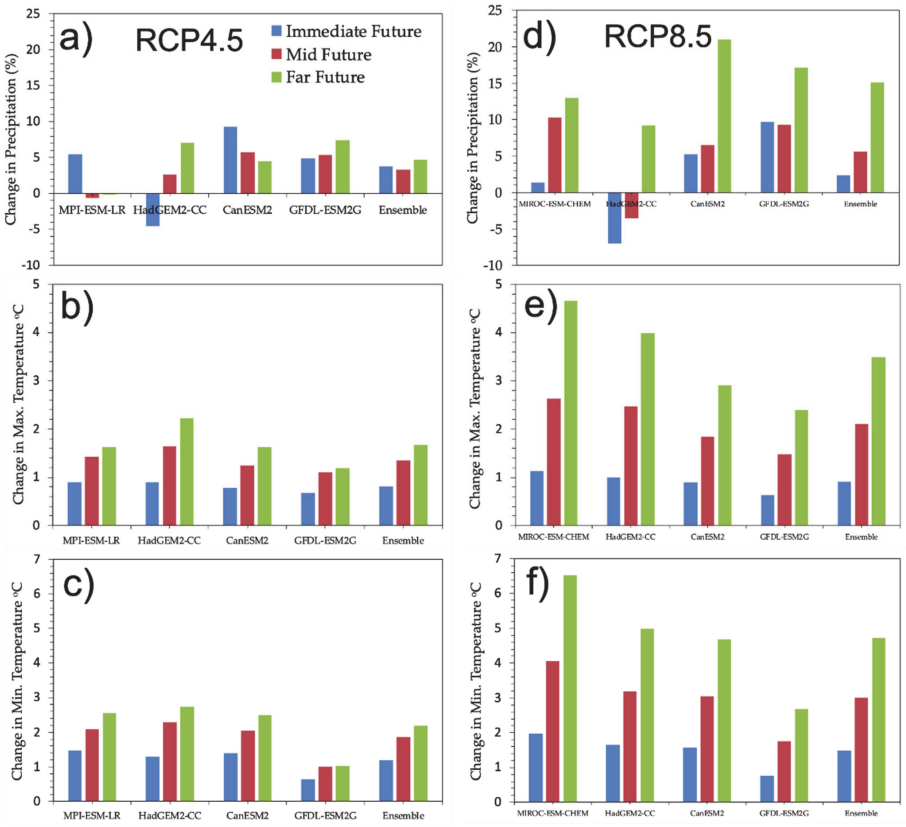

Figure 5. Change in precipitation (**a**,**d**) and change in temperature [maximum (**b**,**e**), minimum (**c**,**f**)] pattern of the four selected GCMs and ensemble of RCPs 4.5 (left) and 8.5 (right) with their respective time windows: blue (IF), red (MF), and green (FF).

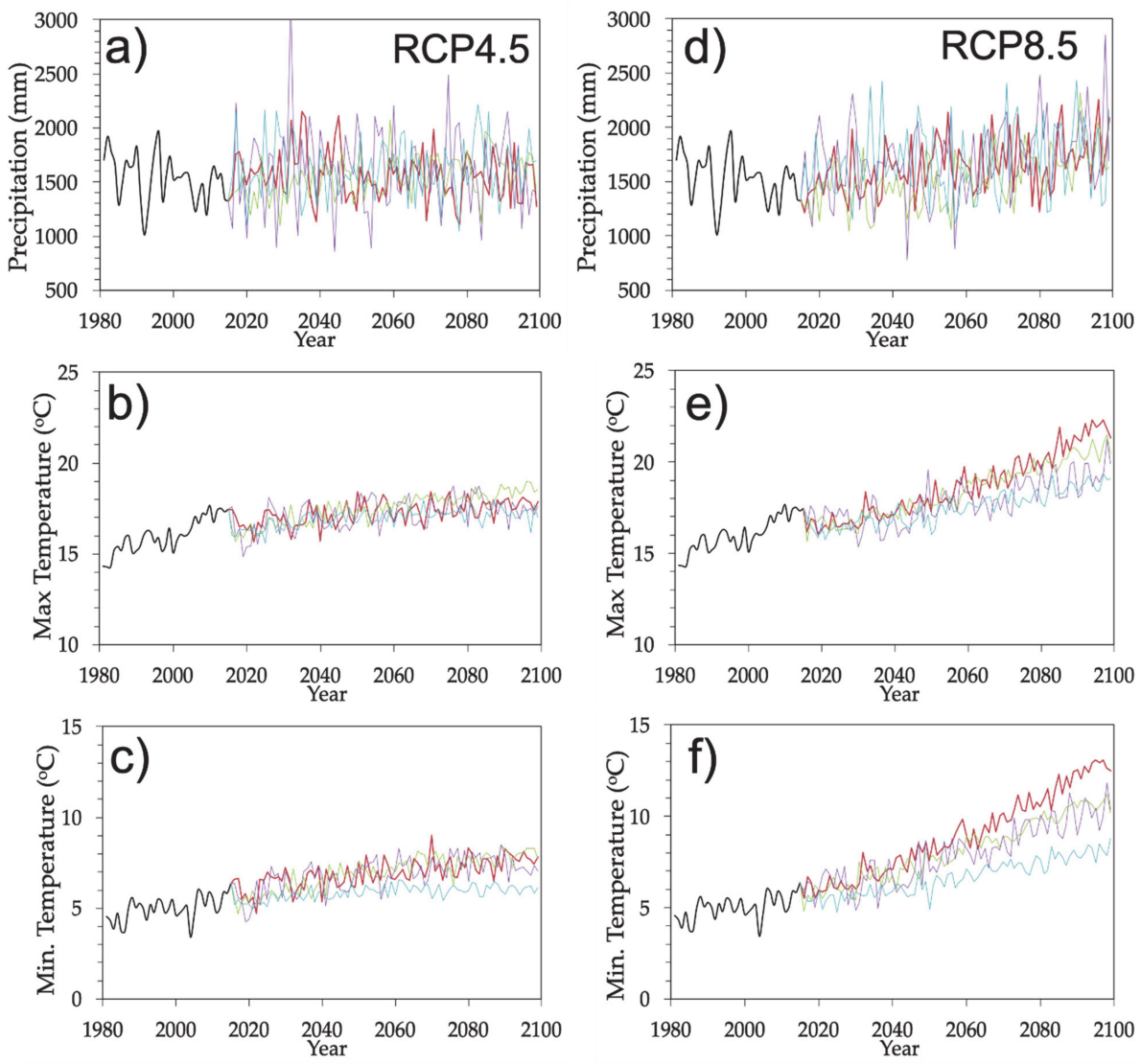

Figure 6. Precipitation and temperature (observed, bias corrected) of RCP 4.5 (**a**–**c**) and 8.5 (**d**–**f**) of the selected GCMs; black (baseline), red (MIROC/MPI), blue (GFDL), green (HadGEM), and purple (CanESM2).

3.4. General Hydrology under Climate Change

The simulated average annual flow at the outlet of BRB for the baseline period is 240 m^3/s [37]. Table 2 presents the predicted flow and corresponding percentage changes by all selected GCMs for four climatic conditions (warm-wet: projected by CanESM2; warm-dry: MPI (RCP 4.5/MIRCO (RCP 8.5), cold-wet: GFDL, and cold-dry: by HadGEM2) and their ensemble for all time windows.

The maximum increase of annual flow in RCP 4.5 is more than 30% in the cold-dry condition of FF and the minimum increase is about 10% in IF for the same condition predicted by the HadGEM2 model. It shows that the HadGEM2 predicted flow has a higher variability range than other GCMs in terms of annual averages. The increased flow of the long-term annual average is almost the same for the warm-wet condition projected by CanESM2 (IF: 29%, MF: 30% and FF 28%), whereas it has a decreasing trend for the warm-dry condition projected by the MPI model (IF: 26%, MF: 20% and FF: 17%). The flow of the other remaining two conditions have an increasing trend while moving from IF to FF [GFDL: 18% (IF), 20% (MF) and 24% (FF); and HadGEM2: 10% (IF), 24% (MF) and 31% (FF)].

Table 2. Impact of climate change on long-term annual flow.

Conditions	Time Window	RCP 4.5		RCP 8.5	
		Flow (m^3/s)	% Change	Flow (m^3/s)	% Change
Baseline		240	-	240	-
Cold-Wet (GFDL-ESM2G)	Immediate Future	283	18	304	27
	Mid Future	287	20	317	33
	Far Future	297	24	358	49
Warm-Wet (CanESM2)	Immediate Future	309	29	311	30
	Mid Future	311	30	315	32
	Far Future	306	28	377	57
Cold-Dry (HadGEM)	Immediate Future	263	10	251	5
	Mid Future	297	24	272	14
	Far Future	314	31	331	38
Warm-Dry (MPI-ESM-LR/MIROC-ESM)	Immediate Future	301	26	287	20
	Mid Future	288	20	334	39
	Far Future	281	17	350	46
Ensemble	Immediate Future	289	21	288	20
	Mid Future	296	23	310	29
	Far Future	299	25	354	48

The long-term average annual flow predicted by all GCMs for all time windows in RCP 8.5 are also more than the baseline flow, in increasing order from IF to FF for all climatic conditions, similar to RCP 4.5. The increase in annual projected flow is between 5% (cold-dry/IF) and 57% (warm-wet/FF).

Thus, it can be observed that the long-term average annual flows are projected to increase in all climatic conditions for both RCPs. The range of increment of ensembled flow is in between 21% and 25% in RCP 4.5 and 20% and 48% in RCP 8.5. This shows that the magnitude of increment of future flow is expected to be more for the higher emission scenario.

3.5. Variation in Monthly Flows

Knowledge on the monthly variability under CC is useful for risk assessment of water resource development projects, such as hydropower, irrigation, and municipal water supplies. The long-term monthly flow for the three-time windows projected by the four GCMs representing four climatic conditions of RCP 4.5 and RCP 8.5 emission scenarios are given in Supplementary Tables S3 and S4, respectively. The data show that the range of change in monthly projected flow in RCP 4.5 is from −17% (June/MF/cold-dry) to 68% (March/FF/warm-wet) with respect to the baseline flows. It is noted here that only 4 out of 144 cases (12 months × time windows × 4 climatic conditions) have more than 5% decrease in monthly flows. In almost 60% of the cases, the flows are in the range of +10% to +25% of the baseline flows. Monthly flows more than 25% of the baseline flows are found to be in one fourth of the total number of months in the simulated period. In general, in three climatic conditions (warm-wet, cold-wet, and warm-dry), more than 25% increase is found in the month of March. Even for the cold-dry condition, the increased percentage is high (>15%). The monsoon flow is expected to increase significantly in all time windows except for the cold-dry condition in June. The highest absolute magnitude of the projected monthly maximum flow in all time windows for all climatic conditions is found to occur in August, similar to the baseline, except for the far-future of the cold-wet condition. In this case, the flow value is at its maximum in July.

In the case of RCP 8.5, the range of change of the monthly flow is from nearly −50% (July/MF/cold-dry) to 200% (October and November/MF/cold-dry). Almost two-thirds

of the predicted monthly flows are more than 25% of the baseline values for all climatic conditions. Almost one-fourth of the cases are between a 10 and 25% increase in monthly flows. The decrease in predicted flow was found only for cold-dry conditions. It is interesting to note that this decrease is mainly observed in the monsoon season (June, July, and August) and in May. The rate of increase is found to be higher in the post-monsoon season (October and November).

The monthly baseline and predicted ensembled flows as well as the corresponding percentage changes due to CC for both RCPs are given in Figure 7.

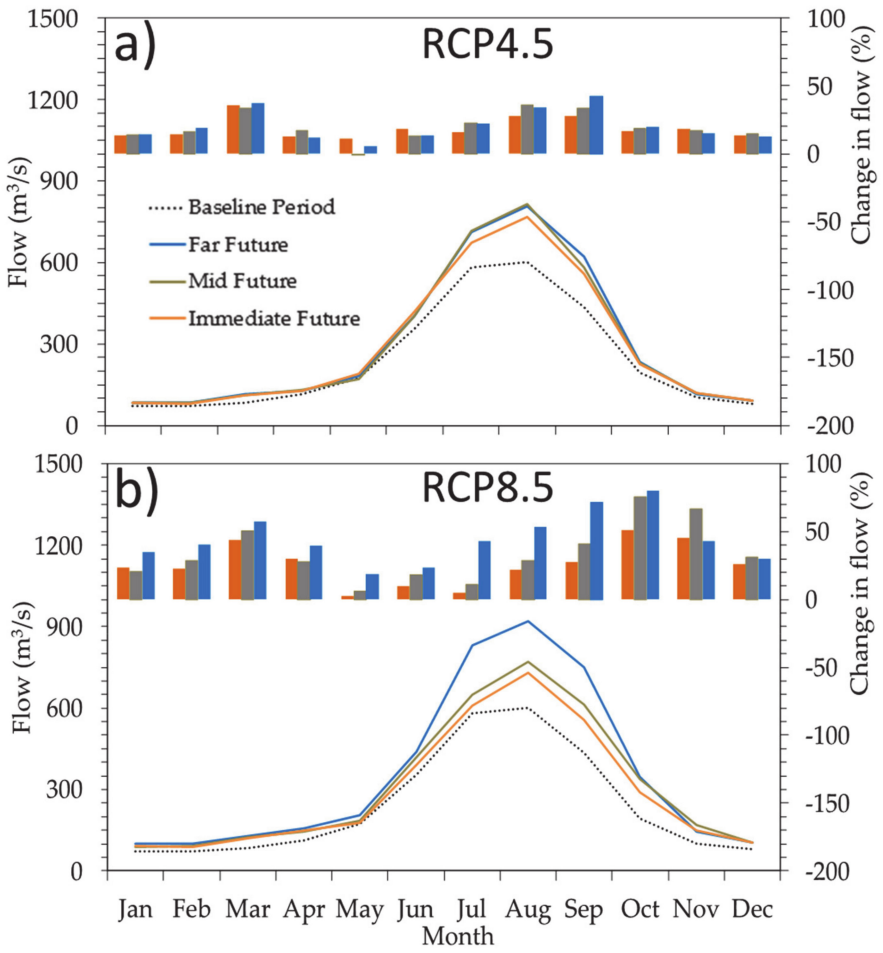

Figure 7. Hydrographs of monthly ensembled and baseline flows and their changes; (**a**: RCP 4.5 and **b**: RCP 8.5) black dashed (baseline), red (Immediate Future—IF), grey (Mid Future—MF), and blue (Far Future—FF).

The ensembles of the projected mean monthly flow are expected to increase in March, August, September, October, and November for all scenarios except MF (May) of RCP 4.5 (2021–2099). On the other hand, in RCP 8.5, all the ensembles of the projected monthly flow increase in all time windows. The relative changes in the projected mean monthly flow under RCP4.5 are +11 to +28%, −1 to +36%, and +5 to +43% for IF, MF, and FF, respectively. These figures range from +3 to +52%, + 6 to + 77%, and +18 to + 82% for IF, MF, and FF, respectively, in the case of RCP 8.5. Ensembled flows are found to be higher in RCP 8.5 than in RCP 4.5, except for a few months (May to August of IF and July and August of MF). The maximum increases of 43% (September) in RCP 4.5 and 82% in RCP 8.5 occur towards the end of the century.

3.6. Variation in High and Low Flows

The 10th percentile (Q_{10}, high flow) and 90th percentile (Q_{90}, low flow) values were derived from the corresponding baseline and flow duration curves predicted by all four GCMs for the considered time windows. Their fractional differences (Q_{10}:Q_{90}) were calculated separately for each case. The 10th and 90th percentiles of baseline flow are, respectively, 598 m^3/s and 64 m^3/s. This means that the fractional difference of the baseline flow is 9. For RCP 4.5, the fractional differences of the ensembled flow are found to be 11, 12, and 12 for IF, MF, and FF, respectively. However, such ensemble values for RCP 8.5 are, respectively, 14, 17, and 18 for IF, MF, and FF. This result shows that variability is expected to increase with time and be of a higher magnitude in RCP 8.5 than in RCP 4.5.

The number of days exceeding Q_{10} flow and less than Q_{90} were calculated from the results to assess the frequency of incidence of high flow and low flow. The number of days exceeding Q_{10} or not exceeding Q_{90} was 1098 for the baseline period. The number of days (for all the four GCMs) that are expected to have flow exceeding Q_{10} are more than 1098 days and not exceeding Q_{90} are less than 1098 days, except for one case (FF-low flow-warm dry-RCP 4.5). The increase in the number of such days for IF, MF, and FF are, respectively, 58%, 66%, and 71% for RCP 4.5 and 43%, 62%, and 97% for RCP 8.5. On the other hand, the percentage of decrease in number of days in which the flow is expected to be less than Q_{90} are 29%, 26%, and 14% for RCP 4.5 and 43%, 20%, and 42% for RCP 8.5 for IF, MF, and FF, respectively. This result indicates that the likelihood of the number of flooding days would increase during the high flow season, while the number of firm flow days in the low flow season would decrease, both instances pointing towards the negative impact of CC.

3.7. Frequency Analysis of Flow

In this study, the frequency analysis of annual one-day-maximum and -minimum flows at the outlet of the BRB was carried out by the Gumbel Method for the baseline and CC cases as discussed below.

3.7.1. One-Day-Maximum Flow

Maximum instantaneous flows are generally used to estimate design floods [58,59]. Annual one-day-maximum floods and instantaneous floods are positively correlated [59–61]. Therefore, it is assumed that the impact of CC on instantaneous flows is the same as that in the annual one-day-maximum flow.

Changes in the one-day-maximum flood for the different conditions and return periods are given in Table 3, including baseline values. The baseline floods for the 100-, 500-, and 1000-year return period are, respectively, 1544, 1801, and 1911 m^3/s. Table 3 shows that the one-day-maximum flood resulting from CC is higher than the baseline floods for all climatic conditions and in all time windows for the considered return periods. However, the magnitude of predicted values are different depending on the selected GCMs. Such an increase is found in the range of 66% (warm-dry/IF/100 years) to 226% (warm-wet/MF/1000 years) for RCP 4.5 and 69% (cold-dry/IF/100 years) to 317% (cold-wet/FF/1000 years) in the case of RCP 8.5. It is noted here that flood magnitudes are more in RCP 8.5 than RCP 4.5, except in the IF of the cold-dry condition. On an average, the change in ensembled projected flood is around 110%, 125%, and 140% of baseline floods, respectively, for IF, MF, and FF time windows in the case of RCP 4.5. These changes are about 150%, 200%, and 250%, respectively for IF, MF, and FF time windows in RCP 8.5.

3.7.2. One-Day-Minimum Flow

One-day-minimum simulated flows for the different scenarios are given in Table 4. Results showed that the range of change in one-day-minimum flow due to CC with respect to the baseline condition is between −27% (warm-dry/FF/20 years) and +9% (warm-wet/IF/2 years) for RCP 4.5, while it is between −20% (warm-wet/MF/20 years) and +16% warm-wet/FF/2 years) for the RCP 8.5 scenario. Almost half of the flow values in

RCP 4.5 are expected to decrease by more than 10%. This phenomenon is mainly observed in MF and FF. Similar results are obtained in RCP 8.5, i.e., almost 50% of the low flows are lower than the base case values. It is more prominent in MF. Such a decrease is mainly clustered for the 10- and 20-year return period flows. The maximum decrease in predicted ensembled one-day-low flows is observed in FF in the case of RCP 4.5 and MF in the case of RCP 8.5.

Table 3. One-day-maximum flood frequency analysis.

Time Window	Return Period (Years)	Baseline Flow (m^3/s)	% Change in Flow (RCP 4.5)					% Change in Flow (RCP 8.5)				
			Warm and Dry	Cold and Dry	Warm and Wet	Cold and Wet	Ensembled	Warm and Dry	Cold and Dry	Warm and Wet	Cold and Wet	Ensembled
IF	100	1544	66	101	153	102	106	204	69	159	137	142
	500	1801	67	109	163	106	111	226	72	171	145	154
	1000	1911	68	111	166	108	113	234	73	175	148	158
MF	100	1544	71	126	205	79	120	215	167	180	200	190
	500	1801	72	131	220	79	125	228	183	189	217	204
	1000	1911	72	133	226	78	127	233	188	192	223	209
FF	100	1544	114	141	183	97	134	238	175	269	285	242
	500	1801	123	149	197	98	142	254	183	280	309	256
	1000	1911	126	151	202	98	144	260	186	283	317	262

Table 4. One-day-minimum flow frequency analysis.

Time window	Return Period (Years)	Baseline Flow (m^3/s)	% Change in Flow (RCP 4.5)					% Change in Flow (RCP 8.5)				
			Warm and Dry	Cold and Dry	Warm and Wet	Cold and Wet	Ensembled	Warm and Dry	Cold and Dry	Warm and Wet	Cold and Wet	Ensembled
IF	2	56	7	0	9	4	5	5	2	9	7	6
	10	47	2	0	−9	−4	−3	6	−2	−4	4	1
	20	45	0	0	−13	−7	−5	7	−2	−7	4	1
MF	2	56	−4	5	4	−7	0	0	−2	4	−2	0
	10	47	−11	0	−11	−15	−9	−11	−15	−15	−15	−14
	20	45	−13	−2	−16	−16	−12	−13	−20	−20	−18	−18
FF	2	56	−13	2	−2	−5	−4	−5	4	16	4	4
	10	47	−23	−4	−17	−15	−15	−15	−13	2	−2	−7
	20	45	−27	−7	−20	−18	−18	−18	−18	−2	−4	−11

4. Discussion

Precipitation and temperature are considered to be the most important climatic variables influencing the water availability of a basin. The influence of CC has significant implications on water resource planning and management. Recent studies have used varying models and datasets (GCMs and/or RCMS) and climate scenarios to assess CC through precipitation and temperature in various parts of Nepal, considering different time windows to the end of this century [31,62–65]. Expected changes in precipitation are not consistent across the country; however, all these studies predicted an increase in precipitation with time. Our results are comparable with these, showing that projected precipitation by almost all GCMs for all time windows (IF, MF and FF) is most likely to increase in both RCPs. In the case of temperature, expected changes quantified by the aforementioned studies are not uniform in this region. Nevertheless, most have predicted a rise in both maximum and minimum temperature [29,39,64,65]. In this study too, both the maximum and minimum temperatures projection by all the selected GCMs (in all climatic conditions) are expected to increase while moving from IF to FF in both emission scenarios.

This study found that the projected annual flows by all GCMs and for all time windows are greater than the base case. A similar trend has been reported in other studies made in Nepalese rivers basins: for example, Indrawati [31], in Bagmati [62], Kaligandaki [66], Bheri [67], Karnali [29], and Koshi [32,40,59], except [39] in Tamor. Among these results, the trend of increase in ensembled future flows is surprisingly found similar to that of [40]. The percentage change in flow due to CC in IF/MF/FF of this study and [40] are, respectively, 21/23/25 and 16/22/28 for RCP 4.5 and 20/29/48 and 18/31/57 for RCP 8.5. From the results presented above, we can see that the range of increase in annual flow is more in

RCP 8.5 (5–57%) than in RCP 4.5 (10–30%), except in IF and MF of the cold-dry and in IF of the warm-dry conditions. The lower values of the predicted flows in RCP 8.5 are attributed to less precipitation in RCP 8.5 in these cases. Although the overall trend of the projected flow is found increasing, the individual scenarios show differences in the magnitude of changes in flows. Depending on the GCM used and the location of the studied catchments, the magnitude (in some cases even the direction) of changes in flow as the impact of CC are reported differently in previous studies [38,40,68–70]. For example, in the study by [69] using the SWAT model, the authors found that the annual runoff of the Yinma River Basin (China) in the future (2021–2050) would increase by 88% for RCP 4.5 and by 48% for RCP 8.5 in comparison to the baseline period (1981–2010). On the other hand, decreases of mean annual runoff are projected by the VIC model in all future time windows of 2010–2039, 2040–2069, and 2070–2099 in a similar study by [70] conducted in the Upper Yangtze River Basin of China (the decrease in mean annual flow was 7.84% under RCP 8.5 and 9.81% under RCP 4.5, in their case). Phi Hoang et al. [68] found that the ensemble flow due to CC shows increases in annual river flows between +5 and +16% in the Mekong river. Results from these studies highlight the need for the localized prediction of future flows for water resource management considering the uncertainties.

Except in May and June, the future flows predicted by all GCMs are likely to increase in all other months of the year for all time windows. This is similar to the results of the Koshi Basin in Nepal [40]. As in the case of annual flows, the range of predicted changes in future flows shows a high level of uncertainty depending on the choice of GCM. Such variation is quite high in RCP 8.5 (–50% to +200%). However, similar monthly variations in flow between −70% and +190% are found in Wagener et al. [71]. Similarly, maximum monthly flow increases of 143% and 99%, respectively, for RCP 4.5 and 8.5 were reported in [69]. On the other hand, [72] found that the mean monthly river flow varies from −16% to +55%, with the greatest decreases in July and August and the greatest increases in May and June.

Our results predict a higher increase in high flows than that of low flows. The average increases (predicted by all GCMs for all time windows) of high flow (Q_{10}) are 23 and 26%, and those of low flow (Q_{90}) are 14 and 17% with respect to the baseline for RCP 4.5 and RCP 8.5, respectively. This shows that the negative impacts of CC can be expected in both the high flows (increasing) and low flows (decreasing). Similar results are reported for the Ljubljanica River of Slovenia in all three investigated future time windows, i.e., 2011–2040, 2041–2070, and 2071–2100 under RCP 4.5 [73]. The highest change in one-day-maximum flood is expected in the warm-wet climatic condition for the case of RCP 4.5 in all time windows. w However, for RCP 8.5, the warm-dry condition in IF and MF predicts higher values of flood, while the cold-wet does so in the FF.

The expected rise in temperature will most likely lead to increase in water demand: for example, ET. This will further stress the water availability of the basin. On the other hand, increased snow melt during the dry season and thus addition to the current water availability might be beneficial to some users, such as hydropower projects. Moreover, the projected shift in precipitation patterns will most likely impact floods and droughts by altering their timing and magnitude. These consequences are further exacerbated by the various uncertainties in the method of analysis and results. Nevertheless, the increase in predicted floods by all the GCMs in our study show that the flood disposal structure should be designed at a higher capacity than the one designed based on baseline flood values to achieve climate resilience. Additionally, the projected decrease in the future low-flows due to CC strongly indicates the need for storage over run-of-river projects for optimal water use planning. Overall, it is seen that the impacts of CC are essential for the design of hydraulic structures, flood and drought management, and overall water resource planning and development of the basin.

5. Conclusions

The impact of CC on future water availability in the BRB was analysed by using a well-calibrated and validated SWAT hydrological model. Climate data were projected by four GCMs representing cold-dry, warm-dry, cold-wet, and warm-wet conditions for two emission scenarios, i.e., RCPs 4.5 and 8.5, adopting an envelope method. Most of the selected GCMs predict an increase in annual precipitation and temperature for RCP 4.5. In the case of RCP 8.5, most of the GCMs predict higher annual precipitation and temperature compared with the baseline condition, while some project a decrease in annual precipitation. The projected precipitation by almost all GCMs for all time windows (IF, MF, and FF) is most likely to increase in both RCPs. Both the maximum and minimum temperature projections by all the selected GCMs (in all climatic conditions) are found increasing while moving from IF to FF in both emission scenarios.

This study concludes that the increasing temperature and variation in precipitation patterns in the BRB resulting from CC will impact the water resource availability in the future. The monsoon flow is expected to increase significantly for all time windows in the case of both RCPs. While the variation in the monthly flows from the baseline values of RCP 8.5 is projected to be higher than that of RCP 4.5, the rate of increase is found to be more in the post-monsoon season. The greatest magnitude of the projected monthly maximum flow in all time windows for all climatic conditions except FF of the cold–wet condition is found to occur in August, similar to the baseline condition. The long-term average annual flow predicted by all GCMs for all time windows in RCP 4.5 and 8.5 is projected to continuously increase from IF to FF. The relative change in the mean monthly flow under RCP 4.5 and 8.5 is projected to increase for IF, MF, and FF. Ensembled flows are expected to be higher in RCP 8.5 than in RCP 4.5.

The fractional differences (Q_{10}:Q_{90}) for the projected flow were found to be progressively increasing with RCPs and over time. Additionally, the number of days exceeding the 10th percentile (Q_{10}, high flow) and not exceeding the 90th percentile (Q_{90}, low flow) are predicted to be more by all the GCMs. Likewise, the one-day-maximum floods of different return periods are projected to be higher than those of the baseline floods for all climatic conditions and for all time windows in both RCPs. Similarly, the one-day-minimum flows for different return periods are most likely to be lower than the base case. However, the predicted values are different in magnitude and direction depending on the selected GCMs.

The increase in future predicted floods implies the designing of flood disposal structures at a higher capacity than those designed based on historical data. Furthermore, the decrease in projected firm flows in the future suggests that storage-type water resource projects are preferred over run-of-river projects for optimal water use planning from the perspective of climate resilience.

Supplementary Materials: The following are available online at https://www.mdpi.com/article/10.3390/w13111548/s1. Table S1. Detail of scores for the changes in precipitation and temperature indices of selected GCMs in each corner before intermediate selection step (Step 2); Table S2. Selected GCMs in intermediate selection step (Step 3) using Taylor score; Table S3. The long-term monthly flow of three-time windows projected by four GCMs representing four climatic conditions of RCP 4.5 emission scenario; Table S4. The long-term monthly flow of three-time windows projected by four GCMs representing four climatic conditions of RCP 8.5 emission scenario

Author Contributions: Conceptualization, S.M., D.A. and L.P.D.; methodology, S.M., D.A., L.P.D., U.B. and D.S.; software, validation, formal analysis, investigation, resources, data curation, writing—original draft preparation, S.M., D.A., L.P.D., U.B. and D.S.; Writing—Review and editing, S.M., D.A. and L.P.D.; supervision, D.A. and L.P.D. All authors have read and agreed to the published version of the manuscript.

Funding: This research was partially funded by Tribhuvan University, Nepal.

Institutional Review Board Statement: Not applicable.

Informed Consent Statement: Not applicable.

Data Availability Statement: The datasets used in this study can be accessed freely.

Acknowledgments: The authors would like to thank the Department of Hydrology and Meteorology, Government of Nepal, for providing hydroclimatic data. Budhigandaki Hydroelectric Project Development Committee is also acknowledged for providing hydrological data. The authors would like to thank three anonymous reviewers for constructive comments which helps to improve our manuscript substantially.

Conflicts of Interest: The authors declare no conflict of interest.

References

1. Wrigley, E.A. Energy and the English industrial revolution. *Philos. Trans. R Soc. A Math. Phys. Eng. Sci.* **2013**, *371*, 20110568. [CrossRef] [PubMed]
2. O'Connor, P.A.; Cleveland, C.J. U.S. Energy transitions 1780–2010. *Energies* **2014**, *7*, 7955–7993. [CrossRef]
3. United Nations. *Pathways to Sustainable Energy-Accelerating Energy Transition in UNECE Region*; ECE Energy Series no.67; United Nations Publication: New York, NY, USA, 2020; ISBN 9789211172287.
4. Mohajan, H.K. The First Industrial Revolution: Creation of a New Global Human Era. *J. Soc. Sci. Humanit.* **2019**, *5*, 377–387.
5. Stern, D.I. The role of energy in economic growth. In *International Energy and Poverty*; Routledge: Milton, UK, 2012; pp. 35–47. ISBN 9781315762203. [CrossRef]
6. IPCC Drivers, Trends and Mitigation. In *Climate Change 2014: Mitigation of Climate Change*; Cambridge University Press: Cambridge, UK, 2015; pp. 351–412. [CrossRef]
7. Yoro, K.O.; Daramola, M.O. *CO_2 Emission Sources, Greenhouse Gases, and the Global Warming Effect*; Elsevier Inc.: Amsterdam, The Netherlands, 2020; ISBN 9780128196571.
8. Stern, N.H.; Peters, S.; Bakhshi, V.; Bowen, A.; Cameron, C.; Catovsky, S.; Zenghelis, D. *Stern Review: The Economics of Climate Change*; Cambridge University Press: Cambridge, UK, 2006; Volume 30, p. 2006.
9. Le Treut, H.; Cubasch, U.; Allen, M. Historical Overview of Climate Change Science. In *Notes*; Cambridge University Press: Cambridge, UK; New York, NY, USA, 2005; Volume 16.
10. United Nations. *United Nations Conference on the Human Environment*; United Nations: New York, NY, USA, 1973; Volume 3.
11. Houghton, E. *Climate Change 1995: The Science of Climate Change: Contribution of Working Group I to the Second Assessment Report of the Intergovernmental Panel on Climate Change*; Cambridge University Press: Cambridge, UK; New York, NY, USA, 1996; Volume 2, ISBN 0521564360.
12. United Nations. *Report of the United Nations Conference on Environment and Development*; United Nations: New York, NY, USA, 1992; Volume l.
13. United Nations. *Kyoto Protocol to the United Nations Framework Convention on Climate Change*; United Nations: New York, NY, USA, 1998.
14. UNFCCC. Addendum Part Two: Action Taken by the Conference of the Parties at Its Twenty-First Session. In *Proceedings of the Report of the Conference of the Parties on Its Fifteenth Session*; Copenhagen, Denmark, 7–19 December 2009, United Nations: New York, NY, USA.
15. UNFCCC. Addendum Part Two: Action Taken by the Conference of the Parties at Its Twenty-First Session (FCCC/CP/2015/10/Add.1) and (FCCC/CP/2015/10/Add.3). In *Proceedings of the Report of the Conference of the Parties on Its Twenty-First Session*; Paris, France, 30 November–13 December 2015, United Nations: New York, NY, USA; p. 01192.
16. IPCC. *Global Warming of 1.5 °C An IPCC Special Report on the Impacts of Global Warming of 1.5 °C above Pre-Industrial Levels and Related Global Greenhouse Gas Emission Pathways, in the Context of Strengthening the Global Response to the Threat of Climate Change*; Pörtner, H.-O., Skea, J., Matthews, J.B.R., Tignor, M., Gomis, M.I., Zhai, P., Shukla, P.R., Pidcock, R., Connors, S., Maycock, T., et al., Eds.; IPCC: Geneva, Switzerland, 2018.
17. Robock, A.; Turco, R.P.; Harwell, M.A.; Ackerman, T.P.; Andressen, R.; Chang, H.S.; Sivakumar, M.V.K. Use of general circulation model output in the creation of climate change scenarios for impact analysis. *Clim. Chang.* **1993**, *23*, 293–335. [CrossRef]
18. Tapiador, F.J.; Navarro, A.; Moreno, R.; Sánchez, J.L.; García-Ortega, E. Regional climate models: 30 years of dynamical downscaling. *Atmos. Res.* **2020**, *235*, 104785. [CrossRef]
19. Oceanic, N.; Brunswick, N.; Oceanic, N.; Survey, U.S.G.; Oceanic, N.; Biology, E. GFDL's CM2 Global Coupled Climate Models. Part I: Formulation and simulation characteristics. *J. Clim.* **2006**, *19*, 643–674.
20. Edwards, P.N. History of climate modeling. *Wiley Interdiscip. Rev. Clim. Chang.* **2011**, *2*, 128–139. [CrossRef]
21. Collins, W.J.; Bellouin, N.; Doutriaux-Boucher, M.; Gedney, N.; Halloran, P.; Hinton, T.; Hughes, J.; Jones, C.D.; Joshi, M.; Liddicoat, S.; et al. Development and evaluation of an Earth-System model—HadGEM2. *Geosci. Model Dev.* **2011**, *4*, 1051–1075. [CrossRef]
22. Chylek, P.; Li, J.; Dubey, M.K.; Wang, M.; Lesins, G. Observed and model simulated 20th century Arctic temperature variability: Canadian Earth System Model CanESM2. *Atmos. Chem. Phys. Discuss.* **2011**, *11*, 22893–22907. [CrossRef]
23. Mauritsen, T.; Bader, J.; Becker, T.; Behrens, J.; Bittner, M.; Brokopf, R.; Brovkin, V.; Claussen, M.; Crueger, T.; Esch, M.; et al. Developments in the MPI-M Earth System Model version 1.2 (MPI-ESM1.2) and Its Response to Increasing CO_2. *J. Adv. Model. Earth Syst.* **2019**, *11*, 998–1038. [CrossRef]
24. Lee, D.K.; Cha, D.H. Regional climate modeling for Asia. *Geosci. Lett.* **2020**, *7*, 13. [CrossRef]

25. Müller, W.A.; Jungclaus, J.H.; Mauritsen, T.; Baehr, J.; Bittner, M.; Budich, R.; Bunzel, F.; Esch, M.; Ghosh, R.; Haak, H.; et al. A Higher-resolution Version of the Max Planck Institute Earth System Model (MPI-ESM1.2-HR). *J. Adv. Model. Earth Syst.* **2018**, *10*, 1383–1413. [CrossRef]
26. Thatcher, M.; McGregor, J.; Dix, M.; Katzfey, J. A new approach for coupled regional climate modeling using more than 10,000 cores. *IFIP Adv. Inf. Commun. Technol.* **2015**, *448*, 599–607. [CrossRef]
27. Barnett, T.P.; Adam, J.C.; Lettenmaier, D.P. Potential impacts of a warming climate on water availability in snow-dominated regions. *Nature* **2005**, *438*, 303–309. [CrossRef]
28. Lutz, A.F.; ter Maat, H.W.; Biemans, H.; Shrestha, A.B.; Wester, P.; Immerzeel, W.W. Selecting representative climate models for climate change impact studies: An advanced envelope-based selection approach. *Int. J. Climatol.* **2016**, *36*, 3988–4005. [CrossRef]
29. Dahal, P.; Shrestha, M.L.; Panthi, J.; Pradhananga, D. Modeling the future impacts of climate change on water availability in the Karnali River Basin of Nepal Himalaya. *Environ. Res.* **2020**, *185*, 109430. [CrossRef]
30. Lutz, A.F.; Immerzeel, W.W.; Kraaijenbrink, P.D.A.; Shrestha, A.B.; Bierkens, M.F.P. Climate change impacts on the upper indus hydrology: Sources, shifts and extremes. *PLoS ONE* **2016**, *11*, e0165630. [CrossRef]
31. Shrestha, S.; Shrestha, M.; Babel, M.S. Modelling the potential impacts of climate change on hydrology and water resources in the Indrawati River Basin, Nepal. *Environ. Earth Sci.* **2016**, *75*, 1–13. [CrossRef]
32. Bharati, L.; Bhattarai, U.; Khadka, A.; Gurung, P.; Neumann, L.E.; Penton, D.J.; Dhaubanjar, S.; Nepal, S. *From the Mountains to the Plains: Impact of Climate Change on Water Resources in the Koshi River Basin*; International Water Management Institute (IWMI): Colombo, Sri Lanka, 2019; Volume 187, ISBN 9290908858.
33. Molden, D.J.; Shrestha, A.B.; Nepal, S.; Immerzeel, W.W. Downstream implications of climate change in the Himalayas. *Water Secur. Clim. Chang. Sustain. Dev.* **2016**, 65–82.
34. Devkota, R.P.; Pandey, V.P.; Bhattarai, U.; Shrestha, H.; Adhikari, S.; Dulal, K.N. Climate change and adaptation strategies in Budhi Gandaki River Basin, Nepal: A perception-based analysis. *Clim. Chang.* **2017**, *140*, 195–208. [CrossRef]
35. Khatri, H.B.; Jain, M.K.; Jain, S.K. Modelling of streamflow in snow dominated Budhigandaki catchment in Nepal. *J. Earth Syst. Sci.* **2018**, *127*, 1–14. [CrossRef]
36. Pangali Sharma, T.P.; Zhang, J.; Khanal, N.R.; Prodhan, F.A.; Paudel, B.; Shi, L.; Nepal, N. Assimilation of snowmelt runoff model (SRM) using satellite remote sensing data in Budhi Gandaki River Basin, Nepal. *Remote Sens.* **2020**, *12*, 1951. [CrossRef]
37. Marahatta, S.; Aryal, D.; Devkota, L.P. Application of SWAT in Complex Mountainous River Basin (Part I: Model Development). *Water* **2021**. submitted for publication.
38. Pandey, V.P.; Dhaubanjar, S.; Bharati, L.; Thapa, B.R. Spatio-temporal distribution of water availability in Karnali-Mohana Basin, Western Nepal: Hydrological model development using multi-site calibration approach (Part-A). *J. Hydrol. Reg. Stud.* **2020**, *29*, 100690. [CrossRef]
39. Bhatta, B.; Shrestha, S.; Shrestha, P.K.; Talchabhadel, R. Evaluation and application of a SWAT model to assess the climate change impact on the hydrology of the Himalayan River Basin. *Catena* **2019**, *181*, 104082. [CrossRef]
40. Kaini, S.; Nepal, S.; Pradhananga, S.; Gardner, T.; Sharma, A.K. Impacts of climate change on the flow of the transboundary Koshi River, with implications for local irrigation. *Int. J. Water Resour. Dev.* **2020**, 1–26. [CrossRef]
41. van Vuuren, D.P.; Edmonds, J.; Kainuma, M.; Riahi, K.; Thomson, A.; Hibbard, K.; Hurtt, G.C.; Kram, T.; Krey, V.; Lamarque, J.F.; et al. The representative concentration pathways: An overview. *Clim. Chang.* **2011**, *109*, 5–31. [CrossRef]
42. Arnold, J.G.; Srinivasan, R.; Muttiah, R.S.; Williams, J.R.; Ramanarayanan, T.S.; Arnold, J.G.; Bednarz, S.T.; Srinivasan, R.; Muttiah, R.S.; Williams, J.R. Large area hydrologic modeling and assessment part I: Model development 1. *JAWRA J. Am. Water Resour. Assoc.* **1998**, *34*, 73–89. [CrossRef]
43. Arnold, J.G.; Kiniry, J.R.; Srinivasan, R.; Williams, J.R.; Haney, E.B.; Neitsch, S.L. Soil & Water Assessment Tool: Input/output documentation. Version 2012. *Texas Water Resources Institute TR-439*. 2013. Available online: https://swat.tamu.edu/media/69296/swat-io-documentation-2012.pdf (accessed on 29 May 2021).
44. Taylor, K.E. Summarizing multiple aspects of model performance in a single diagram. *J. Geophys. Res.* **2001**, *106*, 7183–7192. [CrossRef]
45. Jakob Themeßl, M.; Gobiet, A.; Leuprecht, A. Empirical-statistical downscaling and error correction of daily precipitation from regional climate models. *Int. J. Climatol.* **2011**, *31*, 1530–1544. [CrossRef]
46. Pandey, V.P.; Dhaubanjar, S.; Bharati, L.; Thapa, B.R. Hydrological response of Chamelia watershed in Mahakali Basin to climate change. *Sci. Total Environ.* **2019**, *650*, 365–383. [CrossRef]
47. Lenderink, G.; Buishand, A.; Van Deursen, W. Estimates of future discharges of the river Rhine using two scenario methodologies: Direct versus delta approach. *Hydrol. Earth Syst. Sci.* **2007**, *11*, 1145–1159. [CrossRef]
48. Schmidli, J.; Frei, C.; Vidale, P.L. Downscaling from GCM precipitation: A benchmark for dynamical and statistical downscaling methods. *Int. J. Climatol.* **2006**, *26*, 679–689. [CrossRef]
49. Terink, W.; Hurkmans, R.T.W.L.; Torfs, P.J.J.F.; Uijlenhoet, R. Evaluation of a bias correction method applied to downscaled precipitation and temperature reanalysis data for the Rhine basin. *Hydrol. Earth Syst. Sci.* **2010**, *14*, 687–703. [CrossRef]
50. Piani, C.; Weedon, G.P.; Best, M.; Gomes, S.M.; Viterbo, P.; Hagemann, S.; Haerter, J.O. Statistical bias correction of global simulated daily precipitation and temperature for the application of hydrological models. *J. Hydrol.* **2010**, *395*, 199–215. [CrossRef]
51. Teutschbein, C.; Seibert, J. Is bias correction of regional climate model (RCM) simulations possible for non-stationary conditions. *Hydrol. Earth Syst. Sci.* **2013**, *17*, 5061–5077. [CrossRef]

52. Maraun, D.; Widmann, M. Cross-validation of bias-corrected climate simulations is misleading. *Hydrol. Earth Syst. Sci.* **2018**, *22*, 4867–4873. [CrossRef]
53. Gudmundsson, L.; Bremnes, J.B.; Haugen, J.E.; Engen-Skaugen, T. Technical Note: Downscaling RCM precipitation to the station scale using statistical transformations—A comparison of methods. *Hydrol. Earth Syst. Sci.* **2012**, *16*, 3383–3390. [CrossRef]
54. Themeßl, M.J.; Gobiet, A.; Heinrich, G. Empirical-statistical downscaling and error correction of regional climate models and its impact on the climate change signal. *Clim. Chang.* **2012**, *112*, 449–468. [CrossRef]
55. Gumbel, E.J. Return Period of Flood Flows. *Ann. Math. Stat.* **1941**, *12*, 163–190. [CrossRef]
56. Devkota, R.P.; Maraseni, T. Flood risk management under climate change: A hydro-economic perspective. *Water Sci. Technol. Water Supply* **2018**, *18*, 1832–1840. [CrossRef]
57. Devkota, R.P.; Bhattarai, U. Assessment of climate change impact on floods from a techno-social perspective. *J. Flood Risk Manag.* **2018**, *11*, S186–S196. [CrossRef]
58. Chow, V.T.; Maidment, D.R.; Mays, L.W. *Applied Hydrology*; TATA McGrawHill Inc.: New York, NY, USA, 1988.
59. Devkota, L.P.; Gyawali, D.R. Impacts of climate change on hydrological regime and water resources management of the Koshi River Basin, Nepal. *J. Hydrol. Reg. Stud.* **2015**, *4*, 502–515. [CrossRef]
60. Chen, B.; Krajewski, W.F.; Liu, F.; Fang, W.; Xu, Z. Estimating instantaneous peak flow from mean daily flow. *Hydrol. Res.* **2017**, *48*, 1474–1488. [CrossRef]
61. Devkota, R.; Bhattarai, U.; Devkota, L.; Maraseni, T.N. Assessing the past and adapting to future floods: A hydro-social analysis. *Clim. Chang.* **2020**, *163*, 1065–1082. [CrossRef]
62. Dahal, V.; Shakya, N.M.; Bhattarai, R. Estimating the impact of climate change on water availability in Bagmati Basin, Nepal. *Environ. Process.* **2016**, *3*, 1–17. [CrossRef]
63. Dhaubanjar, S.; Prasad Pandey, V.; Bharati, L. Climate futures for Western Nepal based on regional climate models in the CORDEX-SA. *Int. J. Climatol.* **2020**, *40*, 2201–2225. [CrossRef]
64. Pandey, V.P.; Dhaubanjar, S.; Bharati, L.; Thapa, B.R. Spatio-temporal distribution of water availability in Karnali-Mohana Basin, Western Nepal: Climate change impact assessment (Part-B). *J. Hydrol. Reg. Stud.* **2020**, *29*, 100691. [CrossRef]
65. MoFE. *Climate Change Scenarios for Nepal for National Adaptation Plan (NAP)*; Ministry of Forests and Environment: Kathmandu, Nepal, 2019.
66. Bajracharya, A.R.; Bajracharya, S.R.; Shrestha, A.B.; Maharjan, S.B. Climate change impact assessment on the hydrological regime of the Kaligandaki Basin, Nepal. *Sci. Total Environ.* **2018**, *625*, 837–848. [CrossRef]
67. Mishra, Y.; Nakamura, T.; Babel, M.S.; Ninsawat, S.; Ochi, S. Impact of climate change on water resources of the Bheri River Basin, Nepal. *Water* **2018**, *10*, 220. [CrossRef]
68. Phi Hoang, L.; Lauri, H.; Kummu, M.; Koponen, J.; Vliet, M.T.H.V.; Supit, I.; Leemans, R.; Kabat, P.; Ludwig, F. Mekong River flow and hydrological extremes under climate change. *Hydrol. Earth Syst. Sci.* **2016**, *20*, 3027–3041. [CrossRef]
69. Zhou, Y.; Xu, Y.J.; Xiao, W.; Wang, J.; Huang, Y.; Yang, H. Climate change impacts on flow and suspended sediment yield in headwaters of high-latitude regions-A case study in China's far Northeast. *Water* **2017**, *9*, 966. [CrossRef]
70. Wang, Y.; Yang, X.; Zhang, M.; Zhang, L.; Yu, X.; Ren, L.; Liu, Y.; Jiang, S.; Yuan, F. Projected effects of climate change on future hydrological regimes in the upper Yangtze River basin, China. *Adv. Meteorol.* **2019**, *2019*, 1545746. [CrossRef]
71. Wagener, T.; Wheater, H.; Gupta, H.V. *Rainfall-Runoff Modelling in Gauged and Ungauged Catchments*; World Scientific: Singapore, 2004; ISBN 1860944663.
72. Kingston, D.G.; Thompson, J.R.; Kite, G. Uncertainty in climate change projections of discharge for the Mekong River Basin. *Hydrol. Earth Syst. Sci.* **2011**, *15*, 1459–1471. [CrossRef]
73. Sapač, K.; Medved, A.; Rusjan, S.; Bezak, N. Investigation of low- and high-flow characteristics of karst catchments under climate change. *Water* **2019**, *11*, 925. [CrossRef]

International Journal of Energy and Water Resources
https://doi.org/10.1007/s42108-021-00174-w

ORIGINAL ARTICLE

Unravelling the water-energy-economics-continuum of hydroelectricity in the face of climate change

S. Marahatta[1] · U. Bhattarai[2,3] · L. P. Devkota[3,4] · D. Aryal[1]

Received: 30 September 2021 / Accepted: 15 December 2021

Abstract
This study is aimed at evaluating the impacts of climate change (CC) on the water-energy-economics-continuum considering a storage type hydroelectricity project (STP). Inflows from ensembled CC scenarios for two RCPs (4.5 and 8.5) and three time-windows (near-future, mid-future, far-future) until the end of this century, generated from an earlier study by the same team, was used for the analysis. The proposed 1200 MW Budhigandaki Hydropower Project in Nepal is taken as a case. A set of reservoir operating rules were derived considering the baseline data which was then used to generate future energy and revenue at the monthly, seasonal and annual timescales. Results show that future annual energy is expected to increase by about 9–13% from the baseline. Furthermore, future revenue generation is projected to increase in the range of 20–28 million USD annually. This overall gain in the revenue due to additional energy generation is an anticipated positive impact of CC which is capable of contributing to the reduction of greenhouse gases and minimizing fossil-fuel laden trade deficit. This study recommends that: STPs with the provision of flexible operating rules are desirable for climate resiliency in hydroelectricity; areas expected to witness decreased future hydroelectricity generation need to explore other alternative sources of renewable energy; and the policy instruments pertaining to the financial aspects of hydroelectricity should be continuously updated considering future conditions.

Keywords Water-energy-economics-continuum · Hydroelectricity · Climate change · Energy economics · Energy policy

Introduction

The urgent world-wide need of switching to green energy has led to hydroelectricity, wind, solar, geothermal and wave receiving global attention (Bogdanov et al., 2021; Davis et al., 2020; Dietzenbacher et al., 2020; Liao et al., 2021). Among the identified renewable sources of clean energy, hydroelectricity is over a century old and a well-proven technology with significant developments in its planning, design of hydraulic structures, electro-mechanical components as well as distribution systems. Likewise, studies have also focused on methane emissions, sediment and overall water environment of reservoirs and dams associated with hydroelectricity projects (Janssen et al., 2021; Li et al., 2018; Liu et al., 2019, 2020).

Hydroelectricity contributes about 3% of the total global energy and has a major share (about 17%) in the total world's electricity generation (IEA, 2020). The contribution of hydro-energy is found to be substantial in countries with a relatively smaller energy/electricity demand and high water availability. However, it varies significantly across countries. The share of hydroelectricity in the gross national supply of electricity is 100% in Albania, 99% in Congo, 97% in Paraguay, 92% in Iceland and 90% in Nepal (IEA, 2020). On the contrary, the contribution of hydroelectricity on the current electricity supply is relatively small for high energy-consuming countries. For instance, it is 1232 Terawatt-hour, TWh (17%) in China, 317 TWh (7%) in USA, and 193 TWh (17%) in Russia (IEA, 2020). Some exceptions of high energy consuming countries with a high share of hydroelectricity

✉ S. Marahatta
suresh.marahatta@cdhm.tu.edu.np

1 Central Department of Hydrology and Meteorology, Institute of Science and Technology, Tribhuvan University, Kathmandu, Bagmati, Nepal

2 Institute for Life Sciences and the Environment, University of Southern, Queensland, Toowoomba, Queensland 4350, Australia

3 Water Modeling Solution Pvt. Ltd., Lalitpur, Bagmati, Nepal

4 Nepal Academy of Science and Technology (NAST), Lalitpur, Bagmati, Nepal

Published online: 06 January 2022

are Brazil 389 TWh (65%), Canada 386 TWh (59%) and Norway 140 TWh (95%) (Martins et al., 2018; Tomczyk & Wiatkowski, 2020). Best (2017) makes an interesting comparison showing that the capital cost of a hydroelectricity project is about 4.0 million USD per Megawatt (MW) which is only slightly more expensive than a coal plant, two-thirds of a nuclear or geothermal plant and one-fourth of the cost of a solar power plant. These figures show that hydroelectricity is an important energy source globally.

Hydroelectricity is mainly dependent on the temporal variation of river flow, which in turn is, largely impacted by climate change (CC). Generally, run-of-the-river (ROR) facilities are more affected than storage type plants (STPs). Several studies have analyzed how runoff will change at the global (Turner et al., 2017a, b; Zhou & Hanasaki, 2018), regional (Ali et al., 2018; Zhong et al., 2019) and local (Devkota & Gyawali, 2015; Pandey et al., 2019; Kaini et al., 2020; Marahatta et al., 2021a) scales in the future due to CC. A common inference from all these studies is that the CC impacts on hydroelectricity is largely influenced by the geographical location of the hydroelectricity plant and choice of climate models despite high levels of uncertainty in the direction and magnitude of the predictions (Marahatta et al., 2021a).

It is seen that the impact of CC on runoff and water availability for hydroelectricity projects have been studied in different countries such as Brazil, Canada, China, and Nepal where hydroelectricity is the dominant electricity provider (Caceres et al., 2021; Liu et al., 2016; Shrestha et al., 2021). Moreover, there are ample studies on renewable energy mostly targeted towards advancement of newer technologies and analyses of the conversion from current fossil-fuel based to a renewables-dominated economy (Davis et al., 2020; Paltsev, 2020; Bogdanov et al., 2021; Liu et al., 2021; Mutezo & Mulopo, 2021; Poletti & Staffell, 2021). The current research trend on energy economics is found to be largely focused on fossil fuels (Barreto, 2018; Belfiori, 2020; Hanif et al., 2019; Poudineh et al., 2020; Ranzani et al., 2018; Rehman et al., 2021) and other water management issues (Pakhtigian et al., 2020). However, research on the effects and economic values of established technologies such as hydroelectricity is rather limited (Mattmann et al., 2016). Extending this gap further is the micro-economic assessment of the cost and revenue aspects of hydroelectricity linked to CC at the project level. This study attempts to address this niche and paves way for integrated economic evaluations of the hydroelectricity sector.

The overarching objective of this study is to evaluate the impact of CC on the water-energy-economics-continuum considering a storage type hydroelectricity project (STP) over a time horizon of a century. The specific objectives are: (i) to examine how the electricity production is impacted in future climate scenarios and time windows; and (ii) to compare the future CC-induced seasonal and annual revenue generation from hydroelectricity with that of the base period. The insightful evidence that is produced shall be extremely useful for climate resilient planning and design of hydroelectricity projects in complex and mountainous river basins. The proposed 1200 MW Budhigandaki Hydropower Project (BGHP, a storage type project) located in Nepal in the central Hindu Kush Himalayan (HKH) region is taken as a case.

To the knowledge of the authors, hydrology (river flow), energy (hydroelectricity) and economics (revenue aspects) including climate change have not been dealt with in a single study. Furthermore, we have attempted to link the research/academic sector to the policy making level by providing evidence-based policy prescriptions. We consider this as a significant contribution from our side, rarely found in many published studies.

Materials and methods

Study area

The Budhigandaki is a complex mountainous river basin. Its drainage area at the confluence of Trishuli River is 4988 km^2 out of which nearly one-fourth lies in Tibetan plateau of People Republic of China and remaining part lies in the Federal Democratic Republic of Nepal (Fig. 1). The basin has a high hydroelectricity potential in which more than 35 hydroelectric projects ranging from 0.5 to 1200 MW are at various stages of development (Marahatta et al., 2021b). Relevant salient features of the study project, BGHP are given in Fig. 1. Readers are referred to Marahatta et al., (2021c) and Devkota et al. (2016) for details on the geography, terrain and topography, hydro-meteorology and supplementary information of the basin.

Terrain data

The reservoir water surface area (A) is estimated as a power function of its depth (y) as given in Eq. (1) (Devkota et al., 2021, 2022)

$$A = \alpha y^{\beta}. \tag{1}$$

The best-fit value of the multiplicative coefficient (α) is 1360 and the power coefficient (β) is 2.0 which have been adopted for further calculations.

Flow data

The baseline and projected ensemble flow data used in this study are respectively from 1983 to 2012 (30 years) and

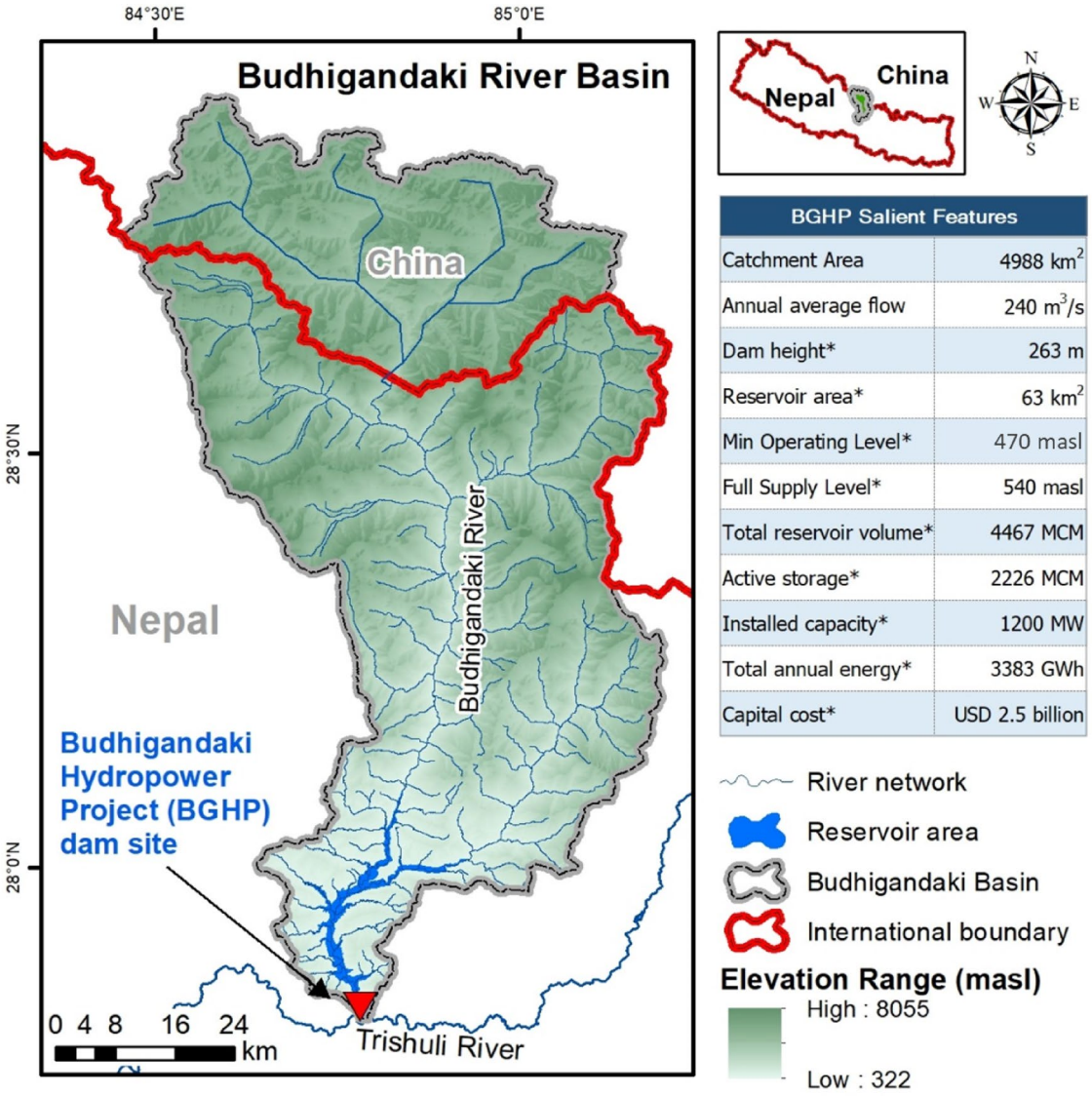

Fig. 1 Location map of Budhigandaki Basin; *source: (BGHP, 2015)

2021 to 2099 (79 years) (Fig. 2). Two RCPs—4.5 (stabilization scenario) and 8.5 (high emission scenario) of the Fifth Assessment Report of Intergovernmental Panel on Climate Change (IPCC) were considered for future climate projections. The flow data were derived from an earlier study (Marahatta et al., 2021a) by the same team. Data of each RCP were divided into three 30-year time windows, viz., immediate future (IF): 2021–2050; mid future (MF): 2046–2075 and far future (FF): 2070–2099. It is seen that there is a consistent increase in the annual flow in both the RCPs over time with the magnitude more prominent in RCP 8.5. The selection procedure of the climate models, bias correction methods and ensemble details are briefly discussed in Marahatta et al., (2021a).

Methodology

Figure 3 depicts the overall methodology applied in this research. This study utilizes the baseline inflows to the BGHP damsite at monthly timestep to generate a set of reservoir operating rules taking into account terrain data and the constraints based on the assumptions (details of the assumptions can be found in Devkota et al., (2021, 2022). The main objective of determination of these rules is to maximize dry season (December–May) energy. Applying these rules on long-term flows, energy was calculated for the baseline period at monthly timescale. Further, using the same operating rules, monthly energy generation for the future (three time-windows: IF, MF and FF) under CC

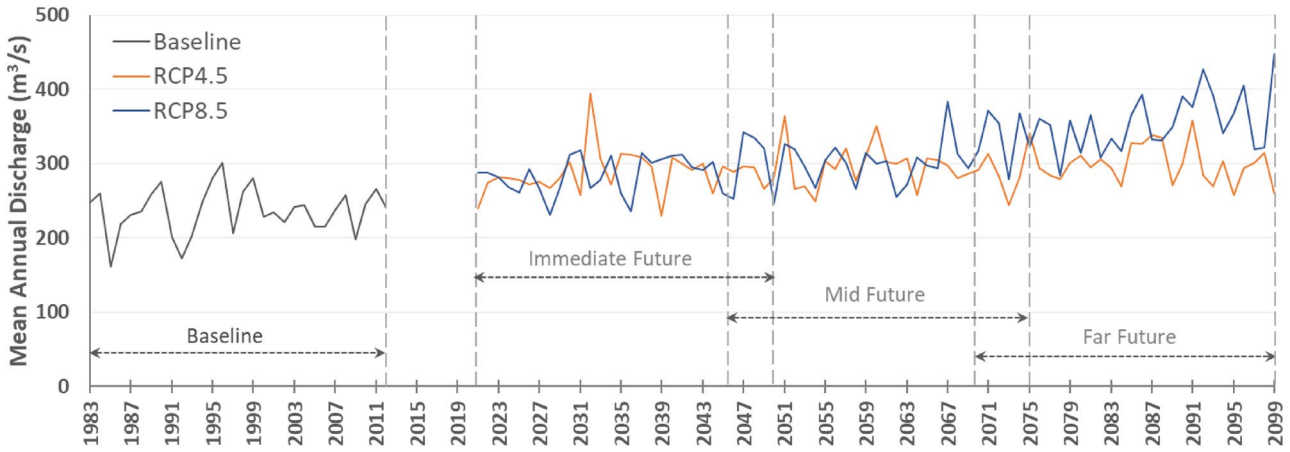

Fig. 2 Mean annual inflows to the BGHP reservoir for the historical (baseline) and ensembled (projected future time periods) used in this study [data from (Marahatta et al., 2021a)]

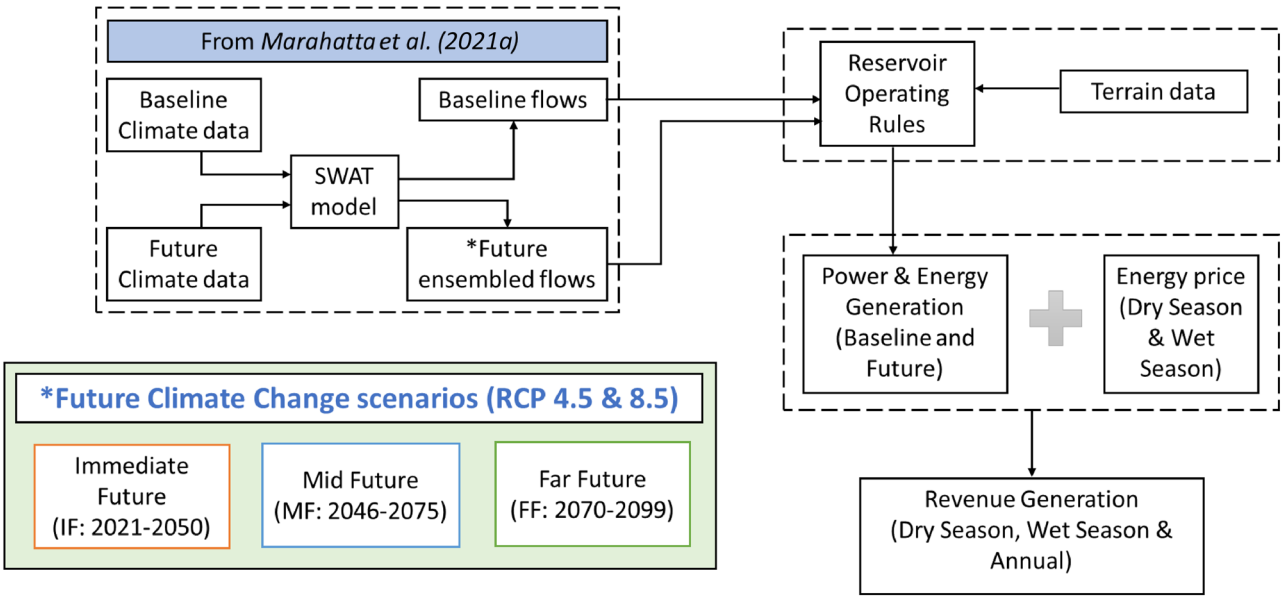

Fig. 3 Overall methodological framework adopted in this study

RCPs 4.5 and 8.5 were also determined. The terrain and other salient features of the project site have been assumed to be constant throughout our period of analysis. Future energy generation was compared with the base case at monthly, seasonal and annual timescales. The seasonal and annual revenues equivalent to the generated monthly energy for the above-mentioned scenarios were then calculated using the power purchasing agreement (PPA) rates fixed by the Nepal Electricity Authority (NEA, 2017) and compared with the base case. The governing equations of this study are listed hereunder.

For any month i of year j, the power that can be generated by a hydroelectric plant is given by Eq. (2) (Devkota et al., 2021, 2022).

$$P_{i,j} = \eta \cdot \gamma \cdot Q_{Ti,j} \cdot H_{i,j}/1000, \tag{2}$$

where, P = generated power (MW), η = overall efficiency of the plant (0.93, considered a constant), γ = unit weight of water (9.8 kN/m^3, considered a constant), Q_T = flow passing through the turbine (m^3/s) and H = available net head (m).

It is assumed that the hydroelectric plant runs continuously and thus the corresponding monthly energy generation (in GWh) is the product of the power and the number of days in a given month in compatible units (Eq. 3). For convenience in comparison, all the analysis was carried out in terms of energy rather than power.

$$E_{i,j} = P_{i,j} \cdot n_{i,j} \cdot \left(\frac{24}{1000}\right), \tag{3}$$

where, E = total energy generated (GWh), n = number of days.

The percentage change in energy production is calculated using Eq. (4).

$$\Delta E_{i,j} = \frac{E_{i,j,\mathrm{CC}} - E_{i,\mathrm{base}}}{E_{i,\mathrm{base}}} \cdot 100, \tag{4}$$

where, $\Delta E_{i,j}$ = change in the total energy generated expressed as percentage, $E_{i,j,\mathrm{CC}}$ = total energy generated in the ith month of the jth year of the CC scenario, $E_{i,\mathrm{base}}$ = total energy generated in the ith month of the base case.

The PPA rates for dry and wet season are different. It is assumed that these rates remain constant throughout the simulation period. Adopted exchange rate is: 1 USD = 119 NRs (NRB, 2021). The monthly and annual revenues (in USD) are calculated as:

$$R_{i,j} = E_{i,j} \cdot \mathrm{PPA}_i, \tag{5}$$

$$\mathrm{DR}_j = \sum_{i=\mathrm{Dec}}^{\mathrm{May}} R_{i,j}, \tag{6.1}$$

$$\mathrm{WR}_j = \sum_{i=\mathrm{Jun}}^{\mathrm{Nov}} R_{i,j}, \tag{6.2}$$

$$\mathrm{AR}_j = \sum_{i=\mathrm{Jan}}^{\mathrm{Dec}} R_{i,j}, \tag{6.3}$$

where, $R_{i,j}$ = revenue generated (USD), DR_j = total dry season revenue, WR_j = total wet season revenue, AR_j = total annual revenue.

The percentage change in revenue at monthly and annual timescales are given as:

$$\Delta R_{i,j} = \frac{R_{i,j,\mathrm{CC}} - R_{i,\mathrm{base}}}{R_{i,\mathrm{base}}} \cdot 100, \tag{7}$$

$$\Delta \mathrm{DR}_j = \frac{\mathrm{DR}_{j,\mathrm{CC}} - \mathrm{DR}_{j,\mathrm{base}}}{\mathrm{DR}_{j,\mathrm{base}}} \cdot 100, \tag{8.1}$$

$$\Delta \mathrm{WR}_j = \frac{\mathrm{WR}_{j,\mathrm{CC}} - \mathrm{WR}_{j,\mathrm{base}}}{\mathrm{WR}_{j,\mathrm{base}}} \cdot 100, \tag{8.2}$$

$$\Delta \mathrm{AR}_j = \frac{\mathrm{AR}_{j,\mathrm{CC}} - \mathrm{AR}_{j,\mathrm{base}}}{\mathrm{AR}_{j,\mathrm{base}}} \cdot 100, \tag{8.3}$$

where, $R_{i,\mathrm{base}}$ = total monthly revenue generated in the base period, $R_{i,j,\mathrm{CC}}$ = total monthly revenue generated in the CC scenario, $\Delta R_{i,j}$ = change in the total revenue, $\Delta \mathrm{DR}_j$ = change in the dry season revenue, $\Delta \mathrm{WR}_j$ = change in the wet season revenue, $\Delta \mathrm{AR}_j$ = change in the annual revenue.

We define the annual profit as the difference between the revenue generated from the hydroelectricity project and the operation and maintenance (O&M) costs at an annual scale. Considering the jth year, it is expressed mathematically as in Eq. (9).

$$\pi_j = \mathrm{AR}_j - C_{\mathrm{O\&M},j}, \tag{9}$$

where, π_j = total annual profit, $C_{\mathrm{O\&M},j}$ = total annual operation and maintenance cost.

The change in annual profit because of the impact of CC is given by Eq. (10).

$$\Delta \pi_j = \left(\mathrm{AR}_{j,\mathrm{CC}} - C_{\mathrm{O\&M},j,\mathrm{CC}}\right) - \left(\mathrm{AR}_{j,\mathrm{base}} - C_{\mathrm{O\&M},j,\mathrm{base}}\right). \tag{10}$$

For the sake of simplicity, the physical infrastructure (e.g., spillway to dispose CC induced excess water) of the BGHP is assumed to be constructed considering the impact of CC. Hence, the annual O&M cost is not affected significantly by CC. Thus, the annual O&M cost is assumed to remain constant for the base case as well as for the future CC cases (i.e., $C_{\mathrm{O\&M},j,\mathrm{base}} = C_{\mathrm{O\&M},j,\mathrm{CC}}$).

With the aforementioned assumptions, it can be safely derived that the change in annual revenue generation in the future CC scenarios compared to the base case is as given by Eq. (11).

$$\Delta \pi_j = \mathrm{AR}_{j,\mathrm{CC}} - \mathrm{AR}_{j,\mathrm{base}}. \tag{11}$$

Results and discussion

Operating rule

The reservoir operating rules were used to generate at monthly timesteps: (i) the average discharge (Q_T) available for the turbine, (ii) available net head (H), (iii) power generation (P) corresponding to the average discharge and available head, (iv) maximum allowable discharge ($Q_{\max}$) to the turbine meeting all the requirements and physical constraints, (v) maximum possible power generation

Table 1 Monthly values of the variables determined as reservoir operating rule for the base case

Base case variables	Months											
	Jan	Feb	Mar	Apr	May	Jun	Jul	Aug	Sep	Oct	Nov	Dec
Q_{LTMA} (m^3/s)	73	71	83	114	171	354	577	593	429	191	102	81
Q_T (m^3/s)	266	280	297	322	354	141	231	238	172	191	102	255
H (m)	202	192	181	167	152	153	173	194	209	215	215	211
P (MW)	491	491	491	491	491	198	365	421	328	374	198	491
E (GWh)	365	330	365	353	365	142	272	313	236	278	143	365
Q_{max} (m^3/s)	266	280	297	322	354	351	310	277	257	251	251	255
P_{max} (MW)	491	491	491	491	491	491	491	491	491	491	491	491
E_{max} (GWh)	365	330	365	354	365	354	365	365	354	365	354	365

Q_{LTMA} is the long-term mean monthly flow of baseline period; Q_T is the available monthly discharge used to calculate the power (P) for the baseline period (base case); H is the available net head; Q_{max} is the maximum allowable discharge for a given month meeting reservoir filling and turbine capacity constraints; P_{max} and E_{max} are the maximum possible power and energy generation corresponding to Q_{max}

(P_{max}) and (vi) maximum possible energy generation for the base case (Table 1). It is evident that Q_T is the lowest (102 m^3/s) in November while it is more than triple in May (353 m^3/s). The maximum net head (H) is available during the months of October and November (215 m) which corresponds to the full supply level (FSL) of the reservoir. Head is the lowest in May (152 m). The highest P has been calculated as 491 MW for dry months and the lowest of 198 MW in June and November. It can also be seen that Q_{max} in April, May, June and July are higher (322, 354, 351 and 310 m^3/s, respectively) than the other months of the year (251–297 m^3/s). P_{max} is 491 MW while the corresponding E_{max} is in the range of 330–365 GWh amounting to a maximum annual value of 4301 GWh.

The operating rules prioritize dry season energy maximization. They are derived in such a way that the inflow of the wet months (June–November) is first used to fill up the reservoir to a pre-defined level and then generate energy from the remaining available water (Devkota et al., 2021, 2022). Water stored in the reservoir during the monsoon is slowly released in the dry months (December–May) such that it is at the minimum operating level in the end of pre-monsoon (May), ready to be refilled by the monsoon. In October and November, the reservoir is kept full and the hydroelectricity plant operates as an ROR project. In the dry months, the discharge available to the turbine is the sum of natural inflow as well as a part of the stored reservoir water. The excess available discharge is spilled out from the reservoir only in cases when $Q > Q_{max}$ such that the condition of $P = P_{max}$ and $E = E_{max}$ is maintained. This shows that there is a high flexibility in varying the operating rules according to the projected future climatic conditions in STPs to minimize spill and maximize power generation.

Baseline energy generation

Figure 4a gives a snapshot of the monthly variability in the energy generation of the BGHP over the 30 years baseline period considering (30 years × 12 months =) 360 data points. The vertical rectangle is the spread of the data within the first quartile (Q_1)–third quartile (Q_3) range while the values beyond 1.5 times this Q_1–Q_3 interquartile range (in both positive and negative directions) are treated as outliers. They have been replaced by values in the respective limits of the quartiles. It can be seen that the mean generated energy is about 350 GWh from December to May while the variability is quite high in the monsoon months of June through October ranging from about 145 (November) to 280 (August) GWh. Some dry years have zero energy generation even in the monsoon months. Figure 4b is a distribution plot of the monthly energy generation for the baseline. During this period, 135 months (~38%) produce energy in the range of 350–400 GWh, 87 months (~27%) are capable of generating 300–350 GWh while 6 months (<2%) are able to generate only 50–100 GWh for the baseline period. The average annual energy generated in this period is 3385 GWh. It can be seen from Fig. 4c that the dry season energy generation is almost constant at 2000 GWh throughout the baseline period. However, a variation of 484 (in 1985)–1782 GWh (in 1999) is noted in the wet season energy generation. This variability is also carried over to the respective annual energy generation values of 2552–3875 GWh.

Future energy generation

The projected average annual energy generations in IF, MF and FF are respectively 3871, 3861 and 3877 GWh, clearly indicating increases of about 14% compared to the baseline.

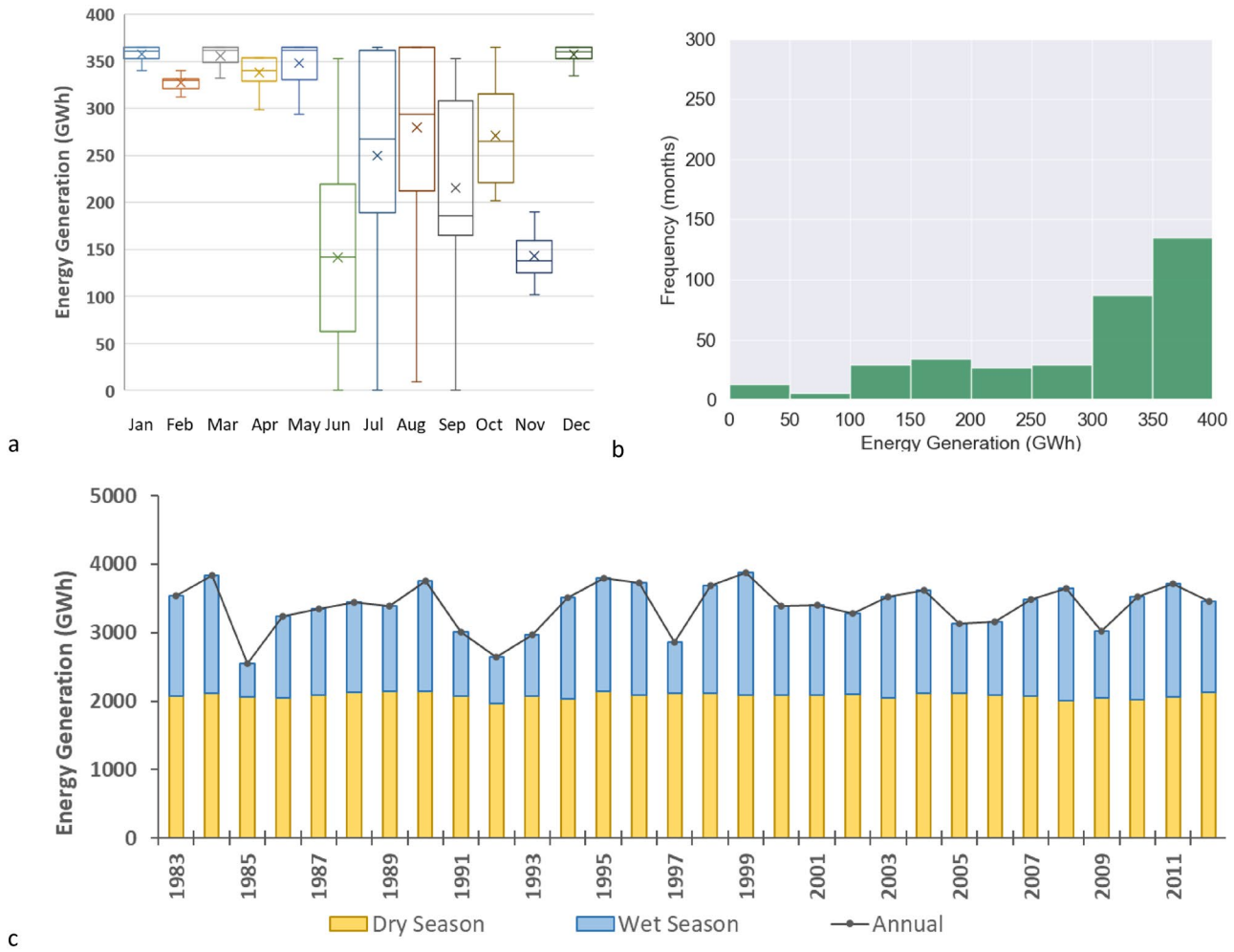

Fig. 4 **a** Monthly variability; **b** frequency histogram; and **c** seasonal and annual variation of energy generation for the baseline period (1983–2012). In **a**, for a given month, the rectangular boxes show the Q_1–Q_3 quartiles range while the error bars represent the maximum-minimum range. The median values are shown as horizontal lines inside the boxes and the cross-marks indicate mean values. In **c**, orange bars represent dry season, blue bars wet season and the solid line with black markers indicates annual energy generation values. Number of data points = 360

Energy distribution plots were generated for the three future time windows for RCP 4.5 and RCP 8.5 (Fig. 5). Very interestingly, in the case of RCP 4.5 (Fig. 5 top pane), more than 220 months (61%) are expected to generate energy in the range of 350–400 GWh for all the three time-windows which shows a significant increase in the expected energy generation compared to the baseline (38% of time). The total number of months with expected energy generation in the range of 300–350 GWh is 66, 64 and 68 for IF, MF and FF, respectively (~ 18% of the time). Notably, the cumulative number of months generating energy less than 300 GWh is below 72 (~ 20%) for all the time windows; about half that value of the baseline (138 months, 43%).

In the case of RCP 8.5 (Fig. 5-bottom pane), 228 (63%), 242 (67%) and 269 (75%) months are expected to generate energy in the range of 350–400 GWh for IF, MF and FF, respectively: a notable similarity with the RCP 4.5 case. The total number of months in IF, MF and FF with expected energy generation in the range of 300–350 GWh are respectively 59 (16%), 58 (16%) and 41 (11%). It can be further seen that the number of months generating 250–300 GWh are less than 20 (6%) for all the three time-windows: a slight decrease in comparison to the baseline. Only 1 month each in IF and FF and 2 months in MF are expected to generate energy up to 50 GWh which is a significant reduction compared to the base case of 13 months. The projected average annual energy generation are 3864 (IF), 3949 (MF) and 3999 (FF) GWh which clearly indicate increases by 14%, 17% and 18% respectively from the baseline.

Interestingly, when future energy generation is plotted temporally (Fig. 6), an almost constant dry season energy generation (~ 2000 GWh) across all the six CC scenarios

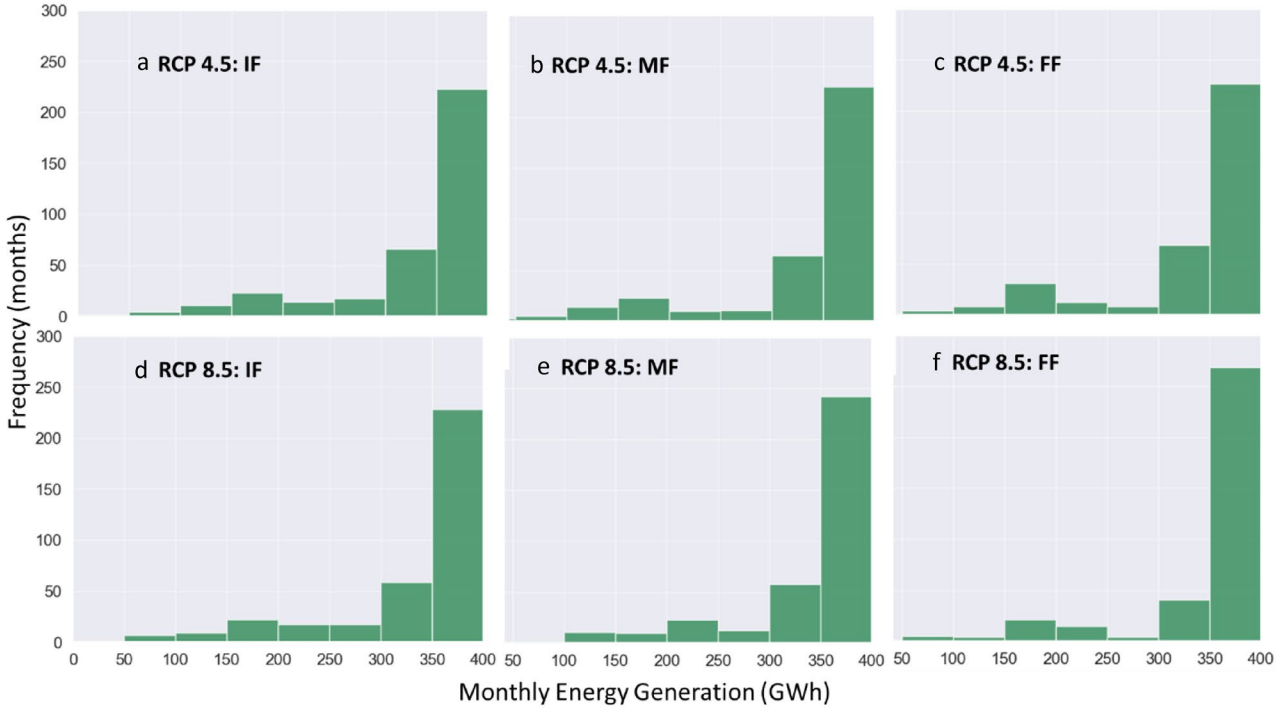

Fig. 5 Monthly frequency histogram of energy generation for RCP 4.5 (top) and RCP 8.5 (bottom) and three time-windows—**a** and **d** immediate future (IF: 2021–2050); **b** and **e** mid future (MF: 2046–2075); and **c** and **f** far future (FF: 2070–2099). Number of data points = 360 for each case

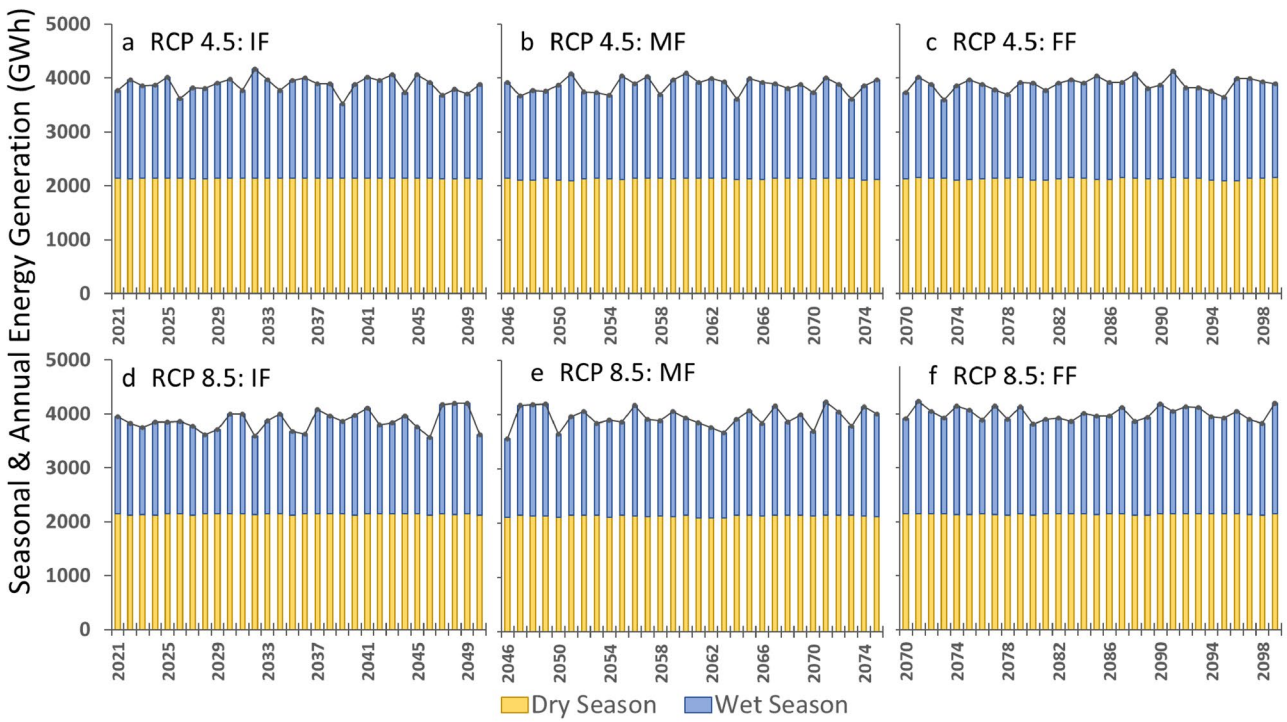

Fig. 6 Seasonal and annual energy generation for RCP 4.5 (top) and RCP 8.5 (bottom) and three time-windows—**a** and **d** immediate future (IF: 2021–2050); **b** and **e** mid future (MF: 2046–2075); and **c** and **f** far future (FF: 2070–2099). Orange bars represent dry season, blue bars wet season and the solid line with black markers indicates annual energy generation values. Number of data points = 360 for each case

Table 2 Comparison of monthly and annual energy generation (in GWh) of RCP 4.5 and RCP 8.5 (each averaged over the respective time window) with the base case

Energy (GWh)	Jan	Feb	Mar	Apr	May	Jun	Jul	Aug	Sep	Oct	Nov	Dec	Annual
Base case	365	330	365	353	365	142	272	313	236	278	143	365	3528
RCP 4.5													
IF	365	330	365	354	359	201	349	365	333	319	168	365	3871
% change	0.0	0.0	0.0	0.0	−1.7	41.0	28.2	**16.6**	40.8	14.8	17.2	0.0	9.7
MF	365	330	365	353	350	179	352	365	353	318	166	365	3861
% change	0.0	0.0	0.0	−0.3	**−4.2**	26.1	29.3	**16.6**	**49.4**	14.4	16.4	0.0	9.4
FF	365	333	365	349	353	192	352	365	353	321	165	365	3877
% change	0.0	**0.87**	0.0	**−1.2**	−3.4	34.9	29.3	**16.6**	**49.4**	15.5	15.1	0.0	9.9
RCP 8.5													
IF	365	330	365	353	358	179	283	365	336	356	207	365	3864
% change	0.0	0.0	0.0	−0.3	−1.9	26.1	4.2	**16.6**	42.3	28.1	45.1	0.0	9.5
MF	365	330	365	351	356	200	300	365	353	365	235	365	3949
% change	0.0	0.0	0.0	−0.8	−2.5	40.8	10.2	**16.6**	**49.4**	**31.1**	**64.4**	0.0	11.9
FF	365	330	365	353	360	210	365	365	353	365	203	365	3999
% change	0.0	0.0	0.0	−0.3	−1.5	**47.8**	**34.2**	**16.6**	**49.4**	**31.1**	42.2	0.0	**13.3**

Maximum values of each column are bold-faced

IF immediate future (2021–2050), *MF* mid future (2046–2075), *FF* far future (2070–2099)

is observed. This is very similar to the baseline condition. However, there is a noticeable variation in the wet season ranging from the lowest 1377 GWh in RCP 4.5 (IF) to the highest of 2095 GWh in RCP 8.5 (MF). Consequently, a variation in the range of 3520 GWh (RCP 4.5: IF)–4239 GWh (RCP 8.5: MF) is seen in the annual energy values.

Change in future energy generation

Monthly and annual energy generation for both RCPs were calculated and averaged over the respective time-windows to compare the changes with the base case (Table 2). Very little change is expected in the dry season while it is considerable in the wet months. No change can be expected in the months of December–March; and a nominal decrease during April and May with respect to the base case. Highest change of 64.4% can be expected in November in MF of RCP 8.5. Variation in the annual energy generation ranges from 9.4% (RCP 4.5, MF) to 13.3% (RCP 8.5, FF).

Due to the variation in the geographical location, climate, terrain, hydro-geology and physical setting of the hydroelectricity projects across the world, results from similar other studies cannot be directly compared without due consideration to these differences. Furthermore, the size and type of the hydroelectricity plant and the adopted operating rules play a very important role in the power potential as well as generation (Chang et al., 2018). Therefore, it is found logical to compare the results of our study with those carried out in the HKH region. For instance, Ali et al., (2018) estimate an increase up to 45% in the streamflow and 25% in the hydroelectricity generation in the Ganga Basin (India). Fourteen percent increase is projected in hydro-energy generation in the Tamakoshi Basin (Nepal) (Shrestha, 2016); 1.7% increase in hydroelectricity potential in Kabul (Afghanistan) (Shirsat et al., 2021) and expected variation of −5 to +40% in Upper Indus (Casale et al., 2020). CC studies have also shown projected decline in hydroelectricity generation in the HKH region, for example, up to 13% in the Kulekhani Basin (Nepal) which is attributed to the decrease in future runoff (Shrestha et al., 2021). Hence, our results of the Budhigandaki Basin with a projected 9–13% increase in future hydroelectricity generation is comparable to the findings of the above-mentioned studies.

Change in future revenue generation

In the base case, dry season contributes about 73% (223 million USD) while the wet season has a share of 27% (83 million USD) in the total annual revenue of 36.4 billion USD (Fig. 7a). It is clearly seen that future revenue during the wet season and also at the annual scale can be expected to increase significantly in all the three time-windows for both the RCPs (Fig. 7b). Wet season revenue is expected to increase by about 20 million USD per year on an average for the RCP 4.5 and IF of RCP 8.5 cases. The magnitudes are slightly more pronounced for the MF (26 million USD) and FF (28 million USD) of RCP 8.5. There is an expected decrease in the dry season revenues in all the future climate scenarios but with a relatively much smaller amount

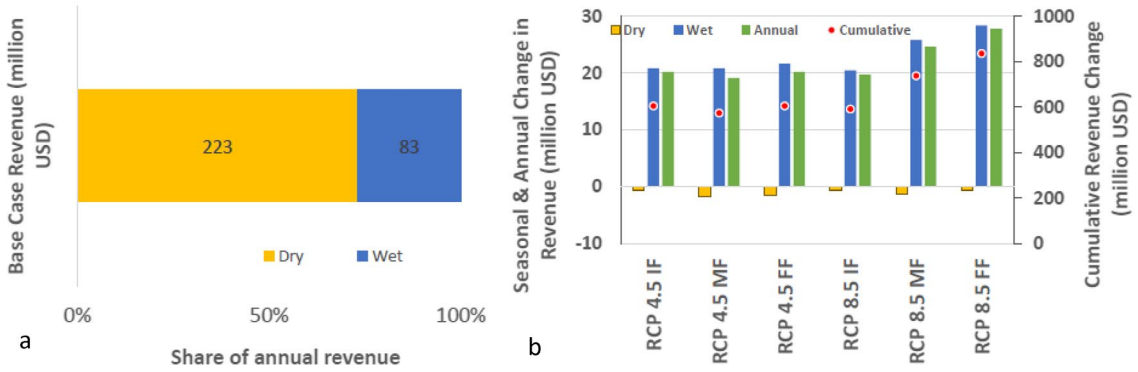

Fig. 7 **a** Seasonal revenue generation and their share on the annual revenue for the base case. **b** Change in dry season (orange bars), wet season (blue bars), annual (green bars) revenue generation compared to the base case for the two future climate change scenarios (RCP 4.5 and RCP 8.5) and three time-windows: immediate future (IF: 2021–2050); mid future (MF: 2046–2075) and far future (FF: 2070–2099); red dots show the total cumulative revenue change in 30 years for each time window

(~ 1 million USD). When accumulated over 30 years for each time window, the total increase in revenue is about 600 million USD for RCP 4.5. These cumulative increases are 590 (IF), 740 (MF) and 835 million USD (FF) for the RCP 8.5 scenario with respect to the base case.

The total cost of constructing the BGHP was calculated to be 2550 million USD in 2015 (BGHP, 2015). Comparing this capital cost with the additional estimated revenue as a result of CC in this study, it can be seen that CC will have an extremely positive impact by earning the cost required for construction of an additional STP with approximately 30% generation capacity (~ 1015 GWh annually) of the proposed BGHP. The annual energy consumption of Nepal was 14.5 Mtoe (169 TWh) for the fiscal year 2019/020 (MoF, 2021) out of which liquified petroleum gas (LPG) was 449,063 metric tonnes[1] (equivalent to 6295 GWh). LPG has an approximately 3.7% share of the total energy consumption of Nepal. Thus, these figures clearly indicate that about 16% of the current national LPG consumption of Nepal can be substituted by the CC-induced additional energy from a single BGHP project. Furthermore, the national trade deficit for the fiscal year 2019/020 was 11.37 billion USD out of which 1.80 billion USD (~ 16%) was from fuel import (MoF, 2021). The estimated additional revenue generation due to CC from the BGHP alone in the high emission scenario is capable of replacing 28 million USD (more than 1.5%) of the national fuel import. These are significant contributions to the economy especially for a developing country, like Nepal, which is largely dependent on hydroelectricity for its electricity and overall energy needs. Upscaling this value to the national level considering all the proposed and planned STPs in Nepal possesses the capacity to displace the existing fossil-fuel consumption by hydroelectricity (clean renewable energy) with tremendous surplus economic benefits.

Additionally, it is seen that exploitation of the available hydroelectricity potential is governed by the economic condition and availability of water resources of a country. For example, the Scandanavian countries, Australia, New Zealand, Japan and Canada have already exploited a large share of their hydroelectricity potential and are switching to other forms of renewable energy to meet the future energy demands (Gunturu & Hallgren, 2017; Amir Jabbari & Nazemi, 2019; Wagner et al., 2019; Poletti & Staffell, 2021). As a result, the impacts of CC on hydroelectricity generation of these countries are expected to be less. Another notable example is China which has generated about 3000 GW from hydropower mainly due to its financial capacity, resources and technology (Liu et al., 2016; IEA, 2020; Qin et al., 2020). However, Africa is able to harness only less than 3% of its total hydro-potential because of the lack of budget to construct megaprojects despite having a tremendous amount of water resources available (Hamududu & Killingtveit, 2016; Mtilatila et al., 2020; Uamusse et al., 2020), a condition very similar to Nepal (Jha, 2011). Brazil has exploited a considerable amount of its hydroelectricity potential and supplies about 30% of the total electricity consumption to the other South American countries. As a result, there is an equally large risk because of possible reduction in its power generation due to CC (Caceres et al., 2021; de Faria & Jaramillo, 2017; de Jong et al., 2018, 2021; de Oliveira et al., 2017; de Queiroz et al., 2019; Donk et al., 2018). Countries which are already heavily reliant on hydroelectricity need to assess the impacts of CC seriously for energy security and economic loss minimization, amidst uncertainties. Moreover, developing countries like Nepal with a high hydroelectricity potential should harness the benefits of this clean renewable energy technology both in terms of

[1] http://noc.org.np/import accessed on 28 July 2021.

its contribution to greenhouse gas reduction and economic gains from increased revenue.

Conclusion

This research evaluated the impacts of CC on the water-energy-economics-continuum considering a storage type hydroelectricity project over a time horizon of a century. An ensemble of different CC scenarios for two RCPs (4.5 and 8.5) and three 30-year time-windows (IF, MF, FF) derived in a previous study by the same research team (Marahatta et al., 2021a) was used as input to the analysis. A set of reservoir operating rules was derived for the BGHP considering the baseline flows, terrain data and other site constraints such that dry season (December–May) energy is maximized. Utilizing the same operating rules and monthly average flows for the baseline and future time-windows, energy for the respective cases were determined and compared at monthly, seasonal and annual timescales. Furthermore, the corresponding seasonal and annual revenues for these scenarios were then calculated and also compared with the base case. Results show that future annual energy is expected to increase by about 9–13% of the base case which indicates an optimistic picture of the future for the hydroelectricity sector as a result of CC. Additionally, projected increment in future revenue generation is in the range of 20–28 million USD annually. Significant gain in the wet season as well as annual revenue due to additional energy generation is an anticipated positive economic impact of CC.

It can be surmised that in areas where future flow and hydroelectricity generation are expected to increase, operating rules based on the historical baseline conditions are likely to turn out to be inefficient. Hence, provision of flexible operating rules in the energy/hydroelectricity policy considering future hydro-climatic conditions is required. Additionally, regions where decreasing flow and/or hydroelectricity generation are expected in the future, other alternative sources of renewable energy like wind, solar and geothermal are to be explored for future energy security. Furthermore, revenue aspects such as the power purchasing rates, rebates and subsidies, penalties, among others, should be revised accordingly considering future projected conditions for the sustainability of the hydroelectricity projects. It is felt necessary for developing countries like Nepal with a high hydroelectricity potential to harness the benefits of this clean renewable energy technology for greenhouse gas reduction along with economic gains from increased revenue.

Acknowledgements The first author would like to thank the University Grants Commission (UGC), Nepal for the research grant (UGC Award No: PhD/73-74/S&T-9). The Budhigandaki Hydroelectric Project Development Committee (BGHP) and the Department of Hydrology and Meteorology (DHM), Government of Nepal are duly acknowledged for providing the necessary data for this research. We acknowledge Mr. Pawan Khatri and Mr. Dibesh Shrestha of Water Modeling Solutions Pvt. Ltd. (Nepal) for their inputs to the paper.

Funding This research was partially funded by University Grants Commission (UGC), Nepal.

References

Ali, S. A., Aadhar, S., Shah, H. L., & Mishra, V. (2018). Projected increase in hydropower production in India under climate change. *Scientific Reports, 8*(1), 1–12. https://doi.org/10.1038/s41598-018-30489-4.

Amir Jabbari, A., & Nazemi, A. (2019). Alterations in Canadian hydropower production potential due to continuation of historical trends in climate variables. *Resources, 8*, 163. https://doi.org/10.3390/resources8040163.

Barreto, R. A. (2018). Fossil fuels, alternative energy and economic growth. *Economic Modelling, 75*, 196–220. https://doi.org/10.1016/j.econmod.2018.06.019.

Belfiori, M. E. (2020). Fossil fuel subsidies, the green paradox and the Fiscal paradox. *Economics of Energy and Environmental Policy, 10*(1), 183–193. https://doi.org/10.5547/2160-5890.10.1.MBEL.

Best, R. (2017). Switching towards coal or renewable energy? The effects of financial capital on energy transitions. *Energy Economics, 63*, 75–83. https://doi.org/10.1016/j.eneco.2017.01.019.

BGHP. (2015). *Feasibility study and detailed design of Budhigandaki hydropower project part 1*. Budhigandaki: Vol. Main (Issue December).

Bogdanov, D., Ram, M., Aghahosseini, A., Gulagi, A., Oyewo, A. S., Child, M., Caldera, U., Sadovskaia, K., Farfan, J., De Souza Noel Simas Barbosa, L., Fasihi, M., Khalili, S., Traber, T., & Breyer, C. (2021). Low-cost renewable electricity as the key driver of the global energy transition towards sustainability. *Energy, 227*, 120467. https://doi.org/10.1016/j.energy.2021.120467.

Casale, F., Bombelli, G.M., Monti, R., & Bocchiola, D. (2020). Hydropower potential in the Kabul River under climate change scenarios in the XXI century. *Theoretical and Applied Climatology, 139*, 1415–1434. https://doi.org/10.1007/s00704-019-03052-y.

Caceres, A. L., Jaramillo, P., Matthews, H. S., Samaras, C., & Nijssen, B. (2021). Hydropower under climate uncertainty: Characterizing the usable capacity of Brazilian, Colombian and Peruvian power plants under climate scenarios. *Energy for Sustainable Development, 61*, 217–229. https://doi.org/10.1016/j.esd.2021.02.006.

Chang, J., Wang, X., Li, Y., Wang, Y., & Zhang, H. (2018). Hydropower plant operation rules optimization response to climate change. *Energy, 160*, 886–897. https://doi.org/10.1016/j.energy.2018.07.066.

Davis, M., Moronkeji, A., Ahiduzzaman, M., & Kumar, A. (2020). Assessment of renewable energy transition pathways for a fossil fuel-dependent electricity-producing jurisdiction. *Energy for Sustainable Development, 59*, 243–261. https://doi.org/10.1016/j.esd.2020.10.011

de Faria, F. A. M., & Jaramillo, P. (2017). The future of power generation in Brazil: an analysis of alternatives to Amazonian hydropower development. *Energy for Sustainable Development, 41*, 24–35. https://doi.org/10.1016/j.esd.2017.08.001.

de Jong, P., Barreto, T. B., Tanajura, C. A. S., Oliveira-Esquerre, K. P., Kiperstok, A., & Andrade Torres, E. (2021). The impact of regional climate change on hydroelectric resources in South

America. *Renewable Energy, 173*, 76–91. https://doi.org/10.1016/j.renene.2021.03.077.

de Jong, P., Tanajura, C. A. S., Sánchez, A. S., Dargaville, R., Kiperstok, A., & Torres, E. A. (2018). Hydroelectric production from Brazil's São Francisco River could cease due to climate change and inter-annual variability. *Science of the Total Environment, 634*, 1540–1553. https://doi.org/10.1016/j.scitotenv.2018.03.256.

de Oliveira, V. A., de Mello, C. R., Viola, M. R., & Srinivasan, R. (2017). Assessment of climate change impacts on streamflow and hydropower potential in the headwater region of the Grande river basin, Southeastern Brazil. *International Journal of Climatology, 37*(15), 5005–5023. https://doi.org/10.1002/joc.5138.

de Queiroz, A. R., Faria, V. A. D., Lima, L. M. M., & Lima, J. W. M. (2019). Hydropower revenues under the threat of climate change in Brazil. *Renewable Energy, 133*, 873–882. https://doi.org/10.1016/j.renene.2018.10.050.

Devkota, L.P., & Gyawali, D.R. (2015). Impacts of climate change on hydrological regime and water resources management of the Koshi River Basin, Nepal. *Journal of Hydrology: Regional Studies, 4*, 502–515. https://doi.org/10.1016/j.ejrh.2015.06.023.

Devkota, R.P., Pandey, V.P., Bhattarai, U., Shrestha, H., Adhikari, S., & Dulal, K.N. (2016). Climate change and adaptation strategies in Budhi Gandaki River Basin, Nepal: a perception-based analysis. Climatic Change. https://doi.org/10.1007/s10584-016-1836-5.

Devkota, L. P., Bhattarai, U., Khatri, P., Marahatta, S., & Shrestha, D. (2021). Resilience of hydropower plants to flow variation through the concept of flow elasticity of power: theoretical development renewable energy. *Renewable Energy*. https://doi.org/10.1016/j.renene.2021.11.051 in press.

Devkota, L.P., Bhattarai, U., Khatri, P., Marahatta, S., & Shrestha, D. (2022). Resilience of hydropower plants to flow variation through the concept of flow elasticity of power: Theoretical development. *Renewable Energy, 184,* 920–932. https://doi.org/10.1016/j.renene.2021.11.051.

Dietzenbacher, E., Kulionis, V., & Capurro, F. (2020). Measuring the effects of energy transition: a structural decomposition analysis of the change in renewable energy use between 2000 and 2014. *Applied Energy, 258*, 114040. https://doi.org/10.1016/j.apenergy.2019.114040.

Donk, P., Van Uytven, E., Willems, P., & Taylor, M. A. (2018). Assessment of the potential implications of a 1.5 °C versus higher global temperature rise for the Afobaka hydropower scheme in Suriname. *Regional Environmental Change, 18*(8), 2283–2295. https://doi.org/10.1007/s10113-018-1339-1.

Gunturu, U.B., & Hallgren, W. (2017). Asynchrony of wind and hydropower resources in Australia. *Scientific Reports, 7*, 1–9. https://doi.org/10.1038/s41598-017-08981-0.

Hanif, I., Muhammad, S., Raza, F., Gago-de-santos, P., & Abbas, Q. (2019). Fossil fuels, foreign direct investment, and economic growth have triggered CO_2 emissions in emerging Asian economies: some empirical evidence. *Energy, 171*, 493–501. https://doi.org/10.1016/j.energy.2019.01.011.

Hamududu, B.H., & Killingtveit, Å. (2016). Hydropower production in future climate scenarios; the case for the Zambezi River. *Energies, 9*, 1–18. https://doi.org/10.3390/en9070502.

IEA. (2020). Key world energy statistics 2020. In *Key World Energy Statistics* (Issue August).

Janssen, A. B. G., Droppers, B., Kong, X., Teurlincx, S., Tong, Y., & Kroeze, C. (2021). Characterizing 19 thousand Chinese lakes, ponds and reservoirs by morphometric, climate and sediment characteristics. *Water Research, 202*, 117427. https://doi.org/10.1016/j.watres.2021.117427.

Jha, R. (2011). Total Run-of-River type Hydropower Potential of Nepal. *Hydro Nepal: Journal of Water, Energy and Environment, 7*, 8–13. https://doi.org/10.3126/hn.v7i0.4226

Kaini, S., Nepal, S., Pradhananga, S., Gardner, T., & Sharma, A.K. (2020). Impacts of climate change on the flow of the transboundary Koshi River, with implications for local irrigation. *International Journal of Water Resources Development, 00*, 1–26. https://doi.org/10.1080/07900627.2020.1826292.

Li, S., Bush, R. T., Santos, I. R., Zhang, Q., Song, K., Mao, R., Wen, Z., & Lu, X. X. (2018). Large greenhouse gases emissions from China's lakes and reservoirs. *Water Research, 147*, 13–24. https://doi.org/10.1016/j.watres.2018.09.053.

Liao, C., Erbaugh, J. T., Kelly, A. C., & Agrawal, A. (2021). Clean energy transitions and human well-being outcomes in Lower and Middle Income Countries: a systematic review. *Renewable and Sustainable Energy Reviews, 145*, 111063. https://doi.org/10.1016/j.rser.2021.111063.

Liu, X., Tang, Q., Voisin, N., & Cui, H. (2016). Projected impacts of climate change on hydropower potential in China. *Hydrology and Earth System Sciences, 20*(8), 3343–3359. https://doi.org/10.5194/hess-20-3343-2016.

Liu, M., Xie, H., He, Y., Zhang, Q., Sun, X., Yu, C., Chen, L., Zhang, W., Zhang, Q., & Wang, X. (2019). Sources and transport of methylmercury in the Yangtze River and the impact of the Three Gorges Dam. *Water Research, 166*, 115042. https://doi.org/10.1016/j.watres.2019.115042.

Liu, L., Yang, Z. J., Delwiche, K., Long, L. H., Liu, J., Liu, D. F., Wang, C. F., Bodmer, P., & Lorke, A. (2020). Spatial and temporal variability of methane emissions from cascading reservoirs in the Upper Mekong River. *Water Research, 186*, 116319. https://doi.org/10.1016/j.watres.2020.116319.

Liu, X., Zhao, T., Chang, C., & James, C. (2021). China's renewable energy strategy and industrial adjustment policy. *Renewable Energy, 170*, 1382–1395. https://doi.org/10.1016/j.renene.2021.02.045.

Martins, F., Felgueiras, C., & Smitková, M. (2018). Fossil fuel energy consumption in European countries. *Energy Procedia, 153*, 107–111. https://doi.org/10.1016/j.egypro.2018.10.050.

Mattmann, M., Logar, I., & Brouwer, R. (2016). Hydropower externalities: a meta-analysis. *Energy Economics, 57*, 66–77. https://doi.org/10.1016/j.eneco.2016.04.016.

Marahatta, S., Aryal, D., Devkota, L.P., Bhattarai, U., & Shrestha, D. (2021a). Application of swat in hydrological simulation of complex mountainous river basin (Part II: Climate Change Impact Assessment). *Water (Switzerland)* 13. https://doi.org/10.3390/w13111548.

Marahatta, S., Devkota, L.P., & Aryal, D. (2021b). Impact of flow variation on hydropower projects in Budhigandaki River Basin of Nepal. *Journal of Institute of Science and Technology, 26*, 89–98. https://doi.org/10.3126/jist.v26i1.37831.

Marahatta, S., Devkota, L.P., & Aryal, D. (2021c). Application of swat in hydrological simulation of complex mountainous river basin (Part I: Model Development). *Water* (Switzerland) 13. https://doi.org/10.3390/w13111546.

Mutezo, G., & Mulopo, J. (2021). A review of Africa's transition from fossil fuels to renewable energy using circular economy principles. *Renewable and Sustainable Energy Reviews, 137*, 110609. https://doi.org/10.1016/j.rser.2020.110609.

MoF. (2021). *Economic Survey 2077/78*.

Mtilatila, L., Bronstert, A., Shrestha, P., Kadewere, P., & Vormoor, K. (2020). Susceptibility of water resources and hydropower production to climate change in the tropics: The case of Lake Malawi and Shire River Basins, SE Africa. *Hydrology, 7*. https://doi.org/10.3390/HYDROLOGY7030054

NEA. (2017). NEA board decisions on the power purchase rates and associated rules for PPA of RoR / PRoR / Storage.

Nepal Rastra Bank, n.d. NRB Forex [https://www.nrb.org.np].

Pakhtigian, E. L., Jeuland, M., Dhaubanjar, S., & Pandey, V. P. (2020). Balancing intersectoral demands in basin-scale planning: the case

of Nepal's western river basins. *Water Resources and Economics, 30*, 100152. https://doi.org/10.1016/j.wre.2019.100152.

Paltsev, S. (2020). Projecting energy and climate for the 21st Century. *Economics of Energy & Environmental Policy, 9*, 43–62. https://doi.org/10.5547/2160-5890.9.1.SPAL.

Pandey, V.P., Dhaubanjar, S., Bharati, L., & Thapa, B.R. (2019). Hydrological response of Chamelia watershed in Mahakali Basin to climate change. *Science of The Total Environment, 650*, 365–383. https://doi.org/10.1016/j.scitotenv.2018.09.053.

Poletti, S., & Staffell, I. (2021). Understanding New Zealand's wind resources as a route to 100 % renewable electricity. *Renewable Energy, 170*, 449–461. https://doi.org/10.1016/j.renene.2021.01.053.

Poudineh, R., Sen, A., & Fattouh, B. (2020). Electricity markets in the resource-rich countries of the MENA: adapting for the transition era. *Economics of Energy and Environmental Policy, 10*(1), 1–25. https://doi.org/10.5547/2160-5890.10.1.RPOU.

Qin, P., Xu, H., Liu, M., Du, L., Xiao, C., Liu, L., & Tarroja, B. (2020). Climate change impacts on Three Gorges Reservoir impoundment and hydropower generation. *Journal of Hydrology, 580*, 123922. https://doi.org/10.1016/j.jhydrol.2019.123922.

Ranzani, A., Bonato, M., Patro, E. R., Gaudard, L., & Michele, C. D. (2018). Hydropower future: between climate change, renewable deployment, carbon and fuel prices. *Water*. https://doi.org/10.3390/w10091197.

Rehman, A., Ma, H., Chishti, M. Z., Ozturk, I., Irfan, M., & Ahmad, M. (2021). Asymmetric investigation to track the effect of urbanization, energy utilization, fossil fuel energy and CO_2 emission on economic efficiency in China : another outlook. *Environmental Science and Pollution Research, 28*, 17319–17330.

Shirsat, T.S., Kulkarni, A. V., Momblanch, A., Randhawa, S.S., & Holman, I.P. (2021). Towards climate-adaptive development of small hydropower projects in Himalaya: A multi-model assessment in upper Beas basin. *Journal of Hydrology: Regional Studies, 34*, 100797. https://doi.org/10.1016/j.ejrh.2021.100797.

Shrestha, A., Shrestha, S., Tingsanchali, T., Budhathoki, A., & Ninsawat, S. (2021). Adapting hydropower production to climate change: a case study of Kulekhani Hydropower Project in Nepal. *Journal of Cleaner Production, 279*, 123483. https://doi.org/10.1016/j.jclepro.2020.123483

Tomczyk, P., & Wiatkowski, M. (2020). Challenges in the development of hydropower in selected european countries. *Water*. https://doi.org/10.3390/w12123542

Turner, S.W.D., Hejazi, M., Kim, S.H., Clarke, L., & Edmonds, J. (2017a). Climate impacts on hydropower and consequences for global electricity supply investment needs. *Energy, 141*, 2081–2090. https://doi.org/10.1016/j.energy.2017.11.089.

Turner, S.W.D., Ng, J.Y., & Galelli, S. (2017b). Examining global electricity supply vulnerability to climate change using a high-fidelity hydropower dam model. *Science of the Total Environment, 590–591*, 663–675. https://doi.org/10.1016/j.scitotenv.2017.03.022.

Uamusse, M.M., Tussupova, K., & Persson, K.M. (2020). Climate change effects on hydropower in Mozambique. *Applied Science, 10*. https://doi.org/10.3390/app10144842.

Wagner, B., Hauer, C., Habersack, H., 2019. Current hydropower developments in Europe. *Current Opinion in Environmental Sustainability, 37*, 41–49. https://doi.org/10.1016/j.cosust.2019.06.002.

Zhou, Q., Hanasaki, N. (2018). Economic consequences of global climate change and mitigation on future hydropower generation, 77–90.

Zhong, R., Zhao, T., He, Y., & Chen, X. (2019). Hydropower change of the water tower of Asia in 21st century: A case of the Lancang River hydropower base, upper Mekong. *Energy, 179*, 685–696. https://doi.org/10.1016/j.energy.2019.05.059.

APPENDIX -2 FIELD PHOTOGRAPHS

Rainfall Station at Chhekampar (Index no. 833)

Rainfall Station at Arughat (Index no.1002)

Rainfall Station at Chunchet (Index no. 869)

Rainfall Station at MachhaKhola (Index no. 840)

Rainfall Station at Salleri (Installed in 2020)

Rainfall Station at Jagat (Index no. 801)

Hydrological Station BG-Ka at Tatopani (2009)

Hydrological Station BG-Ka at Tatopani (2021)

Hydrological Station BG-Kha at Machha Khola (2009)

Hydrological Station BG-Kha at Machha Khola (2021)

Hydrological Station of Budhigandaki River at Arughat (Station no. 445)

Gauge House of Budhigandaki River at Arughat (Station no. 445)

Hydrological Station of Budhigandaki River at Dam Site (2013)

Budhigandaki Tom Khola Confluence

Budhigandaki River at Arughat

Proposed Dam Site of Budhigandaki HEP

3-D View of Proposed Dam of Budhigandaki HEP

With Former VDC Chairperson of Chumchet

APPENDIX -3 CERTIFICATES OF CONFERENCE PARTICIPATION

AGU 100
ADVANCING EARTH AND SPACE SCIENCE

Certificate of Participation
AGU Fall Meeting 2018
10-14 December, 2018
Washington, DC

13 December 2018

To Sir or Madam:

This letter confirms that Suresh Marahatta presented a paper titled, "GC43K-1700. Potential Impact of Climate Change on Future Water Availability in Budhigandaki River Basin, Nepal", during a(n) Poster session on Thursday, 13 December, at the AGU Fall Meeting 2018. The AGU Fall Meeting 2018 took place 10-14 December 2018 at the Walter E. Washington Convention Center in Washington, DC.

Should you have any questions, please contact the AGU Meetings office at abstracts@agu.org.

Sincerely,

AGU Staff Representative

2000 Florida Avenue, NW. Washington, DC 20009-1277
Tel: 202.462.6900
Fax: +1 202.328.0566
www.agu.org

AGU 100
ADVANCING EARTH AND SPACE SCIENCE

Certificate of Participation
AGU Fall Meeting 2019
9-13 December, 2019
San Francisco, CA, USA

13 December 2019

To Sir or Madam:

This letter confirms that Suresh Marahatta presented a paper titled, "Impact of Climate Change in Himalayan River Hydrology in Nepal", during a(n) Oral session on 13 December, 2019 at the AGU Fall Meeting 2019. The AGU Fall Meeting 2019 took place 9-13 December, 2019 at the Moscone Convention Center in San Francisco, CA, USA.

Should you have any questions, please contact the AGU Meetings office at abstracts@agu.org.

Sincerely,

OFFICIAL DOCUMENT
AGU100 ADVANCING EARTH AND SPACE SCIENCE

AGU Staff Representative

2000 Florida Avenue, NW, Washington, DC 20009-1227
Tel: 202.328.6900
Fax: +1 202.328.0566
www.agu.org